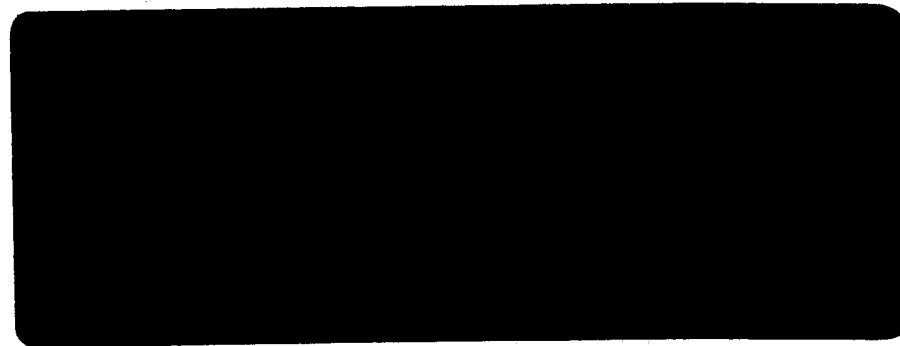


N64-28163
 (ACCESSION NUMBER)
 381
 (PAGES)
 CR-56934
 (NASA CR OR TMX OR AD NUMBER)

28167
 (THRU)
 1
 (CODE)
 10
 (CATEGORY)

The College of William and Mary



381/71



UNPUBLISHED PRELIMINARY DATA

PHYSICS DEPARTMENT

OTS PRICE

Williamsburg, Virginia

XEROX

\$ 21.00 ph

MICROFILM

\$

Supported in part by

NATIONAL AERONAUTICS AND SPACE ADMINISTRATION

(4)

RC# 4

CONFERENCE ON
HIGH ENERGY CYCLOTRON IMPROVEMENT
COLLEGE OF WILLIAM AND MARY
SPONSORED BY THE NATIONAL
AERONAUTICS AND SPACE ADMINISTRATION
FEBRUARY 6-8, 1964

ORGANIZING COMMITTEE

R. E. Welsh

R. T. Siegel

SCIENTIFIC SECRETARIES

M. Bardon

H. O. Funsten

PROCEEDINGS EDITOR

H. O. Funsten

FORWARD

The Conference on High-Energy Cyclotron Improvement was organized to provide an opportunity for exchange of information among those engaged in attempts to increase the usefulness of presently operating proton accelerators in the 100-800 MeV range. These machines, all synchrocyclotrons, have been basically unchanged since their initial operation from five to eighteen years ago. The increasing difficulty of experiments, added to a growing interest in the physics in this energy region, has caused widespread activity directed towards higher proton currents and increased intensity of secondary beams. It is hoped that a pooling of experience and ideas might benefit all engaged in this improvement work. The 64 scientists from five countries who attended the Conference demonstrated that pion-muon and proton research below 1 BeV is presently an active and viable field of research. It remains to be seen whether the ideas and work presented in these Proceedings will enable synchrocyclotrons to provide the beams necessary to sustain research in this energy region until a new generation of accelerators comes into being.

In the interest of making these Proceedings available as soon as possible after the Conference, a method of printing was chosen which leaves something to be desired in the quality of reproduction of photographs. We trust that none of the crucial details are invisible.

It was not possible to submit all the discussions to the participants before publication of these Proceedings. Therefore, any errors which persist are the responsibility of the Editor.

Our thanks to the Sponsors, the Scientific Secretaries, the typists, and those students who aided in various aspects of the Conference.

H. Funsten
R. Siegel
R. Welsh

REGISTRATION - CYCLOTRON IMPROVEMENT CONFERENCE

February 6-8, 1964

C. L. ADAMS Old Dominion College	T. FOELSCH NASA, Langley Research Center
FUJIO ANDO Virginia Polytechnic Institute	M. FOSS Carnegie Institute of Technology
M. BARDON Columbia University	J. H. FREGEAU Office of Naval Research
S. W. BARNES University of Rochester	C. B. FULMER Oak Ridge National Laboratory
H. BEGER CERN	H. FUNSTEN College of William and Mary
R. W. BERCAN NASA, Lewis Research Center	R. A. GOLUB NASA, Langley Research Center
W. M. BROBECK W. M. Brobeck Associates	W. GOODELL Columbia University
R. BURLEIGH University of California, Berkeley	B. GOTTSALK Harvard University
A. CITRON Brookhaven - CERN	R. HANSEN NASA, Langley Research Center
K. M. CROWE University of California, Berkeley	W. HASKINS Virginia Assoc. Res. Center
F. CROWFIELD College of William and Mary	H. D. HENDRICKS NASA, Langley Research Center
G. CULLIGAN University of Chicago	H. H. HEYSON NASA, Langley Research Center
B. W. DELOS REYES Longwood College	H. HINTERBERGER University of Chicago
J. E. DUBERG NASA, Langley Research Center	H. HOLMGREN University of Maryland
M. ECKHAUSE College of William and Mary	W. C. HONAKER NASA, Langley Research Center
R. FINDLEY Carnegie Institute of Technology	R. W. HOOKER NASA, Langley Research Center
A. FLEISCHER W. M. Brobeck Associates	D. I. HOPP University of California, Los Angeles

G. B. HUXTABLE Harwell - A.E.R.E.	G. POLUCCI Harvard University
T. G. JAMES NASA, Langley Research Center	C. M. FRITCHARD Old Dominion College
D. JOHNSON NASA, Langley Research Center	A. ROBSON Virginia Polytechnic Institute
A.M. KOEHLER Harvard University	B. ROSE Harwell - A.E.R.E.
D. LAWRENCE College of William and Mary	W. C. SAUDER Virginia Military Institute
R. S. LIVINGSTON Oak Ridge National Laboratory	R. SHERR Princeton University
K. R. MACKENZIE University of California at Los Angeles	R. T. SIEGEL College of William and Mary
R. B. MARCH University of Chicago	J. SINGH College of William and Mary
S. MARGULIES Columbia University	D. D. SMITH NASA, Langley Research Center
J. A. MARTIN Oak Ridge National Laboratory	S. SOBOTTKA University of Virginia
D. F. MEASDAY Harvard University	H. A. SOULE Hampton, Virginia
E. MICHAELIS CERN	C. STEARNS Virginia Assoc. Res. Center
E. MOLTHEN University of Chicago	A. SUZUKI Carnegie Institute of Technology
R. B. MOORE McGill University	A. SVANHEDEN University of Uppsala
J. MULADY W. M. Brobeck Associates	H. TALKIN NASA, Washington, D. C.
J. B. NEWMAN Virginia Military Institute	V. L. TELEGDI University of Chicago
R. F. NISSEN W. M. Brobeck Associates	H. TYREN University of Uppsala
E. NORDBERG University of Rochester	N. VOGT-NILSEN CERN

R. E. WELSH
College of William and Mary

W. D. WHITEHEAD
University of Virginia

J. R. WORMALD
University of Liverpool

E. WRIGHT
NASA, Langley Research Center

K. O. ZIOCK
University of Virginia - VARC

TABLE OF CONTENTS

	Page
Welcome to Visitors, Davis Y. Paschall, President, College of William and Mary	1
Beam Loss by a Beam-Induced Cross-Mode in the R. F.- Acceleration Programme of the CERN 600 MeV Synchrocyclotron, H. Beger, CERN	3
Some Remarks on Induced Radioactivity, M. Barbier, CERN	16
Preliminary Investigation of Factors Affecting External Beams from the CERN Synchrocyclotron, L. Dick, L. di Lella, L. Feuvralis and M. Spighel, CERN	24
Three Years of Development at the CERN Synchrocyclotron, P. Lapostolle, CERN	35
Improvements to the CERN Synchrocyclotron Extraction System, M. Morpurgo, CERN	59
The Uppsala Synchrocyclotron, Ake Svanheden and Helge Tyren (Presented by Ake Svanheden), University of Uppsala	69
A Beam Pulse Stretcher for the Carnegie Synchrocyclotron, Arata Suzuki, Carnegie Institute of Technology	75
Improvement Designs for the Carnegie Synchrocyclotron, Martyn H. Foss, Carnegie Institute of Technology	85
Facilities Improvements and Activity Problems on the 184 "Cyclotron", Richard J. Burleigh, University of California, Berkeley	92
Some Remarks on the Berkeley 184 "Cyclotron", Kenneth M. Crowe, University of California, Berkeley	108
Multiple Dee System for the Chicago Synchrocyclotron, E. H. Molthen, University of Chicago	128
Columbia University Synchrocyclotron, Marcel Bardon, Columbia University	138
"Stochastic" System at Harvard Cyclotron, B. Gottshalk, Harvard University	143
Monoenergetic Neutron Beams, D. F. Measday, Harvard University	152
Facilities for Biological and Medical Uses of the Harvard Cyclotron, A. M. Koehler, Harvard University	160

	Page
The Harwell Synchrocyclotron, George Huxtable, Harwell, A.E.R.E.	166
Some Remarks on the Rochester Synchrocyclotron, S. W. Barnes, University of Rochester	177
Recent Improvements to the McGill Synchrocyclotron, R. B. Moore, McGill University	192
Improvements on the Princeton 18 MeV Synchrocyclotron, Ruby Sherr, Princeton University	198
Cyclotron Space Charge Limits, K. R. MacKenzie, University of California at Los Angeles	201
Quasi-free Proton-Proton Scattering in Light Nuclii, H. Tyren, University of Uppsala	224
The Chicago Muon Channel, V. L. Telegdi, University of Chicago	237
Performance Tests on the Chicago Muon Channel, Gerald Culligan, University of Chicago	264
Rotating Condensers, M. Foss, Carnegie Institute of Technology	279
Beam Stretching by Excitation of Radial Oscillations, J. R. Wormald, University of Liverpool	283
Residual Radiation Studies, C. B. Fulmer, Oak Ridge National Laboratory	290
Engineering Design of the Space Radiation Effects Laboratory, W. M. Brobeck, W. M. Brobeck Associates	300
The Use of Multiple Dees in the FM Cyclotron, W. M. Brobeck, W. M. Brobeck Associates	306
Beam Transport System for the NASA 600 MeV Synchro- cyclotron, R. F. Nissen, W. M. Brobeck Associates	311
The Design of a 300 MeV Extraction System for the NASA, SREL Synchrocyclotron, J. R. Mulady, W. M. Brobeck Associates	323
Summary, Kenneth M. Crowe, University of California, Berkeley	337
Operating Characteristics of Existing FM Synchrocyclotrons...	347

WELCOME ADDRESS

Davis Y. Paschall

President of the College of William and Mary

Gentlemen of the Cyclotron Conference:

The College of William and Mary is honored to serve as host for this unusual --and, we hope, highly productive--Conference on High Energy Cyclotron Improvement. We look forward to your visiting with us for the next several days, and climaxing your own sessions by joining in our annual observance of Charter Day on Saturday. At that time, as you may have noted in your program, the final address of the Conference will be the Charter Day address, given this year by President Julius A. Stratton of the Massachusetts Institute of Technology.

In the informational material which was prepared for your use, you may already have read some of the history of this institution, and of the man who was certainly one of our most notable graduates--Thomas Jefferson. You have also perhaps seen in your informational material the description of the now-almost-forgotten scientist who was Jefferson's great teacher and whose name has been ascribed to this new Physical Laboratory--William Small.

In mentioning these names, I would simply make the point that Jefferson, so renowned as a statesman, was in his time the example of the broadly educated man--scientist, craftsman, literary creator, and philosopher--that we take as our standard of excellence today. Jefferson viewed man in his infinite potential, and set the basic image and purpose of this College to be that of providing the broadly educated person.

Jefferson's other insistent standard was that education should keep at least abreast, and preferably in advance, of the continually changing need of society. Therefore, in his reorganization of this college in 1779 he introduced what were then radical concepts of education--including a greatly expanded curriculum in "natural philosophy" which has developed into the science faculties of our present

college--and a break in general with the university oriented system of the European tradition.

In the eighteenth century, this campus and this community rode the crest of the wave of the Enlightenment. The Society for the Advancement of Useful Knowledge was a group which stimulated a continuing dialogue on all dimensions of human knowledge. The founding of Phi Beta Kappa on this campus is a well-known story. The role played by College students and faculty in the movement for independence and a new nation is also well known.

But in welcoming you today I wish to emphasize that we consider a conference such as this to be perfectly in keeping with the Jeffersonian tradition, both in its subject-matter and in its response to the intellectual needs of the twentieth century. In Jefferson's day, the times called for intellectual boldness and the scientific mind. Can we seriously dispute that the need is still the same today?

The College greets you cordially, and assures you of our joy in the stimulating association made possible by your presence here.

BEAM LOSS BY A BEAM-INDUCED CROSS-MODE IN THE RF-ACCELERATION
PROGRAMME OF THE CERN 600 MeV SYNCHRO-CYCLOTRON

H. Beger and A. Flebig, CERN

(Presented by H. Beger)

Two different methods have been used in parallel to detect beam losses in the CERN SC:

- Beam intensity measurements by a thermocouple target as function of the radius (Fig. 1).
- Activation measurements in the vacuum tank as function of radius (Fig. 2)

Both measurements show a serious loss of beam at a radius of about 200 cm. By means of the existing RF monitoring system it was possible to establish the existence of a cross-mode at a frequency which also corresponds to a radius of 200 cm.

A circuit diagram of the RF pick-up electrodes is shown in Fig. 3, their mechanical layout in Fig. 4 and the points of their installation in Fig. 5. With these pick-ups RF pictures have been obtained similar to those obtained on other cyclotrons. There were "dips" in the programme, produced by absorption in resonant circuits coupled somehow with the RF structure. Most of these "dips" have been suppressed by the removal of unsuitable decoupling condensers. Other "dips" will be smoothed out in the future by our acceleration voltage modulator. However, at the frequency of 18.2 Mc/s corresponding to an orbit radius of just below 200 cm at normal field, a strange kind of dip with the following characteristics was found:

- 1) This dip disappeared completely if the beam was switched off;
- 2) the phase of this dip was shifted by 180° on the other side of the dee mouth;
- 3) the phase of the dip changed by 180° when the sense of rotation of the beam was changed by inverting the cyclotron magnet field.

These indications suggested that the dip was caused by a beam-excited cross-mode.

The amplitude of this cross-wave at $1.5 \mu\text{A}$ beam current is about 20% of the acceleration voltage at 18.2 Mc/s. The future plans for increasing the internal beam intensity and for improving the beam quality made it necessary to study in detail the possibilities for the suppression of this cross-mode which would cause the loss of the complete beam at higher beam currents.


The provisional installation of an absorption circuit tuned to 18.2 MC/s did not give any improvement, but a measurement inside the cyclotron tank showed a strong resonance at a frequency of 36.4Mc/s in the acceleration gap. When passing the gap at the radius corresponding to half this frequency the protons are decelerated and transfer a part of their energy to a parallel line half wave resonator formed by the acceleration gap (Fig. 6). Due to the high radioactivity within the cyclotron tank no further experiments were possible there.

For further experimental investigations of the fundamental and parasitic modes of oscillation across the dee mouth a 1 : 10 scale RF model was built. This model comprises all parts of the cyclotron relevant to the RF performance : dee, dummy dee, dee liner, stem, the adjustable capacitor replacing the tuning fork capacitor, and stub (Fig. 7).

At a position equivalent to that at which the oscillator is connected in the original RF system a coaxial input was placed in order to check resonant frequency and input impedance for the fundamental mode of oscillation. The resonant frequency versus capacitor position is given in Fig. 8. Because this connection produced a symmetric excitation with respect to the dee mouth the cross-mode suspected of causing beam loss was unlikely to be excited.

In order to check field distributions and to excite antisymmetric modes of oscillations along the dee mouth, some capacitive coupling probes were prepared, which could be inserted into the dummy-dee mouth. They consisted mainly of a coaxial plug, the inner conductor of which was extended and connected to a coupling

plate (Fig. 9). Two of these probes were designed for fixed positions, a third one could be moved along the dummy-dee mouth. The latter one was first used to check the voltage distribution along the dee mouth for the fundamental mode, which was found out to be uniform within the limits of measuring errors. For this measurement an RF generator was connected to the input, and an RF voltmeter to the probe (Fig. 10).

For the investigations of the parasitic modes of oscillations, the RF generator was connected to one of the capacitive probes, which was placed at one side of the dee mouth (Fig. 11). This measuring method was found rather troublesome, because for every position of the tuning capacitor, the generator had to be tuned over the entire frequency range. So the generator and voltmeter were replaced by a wobulator measuring system (Polyskop by Rhode & Schwarz). Here all the modes of oscillation could be simultaneously viewed on the screen, a feature which was extremely instructive. A plot of the modes of oscillation which could be excited at the dee mouth for different positions of the tuning capacitor is given in Fig. 12. For each observed mode the field distribution along the dee mouth was investigated. In the plot the different modes are marked by a voltage distribution symbol at the corresponding trace. For instance, the symbol ===== means an oscillation with constant voltage across the dee mouth, and the symbol  means an antisymmetric mode of oscillation of $1/2 \lambda$ -type.

It may be noted that, besides the main mode of oscillation, the frequency of which changes with the capacitor position, two "spurious" modes exist, which are not or only very little influenced by the capacitance. The antisymmetric spurious mode corresponds to the parasitic one found in the machine, the other one is rather unlikely to be excited by a circulating proton beam of a frequency between 16 and 30 Mc/s. (Since the model is 1:10 scale, the corresponding frequencies are ten times the frequencies existing in the machine.) Discontinuities in the plots for the spurious modes indicate some irregularities. It may be found out from the graphs that these irregularities correspond to positions of the tuning

capacitor, where the ratio between the frequencies of the main and the spurious modes is given by small integers. This effect is most likely due to harmonics in the output voltage of the wobulator.

The obvious method to prevent the appearance of the parasitic mode is to cut a slot into the dee at the plane of symmetry, where the current corresponding to the parasitic mode should be a maximum. Moreover, this slot is very unlikely to influence the wanted main mode.

For this reason, the model was built with a slot in the dee, which was closed with a copper sheet for the measurements described above. With the copper sheet taken out, the measurements were repeated. The results are plotted in Fig. 13. It is clearly seen that the parasitic mode is shifted to a much lower frequency, where it is unlikely to be excited by the beam. The symmetric spurious mode remains unchanged. An additional spurious mode is introduced. Also this one is unlikely to cause trouble, because its frequency is smaller than 300 Mc/s. For additional information, the measurements were repeated with the slot closed by resistive paper (paper containing carbon powder, impedance $\sim 4 \text{ K}\Omega$ per square) which was assumed to damp the spurious transverse modes rather than to shift their frequencies. It is clear from the plot in Fig. 14, that only the main mode and a symmetric spurious mode (2 types) are now present. In the next plot (Fig. 15) the frequency of the parasitic mode as a function of the slot depth is shown. This measurement was done in order to obtain information on the necessary slot depth.

For further measurements, the dee slot was closed only by a metallic conductor at the dee mouth and some intermediate points. This was done in order to find out whether a metallic frame could be tolerated, which in the present dee construction of the SC machine,

gives mechanical strength to the dee. Though the method of cutting a slot into the dee seems to be the obvious means to suppress anti-symmetric oscillations, it does not look very feasible for the machine due to difficulties of dismounting and mounting of the old dee fitted with a slot or of manufacturing a new one. So further investigations were carried out in order to find other solutions. One of these could be to connect series resonant circuits tuned to the proper frequency at points where they are well coupled to the transverse mode. From the practical point of view, a preferable position for these suppressing circuits is given by the high voltage biasing feedthroughs in the stub-liner (indicated on Fig. 7), because points are easily accessible.

Experiments on these suppressing circuits proved unsuccessful because either the influence on the unwanted mode was too small or the influence on the frequency and quality factor of the wanted main mode was too big. Therefore this method had to be abandoned.

As a conclusion from all measurements it may be said that the best method to suppress the parasitic mode of oscillation would be to introduce a slot in the dee which in addition could be filled with resistive material of appropriate conductivity. According to experiments performed with one or several layers of resistive paper in the model and with resistors simply soldered across the slot, the resistance does not seem to be very critical. The order of magnitude should be about 100Ω .

The following conclusions were drawn from the model measurements:

1. There seems no way of suppressing the cross-mode by external circuits without influencing the frequency of the main acceleration programme too much.

2. The cross-mode can be shifted in frequency out of the interesting range by slotting the dee in the middle. However, it is necessary to separate the two parts of the dee completely. If only the copper liner is cut, the internal mechanical supporting structure short-circuits the slot and the cross-mode remains more or less unchanged.

3. The cross-mode may be suppressed completely by putting damping resistors across the slot.

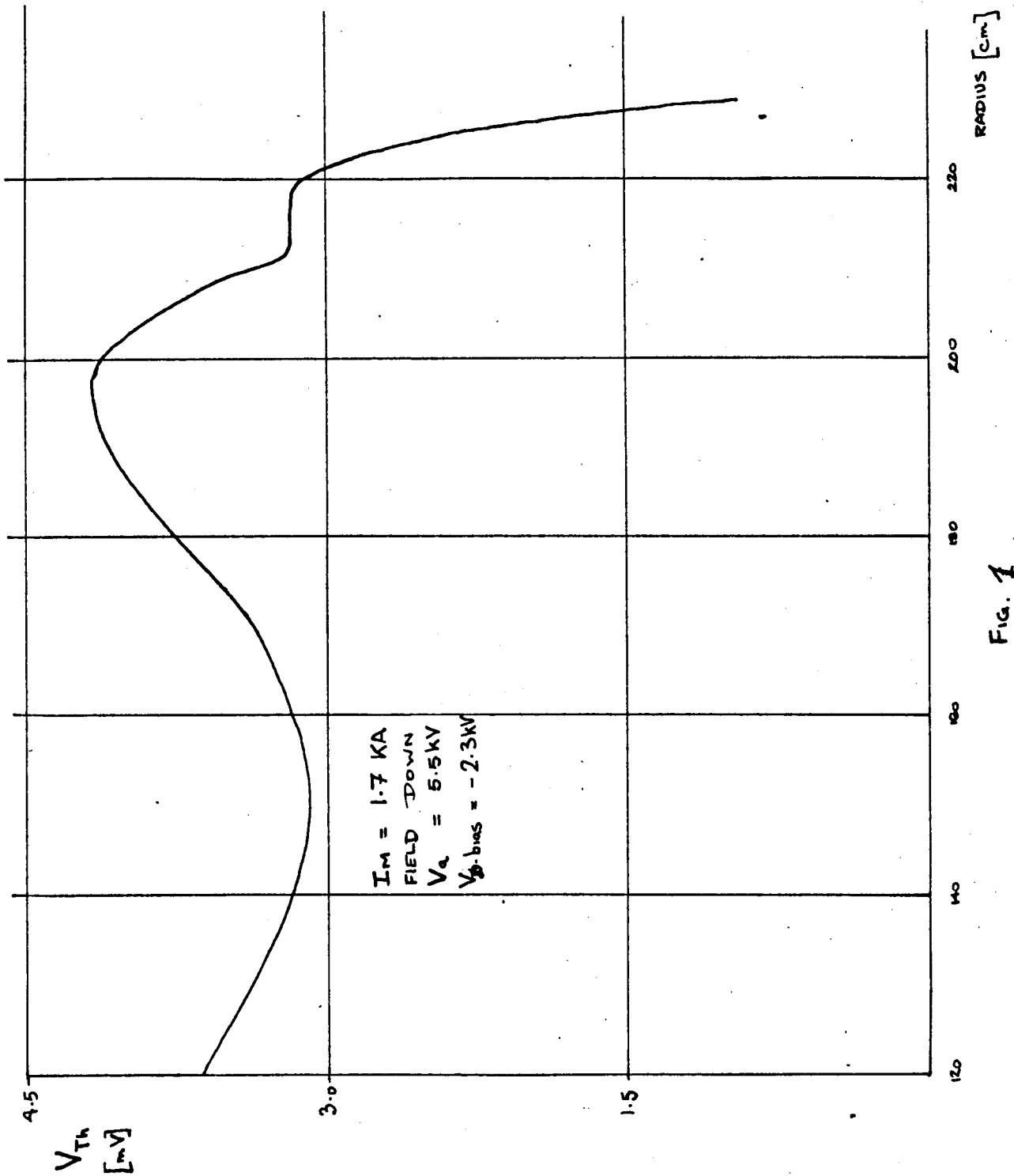


Fig. 1
THERMOCOUPLE READING AS FUNCTION OF RADIUS

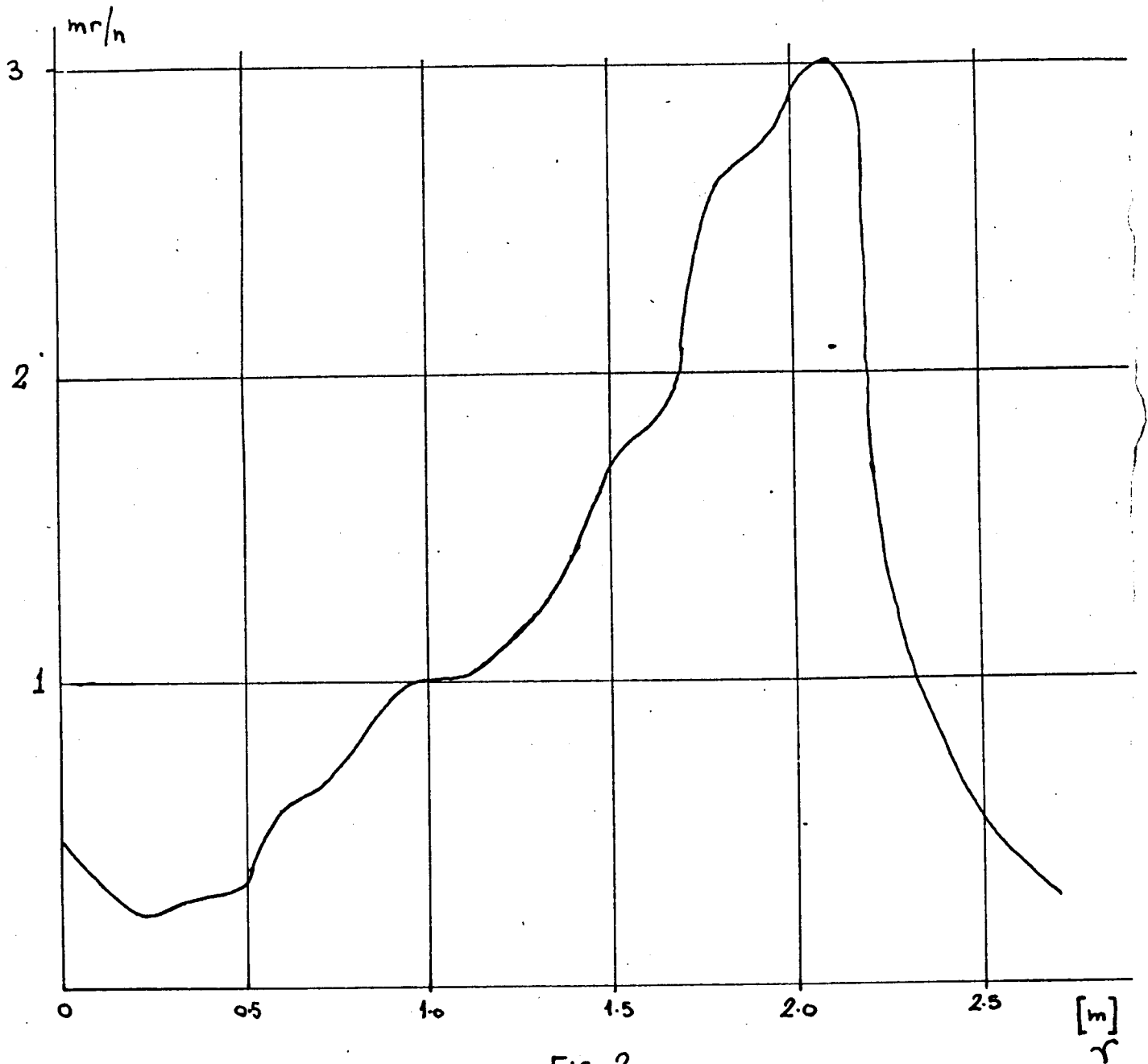
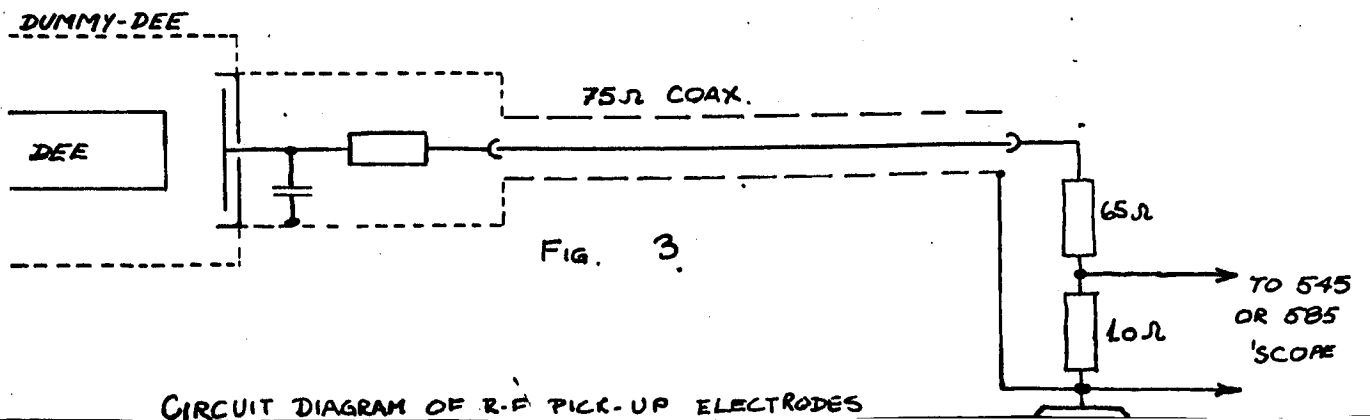


FIG 2

ION-SOURCE RAIL ACTIVATION AS FUNCTION OF RADIUS



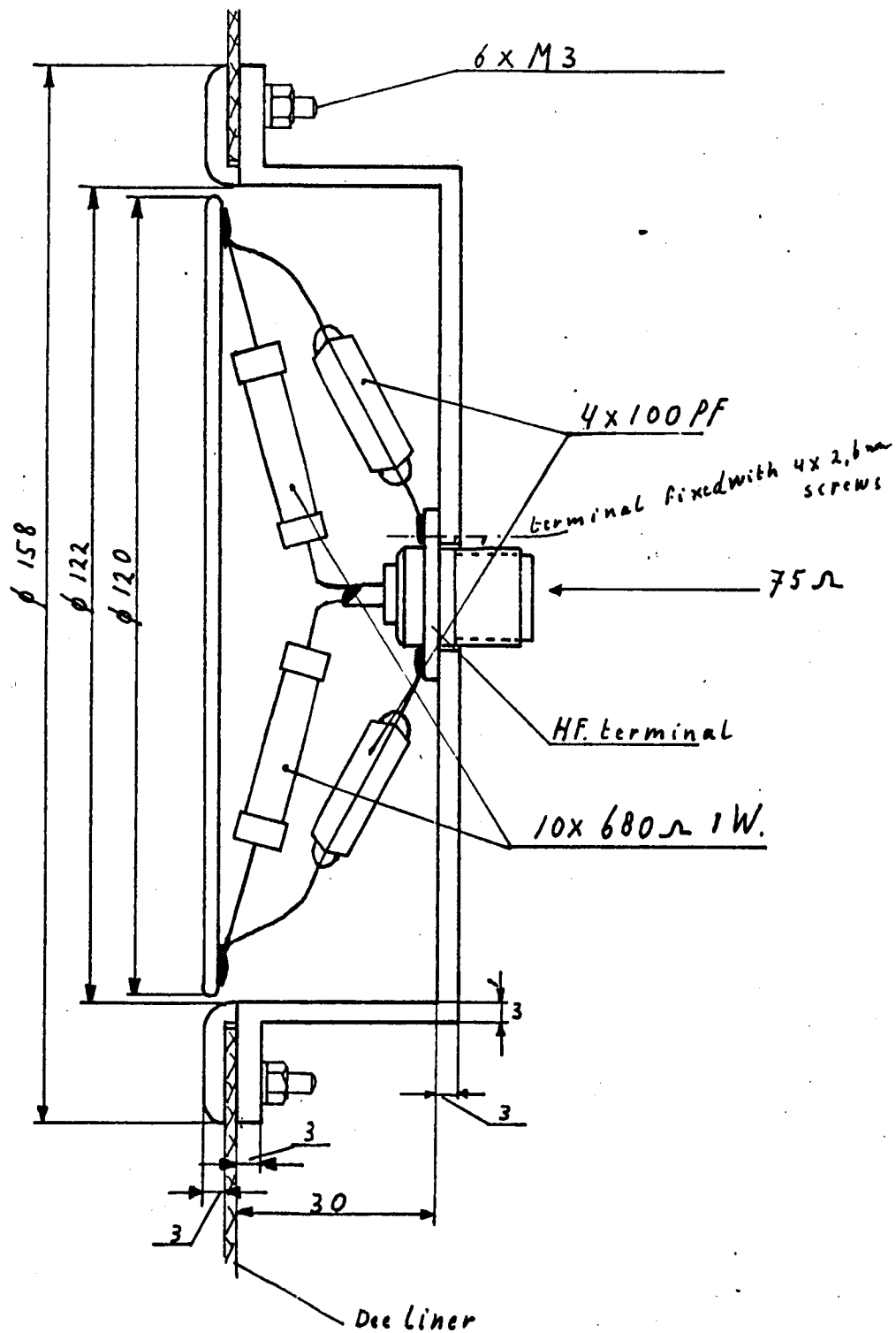


FIG. 4
 MECHANICAL LAYOUT OF RF PICK-UP ELECTRODE

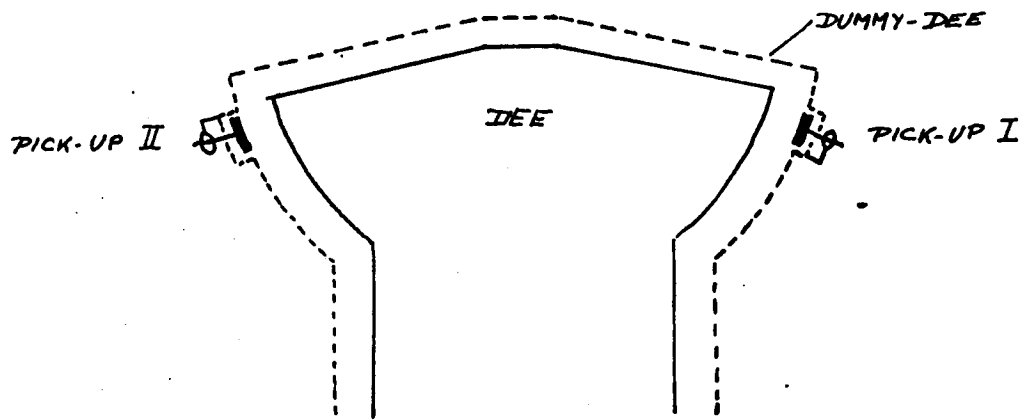


FIG 5

INSTALLATION POINTS OF PICK-UPS IN THE S.C.

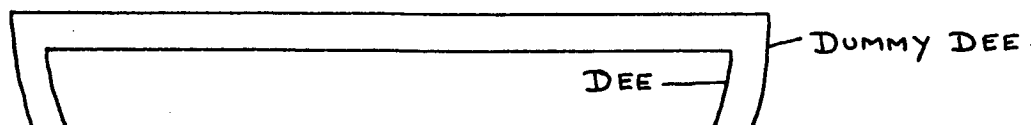
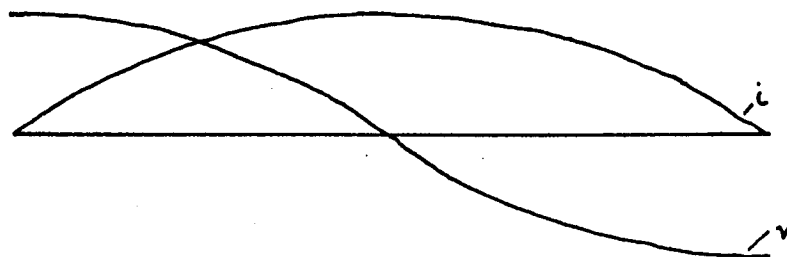


Fig. 6

VOLTAGE AND CURRENT DISTRIBUTION FOR PARASITIC MODE
OF OSCILLATION ALONG THE ACCELERATION GAP

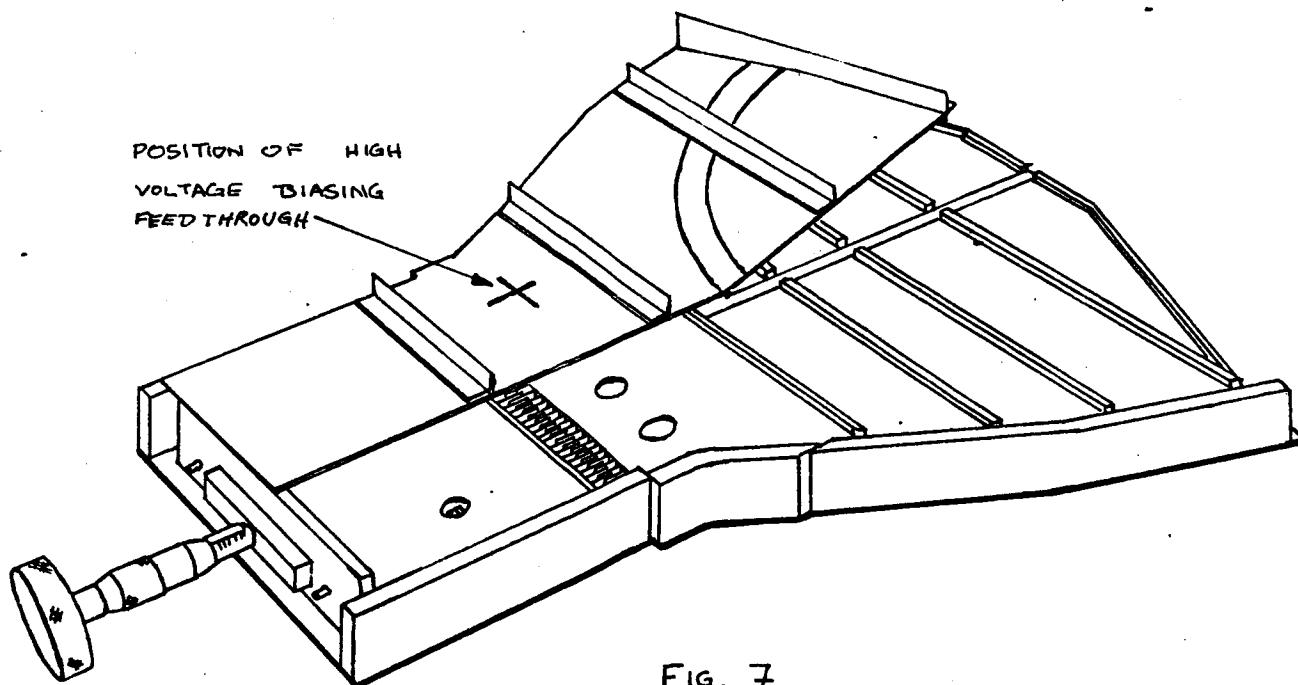


FIG. 7

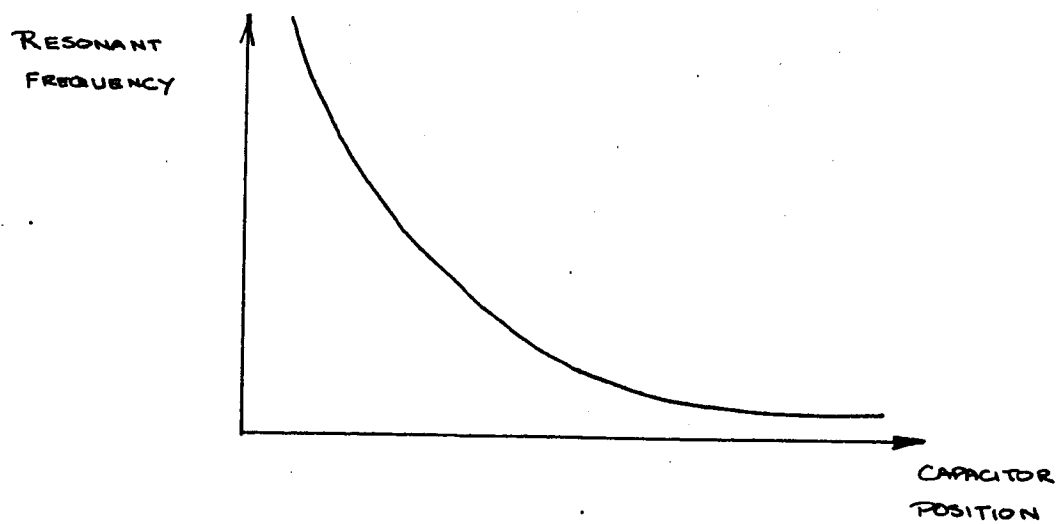


FIG. 8

RESONANT FREQUENCY VS CAPACITOR POSITION
FOR RF MODEL.

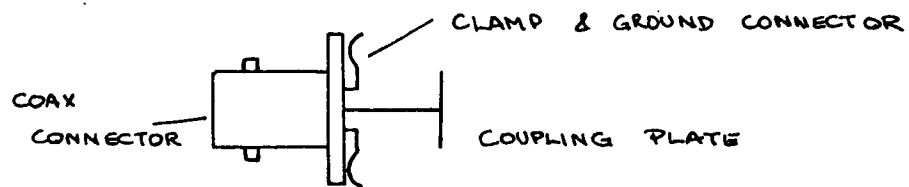


Fig. 9

ELECTRIC COUPLING PROBES

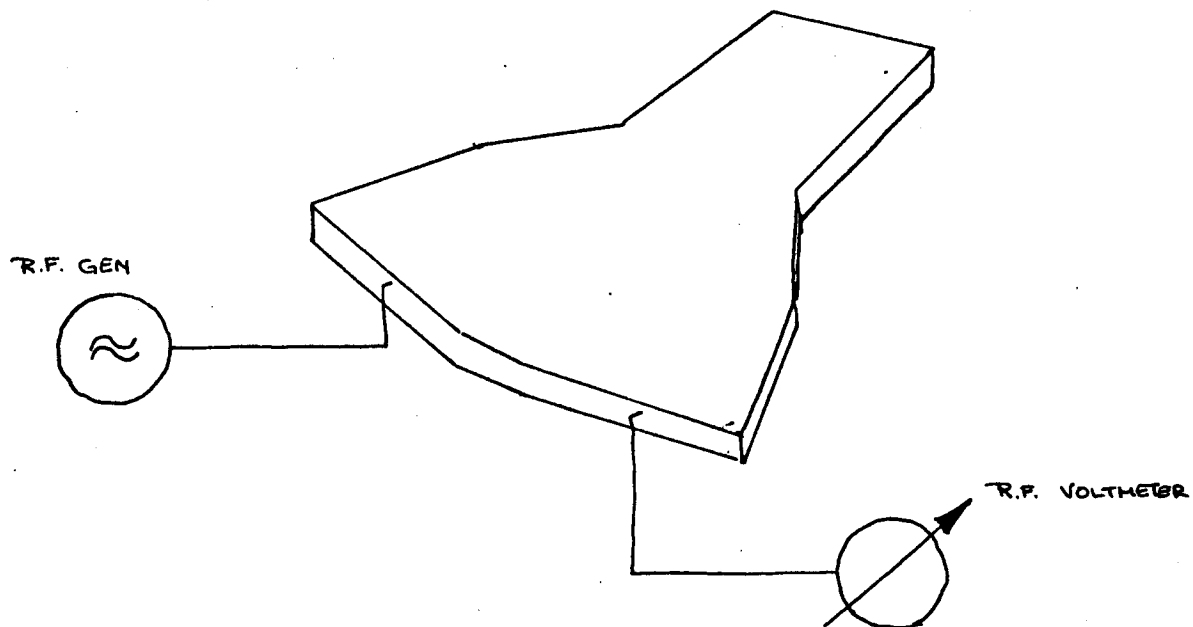


FIG 10

EXPERIMENTAL SET-UP WITH R.F. GENERATOR AND VOLTMETER.

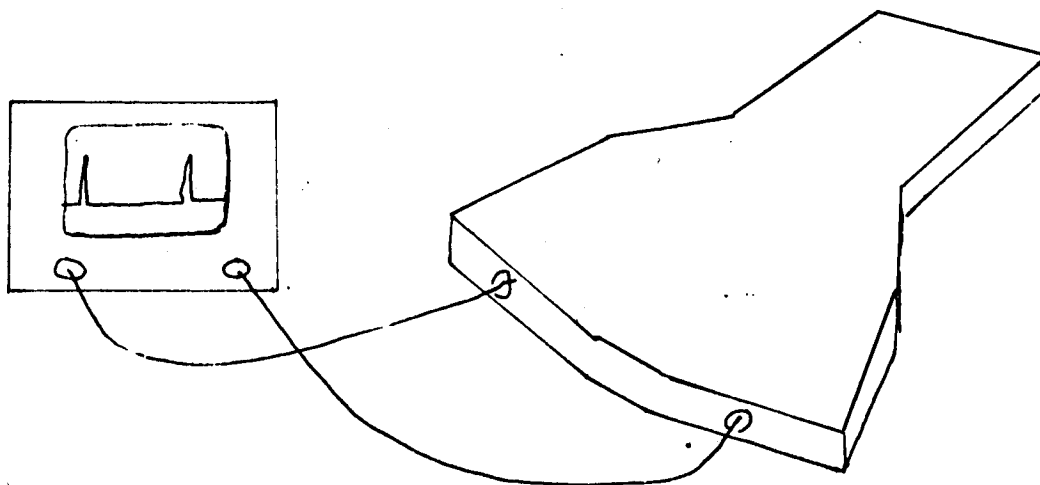
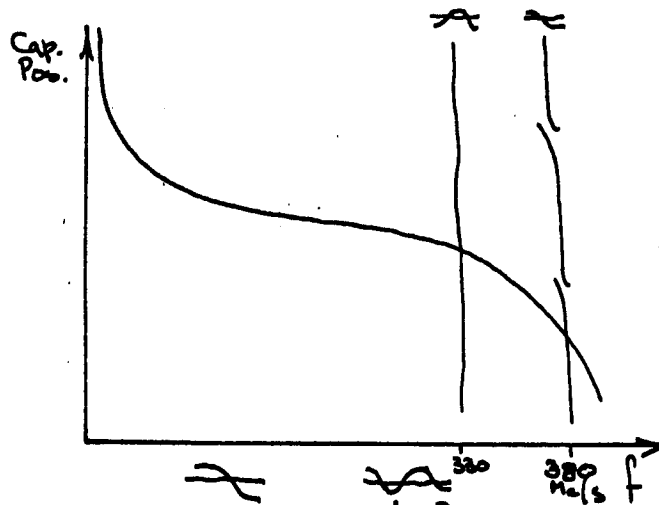


FIG 11

FIG 12

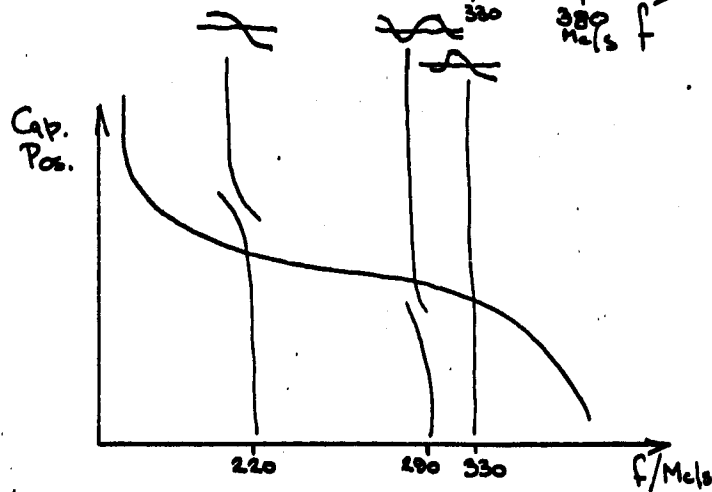


FREQUENCIES & MODES
OF OSCILLATIONS VS.

CAPACITOR POSITION

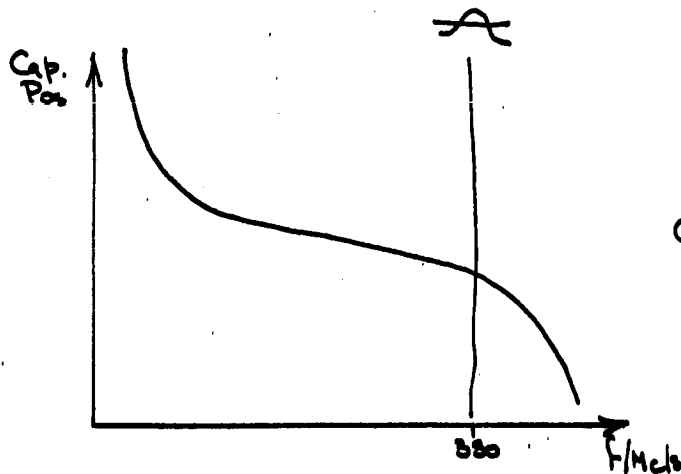
(a) WITHOUT SLOT

FIG 13



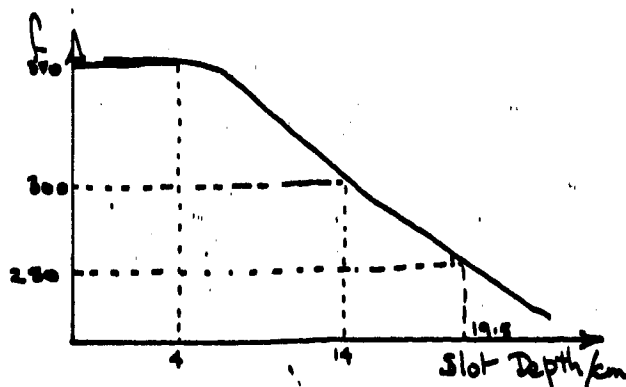
(b) WITH SLOTTED DEE

FIG 14



(c) SLOT CLOSED WITH
RESISTIVE PAPER

FIG 15



FREQUENCY OF PARASITIC
MODE VS. SLOT DEPTH.

SOME REMARKS ON INDUCED RADIOACTIVITY

M. Barbier, CERN

I. Beam Current Limitation due to Induced Radioactivity

An obstacle to the increase of the intensity in existing synchro-cyclotrons is the radiation field caused by induced radioactivity.

The attached figures show the radiation field both inside the tank and outside the CERN synchro-cyclotron, as measured by the CERN Health Physics Group under Dr. J. Baarli, who has kindly permitted my use of the figures.

The field inside the tank is of the order of a few Rem/hour 17 days after shut-down. One day after shut-down, these fields are certainly three times bigger. Clearly there is a limit in beam current for which no human work is possible inside the tank any more. The maximum dose that a person may receive at one time is 3 Rem, and this once a year only. The least figure for the duration of any work inside the tank would be set at about 3 minutes, including time for crawling in and out again. This gives a maximum tolerable radiation field of one Rem per minute, that is 60 Rem/hour, which is five to ten times what we have one day after shut-down, depending upon the location inside the tank.

Clearly all pieces of equipment that need servicing, replacement or repair should be replaced by items that can be taken out and put back into position again by remote control, if any further increase in the circulating beam is contemplated.

II. Behaviour of Various Materials with Respect to Activation

Some consideration has been given at CERN to the difference that may exist between materials with respect to activation hazard. The spallation cross-sections for production of the most important radioactive isotopes from various materials by protons at cyclotron energies have been measured experimentally at several laboratories and are available. We must also take into account the disintegration

scheme. Some radioactive nuclei emit several gamma quanta, others give conversion electrons with a certain probability. Thus the efficiency of the various nuclei in emitting a gamma quantum is different in each case. Furthermore, the number of quanta necessary to produce one Rem depends on the energy of the gamma ray. Finally we must consider the absorption of the gamma quantum in the irradiated material itself in the case of voluminous active parts. We have thus been led to define a "danger parameter" which seems characteristic for a given material with respect to the hazard it represents when it is activated up to saturation. This figure of danger we have derived is

$$D = \frac{N}{A} \sum_{\nu, \mu} \frac{\sigma_{\nu} \epsilon_{\nu, \mu}}{k_{\mu} \chi_{\mu}} \text{ Rem cm}^2$$

where

$N = 6 \cdot 10^{23}$ is Avogadro's number,

A = the atomic number,

σ_{ν} = the spallation cross-section for the ν^{th} isotope in cm^2 ,

$\epsilon_{\nu, \mu}$ = the efficiency of this isotope in emitting a μ^{th} gamma quantum in percent,

k_{μ} = the number of quanta per cm^2 of the type μ to produce one Rem,

χ_{μ} = the narrow beam mass absorption coefficient for the μ -type quantum in $\text{gr}^{-1} \text{cm}^2$.

The following table gives the D-values for various materials in units of $10^{-13} \text{ Rem cm}^2$ calculated with the spallation cross-sections available for protons in the literature. In this table isotopes with life-times less than 24 h are not considered.

TABLE I

Material	H	Be	C	O	Al	Fe	Co	Cu	Zn	Ta
D (in 10^{-13} Rem cm^2)	0	3.4	1.8	1	54	66	160	87	153	5

The danger parameter D has a simple physical meaning. If we multiply D by the flux of protons per sec and cm^2 we get the radiation field in Rem/sec in front of a thick uniformly saturated wall about one day after end of irradiation.

Various experiments have been conducted at CERN in order to compare the activation of different materials.

A series of small samples have been irradiated by protons for two years now and we are for the first time in a position to give measured data on activated materials with such a long irradiation time. The size of the samples was about $30 \times 30 \times 5 \text{ mm}^3$. They were irradiated longitudinally. Table II indicates the activity per gram measured three weeks after the end of irradiation, a) with a $3" \times 3"$ NaI (Tl) crystal at a distance of 36 cm and b) with the tissue equivalent ionization chamber in contact. (The chamber was a Landis & Gyr EQN1, where $80 \cdot 10^{-15}$ Amp is equivalent to one millirad/hour.)

The samples were located inside the tank, 90° downstream from the target region, 9.5 cm below median plane, at a radius of 2.20 m, which is roughly equal to the target radius.

In a second experiment voluminous cylindrical samples were irradiated for 8 months in a uniform flux of neutrons of high energy. These samples were located 3 m from the target region of the CERN Synchro-Cyclotron in the forward direction outside the tank. The diameter was 5 cm, the length 2.5 times the $1/2$ absorption length for a 1 MeV quantum in the respective materials. Table III gives the

TABLE II

Material	a) Counts/gr. min.	b) 10^{-15} Amp/gram
C	500	0.417
Mg	12 700	14.2
Elektron	10 650	10.6
Al	4 940	4.95
SiO ₂	2 950	3.1
Ti	14 400	27.6
Fe	10 900	16.9
Stainless Steel (17% Cr, 11% Ni, 2% Mo)	15 500	21.8
Cu	9 900	12.4
Co	48 500	114
Zn	15 500	19.4
Ni	35 000	71.5
Mo	15 400	22.5
Pb	1 600	1.71

measured activities 3 weeks after the end of irradiation a) at 1.5 m from the NaI (Tl) crystal and b) 6 cm above the tissue equivalent chamber. A 3 cm diameter lead collimator was used in both cases.

The experimental figures quoted in Tables II and III cannot be compared directly with those on Table I. It is impossible to measure the danger parameter directly because of the arbitrary exclusion of all activities under one day, and because the irradiation is supposed to have had an infinite duration. However, it can be estimated as soon as the cross-sections are known. In Table II small samples were measured, thus gamma ray absorption in the samples is absent. Also the Mg, Elektron, Al and SiO₂ samples are clearly not saturated, the intensity increasing

TABLE III

Material	a) Counts/min.	b) 10^{-15} Amp.
Concrete (Ordinary)	865	1.9
Al	1 055	4.5
Fe	10 913	48.5
Cu	7 519	35.5
Zn	12 667	60.5
Pb	401	2.5

by a factor 2.6 when saturation is reached. Column a) gives the number of counts in a NaI crystal, the energy response of which is not flat. Column b) gives the current in the ionization chamber proportional to the Rem-value.

Table III was obtained with thick samples. However, these were activated purely by neutrons, so the results cannot be compared to Table I which was calculated for activation by protons. As the irradiation time was still shorter than in the preceding case, the materials quoted are also less saturated. The missing factor in the materials mentioned above is here 6.4.

We can, however, draw some general conclusions from these preliminary results. In general they show qualitative agreement with the calculated danger parameter values.

The least dangerous materials are those of low atomic number in which Na22 cannot be formed, e.g. C, O, etc.

After these comes the series where Na22 is the most serious hazard : Al, Mg, Si, of which Al is the most favourable. Incidentally Calcium, which was measured in a separate experiment, shows very little Na22 formation. Hence, marble CaCO_3 is an absorber with low activity.

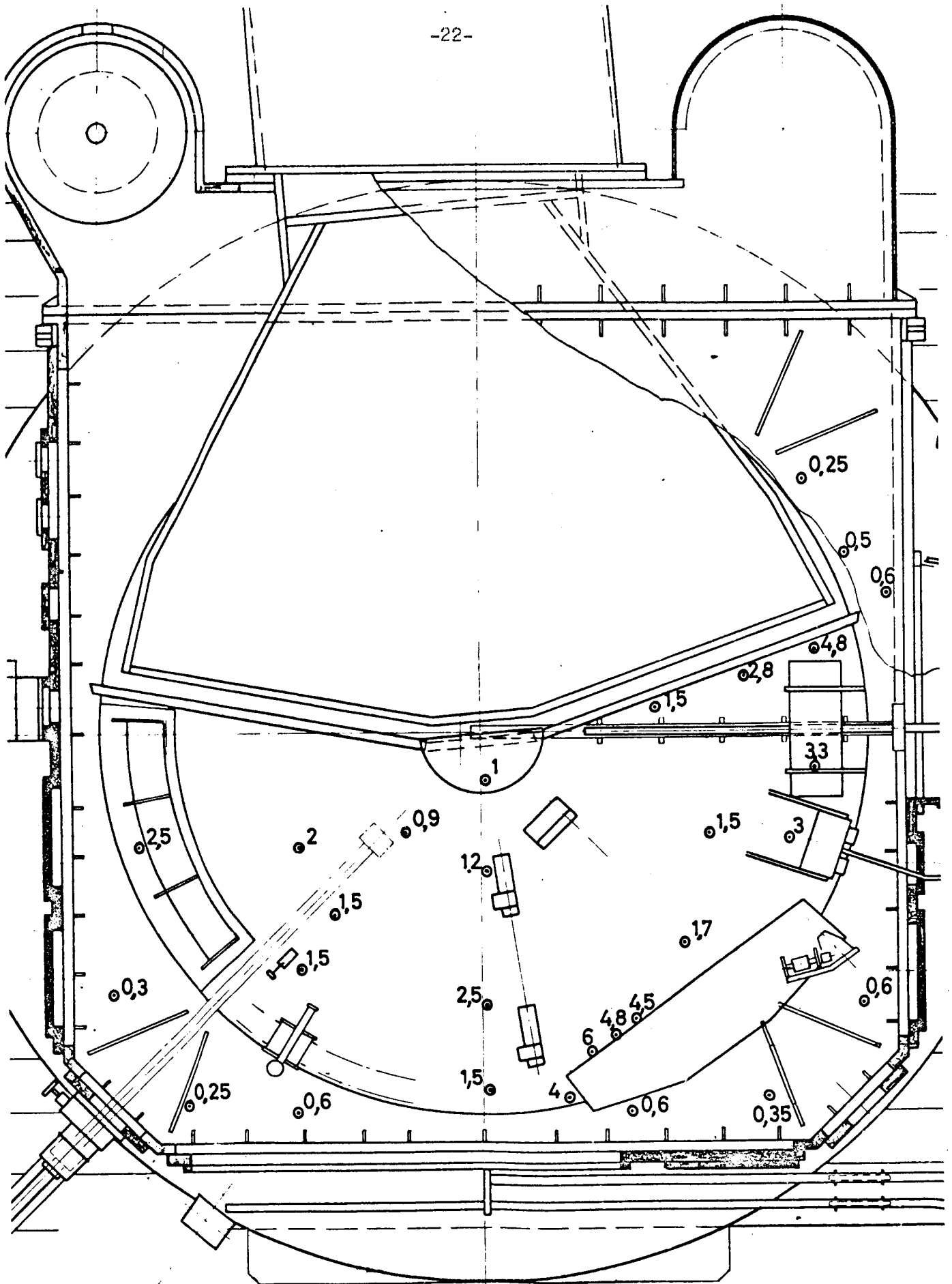
Then comes, from Titanium upwards, the series of the usual metals, which give rise to the heavily radiating isotopes of Scandium, Manganese, etc. Here, surprisingly, iron is more radioactive than expected, at all events more than copper. Stainless steel is worse than iron. Nickel and especially Cobalt are still worse. Aluminium, when saturated, should be a little more favourable than Copper, although Mg and Si are not.

Finally come very heavy but non spontaneously radioactive materials, as Ta or Pb, that appear to have a smaller activity. In fact the measurements made on lead 3 weeks after shut-down and reported here are somewhat misleading, because the activity of lead decreases very rapidly whereas that of Fe, Cu does not. Three days after shut-down, the activity of lead was 5 times bigger than reported, which amounted to about $1/8$ of the iron activity and $1/5$ of the copper activity in counts with the NaI crystal for the thick samples of Table III. Anyhow, lead appears to be promising also as an absorber, if one is prepared to wait several days.

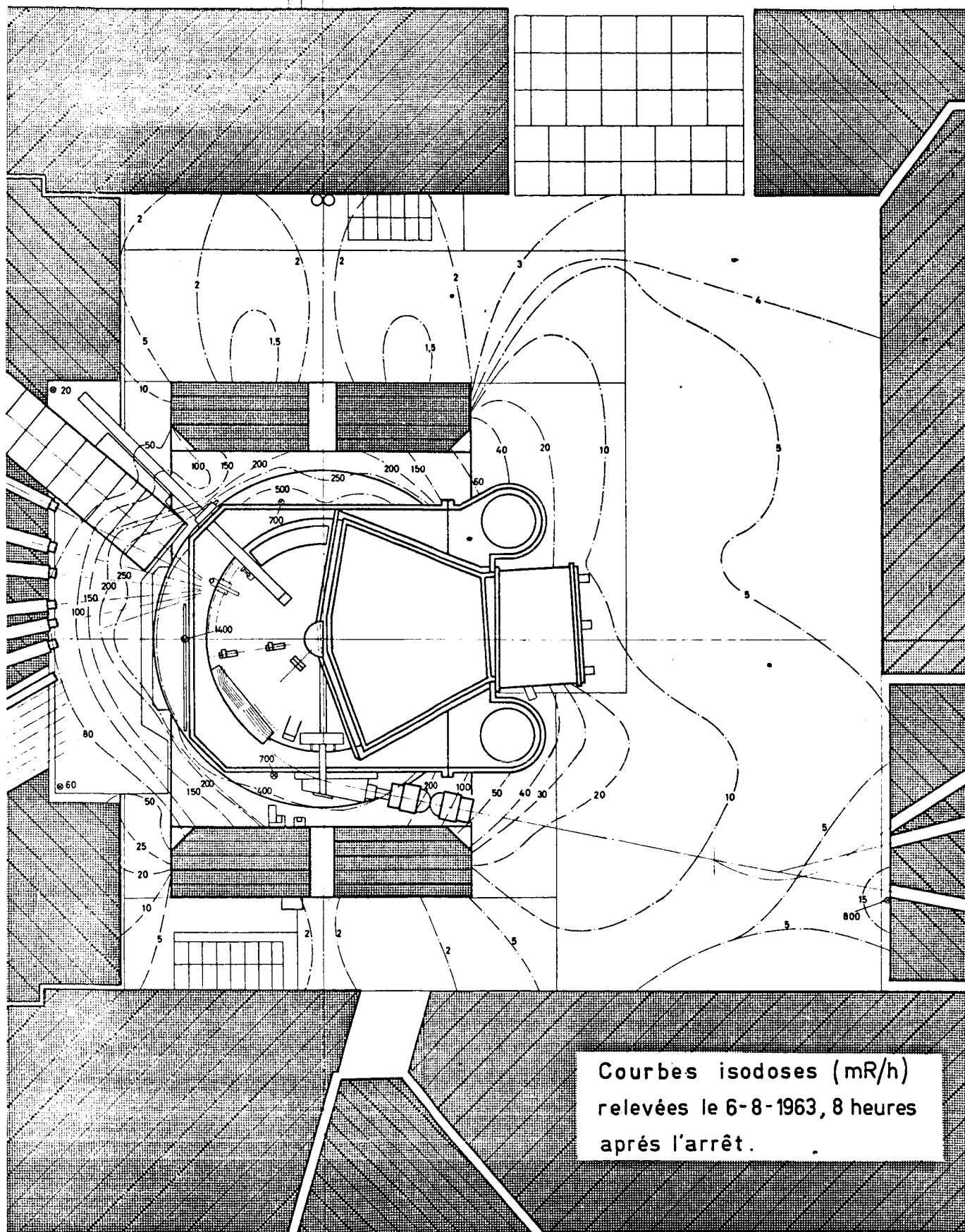
Concluding Remarks

New cyclotrons should be built with distributed absorbers to cover the pole pieces.

One should, however, be cautious in placing absorbers in the tank of an existing cyclotron. One cannot easily distribute them. Concentrated absorbers in form of clippers can only be placed with ease in free regions outside the dees. They will accumulate the activity in localized hot spots near the region where access is necessary. In each case a careful calculation of the expected gamma radiation field would be required.



Répartition de la radioactivité à l'intérieur du tank
en Rem/h, 17 jours après l'arrêt, le 9-1-1963.



PRELIMINARY INVESTIGATION OF FACTORS AFFECTING EXTERNAL
BEAMS FROM THE CERN SYNCHRO-CYCLOTRON

L. Dick, L. di Lella, L. Feuvrais and M. Spighel, CERN

(Presented by L. Dick)

The object of this study is to investigate the influence of different factors influencing the intensity and quality of external beams. Although the measurements are not complete, they allow us to estimate the importance of certain elements with regard to the pion beam intensity. The results reported here were obtained with positive pion beams of 100 and 70 MeV and with the extracted proton beam.

The layout of meson beams used is indicated in Fig. 1 which shows two of the several simultaneous beams available. The pion energies indicated correspond to a target position at 10° azimuth and 224 cm radius. A number of simultaneous beams may also be obtained from a target position around 40° .

The following measurements were carried out :

- a) Beam intensity as a function of the diameter of the pipe in the shielding wall - with and without lens in front of the pipe.
- b) Intensity distribution within the beam and its symmetry with regard to the median plane.
- c) Influence of the thickness of the pion extraction window.
- d) Loss caused by scattering in air.
- e) Extracted proton beam.

The position of the production target (224 cm, 10°) is optimal for the two pion beams in question (70 and 100 MeV), and measurements are performed

taking each of these beams as monitor for the other. This arrangement allows one to vary the different parameters used in pion transport on one of the beams, while at the same time registering the intensity of pions produced in the target by means of the other.

a) Intensity as a Function of the Shielding Wall Pipe Diameter

The principle of this measurement is to decrease in steps the internal diameter of this pipe, which acts as a collimator. The results are given both in linear and log-log scales in Fig. 2 and 3, with and without lenses at the entrance of the pipe.

The increase in intensity is proportional to D^x , where D is the diameter, and x should theoretically equal 5 (2 for solid angle, 2 for the surface of the collimator, and 1 for the momentum band), if the source were large and there were no focusing. If, conversely, the source were small and the focusing perfect, we would expect to find $x = 3$. From the Fig. 2 and 3 we may deduce the value of $x \approx 3.3$ for both the beams. The observed value may be ascribed to the fact that the source is of finite size and that the focusing is different in the horizontal and vertical directions.

Up to the maximal diameter of the pipe (14 cm) no deviation from the 3.3 - law occurs. At present further limitation is given by the aperture of the quadrupole lenses which is 20 cm, but the relative increase in intensity that might be expected for pipes with diameters of 20 and 25 cm by comparison with the present 14 cm pipe are $(20/14)^{3.3} = 3.2$ and $(25/14)^{3.3} = 6.8$ respectively.

Furthermore, the present beam optics is capable of transmitting the momentum bands corresponding to the increased diameters of 20 or 25 cm.

b) The Intensity Distribution within the Beam

This was studied by using two 30 cm thick collimators of aperture 4 cm

placed symmetrically at both ends of the pipe in the five characteristic positions illustrated in Fig. 4.

Without lens at the entrance to the 100 MeV beam pipe, the intensity of this beam is the same for the horizontal positions 1, 2 and 4, and shows a 20 to 30% decrease for the vertically displaced positions 3 and 5.

With the preceding lenses optimized for the intensity corresponding to the maximal pipe aperture, the distribution is practically uniform for positions 1, 2, 3 and 4, but shows a decrease of 65% for the lower position 5. This indicates an asymmetry relative to the median plane of one or several elements effecting the beam transport.

For the 70 MeV beam the same measurements were made and led to a similar conclusion. To correct the asymmetry of the beam relative to the median plane, a horizontal magnetic field was placed at the outlet of the machine. With this a total increase in intensity of 34% was achieved.

c) The Influence of the Thickness of the Pion Extraction Window

To determine the loss of intensity due to multiple scattering in the 3 mm aluminium foil which constitutes the pion extraction window on the CERN SC, we increased its thickness by adding 1, 2 and 3 mm aluminium foils intercepting the beam. As illustrated on Fig. 5 the intensity is a linear function of the square root of the total thickness in the range observed. If one is allowed to extrapolate this law to windows much thinner than 3mm, the maximum possible gain in intensity would be of the order of 70%. With a 0.7 mm thick window, which seems reasonable from the point of view of mechanical resistance, the increase would be 50%.

This measurement was made on the 70 MeV (155 MeV/c) pion beam. The loss caused by multiple scattering will be smaller for more energetic beams, but the gain will exceed 30% for all energies below 300 MeV. The gain obtained

by decreasing the window thickness will be relatively less for bigger pipe apertures.

d) The Loss Caused by Scattering in Air

A preliminary test on the effect of the presence of air along the path of the 70 MeV beam was made by extending the vacuum pipe in the shielding wall by 2 m towards the machine. Measurements performed with and without air in this pipe show a 26% difference in intensity. Only about half the total beam path was in vacuum in this experiment. If the vacuum were extended all the way from the extraction window to the position of the experiments, the gain would be of the order of 40%. For beams of energy above 100 MeV the corresponding gain would probably be 20 to 30%.

Concerning the sections c) and d) which deal mainly with multiple scattering, it must be mentioned that apart from yielding higher intensities, the elimination of scattering also improves the quality of the image by diminishing the blurring of the beam edges.

e) External Proton Beam

A series of experiments with the external proton beam have shown that it is necessary to reconstruct it from the mechanical as well as from the optical point of view. Its direction and size are considerably affected by the optimal position of the regenerator and of the magnetic channel for a given magnetic field in the machine.

The dimensions of the beam image at the exit window are small and should permit a decrease of window diameter from 14 to 5 cm. In this way a minimal window thickness can be maintained without the risk of tearing.

The external proton beam, just as the pion beams, does not lie exactly in the median plane. To direct it into the horizontal plane of the transport system, two small steering magnets will be placed after the first pair of quadrupoles. A further magnet might be placed in front of them.

Fig. 6 shows the principal elements which we propose to install for the proton beam transport.

Despite the mechanical and optical imperfections we extracted a $5 \cdot 10^{11}$ proton/sec beam and focused it to an image of a 2 cm diameter.

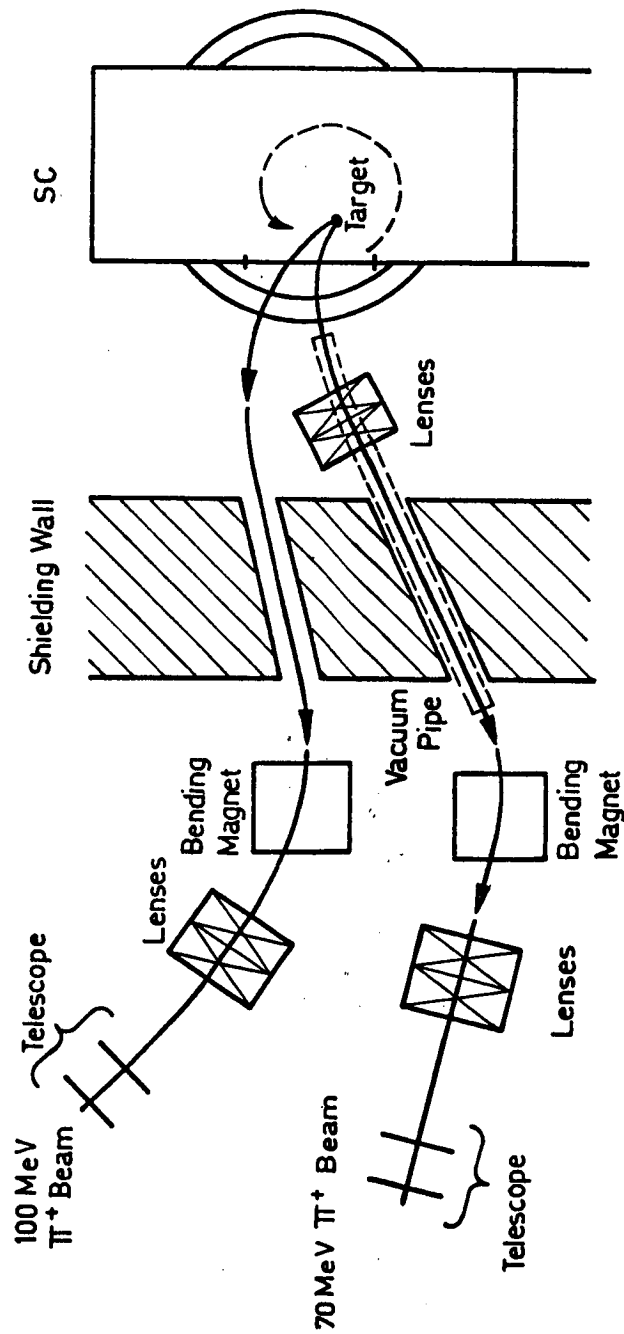
Conclusion Relating to Pion Beams

The experiments described here show that one may obtain a substantial increase in intensity and improvement of the beam quality by relatively simple modifications to those elements that restrict or hamper the secondary beam transport. The main alterations consist in widening the shielding wall pipes to a diameter of 25 cm, and decreasing the thickness and possibly the size of the extraction window. By allowing the beam to run in vacuum and by placing magnets giving a horizontal magnetic field to compensate the vertical asymmetry of the beams, important improvements may be achieved without necessitating costly modifications.

The total increase in intensity which might be expected by carrying out the above alterations would be by a factor of about 5 for a 20 cm shielding wall opening, and by a factor of about 10 for an opening of 25 cm.

For certain experiments where low background is important, it will always be possible to reduce the pipe diameters again by the introduction of thick collimators.

These measurements must be regarded as preliminary. They will be pursued, also taking into account negative pion beams of energies up to 200 MeV. Furthermore, in order to reduce the extraction window dimensions, the exact beam positions at this point must be determined. Finally, a more detailed study of the vertical beam asymmetry will be performed in order to determine the best shape of aperture for the pipes.

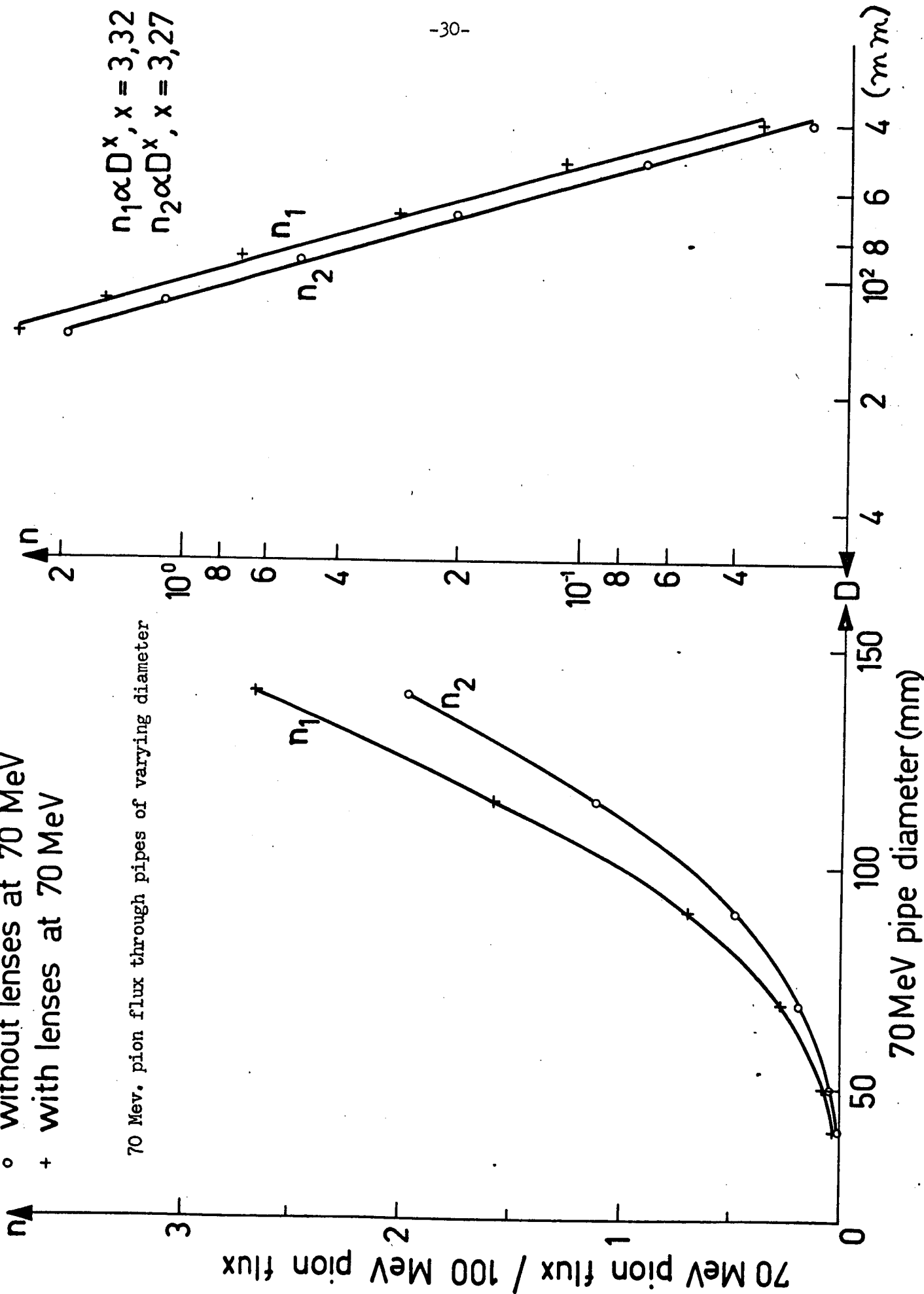


Meson beam layout

FIG.1

° without lenses at 70 MeV
+ with lenses at 70 MeV

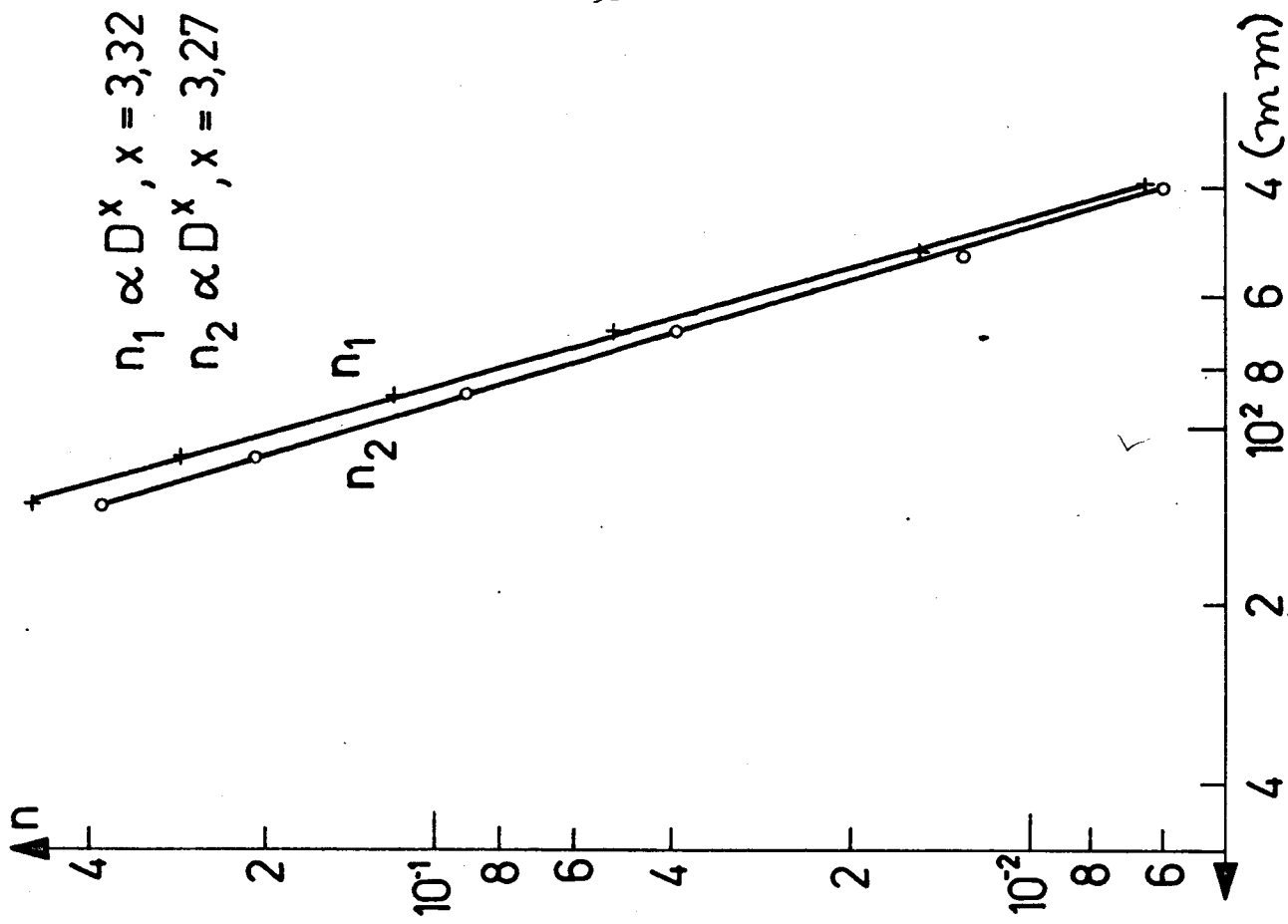
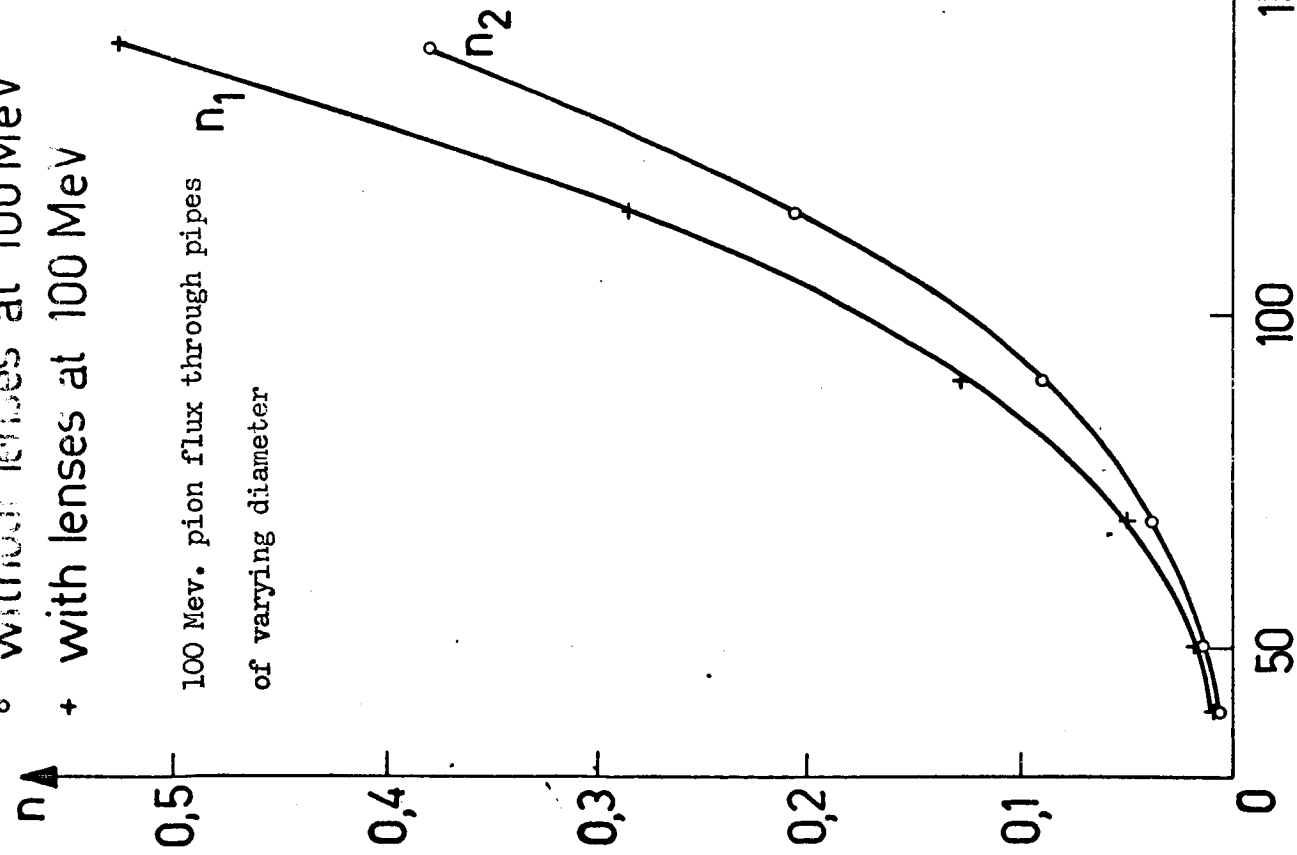
70 MeV. pion flux through pipes of varying diameter



° without lenses at 100 MeV
 + with lenses at 100 MeV

100 MeV pion flux / 70 MeV pion flux

100 MeV. pion flux through pipes
of varying diameter



$n_1 \propto D^x, x = 3,32$
 $n_2 \propto D^x, x = 3,27$

100 MeV pipe diameter (mm)

FIG. 3

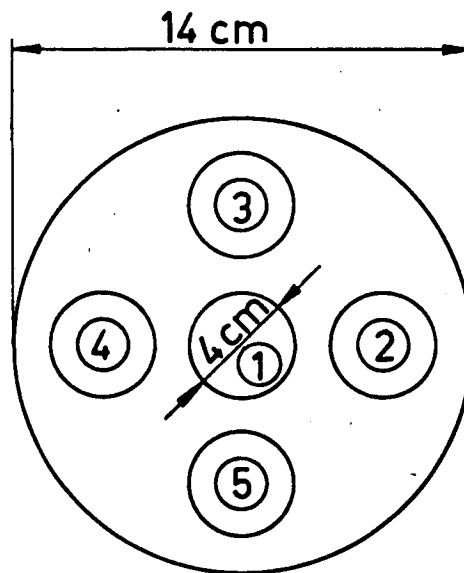
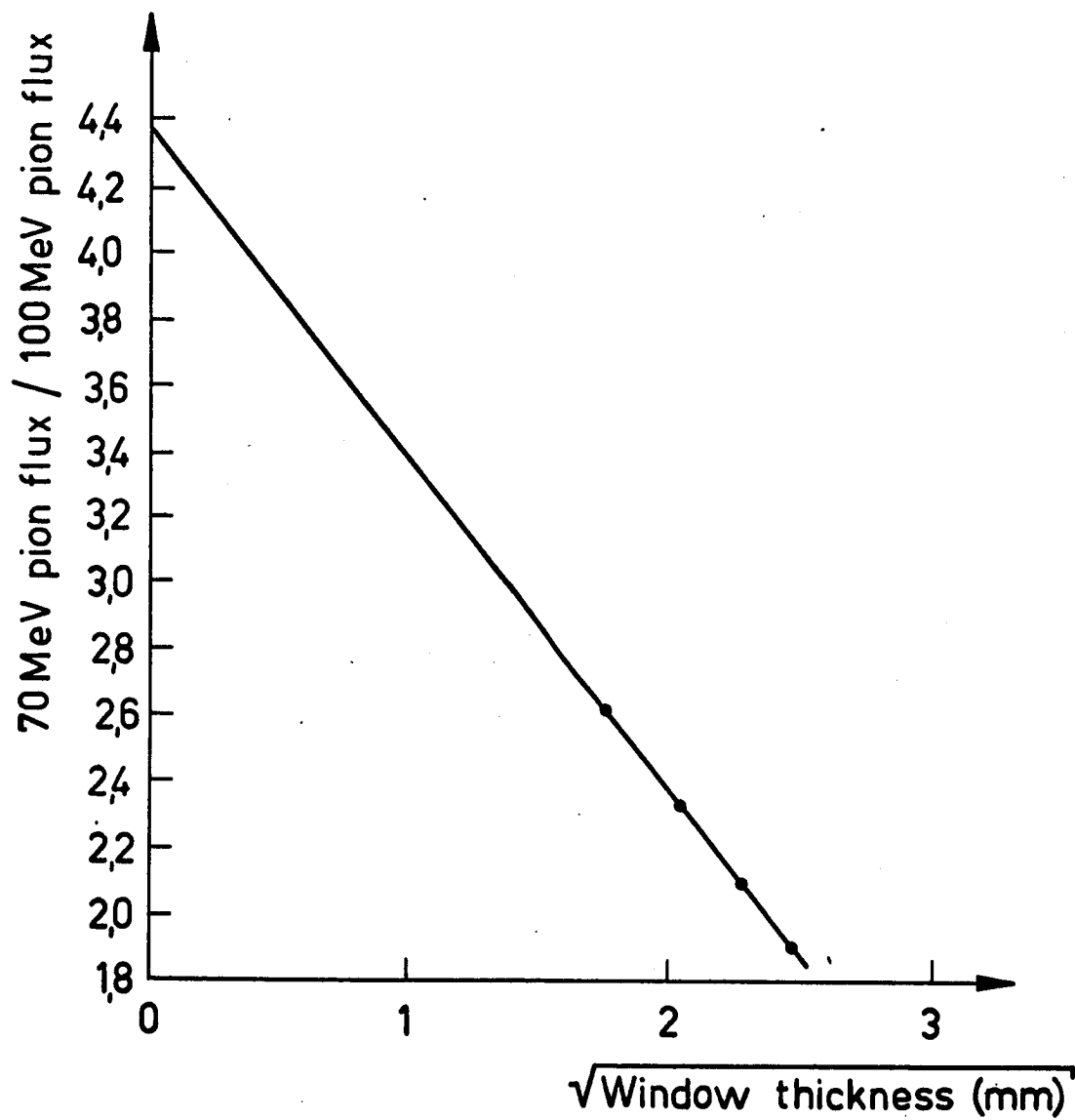


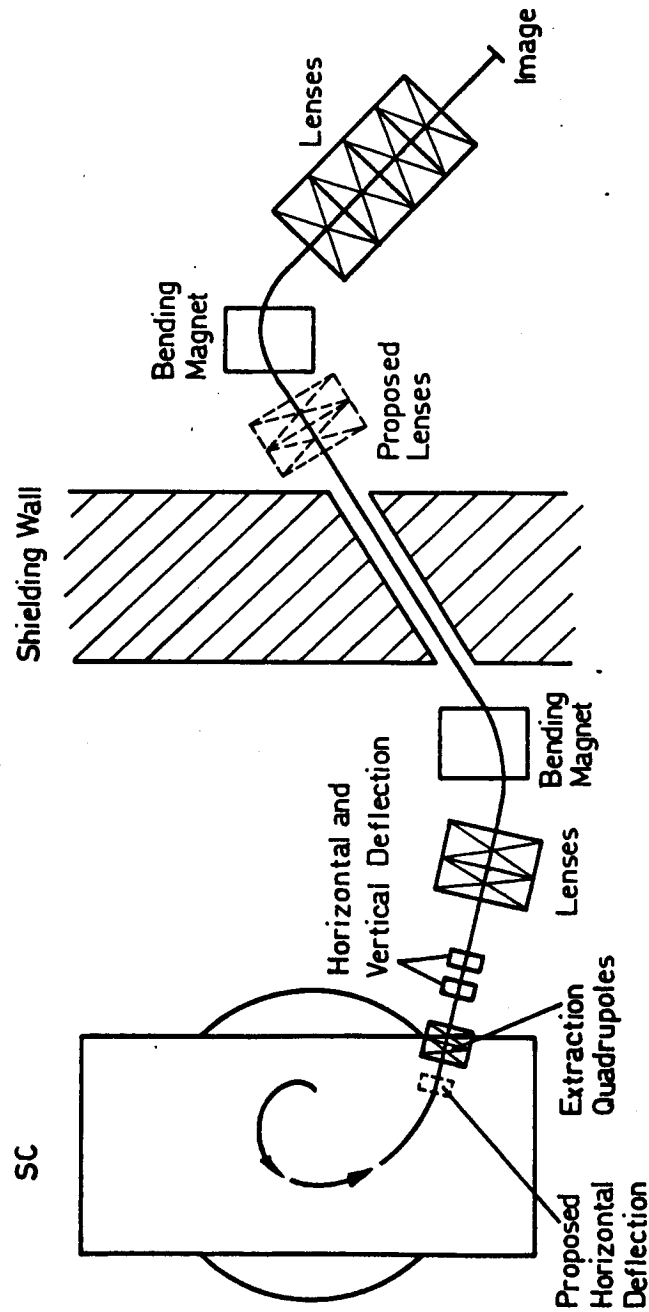
FIG.4

Characteristic positions of collimators to measure pion
intensity distribution



Pion flux measurement made by varying cyclotron
window thickness

FIG. 5



Proton beam transport system

FIG. 6

THREE YEARS OF DEVELOPMENT AT THE CERN SYNCHRO-CYCLOTRON

P. Lapostolle, CERN

During the last three years several developments have been made on the CERN 600 MeV Synchro-cyclotron. Since none of them involved any major change in the machine, in most cases no special report was issued about them until now. Nevertheless, considering Fig. 1 which shows the increase in internal intensity during the period under review, it appears that the sum of these small changes has eventually led to a current 5 to 6 times greater than before. So it does seem worthwhile to report about this work even if in several instances the results are not yet fully understood; and it seems even more appropriate at a time when a more systematic approach has been prepared and when a more fundamental new development programme is being undertaken.

Two main objects have been aimed at : an increase in intensity and an improvement of the machine performance for physics experiments.

We shall restrict ourselves in this description to what has been effectively achieved until now; in this respect we shall speak about the use of :-

- 1) Admixture of argon to the ion source gas.
 - 2) Central auxiliary Dee.
 - 3) RF amplitude modulation.
 - 4) Increased magnetic field.
 - 5) Vibrating target.
 - 6) "Stochastic Cee" acceleration.
- 1) Admixture of argon to the ion source gas.

Until 1961 the SC source was fed with hydrogen mixed with helium in a

similar way to that used in other machines. The source is a cold-cathode Penning source developed by R. Keller and L. Dick and its shape is shown in Fig. 2.

Information received at that time from the 150 MeV Orsay Synchro-cyclotron indicated that the presence of trichlorethylene in the source plasma could lead to an appreciable increase in accelerated proton intensity.

The introduction of C_2HCl_3 in a synchro-cyclotron is of course not very attractive from the vacuum or chemical points of view. But this information gave the idea of trying a heavier inert gas. Argon was suggested.

Since a mixture of gas was already in use, it was easy to replace the helium by argon. Tests were performed by B. Hedin. The best available data for maximal internal beam current are as follows:

Argon flow	$7 \cdot 10^{-3}$ Torr	1/sec = 15	$\mu g/sec$
Hydrogen flow	$15 \cdot 10^{-3}$ Torr	1/sec = 1.7	"
Leakage flow	$14 \cdot 10^{-3}$ Torr	1/sec = 22	"
Total	$36 \cdot 10^{-3}$ Torr	1/sec = 39	$\mu g/sec$

The readings were found from the pressure rise measured by an ionization gauge, corrected for the response for different gases (Dushman: The Scientific Foundations of Vacuum Technique, N. Y. 1949, p. 350). The indicated pressure in the tank was in the range of 10^{-6} Torr with two pumps running (2×12000 l/sec).

If the valve setting is optimized for the extracted proton beam a different adjustment with less argon is found. This seems to indicate that the argon decreases the vertical oscillations but increases the radial oscillations.

The physical process by which the argon increases the beam is not fully understood. Nevertheless the beam intensity was increased from about $0.3 \mu A$ mean current to about $0.55 \mu A$.

The argon has been used since 1961. The adjustment of gas flow is not very critical and it has been found that the source is slightly more stable with argon than it was with helium.

2) Central Auxiliary Dee.

Previous papers ¹⁾ have already reported about the work done at CERN by R. Keller, L. Dick et al. on stochastic acceleration.

The original idea at the CERN Synchro-cyclotron was to achieve stochastic acceleration up to a certain low energy in the centre of the machine by an auxiliary Dee, illustrated in Fig. 2; the beam was then to be stacked and subsequently taken by the main programme up to full energy.

Although the preliminary tests led to an increase in overall intensity by a factor of about 2, the complexity of the installations was such that it did not seem worth while using it on an operational basis.

Nevertheless a closer look at the results showed that apart from the RF voltage on the stochastic Dee, its DC bias also had some influence. At first sight this DC voltage would seem of little importance except perhaps that it controls some asymmetry in the orbits.

We then tried the effect of a pure DC bias on the auxiliary Dee with a proper RF decoupling introduced.

The tests were performed by L. Dick. It was possible to increase the intensity by about 50% with a DC voltage on the auxiliary Dee of the same sign and almost as high as the bias used on the main Dee.

Since then the internal intensity in the SC has been above 0.80 μ A.

It is probable that the auxiliary Dee modifies the vertical electrostatic focusing in the region of the machine where no magnetic focusing exists. This focusing improves the orbit stability and hence the trapping. It is clear, as

will be said later, that there is no reason for the present geometry being optimal, and it should probably be possible to gain even more^{*)}. But it seems necessary to develop a more systematic study of the electrostatic focusing before starting on an extensive series of tests on the machine.

An unexpected advantage of the auxiliary Dee is that it permits a very sensitive control of the intensity of the circulating beam by varying its bias voltage. This method is both cleaner and more reproducible than the use of the "beam chopper" which is normally employed, and its effects on beam quality seem to be less.

A reduction of beam intensity to about 1/10 of its maximum value may be achieved by applying a bias whose polarity is the opposite of that of the main Dee.

The biased auxiliary Dee has been in use on the CERN SC since 1961.

3) RF amplitude modulation.

While the stochastic acceleration was tried at CERN a different central stacking device, of pure cyclotron type, was studied in AERE, Harwell, by Lawson ³⁾ and eventually a proposal was made by Russell ⁴⁾ for increasing the beam output from the Harwell 110 inch SC.

In the latter scheme an auxiliary Dee is used in the central region of the machine with an RF voltage opposite the phase to that of the main Dee in order to increase the accelerating electric field at the beginning of the acceleration cycle, where current limitation is likely to occur.

The RF system of the CERN SC has been described in an early report ⁵⁾. As shown in Fig. 3, the accelerating voltage was changing during the cycle

^{*)} Tests done on the Dubna phasotron indicate a greater improvement ²⁾.

starting from about 5 kV at the beginning and rising up to 25 kV at the end. This variation is due to the type of circuit used, which itself has been chosen in connection with the tuning fork type modulating device.

Due to resonances in the decoupling condensers - mainly in the stub-condenser - there were initially in the RF programme many dips causing beam losses. A new stub-condenser was constructed and gave full satisfaction. A third version for higher acceleration voltages is now going into production; a prototype is shown in Fig. 4.

However, at the frequencies where the stable phase angle is small, the beam loading caused a drop in the RF voltage. An overall rise in the RF voltage turned out to be impossible due to oscillator feedback trouble and sparking difficulties. It was therefore decided to build a plate voltage modulator for the oscillator valve, which would allow the RF amplitude modulation to follow an externally imposed programme.

But before such an installation was ready tests were performed to check the possibilities of improvement. During these tests the RF oscillator was stopped early during the cycle, at a time when the voltage had not yet risen very much; under these circumstances it was possible to use much higher values than in normal operation.

Tests were made by B. Hedin and H. Beger in the middle of 1962. In practice, not only the initial voltage but also the initial rate of change of frequency seems to be an important parameter. The latter can be adjusted by a change in frequency modulation obtained by varying the amplitude of the vibrating fork or, more easily, by an equivalent change in magnetic field. The results are shown in Fig. 5^{*)}, where current, as measured by a

^{*)} It was very interesting to learn during the 1963 Dubna conference about a similar study made on the Dubna phasotron²⁾. The use of a rotating condenser instead of a vibrating fork made a much more appreciable improvement possible.

thermocouple at a radius of 110 cm (corresponding to about 200 MeV), is plotted versus the rate of change of initial frequency.

It is clearly seen that, in contradiction to what would have been expected, the greatest intensity was not obtained with the maximum accelerating voltage but rather at an intermediate value. Nevertheless, as has been mentioned, a reduction of the voltage during the whole cycle causes losses before the end of acceleration, and with the existing voltage distribution the optimal voltage for the full energy beam did not correspond to the optimum for trapping.

An amplitude modulator was therefore still thought to be useful in order to reduce the voltage at the beginning of the cycle and to keep it as high as possible near the end, where the beam is otherwise lost.

The first tests of the modulator were made at the end of 1962 by H. Beger and A. de Groot. The intensity improvement was about 40% using a linear sweep on the anode voltage as shown in Fig. 6. Other shapes of modulation could be considered which might lead to a slightly higher increase.

The modulator has been in continuous operation during the course of 1963.

With the amplitude modulator available we produced at CERN an effect analogous to that initially proposed by Lawson and Russell at Harwell as mentioned earlier. To increase the efficiency of extraction the RF amplitude applied to a main Dee was pulsed to a higher value during the ignition time of the ion source. However, we did not observe an increase of beam. In view of the existence of a comparatively low optimal starting voltage this result is probably not surprising.

4) Increased magnetic field.

It has already been mentioned in the previous paragraph that particles can be lost during acceleration due to insufficient voltage. Furthermore,

there is in practice a difficult point to cross because of the excitation of a transversal harmonic mode of oscillation; we shall come back to this point in the last part of this report.

But apart from losses due to RF, some particles are always lost for lack of sufficient vertical focusing. Furthermore, in case of operation with internal targets, the number of multiple transversals is greatly sensitive to the efficiency of the vertical focusing and even when the accelerated beam is extracted, the extraction efficiency might depend on it.

The vertical focusing is directly related to the index n of the magnetic field; thus it is sensitive to the radial gradient of this field.

When the SC magnet current is increased above the value of 1700 A normally used until 1962, saturation effects are such that the field increases more on the axis than near the edges; this leads to an increase in n .

Accurate measurements of the field were performed by E. Braunerstreuter and M. van Gulik in the middle of 1962⁶⁾. Fig. 7 shows the variations of the field index n derived from these measurements versus radius for different values of the current.

From these results, one can therefore expect an increased yield of secondary particles and perhaps also of high energy protons if a higher magnetic field is used.

The use of a higher field requires a different frequency range for the RF programme. Since the field increases more on the axis than near the edges, the starting high frequency must be increased more than the final low frequency. Such a change required an extension of the RF oscillator circuit.

These modifications and tests on the machine with a higher field were carried out by H. Beger in the course of 1962⁷⁾. Some results are shown in Fig. 8 which indicate an increase in thermocouple reading at 210 cm of

almost 50% and in pion intensity of more than 60%. The decrease in intensity at higher currents seems to be due to a reduction of the internal proton beam in the central region (caused perhaps by a modification of the magnetic bump which is used there). This point has to be examined in more detail.

The operation with higher magnetic field has been currently used since the end of 1962.

5) Vibrating target.

Apart from questions of intensity it is very important for physics experiments to be performed on the machine, that the distribution of the particles in time is suitable. In normal operation of a SC protons are accelerated in bursts of about 200 μ sec duration at 18 msec intervals, but for most of the experiments one should prefer a continuous output.

The vibrating target is one of the devices invented to improve the time distribution of secondary particles from an internal target; it was first installed in the Columbia Machine and described by J. Rosen⁸⁾.

The principle is to stop the acceleration of the particles at a certain radius in order to get a coasting beam and move the target progressively into it at each cycle. In this way, with a target vibrating at the repetition rate of the frequency programme (54 cycles per second) the relative motion of the beam versus the target is much slower than in the case when the beam at the end of the normal programme is accelerated into a fixed target. A detailed description of this work has been already given in a report ⁹⁾ by B. Hedin who also designed the CERN target.

With this target it is possible to produce most of the secondary particles with a duty factor between 25% and 50%. At suitably chosen target positions up to 90% of the short burst intensity is obtained in the long pulse.

The vibrating target offers other interesting possibilities. By programming the RF so that the acceleration is stopped at the radius of the vibrating target only at alternate cycles, beam sharing between two internal targets may be effected. A further development initiated by C. Rubbia is the "Jumping Target" which is pulsed into the beam for a chosen fraction of the time and which has been found suitable for bubble chamber operation in parallel with other experiments. In conjunction with the stochastic extraction system to be described below the jumping target also is extensively used for beam sharing between counter experiments.

6) "Stochastic Cee" acceleration.

Another method to improve the duty cycle of a synchro-cyclotron had been suggested by R. Keller ¹⁾ and tried at that time on the Orsay machine ¹⁰⁾ according to indications given by R. Keller and L. Dick.

As with the vibrating target the main accelerating programme is stopped before the final energy is reached; but in the present system the beam is then slowly accelerated by an auxiliary Cee electrode fed with a special frequency programme.

This device has been developed and tested at CERN by L. Dick, Y. Dupuis and J. Vermeulen in 1961. A 40° Cee between the radii 205 and 230 cm is used. It is fed by a transmitter with a DC input of 13.5 kW giving a 500 c/s saw-tooth frequency programme between 17.3 and 16.8 Mc/s at a peak voltage of about 2.5 kV. The frequency programme is not phase synchronized with the main RF programme ^{*)}, thus a certain fraction of the protons is decelerated and thereby lost. The efficiency is around 50%; but the duty cycle can be

^{*)} A system with an auxiliary slow frequency programme phase locked to the main one has been developed in Berkeley by K. Crowe, and similar systems are now used elsewhere ¹¹⁾.

made slightly larger than 50%. To achieve this it is important that the main RF programme is cut off very sharply. Otherwise an intense burst is produced by the main programme.

This system is at present used for operation with internal targets. It should function as well for the extracted beam; however, the frequency range which has to be covered by the auxiliary programme must then be adjusted differently.

The installation used at present is still a provisional one which had been made for testing purposes (and in practice the one which had been used by R. Keller and L. Dick for the study of stochastic acceleration). It does not allow an easy change from internal target to extracted beam operation. New operational equipment is under construction and will be installed early in 1964¹²⁾.

7) Conclusions and future plans.

In four parts of this report reference has been made to improvements that give an increase in intensity. The question that now arises is "what is still to be done?".

Although parts of the CERN improvement programme will be described in more detail in other reports to be presented at this conference, several points are worth mentioning here:

a) Parasitic resonance on the Dee. As already stated in part 4) a certain fraction of the beam is lost during acceleration. Apart from the approach to the $n = 0.2$ coupling resonance at the end of the cycle, there is an appreciable loss occurring at a radius of about 2 metres. It has been possible to establish that this loss was due to the existence of a transverse mode of oscillation on the Dee, excited on the second harmonic by the beam. The amplitude of this harmonic mode depends on the beam intensity and would tend to limit it at higher values.

The various modes of oscillation have now been extensively studied ¹³⁾ showing that a new Dee must be built in order to prevent the loss. This work will be started in 1964.

b) Central region. Many important aspects of a high energy synchro-cyclotron depend strongly on the conditions achieved in the source region of the machine. This is true for the internal beam intensity, but also for its quality, which in turn reflects on a successful extraction both of the primary and of the secondary beams. The CERN synchro-cyclotron beam is clearly intensity-limited in the acceptance from the source, and is furthermore encumbered with rather violent radial betatron oscillations.

The mechanism responsible for these limitations in our accelerator is not clearly understood. Presumably there is room for wide improvements in this region, and we have therefore decided to initiate a careful study of the phenomena involved. However, to avoid difficulties arising from the heavy experimental load on the CERN SC, from the fact that this machine is by now highly radioactive, and from the rather limited possibilities for varying the parameters involved, we have chosen to perform the source region investigation by means of a specially designed model cyclotron. This model is presently under construction and will be ready for experimentation by end of 1964.

The model comprises a 30 ton, 800 kVA magnet giving a field of 18 kGauss in a 840 mm diameter, 200 mm gap. The RF system is governed by separate amplitude and frequency function generators. The final amplifier is a 40 kW grounded grid type with a frequency band of 26 to 28 Mc/s. The maximum Dee voltage will be about 7 kV peak.

c) Activation. With the present intensity (1.6μ A) in the CERN synchro-cyclotron the level of radioactivity in and around the machine when it

is stopped is already rather high ¹⁴⁾. This problem of activation is now acknowledged to be a serious limitation for high intensity machines, and a thorough investigation is being made for the CERN SC by M. Barbier ¹⁵⁾.

It is clear that important changes involving rather general use of remote controlled gear must be introduced before very large intensities can be tolerated from the point of view of radiation safety during servicing.

If one intends to restrict oneself to a limited number of modifications, the internal intensity should probably not exceed say 10 μ A.

d) Extraction. If the internal beam of the machine has to be limited on account of activation a greater extraction efficiency can offer advantages. At present the pion beams obtainable from internal and external targets are of about the same order. An increase of extraction efficiency will increase the external pion yield without leading to greater machine activation. In fact, its effects will be less serious since the need of servicing internal targets is eliminated, or conversely, somewhat larger internal beams may become permissible. As a final aim one may hope for extraction efficiencies which will sensibly reduce the fraction of particles lost inside the machine.

In practice this problem is not independent from the general study of the central region, as we mentioned already in paragraph b). Such a study may not only lead to a greater beam intensity, but should also yield internal beams of better quality which would facilitate extraction.

A new extraction system for the CERN SC is under development, and will be tested during the current year ¹⁶⁾.

e) Secondary beam optics. For the operation with internal targets the same argument as above leads to a study of secondary beam optics aiming at a better focusing of all the secondary particles produced.

Preliminary measurements ¹⁷⁾ with the present pipes in the shielding wall going to the experimental "neutron" hall show a possibility of increase in pion beam intensities by an appreciable factor by increasing the diameter of those pipes from 14 cm to 20 or 25 cm. These modifications are foreseen for 1964.

We are furthermore in the process of checking the experimental results with beam transport computations in order to optimize the focusing equipment. We are also studying pion production cross-sections experimentally and so hope to arrive at an overall optimization.

f) Polarized proton source. One should eventually mention that the polarized source which has been initiated by R. Keller, L. Dick and M. Fidecaro ¹⁸⁾ is now almost completed and should be installed on the synchro-cyclotron during 1964. When it comes into full operation it is going to constitute an important tool for physics and open a new field of experiments.

ACKNOWLEDGEMENTS.

The developments reported here are the outcome of work done by the whole of the CERN MSC Division.

Although only a few names are mentioned in the text - of those who took particular responsibilities in the work - in actual fact all MSC physicists, engineers and technicians contributed towards making the achievement of these results possible.

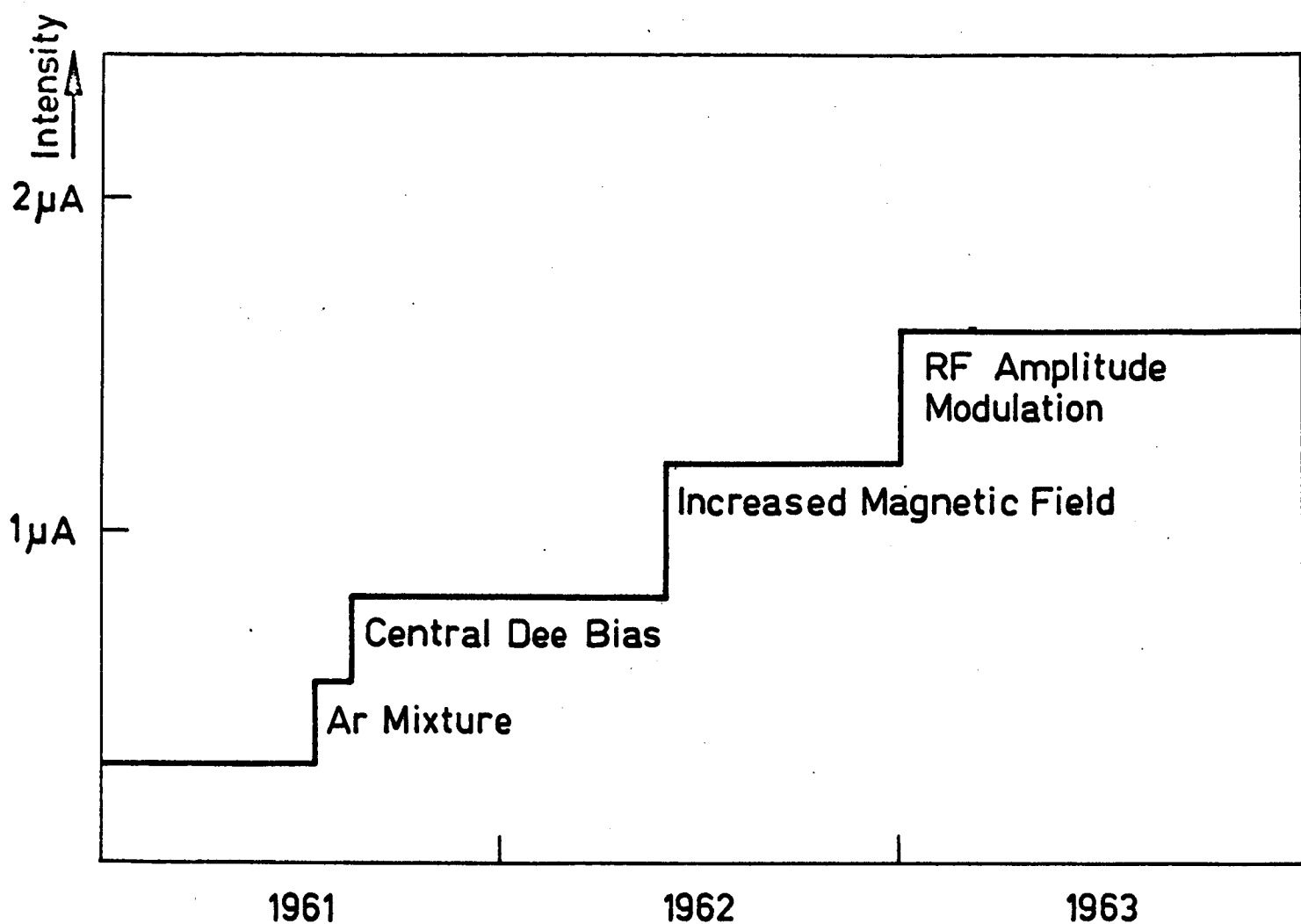
REFERENCES.

- 1) Beam storage with stochastic acceleration and improvement of a synchro-cyclotron beam, by R. Keller and K. H. Schmitter, CERN 58 - 13.
Acceleration Stochastique dans un cyclotron de 5 MeV, R. Keller, L. Dick and M. Fidecaro, CR. Acad. Sci. Paris 248, p. 3154-6, 1959.
Experiments on stochastic acceleration, by R. Keller, International Conference on High-Energy Accelerators, CERN 1959, p. 187.
Les essais d'acceleration stochastique dans le synchrocyclotron de 600 MeV et leur interpretation, par R. Keller, L. Dick et M. Fidecaro, CERN 60-43.
- 2) Increase of the internal beam current of the 680 MeV synchro-cyclotron of the Joint Institute for Nuclear Research (DUBNA), by V. I. Danilov et al, International Conference on Accelerators for charged particles DUBNA 1963.
- 3) On the possibility of increasing the output of a synchro-cyclotron by means of a central high voltage Dee, by J. D. Lawson - AERE Report M 542, 1959.
- 4) A proposal for increasing the beam output from a synchro-cyclotron, by F. M. Russell, Nature, Vol. 190, No. 4773 p. 335, April 22, 1961.
- 5) Synchro-cyclotron du CERN, II L'installation haute frequence, by K. H. Schmitter and S. Kortleven, Revue technique Philips, Tome 22, no. 5, p. 165, April, 1961.
- 6) Magnetic field measurement on the SC Magnet, by E. Braunersreuther and M. van Gulik, CERN, MSC internal report M 88, August, 1962.
- 7) The improvement of the internal beam intensity of the SC, by H. Beger, CERN, MSC internal report M 55, May, 1963.

- 8) Vibrating target for the improvement of synchro-cyclotron duty cycle, by J. Rosen, NEVIS - 92, 1960.
- 9) Longer Pulse length by a vibrating target in the CERN synchro-cyclotron, by B. Hedin, CERN 61-21.
- 10) Methodes permettant d'ameliore la structure en temps du faisceau externe du synchrocyclotron, by A. Cabrespine et al, Le Journal de Physique et le Radium, Tome 21, p. 332, May, 1960.
- 11) Peripheral Cee Beam Extractor for the Chicago 460 MeV Synchro-cyclotron, by E. H. Molthen, EFINS 63-50.
- 12) RF Broad-band amplifiers for driving reactive loads, by A. Fiebig, CERN Yellow report to be issued February, 1964.
- 13) Beamloss by a beam-induced cross-mode in the RF acceleration programme of the CERN 600 MeV Synchro-cyclotron, by H. Beger and A. Fiebig. Paper presented at this conference.
- 14) Shielding and activation of high-intensity cyclotrons, by J. P. Blaser, Ch. Perret, M. Barbier and J. Dutrannois, International Conference on Sector Focused cyclotrons and Meson Factories, CERN 63-19, April, 1963, p. 157.
- 15) Collection of data for spectroscopic analysis of induced activity, by M. Barbier and J. Dutrannois, CERN 62-22.
Some remarks on induced radioactivity, by M. Barbier. Paper presented at this conference.
- 16) Improvements to the CERN Synchro-cyclotron extraction system by M. Morpurgo. Paper presented at this conference.
- 17) Preliminary investigation of factors affecting external beams, by L. Dick, L. di Lella, L. Feuvrais and M. Spighel. Paper presented at this conference.

- 18) Une source de protons polarises. Etat actuel de la construction, by R. Keller, L. Dick and M. Fidecaro, CERN 60-2.

Characteristics of the CERN polarized proton source, by L. Dick, Ph. Levy and J. Vermeulen. International Conference on Sector Focused cyclotrons and Meson Factories. CERN 63-19, p. 127, April, 1963.



INTENSITY INCREASE
ON THE S.C.

FIG. 1

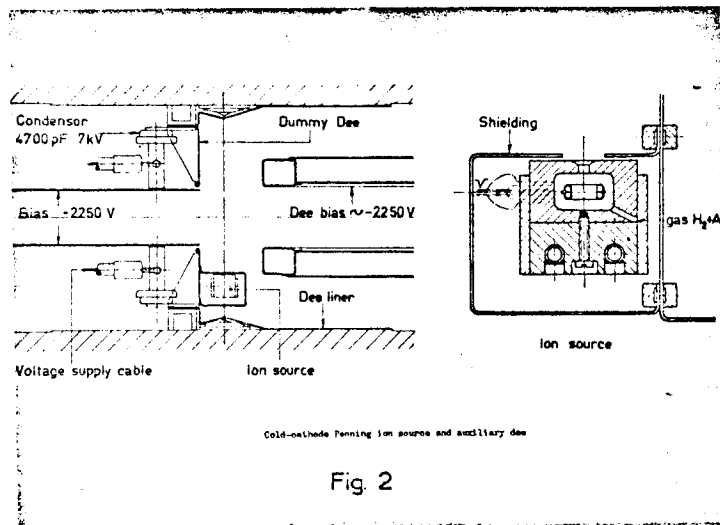
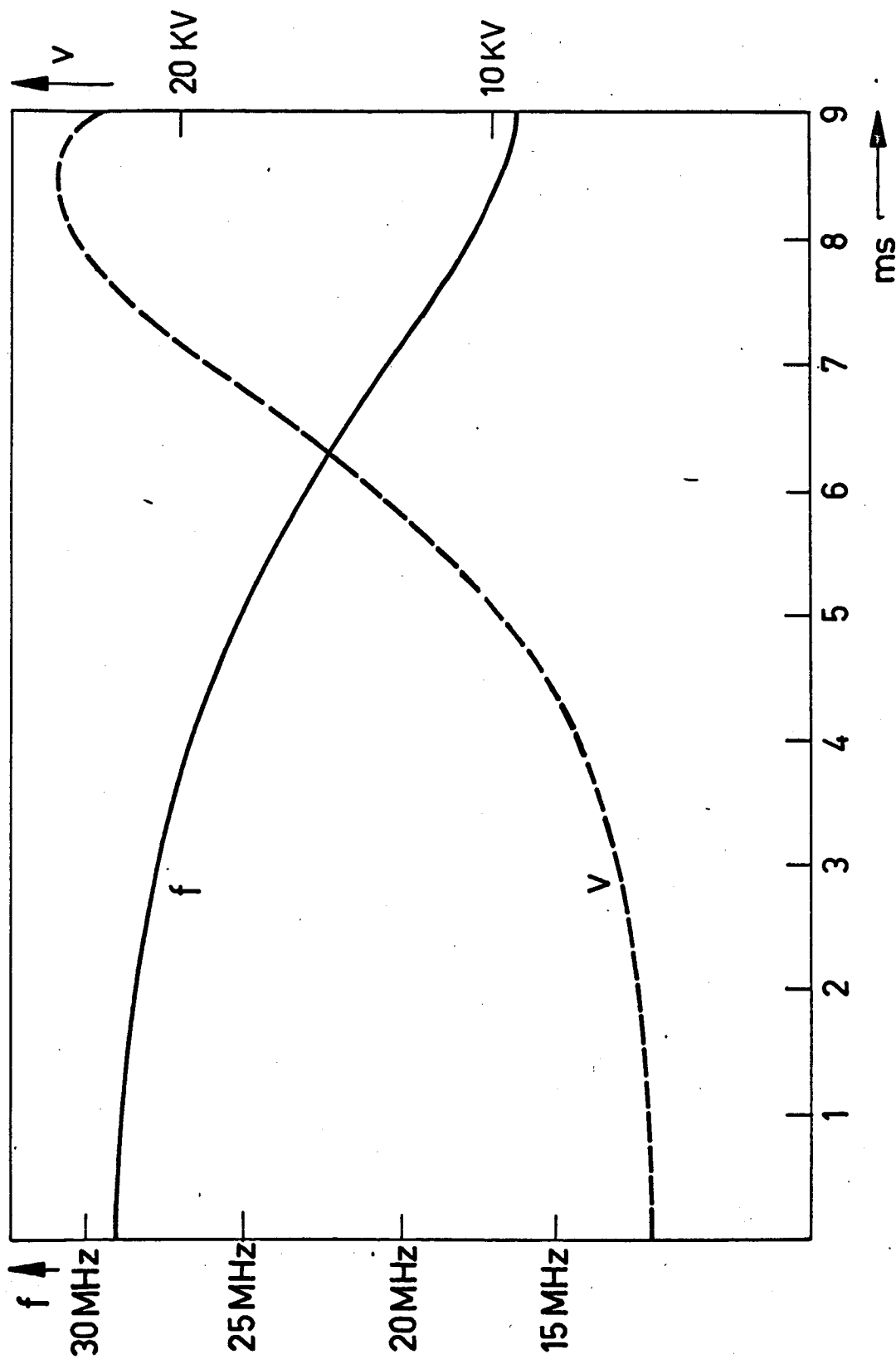


Fig. 2 Cold-cathode Penning ion source and
auxiliary dee.



FREQUENCY AND RF VOLTAGE OF THE DEE DURING THE NORMAL ACCELERATING CYCLE WITHOUT RF-AMPLITUDE MODULATOR.

FIG.3

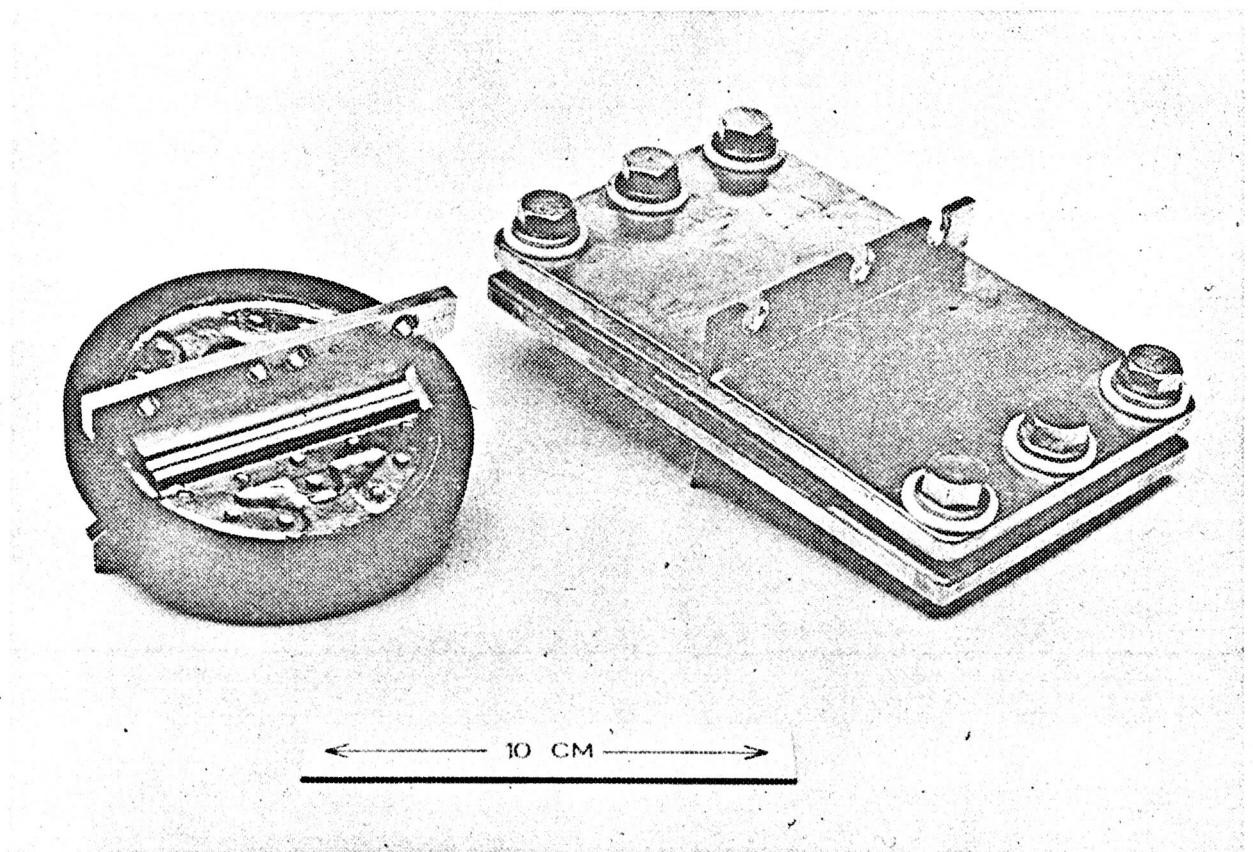
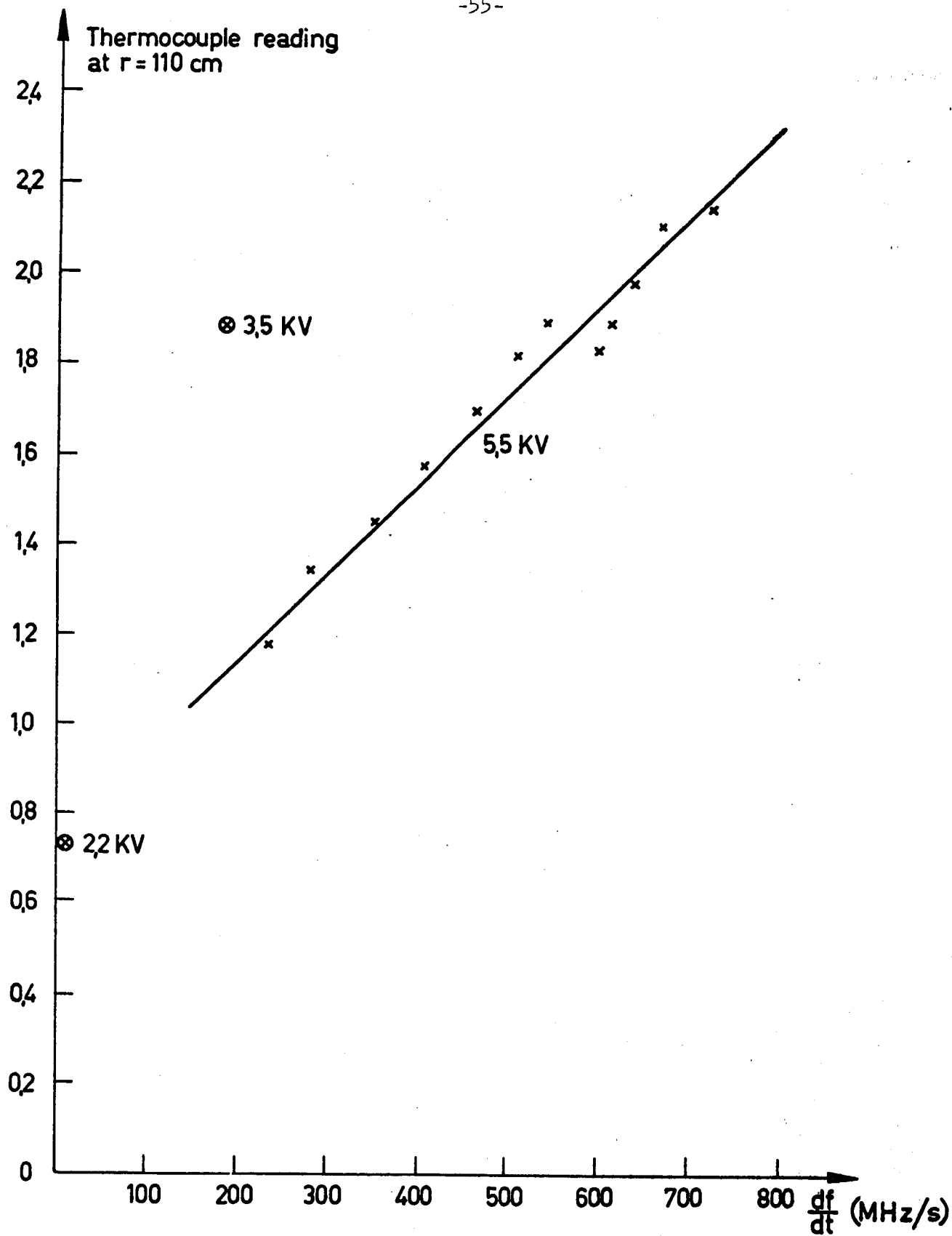
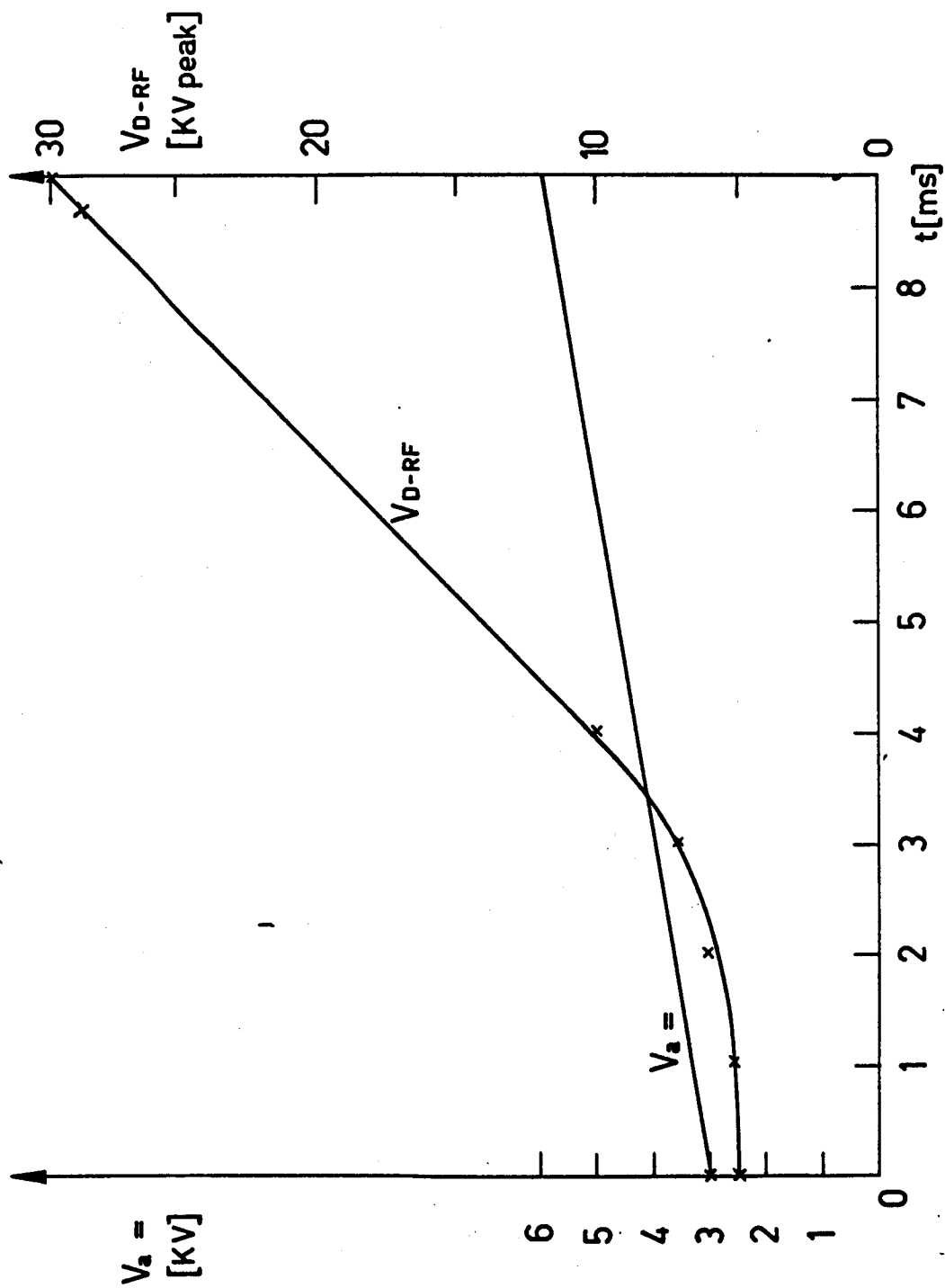


Figure 4
Prototype of high-voltage stub decoupling condenser

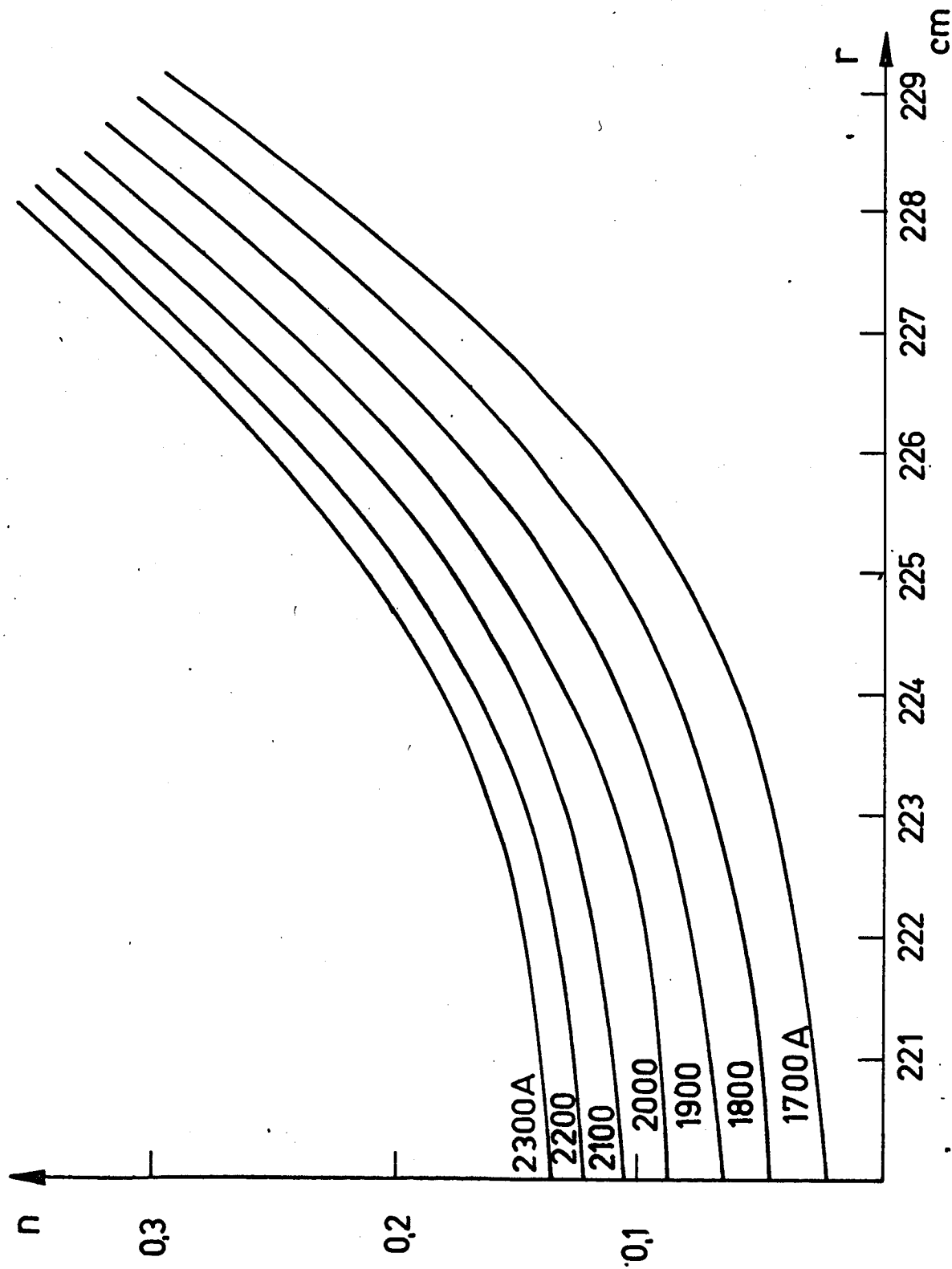


INTERNAL BEAM AS A FUNCTION OF RATE
OF CHANGE OF FREQUENCY AT THE
STARTING FREQUENCY



VARIATIONS OF THE ANODE VOLTAGE ON THE OSCILLATION AND OF THE RF VOLTAGE ON THE DEE, WITH THE MODULATOR

FIG. 6



FIELD INDEX OF THE S.C. MAGNET VERSUS
RADIUS. PARAMETER: MAGNET CURRENT

FIG. 7

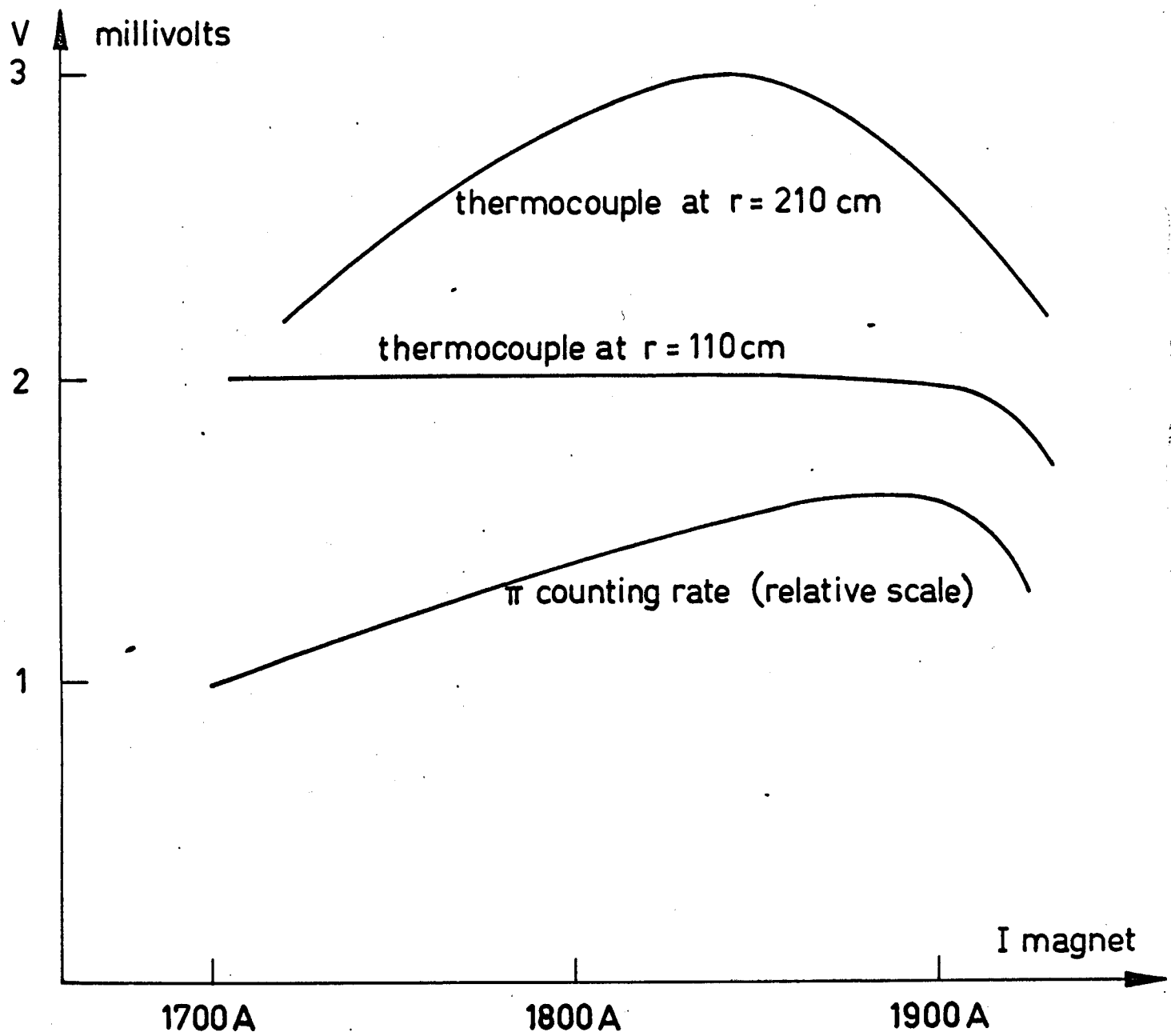


Figure 8 - Effect of the magnet current on pion yield.

IMPROVEMENTS TO THE CERN SYNCHRO-CYCLOTRON EXTRACTION SYSTEM

M. Morpurgo, CERN

The present regenerator and extraction channel developed for the CERN Synchro-cyclotron by B. Hedin and D. Harting has been in use since 1957. Its design was based on the calculations made by Le Couteur for the Liverpool Cyclotron. The extraction efficiency is of the order of 5%. It is in our case mainly limited by the thickness of the iron septum and by the disturbances which are introduced in the cyclotron field.

In the following report we present an outline of the present schemes for improving the CERN extraction system. An improved channel, suitable for both slow and fast extraction, has been designed and will be put under construction during the coming year. Furthermore, a pulsed "kicker" coil, which will provide a highly efficient fast extraction, is being constructed, but has not yet been tested. Other improvements to the more important slow extraction are under consideration.

Fast Extraction.

The extraction system will consist of an arrangement as shown in Fig. 1.

There is a pulsed coil P, which will excite radial betatron oscillations allowing the beam to enter the magnetic channel C. The main advantage of using a pulsed coil is that its effect is felt instantly over the entire width of the beam, whereas it does not disturb the beam at all before it is pulsed.

It is clear that the entire beam could be extracted in one shot without losses if the pulse rise time is shorter than the time taken by a particle to make a revolution and if the induced betatron oscillation is sufficiently

large. In the case of the SC machine it is difficult to fulfil these conditions.

However, if the thickness t of the channel wall is small it is permissible to have a much longer rise time. The extraction will take place during several turns. A part of the beam will be lost against the channel wall but the lost fraction will not be very large.

Let us assume that the particles having R_0 as equilibrium orbit fill with uniform density a circle of diameter $2 \cdot \Delta R$ in a normalized radial phase space (see Fig. 2a). After the particles have traversed the coil P, the circle will be vertically displaced by an amount

$$\gamma = \frac{c B L}{p} \frac{R_0}{\sqrt{1-n}}$$

where:

B = pulsed coil field at the moment

when the particles cross,

L = coil length,

p = particle momentum,

n = field index.

At the channel entrance the situation will be as presented in Fig. 2b. The particles contained in ABCD will enter the channel. Particles contained in ACEF will be lost into the thickness of the channel wall. Particles contained in ABG will be lost against the inside face of the channel wall. The centre of the circle BG will be at a distance from the cyclotron centre

$$R' = \frac{B_c}{B_c - \Delta B_c} R_0 \quad \text{where } \Delta B_c \quad \text{is the field reduction}$$

inside the channel, and B_c is the cyclotron field. Particles contained in

HFI will be lost against the outside face of the channel wall.

The procedure can be repeated for the next particle turns and one can compute the percentage of lost and of extracted particles.

As an example we have made the computation for the following case :

$$\begin{aligned}
 t &= 1 \text{ mm} \\
 \Delta R &= 10 \text{ cm} \\
 B &= B_0 \sin \Omega \tau \\
 B_0 &= 500 \text{ Gauss} \\
 2\pi/\Omega &= 1.2 \text{ } \mu \text{ sec.} \\
 L &= 0.6 \text{ m} \\
 p &= 1200 \text{ MeV/c} \\
 \Delta B_c &= 2000 \text{ Gauss} \\
 n &= 0.05
 \end{aligned}$$

The extraction is completed after six particle turns. Approximately 50 - 60% of the beam is extracted where "extracted" means that the particles have entered the channel and travelled the first section of it.

The maximum stored energy is about 100 Joule at 30 kV. This energy would permit to produce a maximum field of about 1000 Gauss and to complete the extraction in three turns.

Improved Extraction Channel.

The ideal channel for extracting the proton beam from the SC machine should:-

- a) provide a field reduction and a field shape able to accept and guide to the magnetic edge a large fraction of the particles,
- b) not disturb the main cyclotron field,
- c) produce the required field reduction in a very short radial length, say a few millimetres.

We have chosen a DC channel rather than a pulsed one since this has the advantage of the field shape being easier to determine. Furthermore, a DC channel is suitable both for slow and fast extraction.

Among the disadvantages is the large amount of DC power which is required to energize it.

We have designed a DC channel of the coaxial type, very similar to the one proposed for the ORNL cyclotron. This type of channel produces almost no external disturbing field.

A cross-section of this type of channel is given in Fig. 3. The coaxial channel is subdivided into a number of wedge-shaped water-cooled copper conductors, which are connected in series. An angular sector of 30° is left free for the passage of the beam. To reduce the fringing field outside the channel the free sector for the beam has been fitted with a 3 mm thick copper septum. This septum is longitudinally divided into two parts, which are connected in series through a return conductor at the channel centre. The radial position of the septum is chosen to minimize the field outside the channel when the same current is circulating through both the septum and the coaxial channel itself.

The channel shape and its acceptance in phase space have been calculated by a digital computer programme, which calculates the field reduction and the particle trajectories.

Fig. 4 shows the acceptance of the channel in the horizontal plane. The particles which at the entrance of the channel are contained in the hatched region will not touch the channel walls. At the exit the radial spread of these particles will be about 13 cm.

The main features of the channel are:

Total power required	250 kW
Channel length	3.5 m
Wall thickness	3 mm
Power dissipated in the septum	60 kW
Copper weight	2.2 tons

We envisage dividing the channel into short straight sections, each about 0.5 m. The straight sections would be positioned in such a way as to form a polygon which would approach the computed ideal curved shape.

It seems very difficult to construct a curved coaxial channel. However, we plan to fit the first section with a properly curved septum.

Fig. 5 shows the field ΔB_c produced by the channel as a function of radius and the sum of ΔB_c and the cyclotron field at various azimuths starting at the entrance with $\phi = 0$.

This diagram indicates that the field generally decreases with the radius, and we can hope that there will be enough vertical focusing and that the acceptance will thus not be too bad in the vertical plane. This point, however, needs further investigation.

Schematic of extraction system. P is a pulsed coil, C is the magnetic channel.

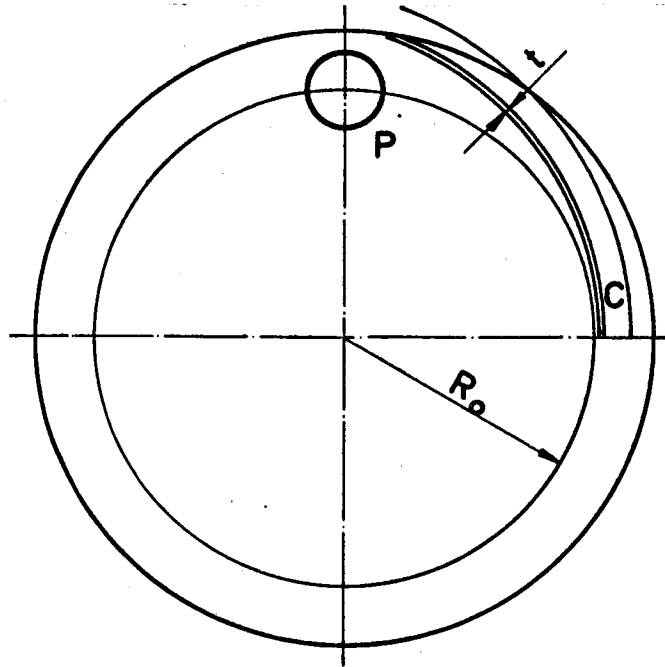


FIG. 1

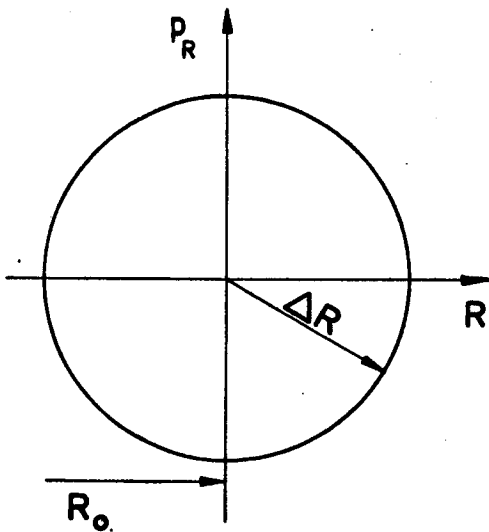


FIG. 2a

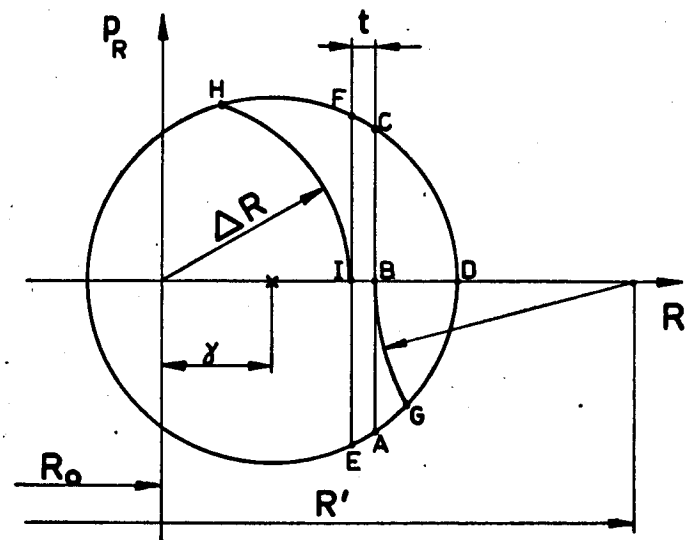
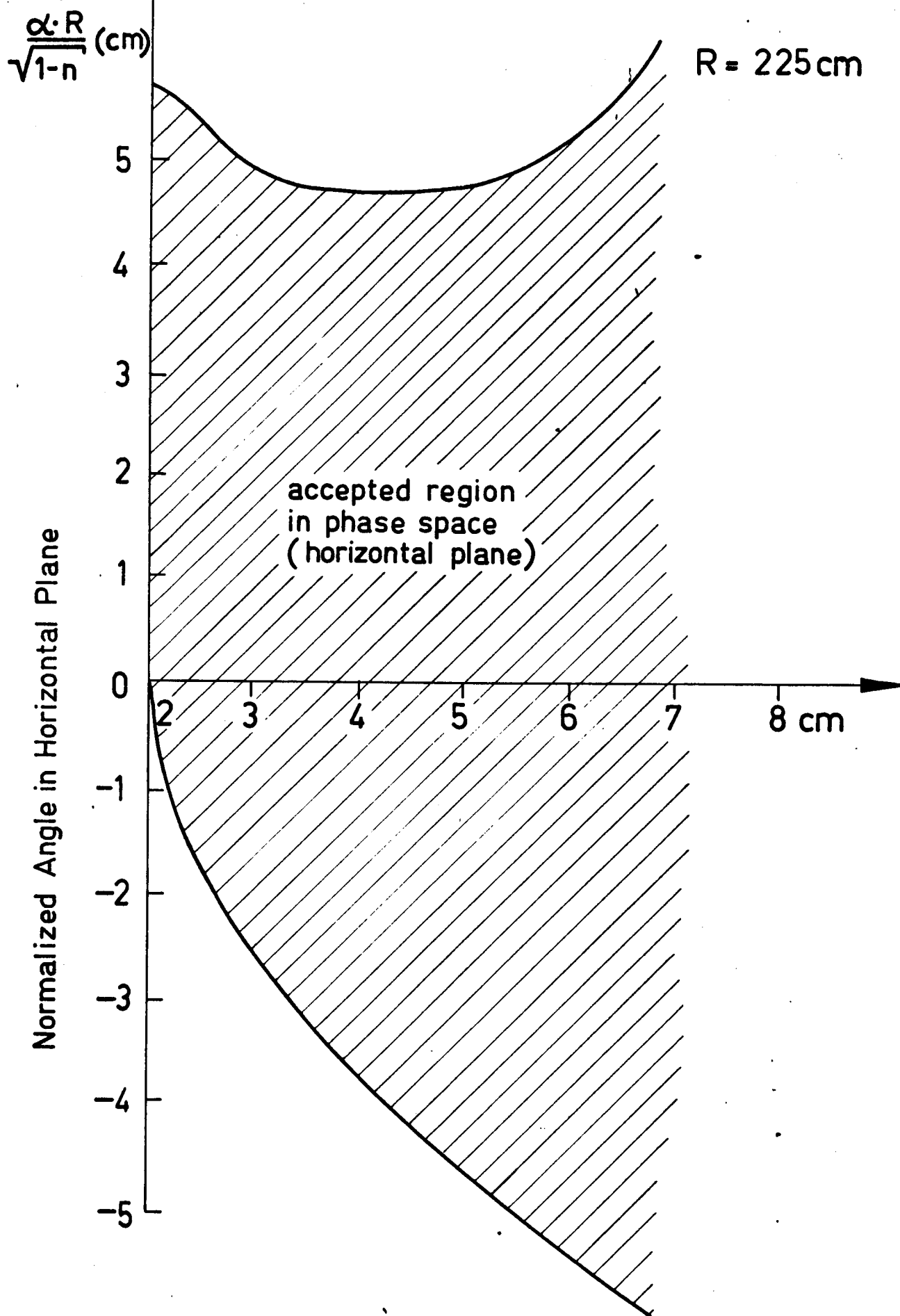


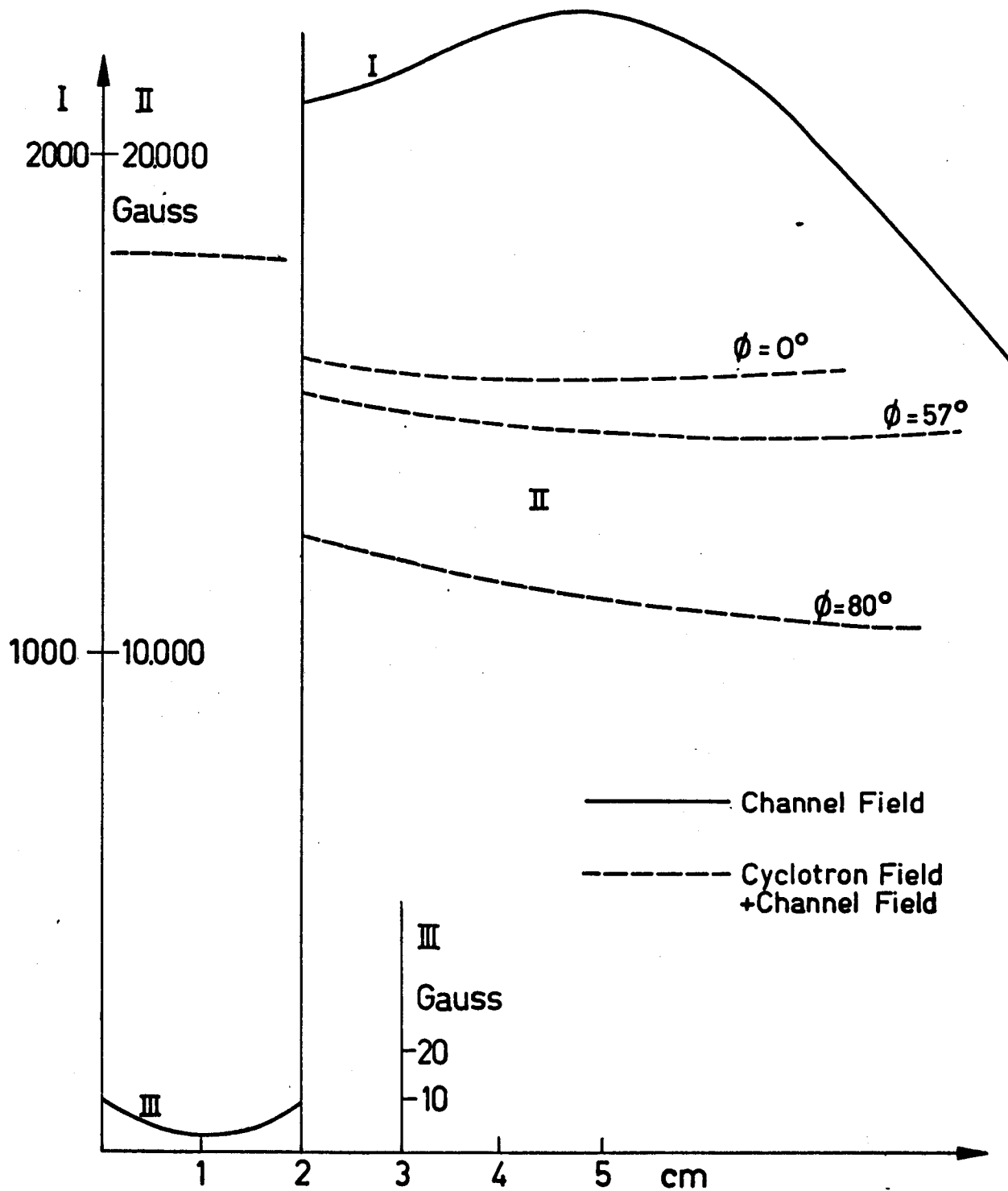
FIG. 2b

- Normalized radial phase space before displacement.
- Radial phase space at the channel entrance after displacement.



Horizontal acceptance of the DC channel

FIG. 4



Field B_c as a function of radius at various
azimuths

FIG. 5

HUXTABLE, Harwell - We have had exactly the same results in stacking the beam near the $n = .2$ radius on the Harwell machine and we find that it is much easier to stack the beam near the $n = .2$ radius if we take the extraction channel out. The perturbation of the extraction channel seems to effect the stacked beam very much.

We have also made exactly the same observations on the cross mode on the dee with our machine that you have made.

THE UPPSALA SYNCHROCYCLOTRON

Åke Svanheden and Helge Tyrén

University of Uppsala, Uppsala, Sweden

The Uppsala synchrocyclotron has been in operation since 1951. It is placed 12 m underground, and is shielded by a 2 m thick roof of concrete and above that 1.5 m earth. (Figure 1) The 650 ton magnet has a pole diameter of 230 cm, and a 25 cm mean gap. The magnetic field strength is 2.15 Wb/m^2 at the center and falls off with about 0.1 Wb/m^2 in 1 meter of radius. The maximum proton energy is 192 MeV at a radius of 102 cm where $n = 0.2$. The high frequency oscillator, which is grounded grid type, has a frequency range of 33.2 - 25.8 MHz and is modulated with a frequency of 250 Hz by a condenser rotating in air. The Dee-voltage is at maximum 15-20 KV, but normally 5-10 kV. The most intense internal proton current measured was $1 \mu\text{A}$. The half width energy spread is 13 MeV at 180 MeV.

The external proton beam was extracted (in 1955) by the nonlinear regenerative method (due to Le Couteur) (Figure 2). Inside the vacuum tank there is a set of focusing channels (forming a strong focusing system) in order to focus and align the beam so that it can enter the first quadrupole magnet. A second quadrupole magnet is used to focus the beam and bring down its cross section at the experimental area. Approximately the whole beam, passing the magnetic channel, is brought out to the experimental room and can be focused to a spot of 0.2 cm^2 . (Figure 3) The kinetic energy of the external beam is 185 MeV with an energy spread of $\leq 0.2 \text{ MeV}$. The maximum intensity is approximately 4×10^{10} protons/sec. The precision

in energy calls for a very high stability of magnetic fields in bending magnets and spectrometers.

In order to debunch the external proton beam (which has pulses of 10-20 μ sec. duration every 4000 μ sec.) a stochastic acceleration system was installed. This oscillator can give about 500 W to the accelerating electrode. The frequency range is 0.5 MHz. With a saw-tooth frequency modulation at 10 kHz about 20% of the normal external beam intensity can be extracted.

The fundamental research performed with the internal and external proton beams has been in the field of nuclear scattering, nuclear chemistry and spectroscopy as well as radiation biology. At the moment experiments are concentrated to nuclear scattering and radiation biology.

For the purpose of nuclear scattering experiments a magnetic spectrometer of the wedge focusing type has been built, the bending angle of which is 135° . The center orbit radius of curvature is 135 cm. The energy resolution of the spectrometer is 0.2 MeV for 180 MeV protons.

Special beam transport facilities are provided for the biological experiments. A general lay-out of the experimental area can be seen in Figure 4.

In many experiments one should like to have the proton beam intensity increased considerably, and therefore it was planned to convert the synchrocyclotron to a sector focused cyclotron. Then the coned pole tips of the magnet had to be altered to cylindrical ones, thus making the pole tips diameter 280 cm. A 4 sector machine was considered with the ridges twice the width of the valleys. With a minimum gap of about 20 cm it would have been possible to get a maximum field strength of 2.3 Wb/m^2 with an average field of 1.84 Wb/m^2 . With a nearly rectangular AVF the minimum field would be 1.03 Wb/m^2 , which in turn requires a spiral angle of around 56° at the maximum useful radius of 1.2 meters. The radius of curvature of the spirals was

planned to be constant. Computer calculations by Vogt-Nielsen have confirmed the rough calculations mentioned above.

Because of the limited knowledge about the possibility of extracting a proton beam of small energy spread from a sector focused cyclotron, and due to the large amount of work and costs involved, the AVFC project was abandoned. Instead the plans were altered to a rebuilding of the oscillator system and to a change of the type of ion source. In this way one hopes to be able to increase the proton beam current to some microamperes. This current would mean a great improvement for most of the experiments to be performed, especially if it is possible to keep the small energy spread of the external beam.

In order to fully use such a beam in nuclear scattering experiments it is necessary to extend the area for experiments in the external beam. In some experiments one should like to have a proton beam of very small energy spread. Therefore it has been considered to build a beam transport system including a set of analyzing magnets capable of giving a lateral energy dispersion of around 4.5 cm/MeV. A special beam transport system is to be provided for the biological experiments.

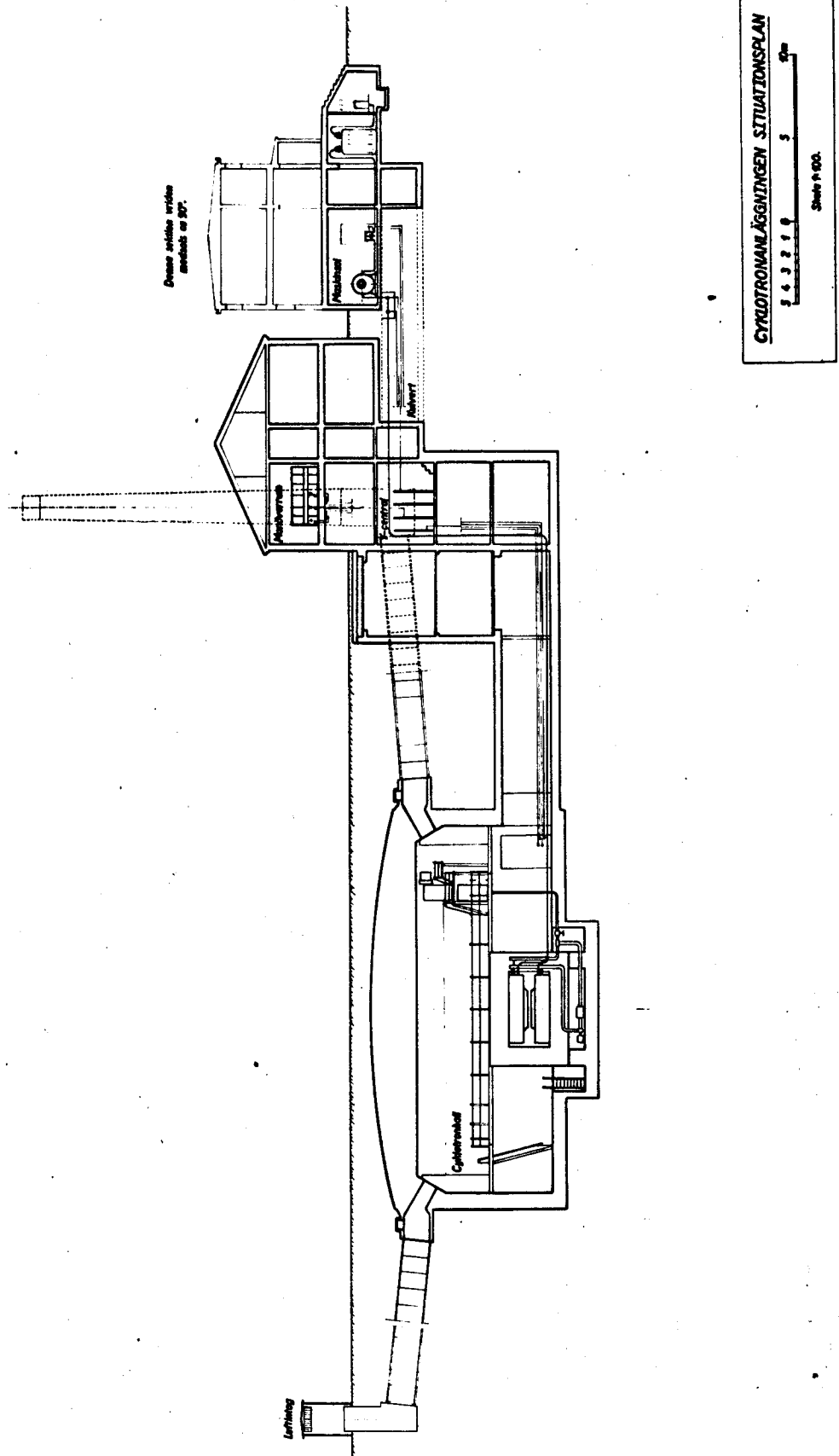


Figure 1 - Vertical section of the cyclotron laboratory.

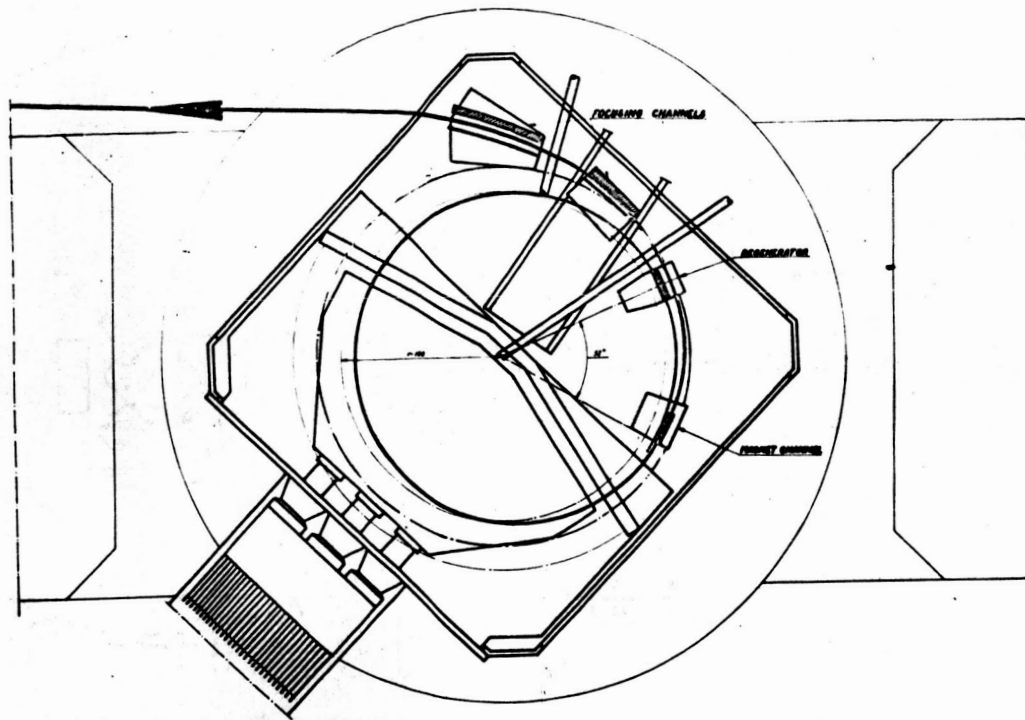


Figure 2 - Beam extraction system.

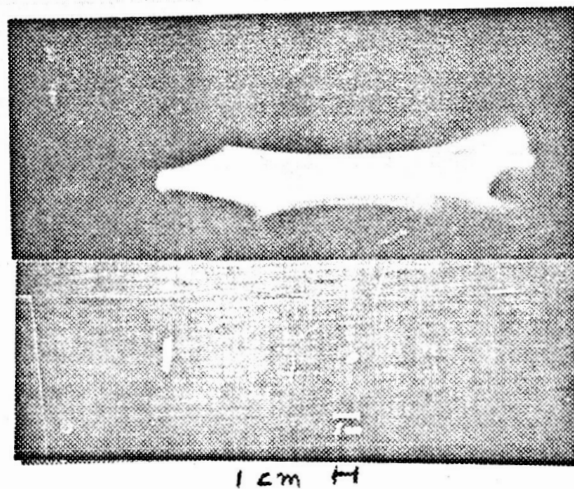


Figure 3 - Cross sections of the external beam at the entrance of the first quadrupole lens, top, and at the scattering center, bottom.

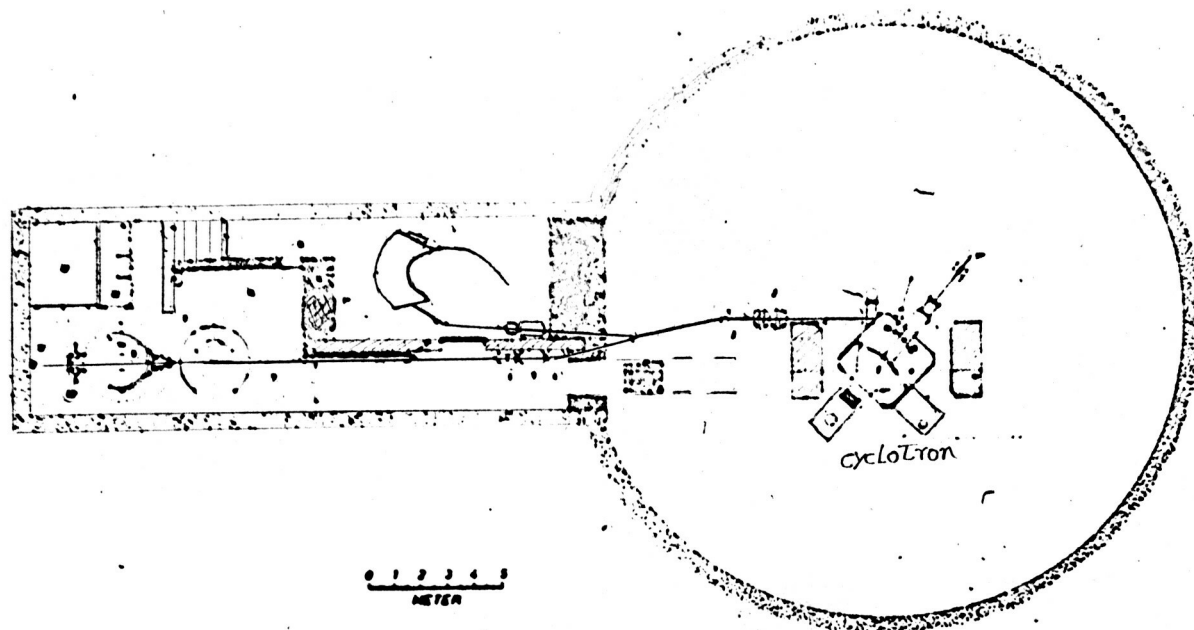


Figure 4 - General lay-out of the experimental area

VOGT-NILSEN, CERN - What was your internal beam?

SVANHEDEN - $1 \mu\text{a.}$

SIEGEL, William and Mary - How did you measure it?

SVANHEDEN - We measured it by Al activation and measuring Na^{24} .

A BEAM PULSE STRETCHER OF THE SYNCHRO-CYCLOTRON*

Martyn H. Foss, Robert W. Findley and Arata Suzuki
 Carnegie Institute of Technology
 (Paper delivered by A. Suzuki)

A radio frequency beam pulse stretcher has been applied to the Carnegie Tech 450 MeV Synchro-cyclotron.

The beam pulses are stretched with an efficiency of about 70%. The duty factors are almost unity for the long time scale and less than two for the nanosecond time scale due to the phase bunch.

The principle of the r-f beam pulse stretcher is as follows: 1,2)

1. Particles are accelerated by the main oscillator until some radius which is just inside of a target position or an extraction radius.
2. After the main oscillator is turned off, a complimentary r-f field takes over the action of the main oscillator.
3. The particles are then accelerated gradually during the cycle of the frequency modulation of the main oscillator.

If the particles are accelerated by a noise field, the energy gain ΔE , in a time interval T , is given as

$$\Delta E \approx \left(\frac{T}{\tau}\right)^{1/2} \cdot \frac{\tau}{\tau_i} e V_{eff} \cdot 2 \sin \frac{\phi}{2}$$

where τ is the averaged time of the phase flips of acceleration or deceleration.

τ_i is the revolving time of the particles at the maximum radius region, and is about 50 nsec for all the machines.

*This work was supported in part by the U. S. Atomic Energy Commission.

V_{eff} is the effective value of the cee voltage and δ is the azimuthal angle covered by the cee.

T/τ is the number of the phase flips in the duration T , and, therefore, the square root gives the statistical deviation from the case where the repetitions of accelerating and decelerating phase are the same.

Namely, the energy of the particles diffuse $\pm \Delta E$ in the time interval T by a noise field.

Fig. 1 is the scheme of the r-f field for the Carnegie Tech beam pulse stretcher. This is the same as the stretcher of the Toyko cyclotron.

By the slow modulation component, the mean energy of the circulating particles is gradually increased, and the probability of the acceleration is changed in order to improve the uniformity and efficiency.

The 100 Kc/s modulation corresponds to τ in the equation. Beam bunches due to this modulation can be eliminated by the noise signal of about 500 Kc/s, because the fast modulation component is effective if the energy change is small.

The minimum band-width of the r-f field can be estimated by the width of the beam pulse and the frequency modulation rate of the main oscillator.

Fig. 2 is a block diagram of the stretcher. The cee is excited by a wide band power amplifier. The r-f voltage on the cee is modulated according to the frequency change of the input signal. Under the normal operating conditions, the time averaged r-f peak voltage on the cee is about 2 KV (V_{eff} is 1.5 KV).

There are three frequency detectors to detect the frequency of the main oscillator: one to generate the stopping signals of the main oscillator; one for gating the counter system, and one for a synchronous timing signal of the stretcher. The jitter of the detectors are less than one microsecond.

The saw-tooth sweep is started by the frequency signals. The frequency of the 20 Mc/s oscillator is decreased gradually by the saw-tooth signal. Also the oscillator is modulated by the 100 Kc/s signal and by the noise signal. The noise is generated by a thyratron in continuous conduction.

Frequency modulated signals from the oscillator are amplified by transistors and are fed to the wide band power amplifier.

The power amplifier consists of four stages. All the stages except the final have more than enough gain and band-width. The frequency response of the amplifier is, therefore, dependent upon the load.

Fig. 3 is an oscilloscope pattern of the stretched beam with an efficiency of about 65%. The spike of the beam pulse is about 5% of total stretched beam.

The fine structure of the stretched beam is shown in Fig. 4 a) was taken without the noise modulation and with increased modulation amplitude of the 100 Kc/s signal. b) was taken under the normal operating conditions.

The effect of the saw-tooth signal is the same as the case of the Tokyo cyclotron.

The r-f phase bunch of the stretched beam was measured by a coincidence circuit. The accidental coincidence counts of two counters was measured as a function of the relative delays. The result is shown in Fig. 5, where the square root of the accidental coincidence rate, namely the beam intensity is shown as a function of time.

For external protons, the resonator must be tuned down changing a shorting bar, and readjusting the frequency setting. Then the beam pulses of the external protons can be stretched efficiently.

The r-f beam stretcher is a very useful device for the synchro-cyclotron and there is no trouble in operation.

It is possible to stretch the r-f phase bunch by installing another electrode which requires a field of about 100 Mc/s. The power of the 100 Mc/s

amplifier (or oscillator) is estimated at about 2 Kw.

The necessary r-f voltage on the cee is rather lower than the value that is estimated by the equation. This might be caused by the radial oscillation of the beam.

The resonator will be replaced by a new high Q wide band resonator which was tested. A 2 Mc/s band width was obtained with $Q = 30$ at 21 Mc/s.

References

- 1) A. Suzuki, Japanese J. Applied Physics 2 (1963) 106.
- 2) M. H. Foss, R. W. Findley and A. Suzuki, to be published.

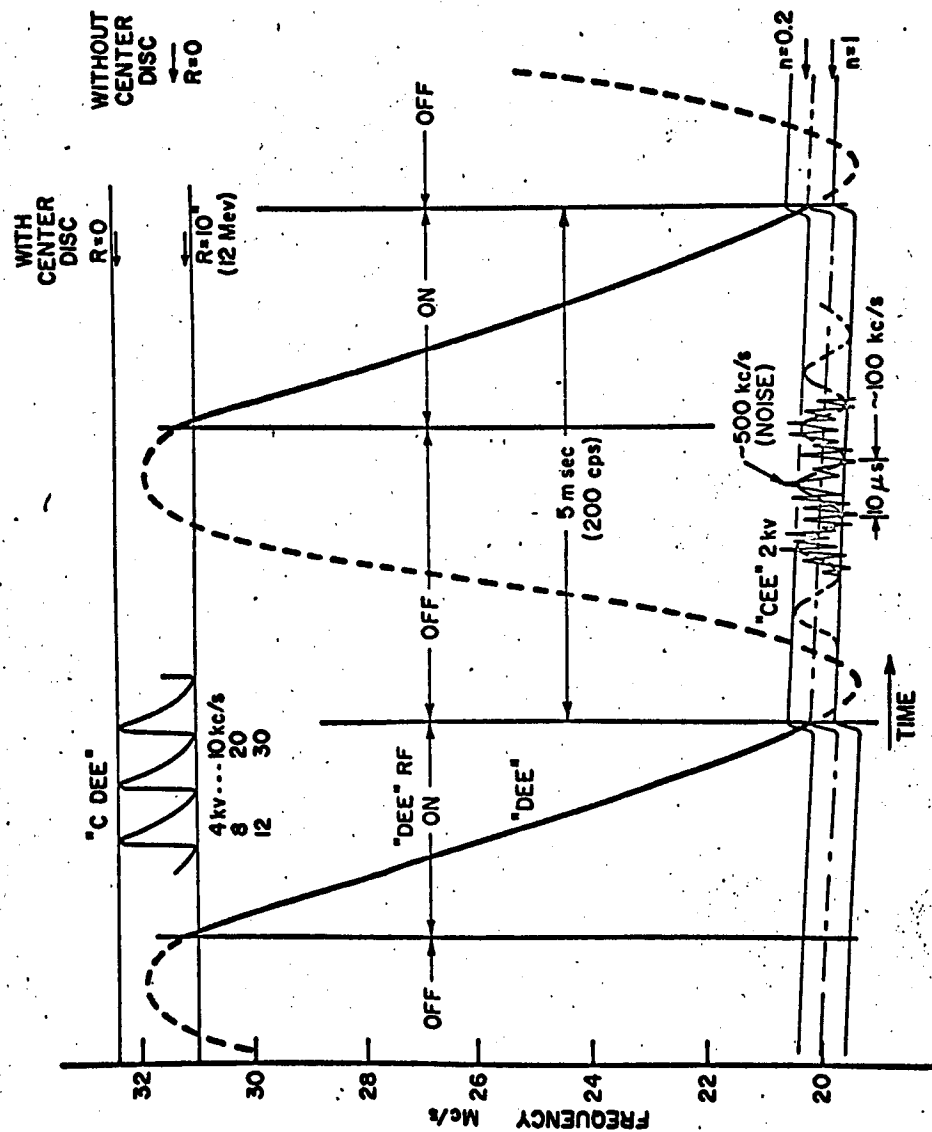


Figure 1 - System modulation pattern employed on the Carnegie Machine.

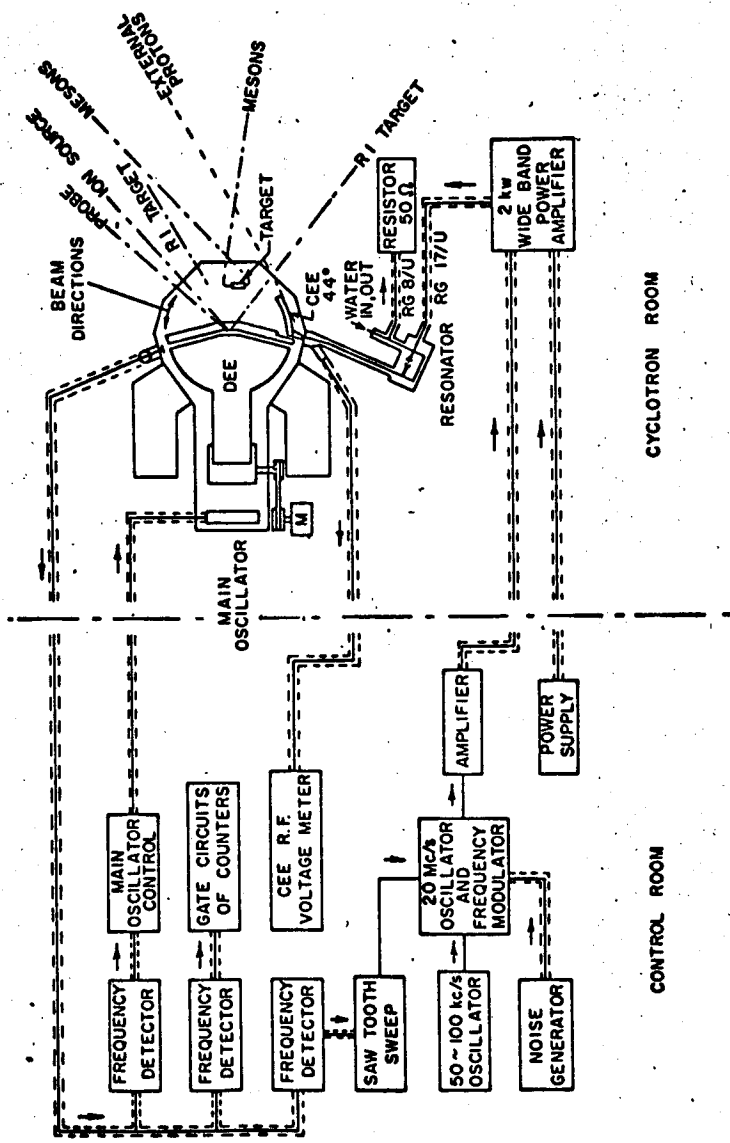


Figure 2 - Block diagram of cee electronics system.

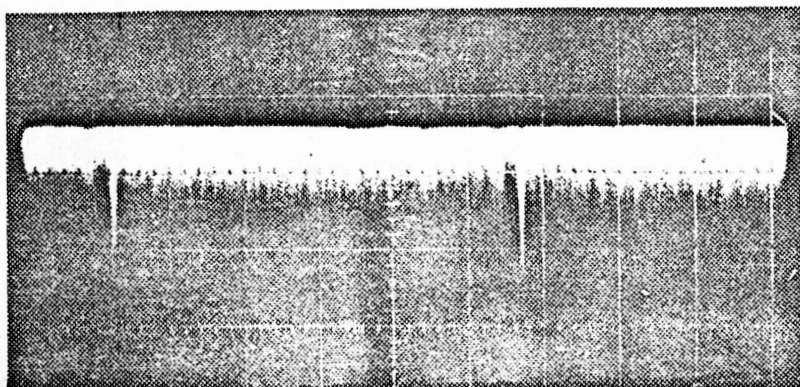


Figure 3 - Oscilloscope pattern of the stretched beam. Stretching efficiency in this photograph is about 65%. The beam spike is less than 5% of the total stretched beam.

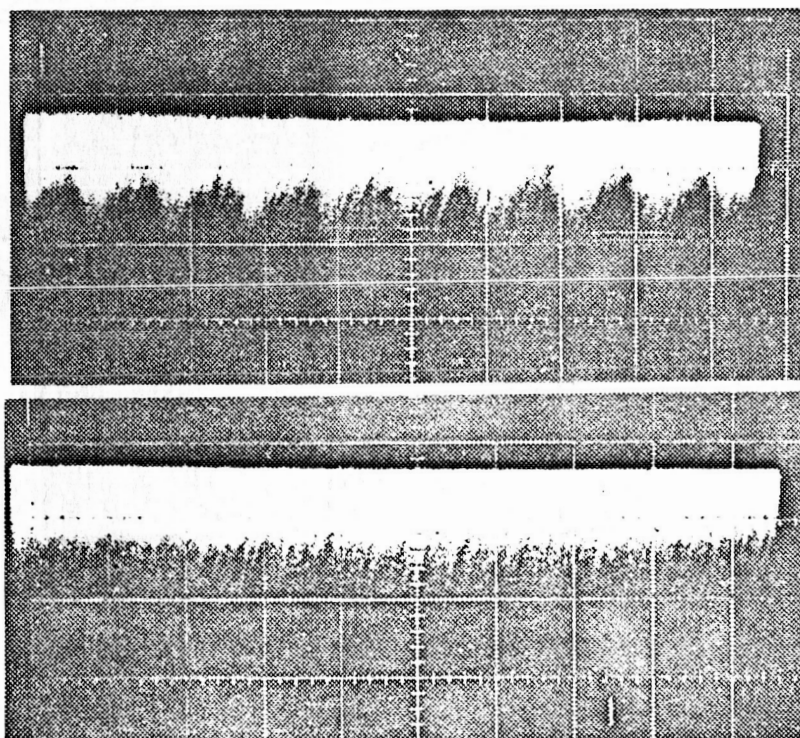


Figure 4 - Fine structures of the stretched beam. Oscilloscope is triggered by the 100 Kc/s signal of the frequency modulation. a) was taken without the noise modulation and b) was taken under the normal operating conditions.

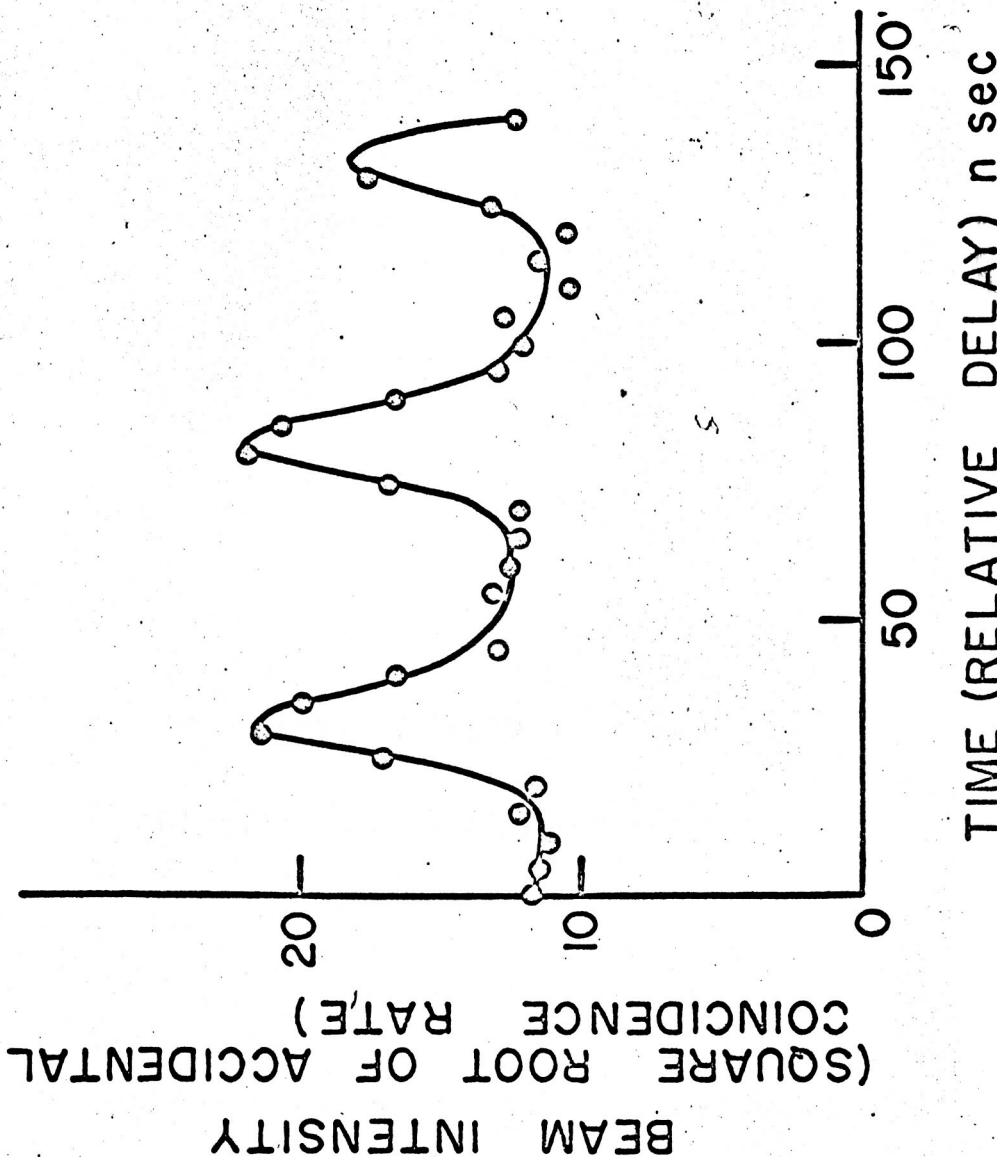


Figure 5 - Accidental coincidence "cable curve". Plotted is the square root of accidental coincidence rate vs time. Note that there is appreciable beam current between r.f. bursts. Resolution of coincidence circuit is 5 nanoseconds.

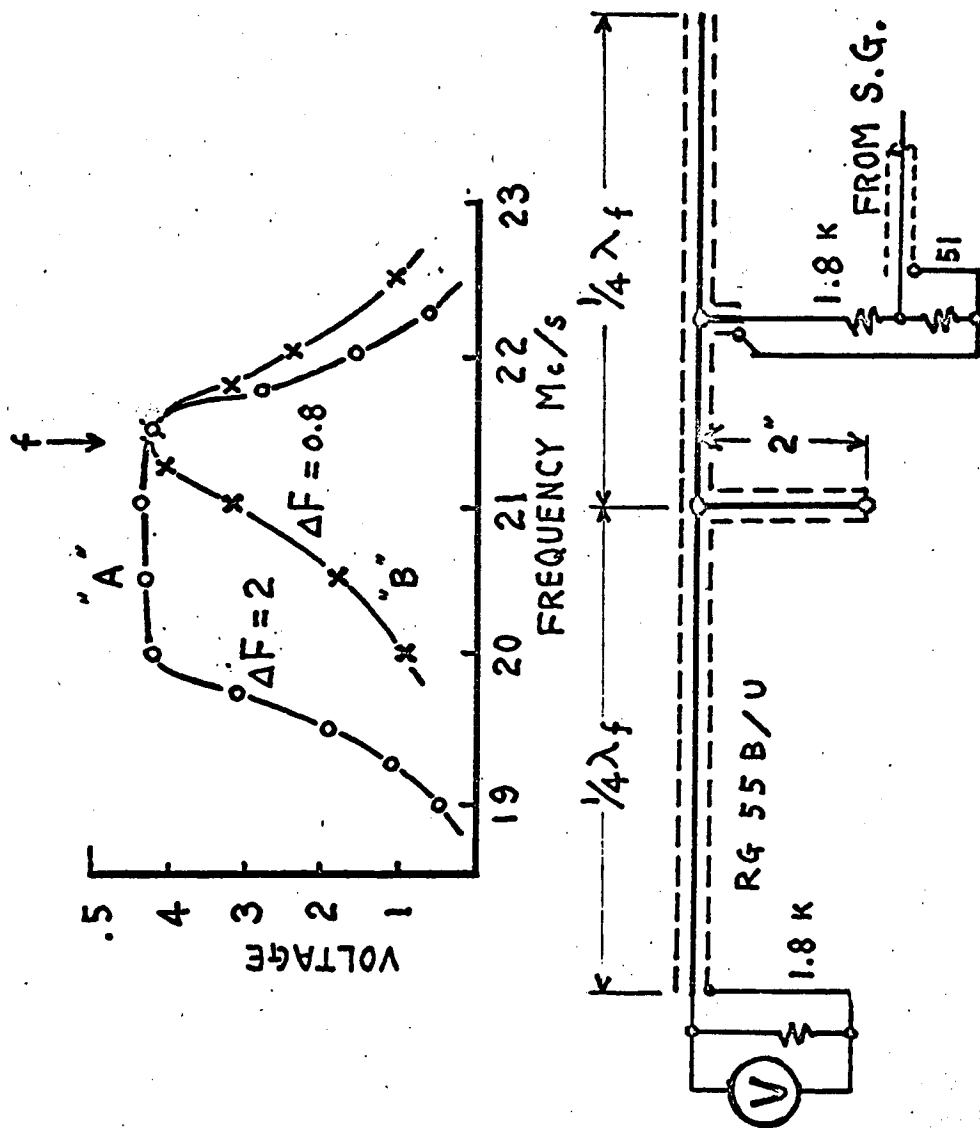
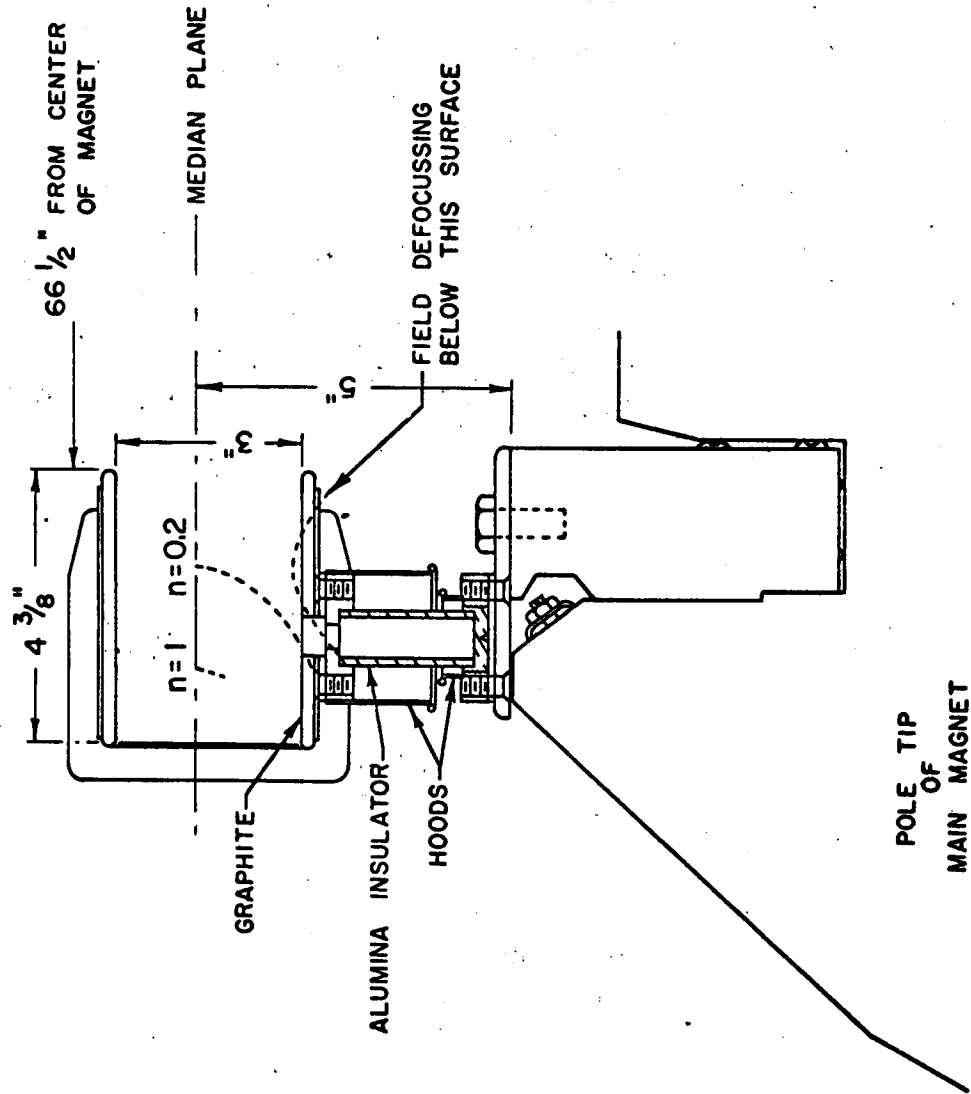


Figure 6 - High Q wide band resonator with one stub. Curve "B" was obtained without 2" short T connection.



Elevation schematic of dee electrode.

IMPROVEMENT DESIGNS FOR THE CARNEGIE SYNCHROCYCLOTRON

Martyn H. Foss, Carnegie Institute of Technology

I would like to list some of the things we are presently doing: First, we are building a poor man's meson channel after a suggestion of van der Meer. A current-carrying wire, Figure 1, has a magnetic field around it producing maximum focusing for a particle traveling parallel to the wire since it has the maximum cross product. The only difficulty is that the particle bends down, hits the wire, and is lost. However, if it has an angular momentum about the wire, then it will make a spiral path about the wire. The device is 30 feet long and has a center conductor composed of 9 conductors in parallel each carrying 2500 amperes and made of $2\frac{1}{4}$ inch pieces of heavy wall copper tubing. The total diameter is about 3 centimeters and the power dissipation is approximately $1/2$ megawatt. We haven't faced up to the matching problems. The beam from the cyclotron must be given a twist to properly match it to the channel. Then on the exit end of the channel the beam has to be untwisted. We are not worrying about these matching problems at the moment. A super-conducting device would avoid the power problem. It might be built in the same way with the turns going around the outside and back through in the center. It is extremely difficult to wind. We've also considered building a super-conducting solenoid which seems to be a nicer device; it acts

as its own matching lens, i.e., the entrance conditions where the field diverges give the beam the necessary twist upon entering and when it leaves it is untwisted. Westinghouse has come out with a 10 mil wire which, in a 20 kilogauss field, will carry 120 amperes. If this wire works, the device would be fairly economical to build and operate.

We are also building an ion source, Figure 2. We had this ion source in a test magnet with a D.C. dee-like extractor and obtained 80 milliamperes. It seemed promising enough to go ahead and try to put it in the machine. It is a type of Von Ardenne ion source, having an upper cone which is grounded and an inner cone spaced quite close to it. There is a little slug of steel in the upper cone that makes a magnetic bottle in the tip of the upper cone. There is a similar piece of steel above the median plane and another inactive cone. The dummy dee and the main dee structures are fastened to the ion source with insulators. We estimate our present cyclotron ion source now gives 1 milliampere. Since our cyclotron is on the borderline of being impossible to maintain, we don't want 80 milliamperes to go into the beam. Hopefully, by discarding the low quality beam near the center of the machine we might be able to decrease the amount of beam being dumped farther out. This might simplify the extraction problem. When high intensity is absolutely necessary, it might be available.

We also built an extractor that didn't extract. It was half as

long as required and showed some promise of acting as it should. It is a septum that produced a regenerator field on the inside and an extractor field on the outside as shown in Figure 3. We usually have about 10% of the internal beam spiraling out and we tried just pushing a bit on the beam with the regenerator field. However, the beam was thrown vertically so we know there is a median plane error. But at a radius where it was supposed to work it did seem to step the beam out.

We are writing fast programs to compute orbits in three dimensions to solve some of the field problems. Each section of the orbit is calculated in a local co-ordinate system which is chosen to make the calculation simple. The program is designed to be fast in "smooth" fields. The errors are cubic in the step size. We have a two-dimensional program already working.



Figure 1 - View of 30' van der Meer type meson channel
The outer conductors are supported on a 10" steel pipe.
The inner conductors are supported by wires. The
conductors crossing the far end can be seen in the
figure. (A string makes an extra line in the foreground.)

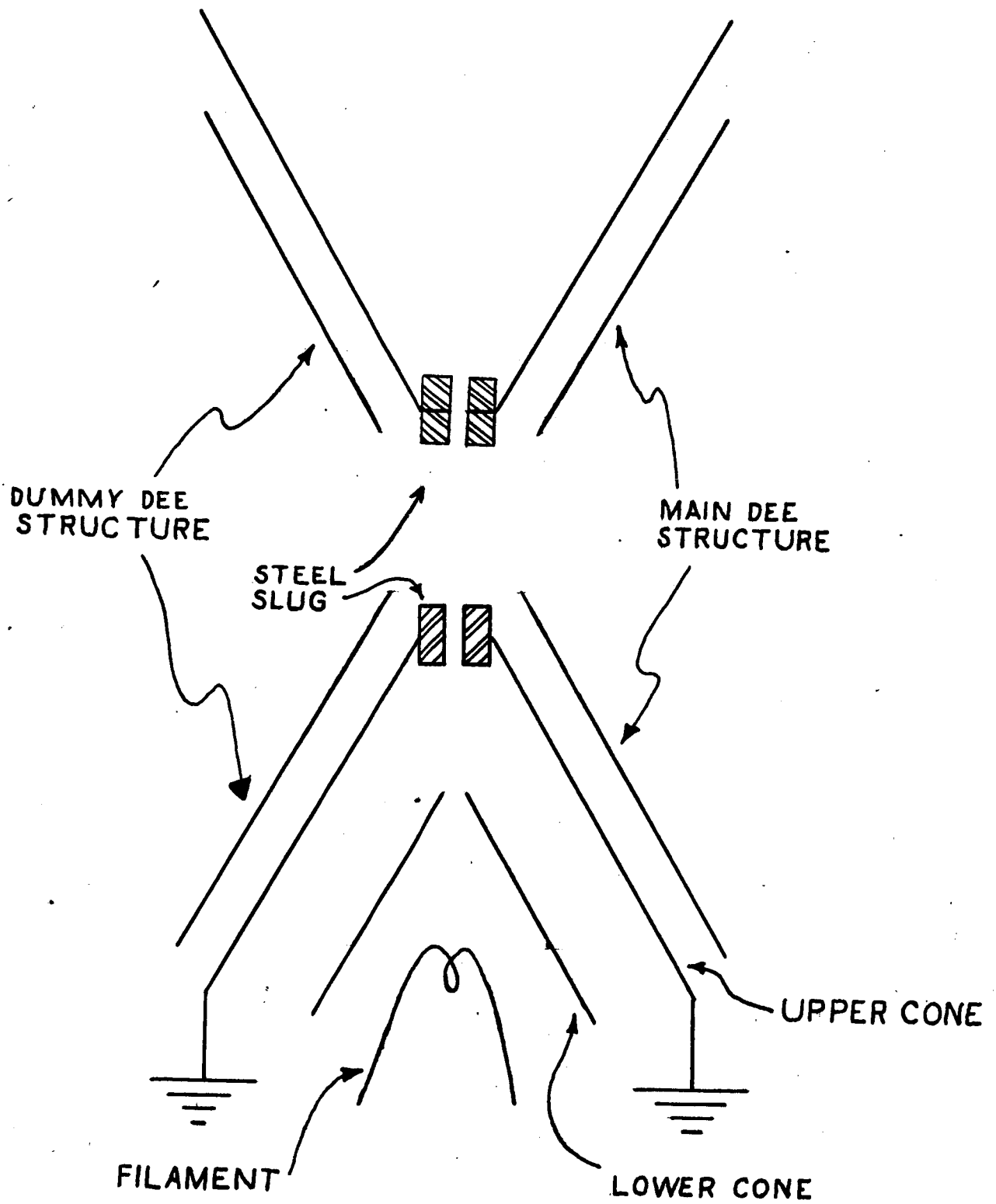


Figure 2 - Von Ardenne type ion source

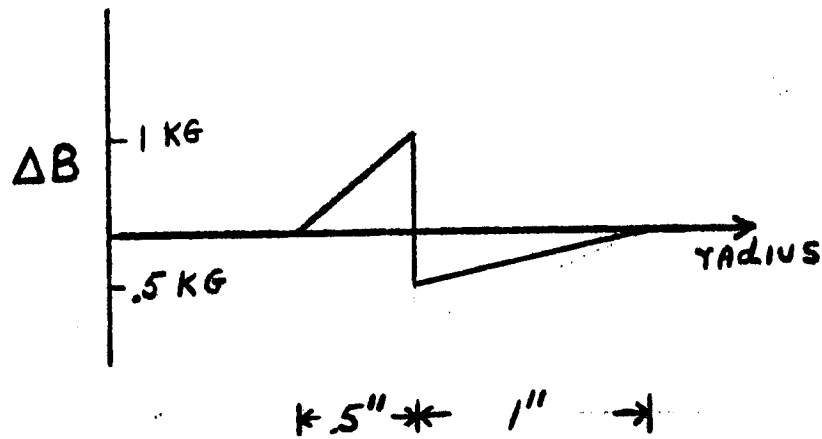


Figure 3 - Radial plot of magnetic field of extractor system.

BROBECK, Brobeck Associates - Was the 80 ma. extracted from the ion source done with r.f. on the dee?

FOSS - No, it was d.c. extraction.

MOLTHEN, Chicago - What was the beam intensity with the cee turned on compared to the beam current under normal operation?

FOSS - about 65%.

MICHAELIS, CERN - What is the intensity of the beam?

FOSS - $10 \mu\text{a}$ from A^2 activation measurements. This is really the product of beam intensity times the number of multiple traversals. We say, though, $1 \mu\text{a}$ just to be agreeable.

SIEGEL, William and Mary - What is the secret of extracting the whole internal beam? The only machine that has extracted a large fraction of its internal beam is the Japanese machine at Tokyo at which Suzuki et al. have succeeded in extracting 80% of the beam. Now Suzuki says that it's the smoothness of the magnetic field which makes it possible to get the beam out to $n = 1$, but no one has come anywhere near this type of extraction efficiency.

FOSS - We put some coils in our machine that improved the residual errors of the magnetic field from probably 2 gauss-feet in the first harmonic to zero and the external beam increased possibly 30%. I think the quality of the beam would have to be better. I also would hope this ion source would improve the quality so we would probably get a higher percentage of extraction by throwing away unextractable junk before it gets to large radii.

FACILITIES IMPROVEMENTS AND
ACTIVITY PROBLEMS ON THE 184" CYCLOTRON

Richard J. Burleigh, Berkley
(Paper delivered by author)

ABSTRACT

The new addition to the building, the new medical and physics caves, and improved equipment associated with the external beams are described. Some problems in working with an active machine are discussed.

Construction on the 184-inch Cyclotron was started in 1940, twenty-four years ago. Since that time the machine has undergone four distinct reincarnations. It is indeed remarkable that such a venerable antique is still considered worth improving!

Within the past few years the experimental facilities associated with the machine have been extensively enlarged and improved. An addition to the building has doubled the experimental area. A new cave for medical and biological research and a new physics cave have been erected. Various improvements and new items have been added to the equipment associated with the external meson beam and with the external proton-deuteron-alpha beams.

BUILDING ADDITION

The new addition to the building is shown in Figs. 1, 2, and 3. This measures approximately 40 feet by 210 feet, or 8,400 square feet net. This was built at a total cost of \$283,000 or a unit cost of \$34 per square foot. These are construction costs only and do not include design, inspection,

the crane, or the cost involved in moving the mechanical vacuum pumps as required by the building addition.

For the greater part the building is of the usual steel frame construction sheathed with corrugated transite. At the back of the physics cave, however, the wall is of monolithic concrete with a smooth uninterrupted surface on both the inside and the outside. "Gun-ports" are provided in this wall at the level of the beam. With this construction the experimental area can be continued outside the building, the concrete wall providing shielding against which blocks can be neatly stacked.

A 30 ton crane, running along curved tracks conforming to the shape of the building, serves the entire area. This cost \$50,000. The existing crane, pivoted at the center of the old part of the building, is still in service. Both cranes may be operated from the floor by pendant controls. In order to move items between the old and new areas an electrically powered truck rolling on rails flush with the floor is provided. When placing a shielding block in the awkward no-man's land between the areas covered by the two cranes, a special handling device is employed. This consists of a beam with one end suspended from the hook of one crane and the other end suspended from the hook of the other crane. A hook may be moved along the beam by means of an electrically driven lead screw controlled from the floor.

PHYSICS CAVE

Full advantage of the addition to the building has been made with the back of the cave now extending to the new outside building wall. The cave is now almost three times longer in the direction of the beam than it was previously: 62 feet compared to 23 feet. The width remains the same. The side walls are 5 feet thick, the back wall 16 feet, and the roof 4 feet. With the exception of the common wall between the physics cave and the medical

cave, all the physics cave shielding is at present of ordinary concrete. However, new composite shielding blocks of steel and heavy concrete are on order. While the actual thickness will remain as shown in Fig. 1 the equivalent thickness in terms of ordinary concrete will be more than doubled.

Entrance to the cave was formerly through a maze. It will be now through a revolving barrel door. This consists of a steel shell, filled with steel plate and heavy concrete. It is mounted on roller bearings at the top and bottom and is driven by an airmotor. This door is $7 \frac{1}{2}$ feet in diameter and weighs 30 tons. This type of door takes up little room and may be readily moved to other locations. It has, however, proven expensive to build.

MEDICAL CAVE

The new cave differs from the old one in that it (1) provides better shielding and (2) provides more space.

The previous medical cave shielding was adequate for alpha bombardment within the cave. The radiation background in the whole building, however, was too high when the full intensity proton beam was used in the medical cave. It is expected that there will be considerable whole-body proton irradiation of animals in connection with a contract with the National Aeronautics and Space Agency (NASA). Furthermore, the increased shielding thickness will now allow people to work in the medical cave in preparation for an experiment while the beam is on in the physics cave. The converse should also be true.

The original cave had a floor area of 17 by $18 \frac{1}{2}$ feet. The new cave is 21 by 24 feet. The original walls were 5 feet thick, of ordinary concrete with a density of 150 lbs/ft³. As indicated in Fig. 1, the new cave shielding is partly ordinary concrete, partly heavy concrete of 300 lbs/ft³ density, and partly steel. The north wall now has an equivalent thickness of

10 feet of ordinary concrete, the east wall (or common wall between the medical and physics caves) has an equivalent thickness of 12 feet, the south or back wall has an equivalent thickness of 20 feet, and the west wall has a thickness of 9 feet. The original roof was 2 feet of ordinary concrete. The new roof is composite steel and ordinary concrete with an equivalent thickness of $8\frac{1}{2}$ feet.

Entrance to the medical cave was formerly through a maze. Again with the thought of better shielding, entrance is now through a door plus maze. This may be seen in Fig. 4. This is a plug door which is moved up and down by a hydraulic cylinder. The door is so constructed that when it is open it is in a pit in the floor and the top of the door serves as the floor of the passageway into the cave. Such a door requires the minimum of floor space but is, of course, fixed in position by the pit in the floor.

The door block is of ordinary concrete, 9 feet thick, 4 feet wide, and 13 feet high. It weighs 34 tons. The cylinder is 8 inches in diameter, has a 7 foot stroke, and operates at an oil pressure of 1350 psi. The hydraulic pump system is driven by a 30 hp electric motor which closes the door in about 30 seconds. Opening is simply by gravity, the rate of fall being determined by controlling the flow of oil through a metering valve.

PROTON-DEUTERON-ALPHA BEAM FACILITIES

The duty factor of the external beam has recently been substantially improved by the use of a second dee. This will be discussed at this conference in a separate paper by Kenneth M. Crowe. The RF system is described in Ref. 4. There has been no change to the regenerative extraction system since it was installed seven years ago. A number of improvements have, however, been made in the external beam equipment.

As the deflected beam emerges from the tank it passes through a recently installed degrader. This is shown in Fig. 5. It consists of a box containing copper plates which may be inserted or removed from the beam path. Any total thickness may be achieved from $1/16$ of an inch to 10 inches in increments of $1/16$ of an inch. The individual plates are actuated by air cylinders remotely controlled from the control room. This degrader is used only when the beam is directed into the physics cave. Energy changes in the medical cave beam are made by another device to be described later.

The beam next goes through the new collimator shown in Fig. 5. This consists of two pairs of brass blocks 4 inches thick, one pair being movable in the vertical direction and the other pair in the horizontal direction. With each pair, both the width of the slit between the blocks and the position of the slit may be varied remotely from the control room. There has been a collimator in this spot for many years but the previous one did not have remote controls on the slit width.

The beam then goes through a steering magnet which steers it into either the physics cave or the medical cave. A new 8-inch quadrupole doublet replaces the 4-inch quadrupole previously installed in the beam to the physics cave. This increases the beam in the cave by a factor of 2. An existing remotely operated beam plug completes the equipment in the physics beam. The equipment along the beam line to the medical cave is all new. The following description is taken largely from reference (2).

Referring again to Fig. 1, this new equipment includes--in the following order--a quadrupole, a beam plug, a scattering target, and a collimator. This array is also shown in Fig. 6.

In order to collect more particles and increase the available beam current in the medical cave, the beam tube diameter was increased from 6 to 8 inches.

A new quadrupole doublet was designed to accommodate this; no quadrupoles were previously in this line. This change has been found to increase the beam current in the cave by a substantial but unknown factor (i.e., beam measurements are not complete). Available beam currents (internal and external for mesons, protons, deuterons, and alphas) are discussed by K. M. Crowe in the paper previously mentioned.

The beam plug is simply a safety device which cuts off the beam to the cave when the cave is not in use. It consists of a cylinder of steel and heavy concrete with two off-center holes parallel to the axis. The cylinder is remotely rotated by an air cylinder so that the holes may be in or out of the beam.

The beam vacuum tube is terminated in a thin vacuum window just ahead of the scattering target. The scattering target serves two purposes: it provides (1) a means of controlling beam energy by placing various thicknesses of absorber in the beam path, and (2) a means of producing a diverging scattered beam for whole-body animal irradiation. This will explain one of the needs for a larger cave: space is needed to place the animal far enough away from the target so that it is entirely within the scattered beam cone. The scattering target is in the form of a turret resembling the magazine of a Colt revolver. This turret is 30 inches in diameter by 42 inches long. It contains four 8 inch diameter holes at 90 degree intervals. Any one of these holes may be rotated into the beam path and various absorber thicknesses may be placed in the holes. The turret is rotated manually from within the cave.

Collimators of various kinds to fit particular experiments may be placed downstream from the scattering target.

MEDICAL CAVE EQUIPMENT

Figure 7 is a view of the inside of the medical cave. The beam enters the cave from the left at (a), (b) is the existing human positioner, (c) is a device for loading the scattering target turret, and (d) is the new animal rotator.

The human positioner shown has been used for many years for the irradiation of the pituitary gland. This is in connection with several diseases including, cancer of the breast, acromegaly, Cushing's disease, and Parkinson's disease. The patient is in a horizontal position with his head intersecting the beam. The bed and the head rest are not shown in this picture. In order to minimize the irradiation of surrounding tissue the bed may be placed at a variety of angles in the horizontal plane. The patient's head is also mechanically oscillated during irradiation.

The patient is viewed by two closed-circuit TV cameras. The TV receivers are located in three places; (1) in the nurse's sentry-box just outside the cave entrance (see Fig. 4), (2) in the main control room, and (3) in the new medical control room (Fig. 8). Facilities in the medical control room - in addition to the TV receivers - include dosimetry, remote controls for the positioner, and "off" control on the Cyclotron.

A new positioner to replace the existing one is currently being designed. Figure 9 is a picture of a model of this new positioner. The new positioner will have the following features. Instead of being designed for irradiation of the head only it is designed so that any part of the body may be irradiated. It will have three degrees of remotely controlled translation and two degrees of remotely controlled rotation. It is designed for a high degree of accuracy and rigidity; reproducibility within 0.010 inch is expected.

The animal rotator (Fig. 7) is for omnidirectional whole-body radiation to simulate conditions in space. The animal is placed in a hollow spherical or dumbbell-shaped shell made of styrofoam. This shell is rotated about a horizontal axis with a speed which may be varied from about 0.5 rpm to about 10 rpm. The shell is also rotated about the vertical axis. In order to provide a uniform distribution of radiation it is necessary that this rotation about the vertical axis varies sinusoidally in time. This sinusoidal variation is provided by a Scotch yoke mechanism in the base. The time for one revolution about the vertical axis may be varied from less than 1 minute to about 15 minutes.

MESON BEAM FACILITIES

The meson facility has been in use for some years. Referring again to Fig. 1 this facility consists of: (1) an internal meson target which may be moved both radially and azimuthally, (2) a thin window through which the mesons emerge from the tank, (3) a meson focusing quadrupole, (4) a wheel in the shielding wall with a diametral hole which may be aligned with the meson beam, and (5) the meson cave. Changes have been made to the window and to the quadrupole.

The previous meson window was actually two separate windows in separate ports on the tank. Then it was found that one of the best positions was in between the two ports. Recently the two ports have been made into one large port and one large window has been installed in this. This window is of aluminum 0.025 inch thick, 8 inches wide and 82 inches long.

The meson focusing quadrupole which had been in service for some years had become quite radioactive. In addition it has to be located in an area which has the highest activity of any place within the shielding but outside the main vacuum tank. This is the area which is bombarded by that part of the

beam which is only partially deflected and does not actually get through the magnetic channel. Positioning of this quadrupole for the various meson beams, both in translation and rotation, was previously done manually and was one of the biggest sources of radioactive exposure for the crew.

The new quadrupole has a remotely controlled mechanism which permits positioning of the magnet from the control room . This is shown in Figs. 10 and 11. The quadrupole may be translated parallel to the shielding wall both vertically and horizontally and also rotated about a vertical axis. Power is supplied by air motors. In addition to reducing radioactive exposure of the crew, more optimum meson beams can be generated since the quadrupole can be positioned during operation of the Cyclotron.

ACTIVITY PROBLEMS

"Improving a synchrocyclotron" somehow implies a rise in the activity level of the machine. At a conference on improving synchrocyclotrons it is therefore appropriate to say a few words about the present problems encountered in making repairs and alterations to an existing "unimproved" machine.

The 184-inch Cyclotron was rebuilt seven years ago in order to double the energy. At that time essentially all the then active parts were replaced. Since then it has been working steadily on a three-shift basis. The average internal beam current has been 1-2 microamperes. At least 95% of the running time has been with 730 MeV protons.

It is possible for the crew to enter the vault immediately after the beam is turned off to make quick changes or minor repairs. After cooling for a day or less, the radiation level in the cyclotron vault has dropped so that a person can safely spend an 8-hour day in it, provided he stays a few feet away from the one or two most active spots.

Two examples of repairs or alterations to the machine will serve to illustrate what can be done at the present levels of activity and what might be done at higher levels of activity.

Last year part of the dummy dee fell off. This was the result of eddy current force due to the collapse of the magnet field under fault conditions. To make the repairs it was, of course, necessary to enter the tank. The machine was cooled off for three days. However, after the first few hours the reduction in activity is very slow. Two men who had had little recent radioactive exposure were elected to do the work. They each stayed in the tank for about ten minutes and during this time each received about 200 - 500 mR. If the annual allowable dose is 5 R and if this is spread evenly over the year, then the allowable weekly dose is 100 mR. On this basis they each received a maximum of a five-weeks' dose. It would have been possible for them to have remained in the tank six times longer (one hour) and still not have exceeded a "reportable incident" dose (3 R). At this time the hottest spot that was observed was on the stainless steel ion source tube, which was near the beam exit radius where it received splatter from the regenerator. The activity measured 50 R/hour. The ion source tube was removed during repairs.

Another example is the work which had to be done to change two ports into one port to accommodate the new meson window. As noted before, this is in the hottest spot inside the shielding but outside the tank. The work involved several days' effort in burining and welding in the active steel. In this case the work was done three weeks after the machine was shut down. A four-inch thick wall of lead bricks was stacked inside the tank to protect the workmen from the activity inside the tank. This reduced the activity in the working area by a factor of two. Each of seven welders

worked eight - ten hours in the area. The maximum dose was 270 mR, the average does was 1140 mR. If one man had done all the work, he would have received about 1 R, still well within an acceptable limit.

It was considered advisable to prevent (1) the inhalation of the active iron vapor by the welders and (2) the spreading of active particles around the building. To achieve this, a wooden frame covered with sheet plastic was built around the immediate area, totally enclosing the welder and the work. The welder wore a mask with a hose leading outside the enclosure. The atmosphere inside the enclosure was continually changed and was passed through a filter before being discharged into the building. The filter was monitored but no activity detectable with an ordinary Geiger counter was found.

It is apparent, then, that the present level of activities can be coped with in a very safe and conservative way. With extreme care and careful planning, activities up to say ten times the present levels could possibly be tolerated. Activities, beyond this point, while not necessarily impossible, would require extraordinary measures and be extremely difficult to handle.

ACKNOWLEDGMENTS

I would like to thank J. T. Vale, L. R. Glasgow, R. L. Fulton and N. W. Yanni for their kind permission to blatantly plagiarize from references (1) and (2). I would also like to thank H. W. Patterson for supplying information on activity levels.

REFERENCES

1. J. T. Vale, 184-inch Cyclotron, Lawrence Radiation Laboratory internal report for May through October, 1963.
2. R. L. Fulton, L. R. Glasgow, N. W. Yanni, Modifications to 88-inch and 184-inch Cyclotrons: Biological Research Facilities, Lawrence Radiation Laboratory Report No. 11128, November 14, 1963.
3. R. W. Boom, K. S. Toth, A. Zucker, Residual Radiation of the IRL 184-inch Cyclotron, Oak Ridge National Laboratory Report No. 3158.
4. R. Smith, K. R. MacKenzie, J. Reidel, Q. Kerns, W. R. Baker, C. W. Park, R. L. Thornton, The Electrical Aspects of the UCRL 740-MeV Synchrocyclotron, 1957 I. R. E. Wescon Convention Record.

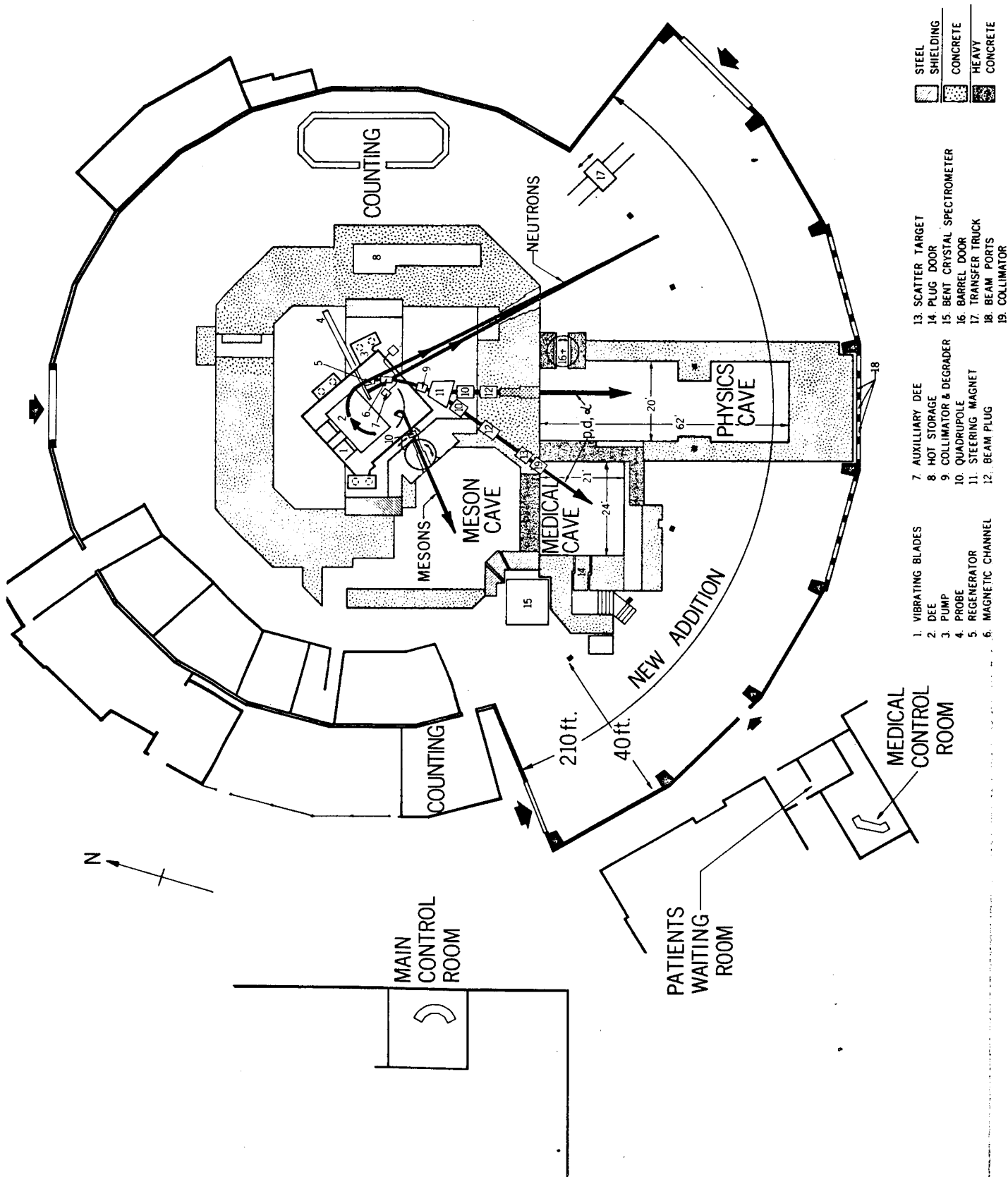


Fig. 1 Schematic plan view of the 131 inch cyclotron and building showing the new experimental facilities.

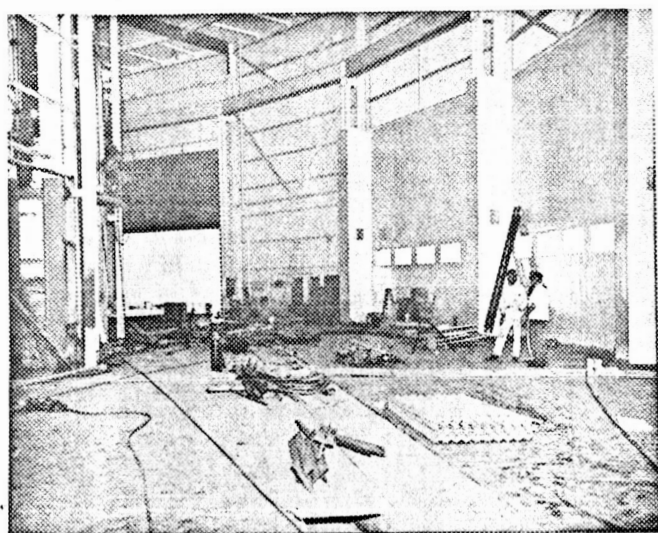


Fig. 2 Interior View of the New addition to the Cyclotron Building. The "gun-ports" for extending particle-beams outside the building may be seen to the right.

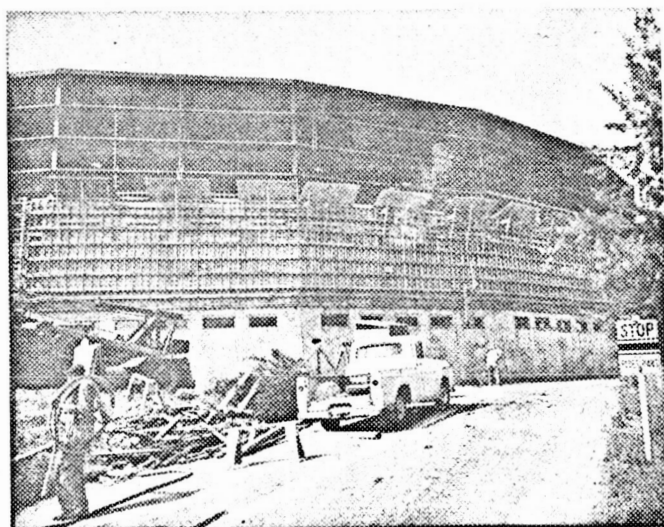


Fig. 3 Exterior View of the New Addition to the Cyclotron Building. The portion of the wall which is concrete is to provide continuous shielding between the exterior and interior experimental areas.

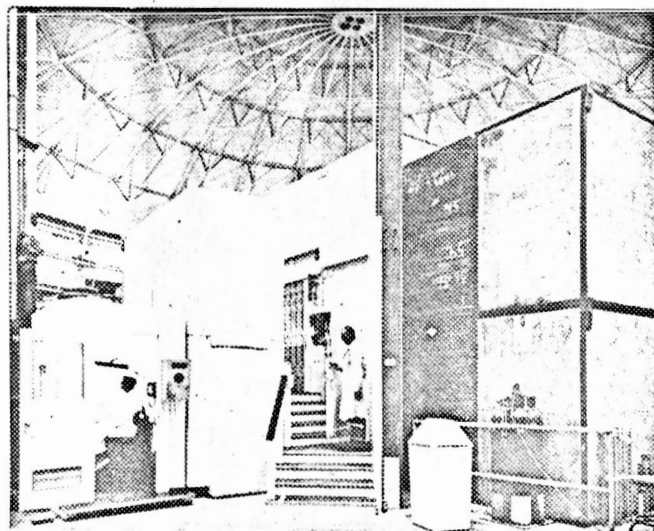


Fig. 4 Entrance to Medical Cave. The hydraulically operated plug door is behind the folding safety door in the center of the picture. The nurses sentry-box to the left is provided with a TV receiver for viewing the patient.

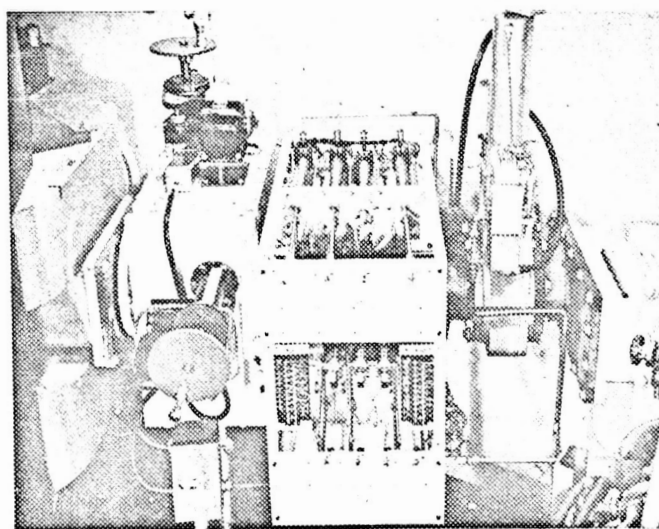


Fig. 5 Degradator and Collimator for Deflected Beam. The beam enters at right. Reading from right to left: beam port, vacuum valve, degrader, collimator, steering magnet.

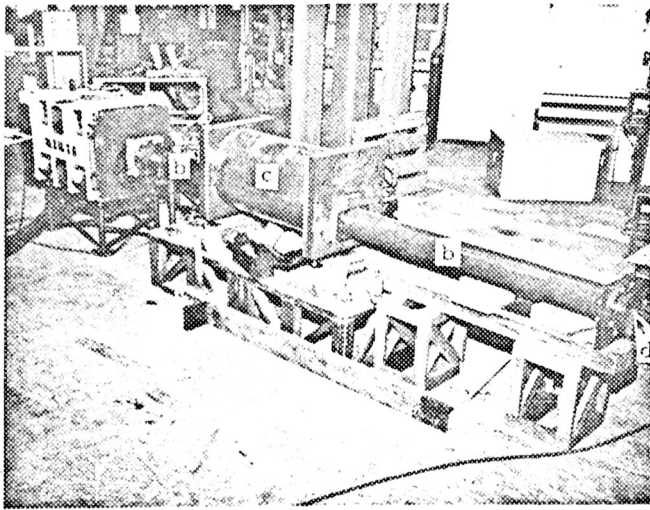


Fig. 6 Part of Beam Transport System for Medical Cave before Installation. Beam enters at left. (a) quadrupole, (b) beam tube, (c) beam plug, (d) vacuum window.

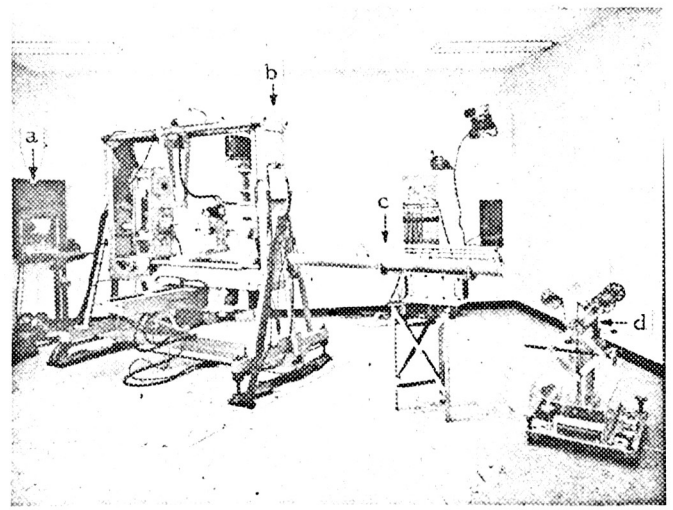


Fig. 7 Interior of Medical Cave. (a) beam entrance, (b) human positioner, (c) scattering-target loader, (d) animal rotator.

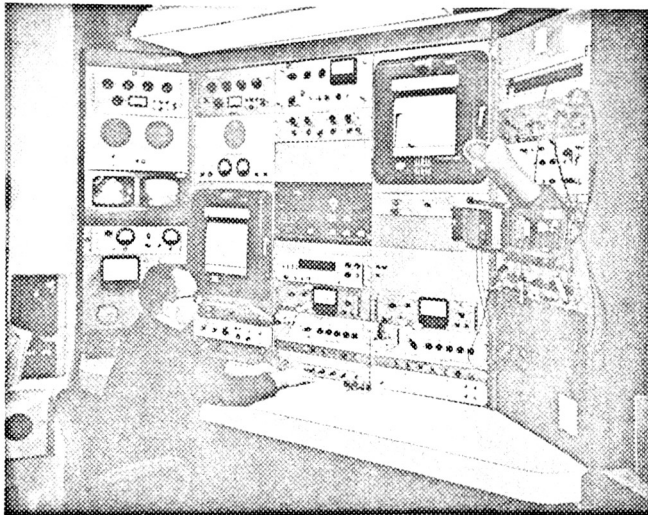


Fig. 8 Medical Control Room. Facilities include TV receivers for viewing patient, dosimetry, remote controls for positioner, and "off" control on the Cyclotron.

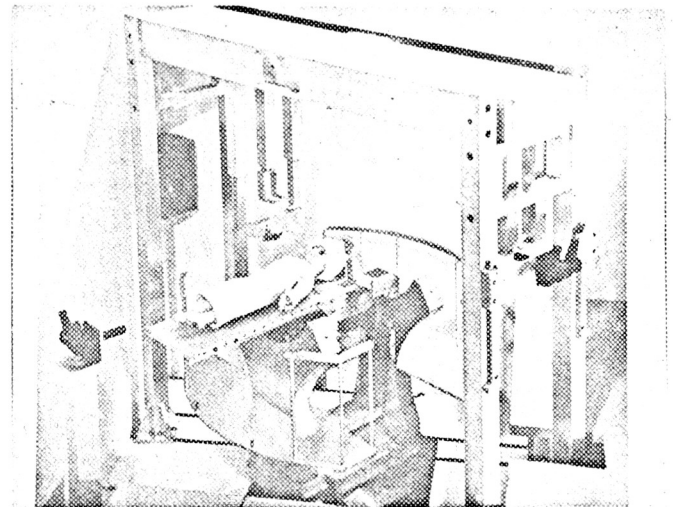


Fig. 9 Model of Proposed Human Positioner. This device is designed for irradiation of any part of the body.

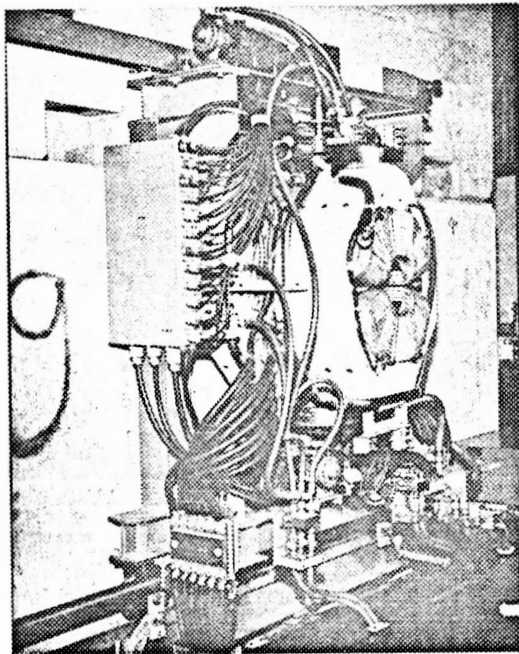


Fig. 10 Meson Focusing Quadrupole before Installation. Quadrupole may be remotely rotated about a vertical axis, and remotely translated horizontally and vertically.

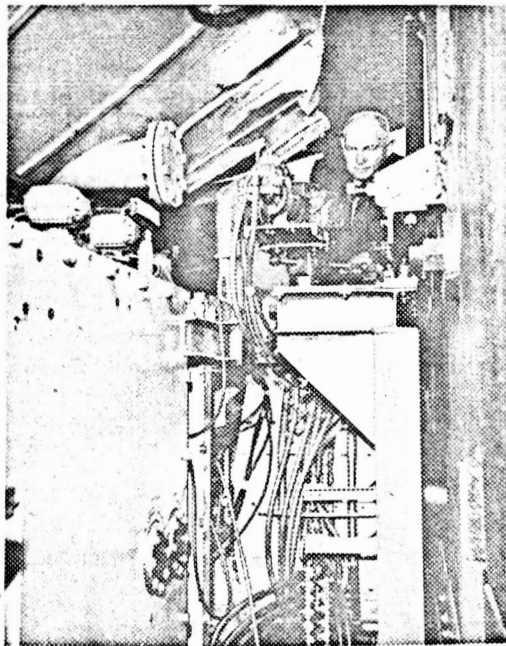


Fig. 11 Meson Focusing Quadrupole after Installation. The dee tank is on the left and the Meson Cave shielding wall is on the right.

SOME REMARKS ON THE BERKELEY 184 "CYCLOTRON"

Kenneth M. Crowe
University of California

In discussing the performance of a machine which has been in operation for many years there are many possible subjects which come to mind. The synchrocyclotron has a reputation of being extremely simple and reliable. The improvements made in the basic operation of the machine in the last 10 years are of two types. On one hand is the item of efficient extraction of the beam to external areas and the improvement in the duty cycle of the beam. The other type of improvement consists of developments of the apparatus, facilities, and reducing backgrounds to increase the usefulness of the machine as an experimental device. In this discussion there will be no mention of possible improvements that do not promise to affect the usefulness of the machine dramatically.

Our ion source is a hooded arc with a filament heated 41 Kc A.C. The ions emerge from a slot $1/8" \times 3/4"$ parallel to the "D" edge, off the center of the machine. The ion beam is 150 ma and delivers an average of 400 μa of ions during an effective pick up time of 30-50 μ sec. The ion beam without the accelerating r.f. is a ribbon along the vertical magnetic field. With r.f. the region of ions probably expands enormously and approximately 1% of the beam is successfully accelerated.

The accelerating voltage is approximately 10 kv peak and has a frequency swing from 38 Mc to 20 Mc, during which the amplitude goes through a flat maximum. The frequency modulation is accomplished by use of a pair of resonant reeds vibrating at 64 cps to approximately 1" amplitude.

The beam is limited in vertical extent by the dee aperture and appears to travel with minor loss from 10" to 60" in radius. (Full radius 82".)

The absolute monitoring of the beam current is poor. One device is a copper block absorber, placed in the beam. It is 6 inches thick in the beam direction and enclosed in an electrostatic shield. It works well as long as the protons don't emerge from the back end of the copper block. It is particularly useless as soon as it gets into the region where the interest would be in the beam behavior because the sign of the collected charge reverses, reversing the current reading. It oscillates around as it goes out in radius so it isn't believed possible to use this device as beam monitor over any variable radius. There is a pressurized ion chamber 1" in diameter which can be put in the beam. However, it is particularly useless because it is usually always saturated; it reads a constant everywhere.

Solid state detectors, selenium rectifiers, copper oxide rectifiers, etc., have been used. They produce very nice signals of high quality in terms of noise background, but their calibration is unknown and subject to uncertainty connected with multiple traversals which are not only unknown but also are variable as the radius is changed.

We have also used a secondary emission monitor probe. It consists of a set of foils tilted at an angle to the magnetic field such that low energy secondary electrons follow the magnetic field paths and can be collected on alternate foils even in the presence of 22 kg fields. It suffers from the same problem as the other types of probes, namely the beam walks its way into the device and if the beam does not have a large turn-to-turn separation, the particles which are scattered off the outside

edges of foil possibly contribute to the reading. It is, in general, not a very reliable device. However, in measurements on the regenerated beam, since the beam does get separated from the circulating beam, the device acts reliably with a very constant and reproducible behavior. In conclusion, we do not have any adequate monitoring devices and none of them are really reliable.

Our machine is unique in the sense that it can presently accelerate protons, deuterons, He^3 , He^4 . In order to do this it requires an extensive and expensive change in the r.f. system but it provides more flexibility. Most of the physics use of the machine is with the protons, whereas the medical exposures that Dick Burleigh mentioned are done with alpha particles to get the highest specific ionization. So the machine is definitely switching back and forth. Operation for medical use represents about 10% of the total time. The down-time for maintenance of the machine is about 5%. Most of that occurs during scheduled shutdown, so that the innage time is greater than 95%.

The beam pulse is approximately 5 nanoseconds wide, separated by the reciprocal of the final frequency, 50 nanoseconds. A normal beam burst will last for about 400 microseconds, with a repetition rate of 64 times a second. The vertical height of the beam at small radii is the dee aperture, about 4 inches. It damps down to about 2 inches at full radius.

The radial oscillations are quite large in the machine. Interestingly, the contribution to the radial oscillation amplitude from magnetic field inhomogeneities is small. By taking the first harmonic content of the field and analyzing it as a function of the radius, it seems as though less than an inch of radial oscillation amplitude can be thus accounted for in this manner. On the other hand if we look at the time spread of the beam as it

arrives on a target, the length of the pulse which occurs can be related to the rate of change of frequency and one can extract the information on the width of the sausage as it bumps into the target. The conclusion is that at least 6 inches of radial oscillation amplitude is present in the beam. In other words it is about a foot wide as it sweeps out. This seems to be quite an extreme number and it will be interesting to see if other people have as large radial oscillations. The conclusion is that this may be connected with have a very large extended ion source for the beam and it is clearly one of the reasons why attempts at regeneration in obtaining an external beam represent rather poor compromises. The vertical size is rather well contained, but the radial size is much larger and causes most of the trouble. An interesting aspect that is observed is that when the temperature of the ion source filament is increased in order to increase the beam, the length of the arrival of the beam on a target fills in, swells, and grows. So it appears that there is partial confirmation that it is the behavior of the ion source that influences the radial oscillation distribution.

Turning next to the extraction system; the beam is regenerated well inside any of the resonances. There is a problem in that the beam must be shot through ports which were determined by the location of the major shielding components at the time the regenerator was designed. This causes some rather severe restrictions as to where things could be placed in the machine. A regenerator design was formulated which involved rather large amplitudes of regeneration in order to feed the beam through a channel which would eventually go into the experimental areas. The main magnetic field is about 22.4 kilogauss, the magnetic perturbation at the full amplitude of the regenerator is about 6 kilogauss, so the peak magnetic field

runs well over 28 kilogauss. The amount of deflection is about 100 kilogauss degrees in radial extent. The final radial orbit separation is about 8-1/2 inches. The node crosses the equilibrium orbit approximately 110 degrees ahead of the center of the regenerator. A probe line is approximately along the same azimuth as the regenerator itself and we can photograph along this line the shape of the beam. Figure 1 shows the beam size at the magnetic channel, an inch in radial dimensions and around 1/4 inch in the vertical direction. The beam is then carried out through a strong focusing lens set, consisting of the fall-off of the field, then a reversed lens having an aperture of $\sim 10''$ of constant gradient of 1.1 kg/in. giving no net deflection, and then the remaining fall-off field of the cyclotron. The beam then emerges from a hole in the tank and enters the beam transport system. This combination of these three lenses represents an attempt to bring the beam through an alternating gradient lens system and to focus it as well as possible. It is only possible by the dimensions and the sizes of gradients to make the beam parallel, whereas the desired effect would be to cause the beam to come to focus at the location of beam-defining copper block slits and degraders. Because of the geometrical confines of the building another lens could not be provided to focus at the slits.

Turning next to a summary of the beam current inside the machine; at r less than 10 inches, it is believed there is between 10 and 50 microamps of beam accelerated. This is a guess; it represents what one calculates from the size of the beam present in the ion source and a reasonable figure calculated for the collection efficiency at the center of the machine. The beam is quite rapidly dropped to around 4 microamps at radii greater than 30 inches and probably 2 microamps survive to about 78 inches. There is no

activity produced on the edges of the dees where the beam should hit and therefore probably not more than half the beam is lost between 10 and 30 inches. Beyond 30 inches, assuming the limiting aperture to be that of the dee, a beam current of two microamps is measured by carbon activation. In the next three inches we lose quite a bit of beam, e.g., about $1/2 \pm 1/4$ microamp at the entrance of the regenerator. Beyond the regenerator, in the fish, we have about .2 microamps with very little uncertainty. So it seems that between 78 inches and 81 inches part of the beam which has large vertical amplitudes is probably lost due to the onset of the regenerator field. About 30% of the beam which remains at the entrance to the regenerator is successfully regenerated. This is not a surprising number. It is typical of what would be calculated if looking at the stability band for the regenerator action. In the experimental cave the maximum beam that has ever been measured is about $1/10$ microampere; in other words, a factor of 2 is lost going from the fish through the channels, through the bends and through the quadrupole out to the cave. A momentum uncertainty, dp/p , is less than 1% and a beam size of $1/2" \times 1/2"$ is obtained by collimation and refocussing out into the cave. This causes a loss by at least another factor of 5. So there is lost a factor of 10^4 going from $400 \mu a$ at the ion source to $0.02 \mu a$ in the experimental cave. This seems to be something which should be able to be improved by at least a factor of 10 and which, it is believed, is one of the outstanding possibilities for this machine.

Turning now to duty cycle considerations, there will probably be repeated some of the things that have been said by other speakers. There are three duty cycle methods. The one most popular for internal bombardment consists of vibrating a target vertically in the magnetic field;

e.g., driving the beam to full radius and then raising a target into the beam. If done at the right rate by intercepting the beam uniformly in time, perhaps a 50% variation in the envelope is possible. This method has the distinct advantage that the fine structure that is present in the beam, as it is delivered to full radius, is lost as soon as the r.f. is turned off. Hence the inherent duty cycle for the vibrating target, including the fine structure, is probably on the order of 50%, whereas the inherent duty cycle for the devices where the r.f. structure is still present, namely the stochastic type or the method that is used at Berkeley which is called the synchronized extracting system, is something like 10%. So using synchronized extraction, even though the beam apparently is stretched to something like 80% of the time, there is still the r.f. structure resulting in around 10% at best for the duty cycle. Since the vibrating target is of no value for external beams and since at least half of the operations on our machine involved using the external beam, concerted effort three or four years ago was given to working out a method of trapping the beam at full radius and then peeling it off slowly into the cave. This method, synchronized extraction, is done by the following system: when the particles reach nearly full radius we turn the main r.f. off and turn on another dee or cee similar to the one at Carnegie Institute of Technology. It looks the same; it is narrower and the voltage is a little higher. It's about 12 degrees in azimuthal extent, 10 inches in radial extent and has a vertical aperture equal to that of the main dee, about 4 inches. It is powered with about 4 kilovolts of peak r. f. voltage compared to 10 kilovolts on the main dee and provides an acceleration on the order of 800-900 volts. The idea is that there is a bucket of particles coming out with the main r.f. program having a well defined boundary in

phase angle and energy. An attempt is made to dump this bucket of particles into another bucket which is represented by the auxiliary dee or cee, and try to make sure that it fits; e.g., the effort was made to make sure the auxiliary bucket is deep enough, the r. f. voltage is high enough, and the phase is more or less centered about the phase of the up-coming bucket so that there is an efficient transfer. Now the best that has been done with the transfer is the order of 50% for the externally regenerated beam and something like 30% for the internal target beams. It is possible to get numbers much higher than this by restricting the way the beam is delivered to the system. Namely, if the beam is turned down and restricted in its radial oscillations and probably its phase oscillations, then something like 80% efficiency is achieved for transfer from the main dee to the cee. The stability and reliability of the system has been improved over the last three years. There are very few experiments outside the medical irradiations where it is not necessary for the experimentors to use this beam stretching device and it is now an accepted part of the machine. Fig. 2 shows the rather small oscillator, using a 10 kilowatt water-cooled tetrode to drive the cee. The system is broad-banded similar to the one that was shown at Carnegie Institute of Technology. A water-cooled resistor is used to drop the Q to about 30. The system is driven with a broad band drive line. The r.f. phase information on the main dee is fed into an oscillator which turns on the r.f. on the cee in phase synchronism with the bunch of arriving particles. Fig. 3 shows the performance of the system. The top trace is an envelope of the main r. f. system. The second trace is the tailored cee r.f. envelope; it was thought that at the point of transfer from the main dee to the cee it might be desirable to have a little more

voltage on the cee at the beginning part of the cycle. However, we found it didn't make any difference. The third trace is a voltage proportional to the frequency of the cee and dee system. The bottom trace shows the external beam current. There is a little spike of beam that comes out at first. This can be adjusted by making sure that the transfer frequency from the dee to the cee is early enough so that no beam can sneak out before it is stacked in the cee. The frequency swing on the cee is about 200 kilocycles and it is made linear in time. However, at the end of the sweep, to make sure that there are no particles left inside, we sweep the cee frequency faster, causing the last bunch of particles to come out almost instantaneously. The time structure in the beam is apparent from the bottom trace. It seems to have the phase oscillation period which corresponds to the voltage on the cee. In other words the particles are rattling back and forth in the cee bucket and when a certain fraction of them get to the extremes of their phase oscillation amplitude they appear to be radially accelerated and will then come out through the extraction system. It is very critical where the change-over from the dee to the cee occurs. It can't jitter by a fraction of a microsecond, surprisingly enough. Fig. 4 shows the effect of bringing out an external beam abruptly but delayed in time. The top trace shows the normal beam. The second trace shows a delayed beam and the third trace shows a beam delayed many times the 64 cycle repetition rate to find beam loss during storage. Experiments made in Berkeley by Crawford and Stubbins many years ago showed that if the r.f. is turned off and the internal beam is left at full radius it stays there for something like 10 minutes. One can turn off the machine, open the door, go in and shove a probe into the beam and there is the beam. However, in the case

of the external beam, Fig. 4, there is evidence that it is decaying. Since the dee r.f. is on each f.m. cycle one might think that the dee r.f., which sweeps through the beam, drives the particles out. It has been determined that it does not. There seems to be a real beam loss due to some other effect. The long time constants associated with the stored beam depend on plural scattering of the beam in the residual gas, and hence depends on the dee aperture. Now the external beam does not have the same aperture requirements as the internal beam since it has had to come out through the regenerator. So as soon as the beam scatters as much as $1/8$ inch off axis it cannot be successfully regenerated. A calculation gives a lifetime of around 20 milliseconds against plural scattering for particles to scatter outside $1/8$ inch, thereby explaining this attenuation. Fig. 5 shows again the effects of storage for the external beam. The top trace shows a normal beam being brought out. (The pips make successive f.m. cycles.) The burst at the far right of the top trace is a successive beam being brought out normally (no delay). The middle and bottom traces show the effect of storing the beam through successive dumps; having gone through two of them on the bottom trace. Noticeable is the effect of loss of external beam intensity due to storage. If the dee r.f. is turned off during storage the situation does not change very much. In other words, there could be another 50% attenuation due to the interference of the r.f. with the beam that is stored. But the main effect that is observed is that the beam is scattered out by the gas.

Fig. 6 shows the measurements that were made at CERN on the stochastic system. In these studies a beam is injected only for one f.m. cycle and the effect of storage during successive cycles is observed. The top trace shows the dee r.f. envelope. Notice that the r.f. envelope at the time

these were taken, which was a year ago, had a maximum at the end of the f.m. cycle. The extracting electrode or cee had a 2 or 3 per cent 60 cycle frequency modulation. The bottom trace represents the cee frequency variation as a function of time. The third trace down shows the r.f. voltage wave form on the cee and shows the effect of the finite Q of the system giving an amplitude variation due to the change in frequency. The second trace down shows the external beam current in time, the bumps lining up with the cee sawtooth frequency variation. Fig. 7 shows a horizontal enlargement of Fig. 6. From top to bottom: external beam, cee r.f. envelope, dee r.f. envelope, and cee frequency. Evidence of the correlation between the peaks of the extracted beam and the frequency modulation sawtooth is apparent, e.g., the system rows the beam out by passing buckets through the original beam bucket. There are about 10 sawtooth periods per f.m. cycle and about 20 sawtooth periods after the maximum of the beam has been obtained. Notice that the parameters which represent the normal operation of the CERN machine have made the decay period of the stored beam about equal to the repetition frequency of the main r.f. system. Chances of this being an accident is unbelievable; however that is just about the way it would work out in trying to achieve both a uniform distribution of particles and an efficient extraction. The periods would probably come out matched as they are. Fig. 8 displays a little clearer the exponential decay of the stored beam, (third trace from the top). Fig. 9 shows the results when the f.m. sweep rate on the cee is decreased. There is a definite correlation in the peaks of the beam current with the frequency that corresponds to extraction.

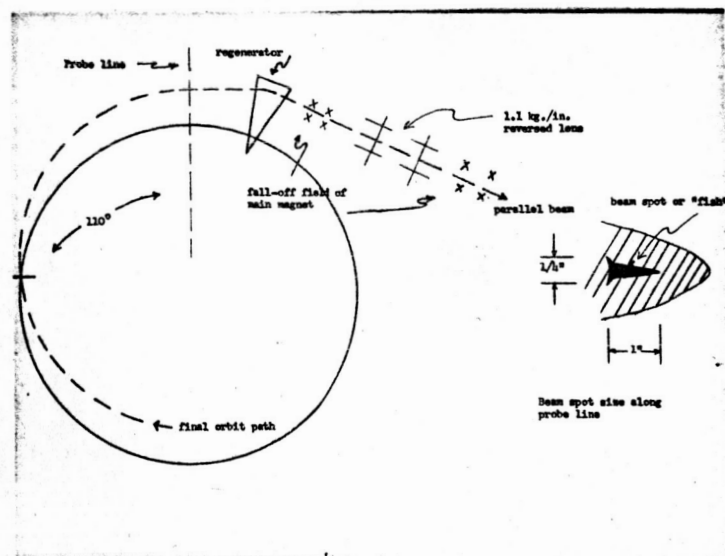


Figure 1 - Schematic of regenerator and focussing lenses for external proton beam. On the right is a representation of the beam spot size of last orbit along probe line.

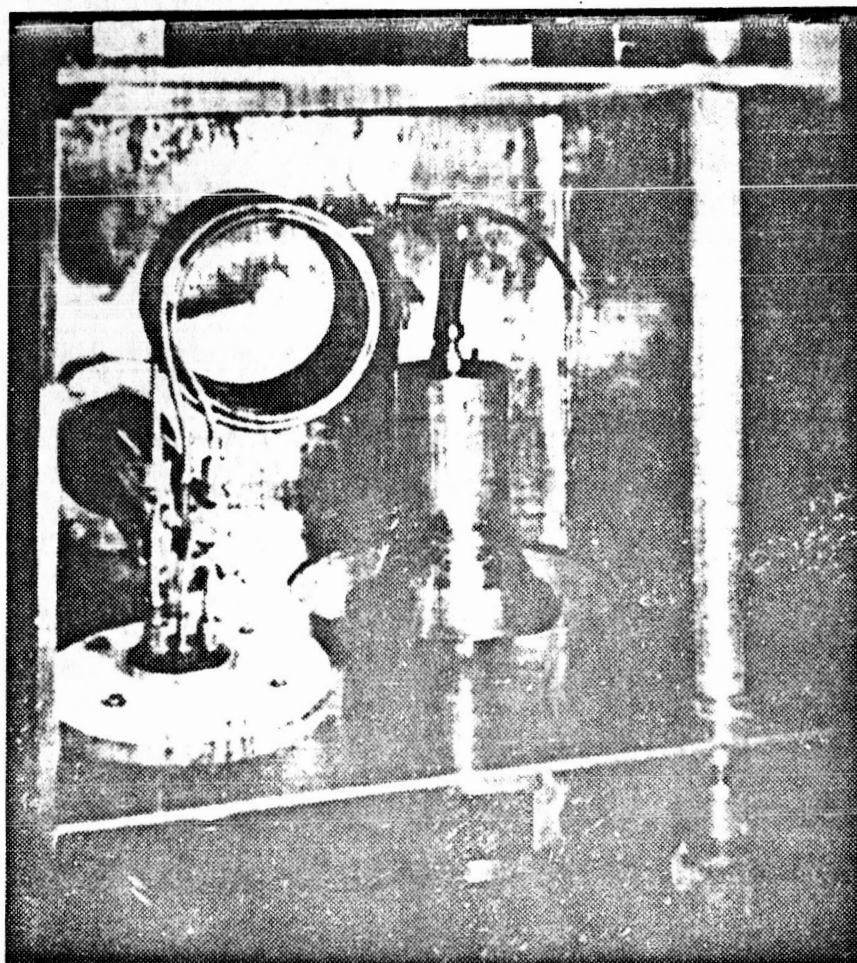


Figure 2 - View of the final amplifier.

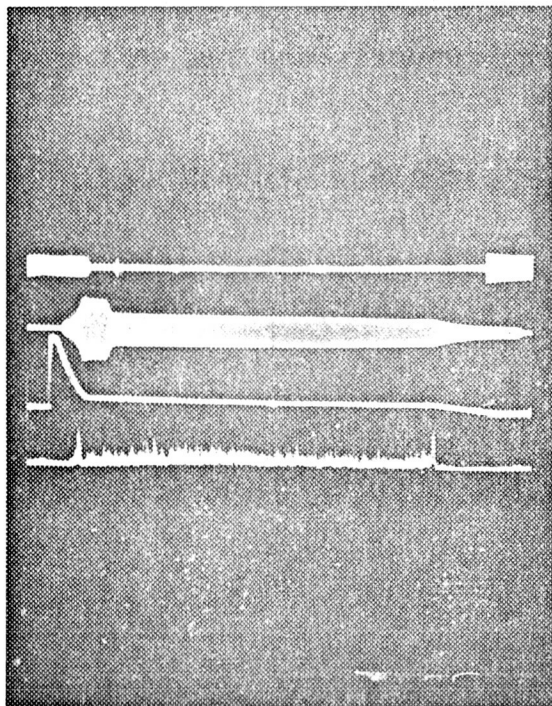


Figure 3 - System performance. From top to bottom dee r.f., cee r.f., system frequency, beam structure.

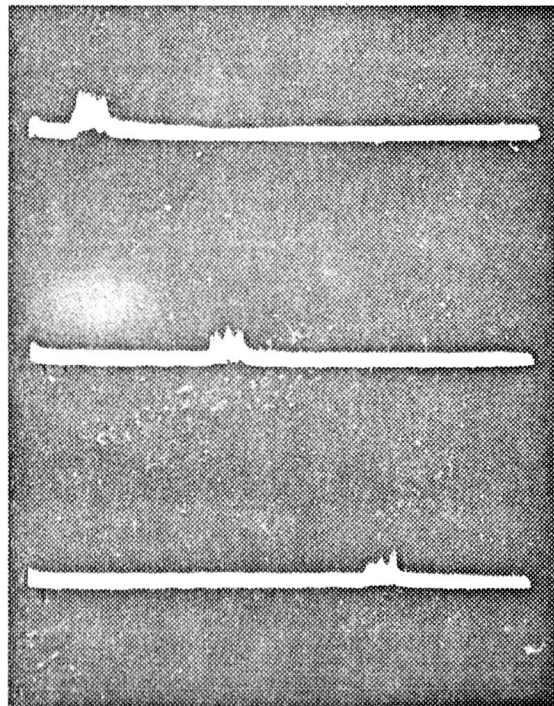


Figure 4 - Results of beam storage for external beam. From top to bottom: normal beam, moderate delay, delay several times the f.m. cycle.

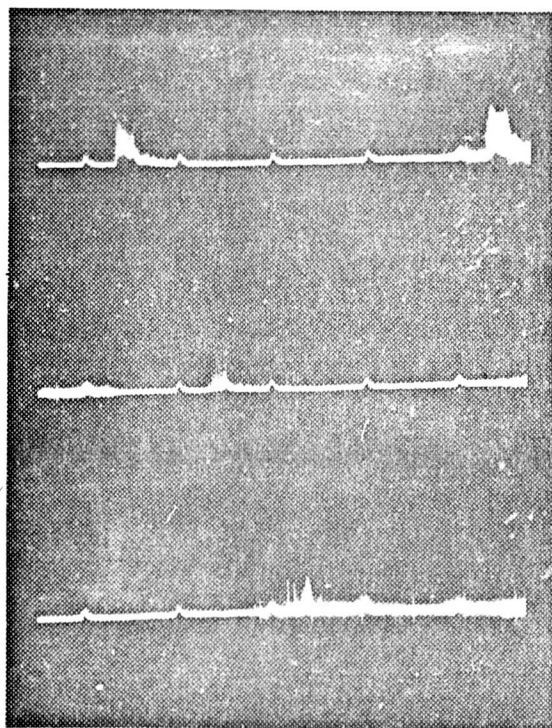


Figure 5 - Results for beam storage for external beam. Top trace shows normal beam. Amount of delay can be judged by number of successive pips, each corresponding to a new f.m. cycle.

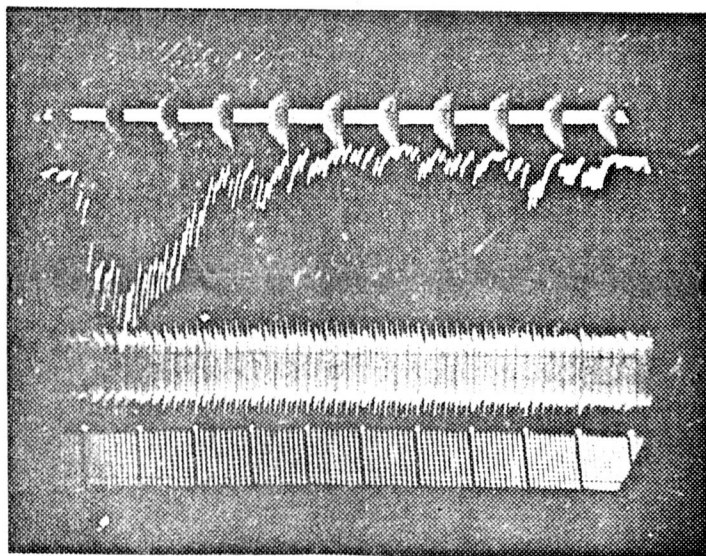


Figure 6 - Results for CERN beam storage and cee extraction. Top to bottom: dee r.f., beam structure, cee r.f., cee frequency with time.

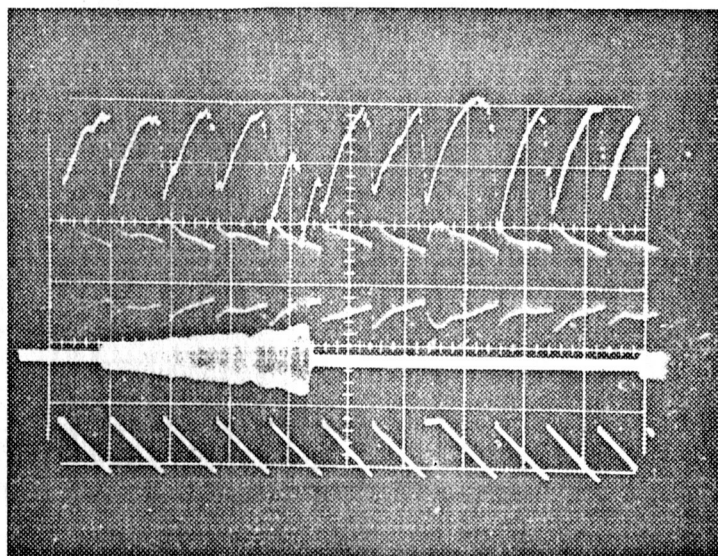


Figure 7 - Results for CERN beam storage and ces extraction. top to bottom: beam structure, ces r.f., des r.f., ces frequency with time.

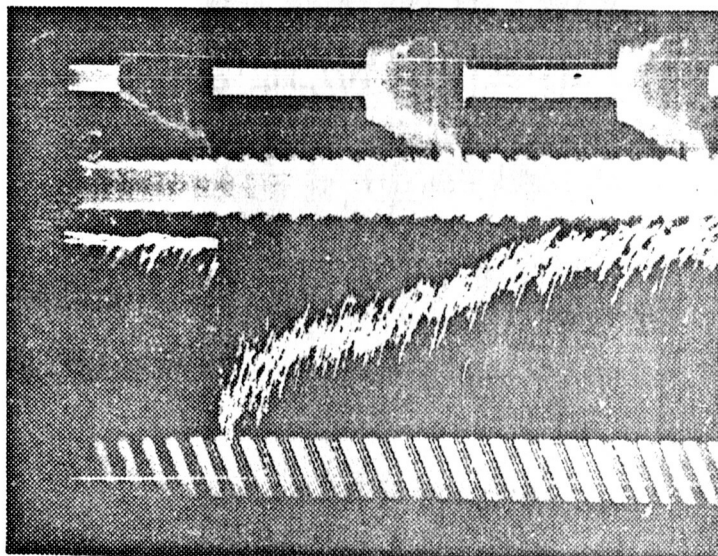


Figure 8 - Display of exponential decay of stored beam, third trace from top.

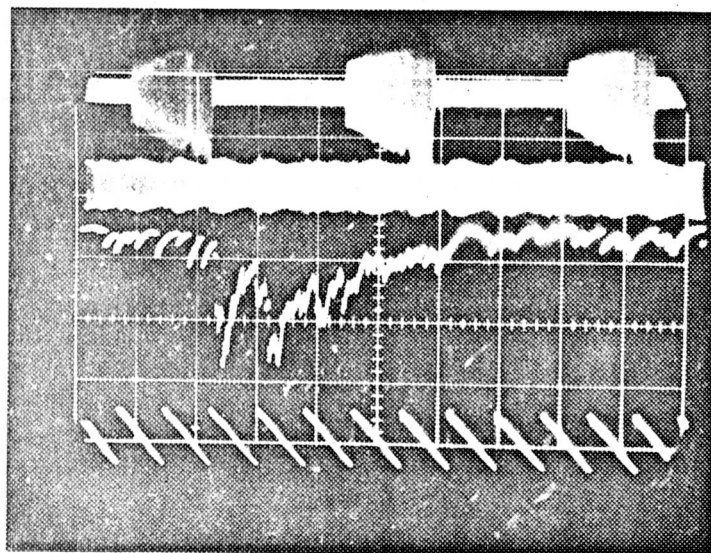


Figure 9 - Same as Fig. 8 but with decreased ces f.m. sweep rate.

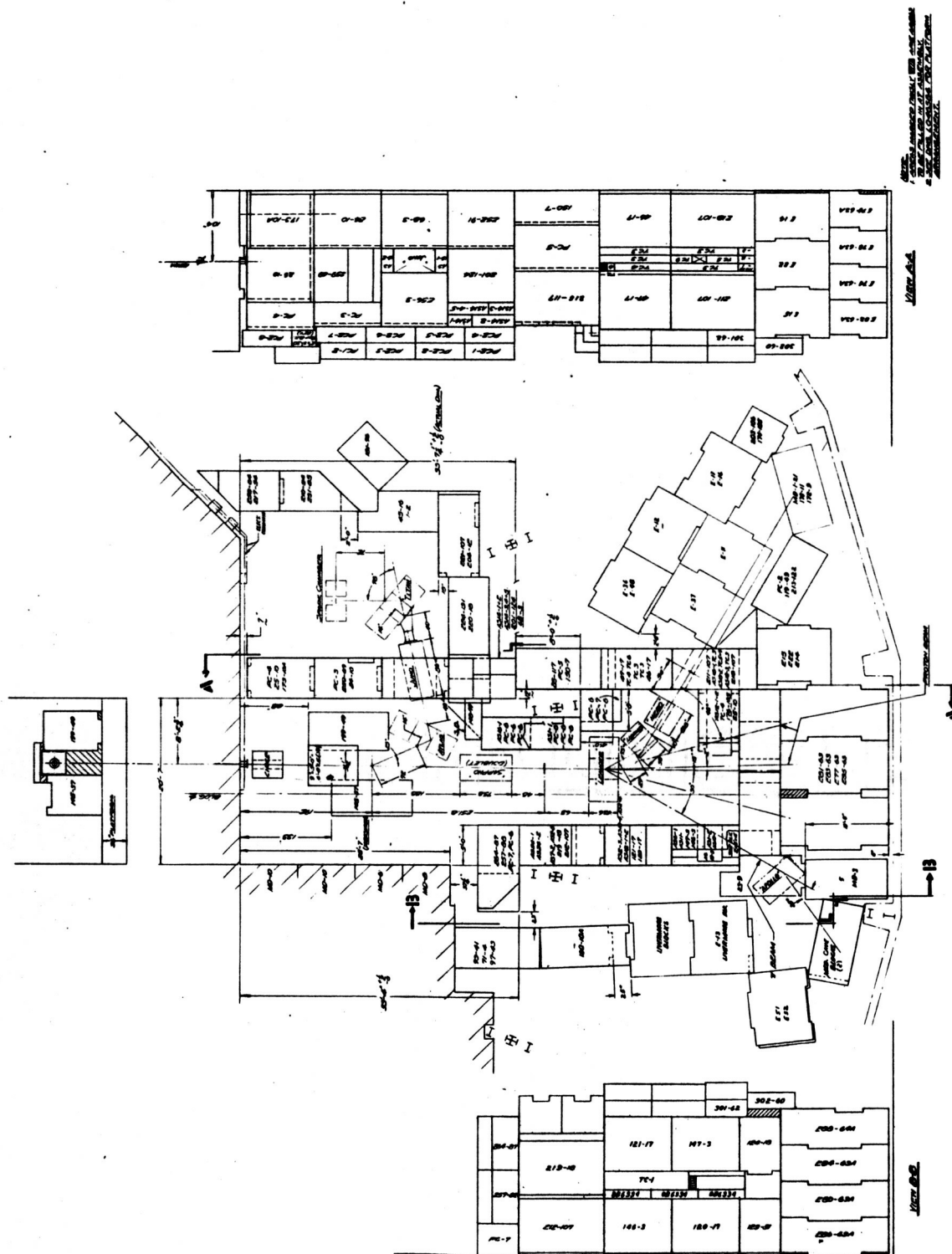


Figure 10 - Plan drawing of external beam facility.

Table I. Results of measurements of the secondary π^+ beam

Momentum (MeV/c)	Main cyclotron field	Meson-wheel angle (deg)	Meson target position		Relative intensity ^a	Remarks
			Radius (in.)	Azimuth (deg)		
170	normal	16.4	82	250	0.6×10^6	b
180	normal	17.5	82	250	3.5×10^6	
200	normal	17.5	80	254	3.2×10^6	
225	normal	17.5	80	259	1.7×10^6	
225	normal	17.5	78	254	1.7×10^6	
250	normal	17.5	80	266	0.7×10^6	
250	normal	17.5	90	242	0.7×10^6	
250	normal	8.5	81	270	1.2×10^6	
275	normal	8.5	79	270	0.7×10^6	c

a. Particles per minute passing through a 4-by-4-in. lead collimator. The meson quad was turned off during these measurements.

b. No space available for internal quadrupole magnet.

c. Greater intensities possible at azimuths greater than 270 deg.

Figure 11 - Fluxes of internally produced π^+ beams.

Table II. Results of measurements of the secondary π^- beam

Momentum (MeV/c)	Main cyclotron field	Meson-wheel angle (deg)	Meson target position		Relative intensity ^a	Remarks
			Radius (in.)	Azimuth (deg)		
150	reversed	16.4	82	215	0.1×10^6	b
180	reversed	17.5	82	251	1.8×10^6	
200	reversed	17.5	80	251	1.1×10^6	
225	reversed	17.5	77.5	251	0.7×10^6	
225	reversed	8.5	82	265	0.9×10^6	
250	reversed	8.5	81	270	2.2×10^6	
275	reversed	8.5	80	261	0.7×10^6	
300	reversed	8.5	80	258	0.3×10^6	
350	normal	-2.25	81	256.5	1.2×10^6	
400	normal	-2.25	81	251	1.5×10^6	
450	normal	-2.25	81	248	1.0×10^6	

a. Particles per min passing through a 1-in.-diam lead collimator. The meson quad was turned off during these measurements.

b. No space available for internal quadrupole magnet.

Figure 12 - Fluxes of internally produced π^- beams.

TELEGDI, Chicago - Do you have a wattmeter on your target?

CROWE - No.

FOSS, Carnegie - Did you observe that the fine structure disappeared when you turned the r.f. off?

CROWE - No, we haven't made any measurements like that.

FOSS - There's a possibility of space charge bunching.

MICHAELIS, CERN - In connection with the amount of your radial oscillation amplitude, we made a similar study by storing the beam at various radii and seeing what came off a target. In this way we got a radial amplitude which is about half the size of yours.

CROWE - That's about 3" in amplitude or 6" in extent. That's not outside of our experimental error.

RIND, NASA - In using the copper oxide and selenium rectifier beam monitors, how long do they stand up under radiation?

CROWE - They stand up long enough to show that they work; we've used them for the order of a day or two.

BEGER - As soon as you can calculate the number of multiple traversals, you can have quite a reliable device by using a thermocouple.

TELEGDI - I think we should measure the internal beam in watts which is really what matters. You can then make a comparison without a knowledge of anything except dE/dx in beryllium.

CROWE - and multiple traversals which are not the same for all machines.

TELEGDI - Yes, but from the experimental point of view the number of multiple traversals enters already in which you can produce.

CROWE - Yes, that tells you the pion yield. We could also measure the pion yield off a target.

SHERR, Princeton - Is there a standard method of measuring the duty factor when using stochastic type extractors?

CROWE - Our method consists of running the beam for around 50% of the time for its gross structure. I didn't mention that we feed back the beam structure into the frequency program to smooth out all its bumps and wiggles. It is a very beautiful operating part of the system. The fine structure duty cycle of the beam, e.g. the structure of the pulses of the main r.f., is 10-12%. It varies with the type of experiment and the specific tune-up of the machine by at least a factor of two. Our main duty factor is about 50%; we could make it 90% but we operate at 50% because it comes out smoother.

SHERR - What does this number mean? Is it $(i \text{ average})^2 / (i^2) \text{ average}$?

CROWE - Yes, it comes out close to this. It is the time during which the beam is on compared to the total time.

GOTTSHALK, Harvard - What are the advantages using your r.f. phase lock cee program vs a non phased program?

CROWE - I think they are quite equivalent, although ours is more difficult.

FUNSTEN, William and Mary - Our results at Princeton seem to indicate that, with our cee operating at very low voltage, if we made the cee frequency increase with time instead of decreasing with time you get a relatively better beam spread and more beam current. This seems to be in agreement with the Symon and Sessler "bucket" theory. How does your stretched beam current increase with r.f. voltage on the cee?

CROWE - With the phased system it is independent with voltage over about a kilovolt and its flat up to about 5 k.v. If you disconnect the phase loop, then there's a gradual increase from about 20% efficiency at 1 k.v. up to around 50% efficiency at 4-5 k.v. It seems to be gaining as you expect.

GOODELL, Columbia - When the Columbia synchrocyclotron was used with the slow neutron velocity spectrometer the beam is pulsed downward electrostatically into a target. The beam is limited in vertical amplitude by a little lollypop at about a 3"-4" radius to about 1" high. When the beam is about 2"-3" within the $n = .2$ point it passes through a pair of bananas of about 3" in radial extent and spaced apart about 1-1/2" and a pulse is applied driving the beam down. We find that 90% or more of the beam is delivered into the target in one r.f. cycle. This would mean that the full radial width at that point is of the order of 3".

CROWE - How long does the beam come out?

GOODELL - It comes out in a time equivalent to the length of the sausage-- a little more than 5 nanoseconds. We do not see two peaks spaced apart by an r.f. period.

CROWE - The 184" used to have an electrostatic extractor at one time and we saw three pulses, a little one, a big one, and a little one more or less the same as you describe.

HUXTABLE, Harwell - We have about the same results that the Columbia group has -- one pulse and about a 3" width.

CROWE - Isn't it possible that the beams at both the Harwell and Columbia machines are a fraction of a microampere? We would say so.

HUXTABLE - one and a half μa .

GOODELL - a fraction of a μa .

HUXTABLE - I would like to make an additional point. Some people find that their beam debunches when they turn the r.f. off and let it coast. We have found that some of the beam in our machine doesn't debunch and that, in fact, you still have a bunch of protons that are circulating around for .1 second or so.

MULTIPLE "DEE" SYSTEM FOR THE CHICAGO SYNCHROCYCLOTRON

E. H. Molthen, Chicago

I. INTRODUCTION

Improvements in the R. F. programming of our machine in view of an increase in intensity center primarily around two parameters of interest:

1. utilization of the dead time in the mechanical process of frequency modulation,
2. increase of voltage on the accelerating electrode.

With a quarter scale mock-up of the vacuum tank, we tested different geometries of accelerating electrodes to see how we could implement improvements along this line, using a Q-meter, RX-meter, and sweep generator at four times the acceleration frequency.

Through these tests, we found that we could use a power amplifier system to drive the accelerating structure. This type of drive would allow us to switch much faster than the mechanical system, and also allow changes in the envelope shape of the modulation program and the frequency wave form with respect to time at a small signal level.

In this report, we will briefly show the changes we intend to make on our machine and the improvements we hope to gain from them.

II. DEAD TIME UTILIZATION

Like most synchrocyclotrons, the Chicago machine uses a rotating condenser in the oscillator circuit for frequency modulation. Thus, somewhat less than half of the available time is used to bring the particles from the center to the periphery of the machine. This frequency program is depicted in Figure 1.

It starts at about 30 Mc (small capacitance of the rotating condenser) and ends at a little less than 20 Mc (large capacitance). Because the condenser blades are symmetrical, the rest of the cycle, represented as a rising change in frequency, is useless for acceleration of particles and is therefore gated out.

Various proposals to use this lost time have been made. Our idea is to use two accelerating electrodes instead of the conventional single dee. These two electrodes will be placed opposite each other, and will cover separate portions radially. The electrode at smaller radii is a "dee", the one at larger radii a "cee". They will be driven by separate power amplifiers that will cover in bandwidth up to the geometric mean of the total bandwidth needed in the system for acceleration. A representation of our system is shown in Figure 2.

We have two small signal oscillators, so constructed that each will put out a signal that covers the entire frequency range needed for the acceleration cycle. The output of each oscillator is connected to a "double-pole, double-throw" electronic switch. One pole of the switch is connected to the power amplifier (PA1) which is tuned to cover the high frequency part of the acceleration cycle, while the other pole is connected to a low frequency power amplifier (PA2) which is tuned to cover the low frequency part. We use this switching system so that either one of the oscillators will control one bunch of particles through its entire cycle and thereby preserve the phase of the bunch when it is transferred from one of the electrodes to the other.

The bottom of Figure 2 shows four cycles of the frequency program. This program starts out with oscillator #1 at about 30 Mc. Oscillator #1's output is now connected to power amplifier #1 and then accelerates the particles to the outer edge of the inner electrode (dee) in the usual manner. When the protons have reached this radius, a signal is sent to the switching network

that causes it to reverse. That is, the output of oscillator #1 is now connected to power amplifier #2 and the outer electrode (cee). Oscillator #1 can now continue its decreasing frequency program accelerating out to the target.

It is seen that the outputs of both oscillators were switched simultaneously, so that while oscillator #1's output was working on a bunch of protons in the cee, oscillator #2's output could capture and accelerate a bunch of particles in the dee. There are thus two bunches of protons being accelerated at the same time in the machine, one bunch in the dee and one bunch in the cee. The continuity of the program accelerates in a like amount of time four times as many bunches as the conventional electrical-mechanical system.

III. GENERATION SYSTEM FOR MULTIPLE ACCELERATION

Some of the problems anticipated for the method of acceleration outlined above are the following:

1. Shaping and synchronism of the frequency program $f(t)$.
2. Allowance of time for the particles to be well within the cee before the dee is turned on.
3. Loss of phase in the oscillators due to the physical spacing of the electrodes and power amplifiers.
4. Amplitude modulation needed during switching and capture.

In Figure 3, we show a block diagram of our modulation scheme and the way we now see how to solve some of these problems. The frequency program is obtained by matched varactors in the tuned circuit of each oscillator. These varactors are controlled by separate sawtooth wave forms that can be individually adjusted. The two oscillator circuits are identical, except for the fact that one of them (#1) is used as a master. That is, oscillator #1 is used to synchronize the low frequency sawtooth that controls oscillator

#2. This arrangement is used to keep the two oscillators from free-running with respect to each other.

The allowance of time that may have to be made for one bunch of particles to be in the cee before the dee is turned on, is provided by allowing each oscillator to start somewhat sooner than is needed (at a frequency greater than 30 Mc) and then simply blanking the output off. This circuit allows up to a msec delay.

To provide for phase delay in the systems, the "end of acceleration cycle sync" along with the "sync delay" associated with each oscillator circuit allows us to put the same R. F., in phase, on the cee and dee simultaneously. The switch for this circuit is shown as the "cee advance". The "normal switching" position of this switch has a delay of about 30 nano-sec before the cee voltage is built up to the same amplitude as that of the dee. These circuits provide us up to 90 n sec time to allow the voltages to build up in phase. Gross changes in time will be taken care of by delay line.

The "AM modulation" circuit allows about six decibels of gain in the R.F. circuit. At this time, the primary function of this circuit allows this gain to be available at capture and switching time.

IV. POWER AMPLIFIERS

The power amplifiers use identical tubes in both the high frequency and low frequency transmitters. The interstages are two double-tuned doublets, and one triplet. The circuits use low permeability ferrite torroids to keep losses to a minimum.

The finals of both power amplifiers are in a grounded-grid class AB 1 circuit. The tubes are Eimac 4 CW 50,000 C's water-cooled tetrodes. Each of these tetrodes are capable of dissipating over 100 KW of power

(depending on the water flow) so there is the ability to dissipate over 200 KW of power in each power amplifier.

V. VOLTAGES ON THE ELECTRODES

During the quarter-scale tests of the system, we found that we were able to maintain a Standing Wave Ratio of about ten on each electrode over the bandwidths of interest. Using a power input of 200 KW, it is found that we will be able to transmit about 65 KW to each electrode. Using this power and the bandwidth of each electrode, the energy delivered to each is found to be about 12 mW/cycle or about 24 mW/cycle total during the entire acceleration cycle.

A comparison with our present systems shows about 96 KW peak being delivered to the dee during the acceleration cycle. This corresponds to an energy of about 6 mW/cycle delivered to the system. We intend to utilize an accelerating structure that has a somewhat higher characteristic impedance and a different place to feed this energy than that of the present system so it is somewhat difficult to make an actual voltage prediction; however, somewhat crude measurements do indicate that we should be able to obtain about double our present voltage, which we believe to be about 14 KV peak.

VI. CONCLUSIONS

With this system of acceleration, we expect a gain of a factor of four over our present system in intensity from the increase in time factor alone. We have chosen two main accelerating electrodes because of the complexity involved with more than two in the phasing and switching system. Figure 4 shows an outline of the electrodes with respect to the rest of the machine. We plan to utilize our peripheral cee stochastically. With the reduction in volume of our stub line and the elimination of the rotating condenser, we also hope that the pump-down time will be substantially decreased.

We intend to test out our system in a full-scale mock-up of the vacuum tank that we have constructed. The small signal generator is almost completed except for a few modifications, and we should be able to turn on the power to the dee sometime in April. It is hoped that the entire system will be ready in the full-scale tank by mid-July.

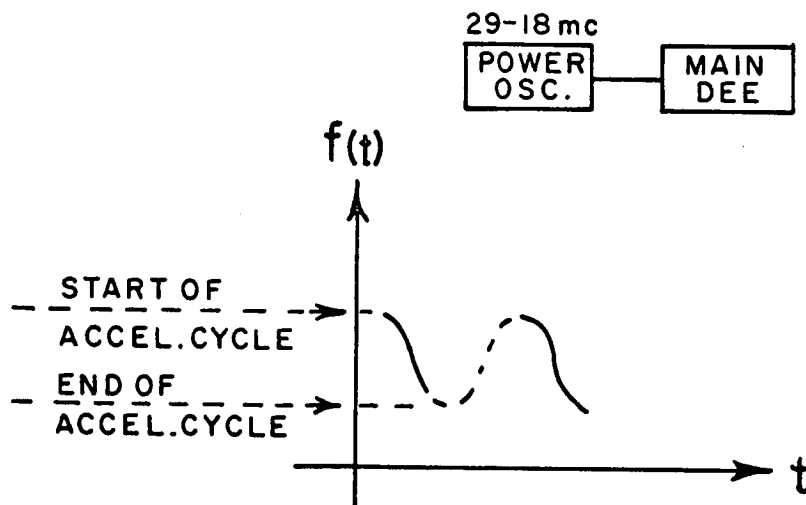


Figure 1 - R.f. frequency on main dee vs. time

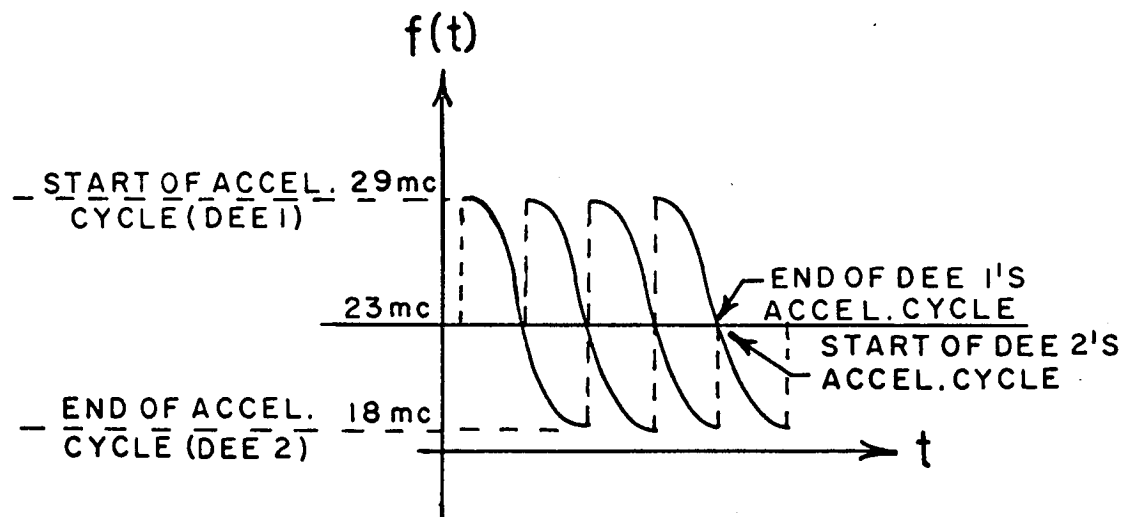
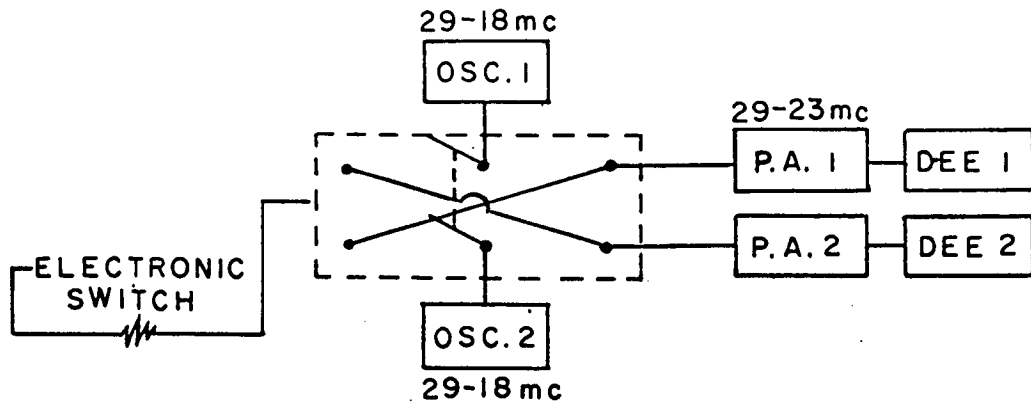
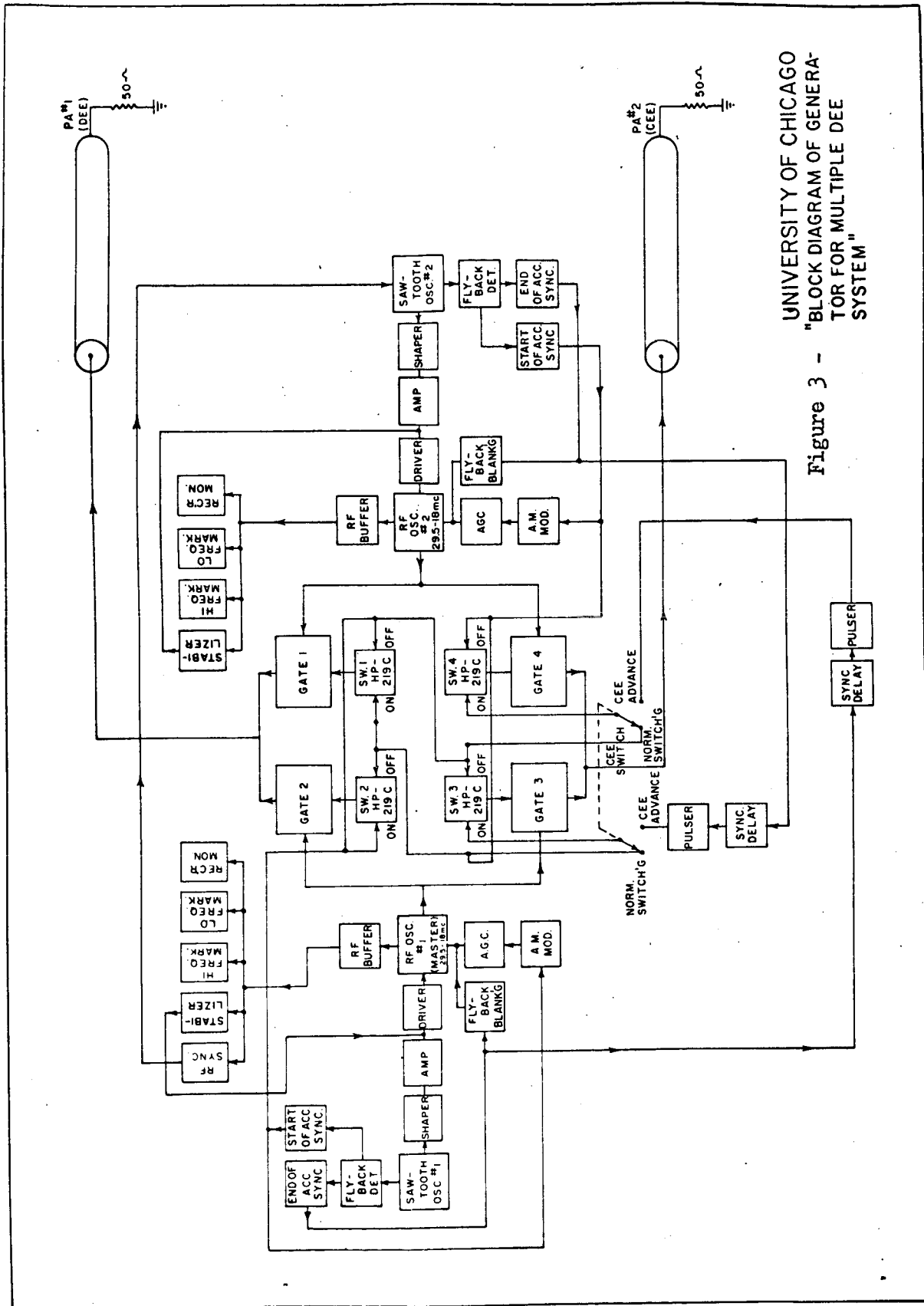


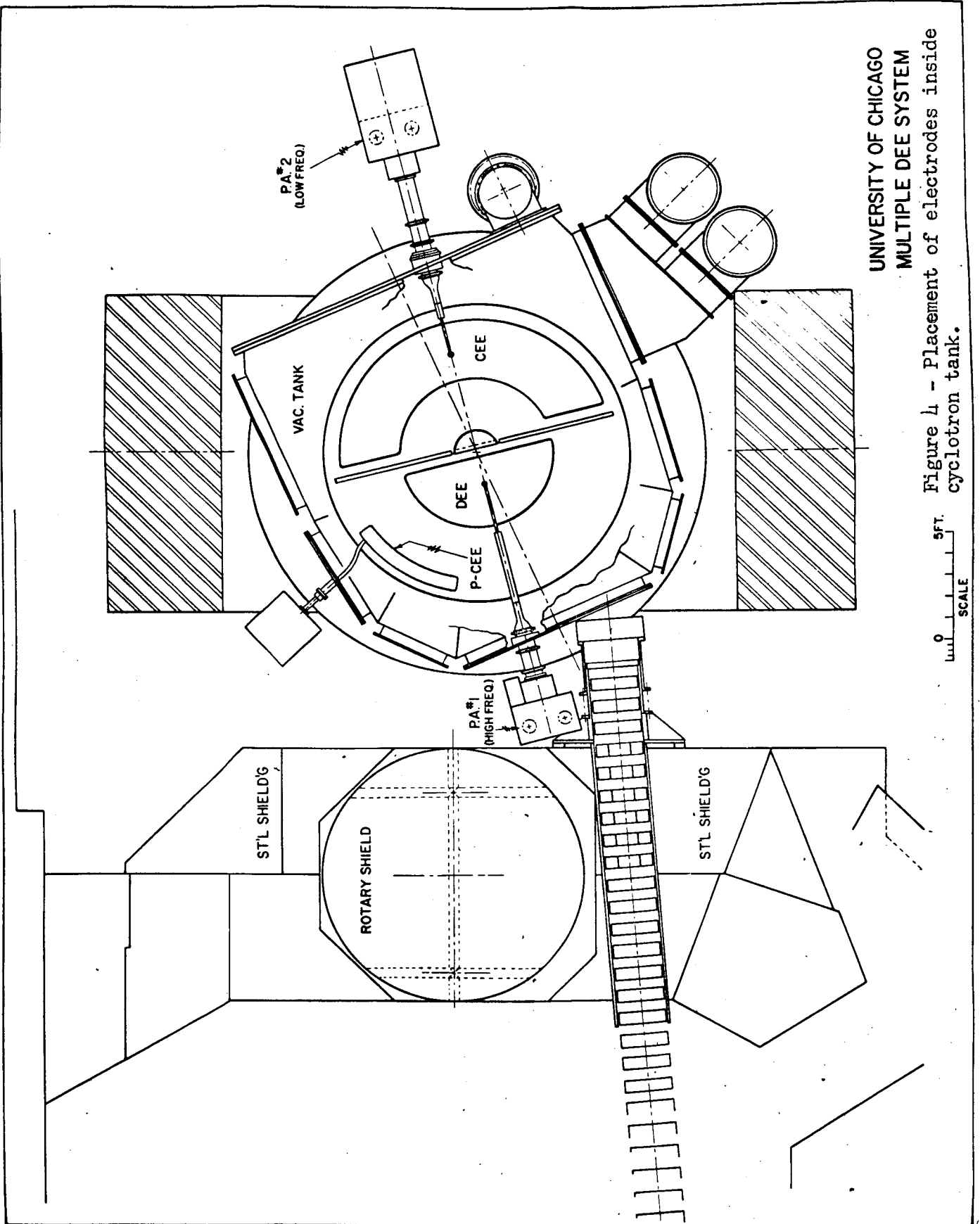
Figure 2 - Proposed system using two electrodes.

Upper figure shows switching arrangement between electrodes. Bottom figure shows frequency on electrodes vs. time.



UNIVERSITY OF CHICAGO
"BLOCK DIAGRAM OF GENERATOR FOR MULTIPLE DEE SYSTEM"

Figure 3 -



UNIVERSITY OF CHICAGO
 MULTIPLE DEE SYSTEM
 Figure 4 - Placement of electrodes inside
 cyclotron tank.

GOTTSHALK, Harvard - Have you considered using a harmonic of the cyclotron frequency in the multiple dee system?

MOLTHEN - It didn't look good from an r.f. engineering standpoint.

BEGER, CERN - What is the average d.c. input that you would expect for each of your two system power stages?

MOLTHEN - 200 k.w.

COLUMBIA UNIVERSITY SYNCHRO-CYCLOTRON

Marcel Bardon, Columbia

(Presented by M. Bardon)

I will limit myself to brief descriptions of some unique features and the present operation of the Columbia synchrocyclotron, and of the plans we have for obtaining more intense beams in the future.

In normal operation, we have a 385 MeV proton beam striking a target placed at 72-in. radius (poles are 82" rad., $n = 0.2$ at $\sim 74"$) to obtain external π and μ beams. No external proton beam has ever been attempted.

The dee system is unique to this machine. It consists of a quarter wave line with one end shorted and the open end located along a diameter of the magnet, as shown in Figure 1. This open end, in the middle of the chamber, is loaded by two long rotating condensers. The frequency is modulated between 28 and 17 mega-c.p.s.

These condensers were a problem in maintenance for a long time, mainly because of troubles with the bearings and with expansion of the 18-ft shaft causing misalignments of the 300 blades. We now have reliable operation by using Teflon impregnated bronze bearings. Also, the 18-ft shaft has been separated into 6 sections, insulated from each other to eliminate a parasitic mode.

This dee system has some problems peculiar to the Columbia machine:

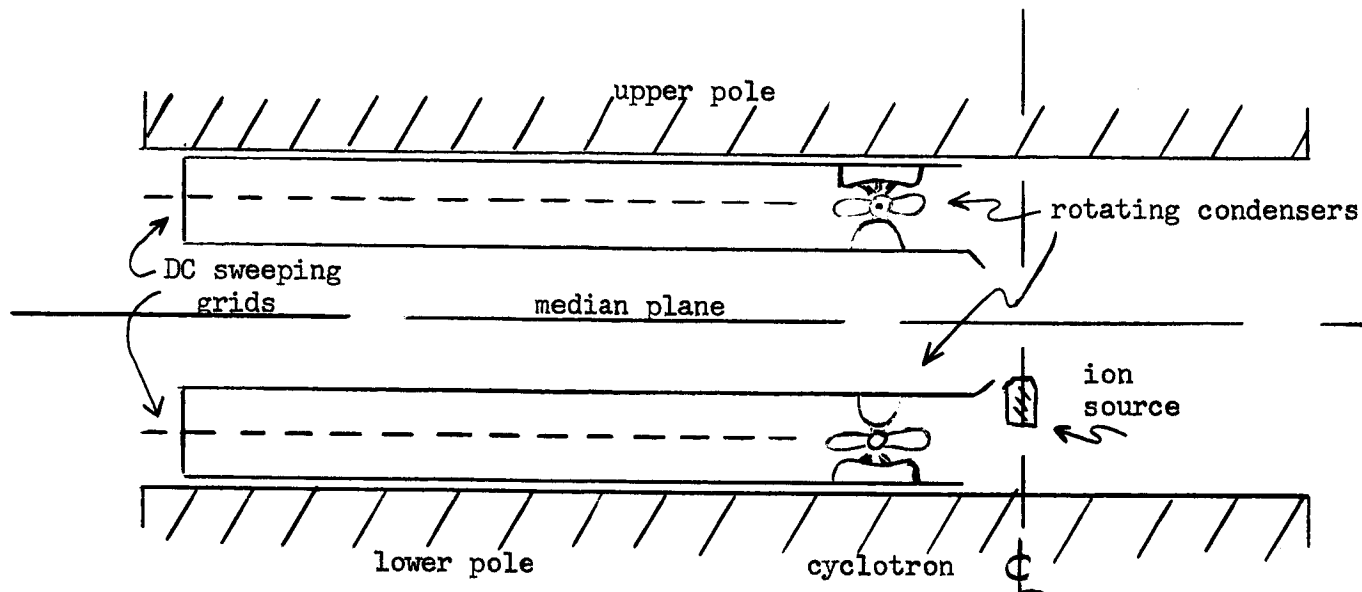


Figure 1 - Elevation view of Columbia cyclotron showing rotating condenser assembly and dee structure

Since one end of the dee is grounded, no D.C. bias could be put on it. For that reason a DC sweeping system is added separately. It consists of an array of 1/2-in. stainless steel tubes 6 inches apart as shown on the diagram. Such a condenser system requires substantial amounts of time spent inside the chamber whenever maintenance becomes necessary. Thus induced activities have been kept as low as possible, by covering surfaces with graphite wherever possible. We have the 5-in. space between dee frames closed down to 3 in. with graphite. Activities vary about 1 rem/hr inside the chamber one day after shutdown.

The condensers have now been running about 10,000 hours (2 years) since the bearings were last changed. Our operation is 3 shifts, 5 days, sometimes weekends as well, with about 90% "on" time.

There have been essentially no changes made in the past four years. At that time we completed a set of improvements which increased our meson beams by about a factor of 5. Some of these are similar to those indicated by the measurements described by Vogt-Nielsen of CERN yesterday. That is, we realigned

and increased the size of the holes through our 12-ft shielding wall to about 8" x 12", and put in a vacuum path. Also we did some tilting down of the meson beam with a horizontal field at the entrance to the shielding wall.

Our interest has been mainly in low energy π and μ beams. To improve these, we inserted an iron channel in a recessed window on the vacuum chamber, to catch the lower energy mesons that would be bent back by the cyclotron fringing field.

We also run sometimes instead with a bending magnet placed in this fringing field. This gives more beam at low energies (45 MeV π^{\pm}) but with not as good a momentum resolution.

Typical beams: (vibrating target, 30% duty cycle)

50,000/sec π^{\pm} stopping in 5-in. diameter,

1-in. C, or 1000/sec μ stopping in 1 1/2-in. C

with $< 2\%$ π contamination.

These mesons are produced internally; as I said, we have no external proton beam. We have been using for the past few years a vibrating target which operates reliably at our 60 cps repetition rate. We get a duty cycle of about 30%, with $\sim 80\%$ of the beam.

It seems clear, however, that we are not likely to get reliable operation from either the target or the rotating condensers at higher repetition rates. This brings me to our future plans.

The question, naturally, is how to make a very substantial increase in our beams. Our present r-f and dee system, with the internal condensers, allow little flexibility for improvements. We feel that the direction in which to look for a large improvement is to study the conversion to a spiral-ridged isochronous or partly isochronous cyclotron. We are looking into this, with

the help of Livingston's group at Oak Ridge. They have both the experience and the facilities that such a difficult project requires. Two principal alternatives are being considered:

- 1) Conversion to partial isochronism by addition of spiral ridges to our present magnet. The frequency swing would be reduced to allow a high repetition rate, possibly by using ferrites and shaping the r-f.

This is attractive only if an efficient extraction system can be devised. We assume that we cannot dump more than $10 \mu A$ inside the machine.

- 2) Conversion to a fully isochronous machine at ~ 450 MeV so that the $3/2$ resonance can be used for extraction.

This would require at least substantial modifications to our magnet. But if it can be done, large extracted currents are possible, limited mainly by shielding problems.

But these studies of the feasibility of such a conversion involve a major amount of model magnet work, orbit calculations, new r-f designs, etc., and one cannot say much in advance about these possibilities.

What we are also considering, and what we would have to do if the studies with the Oak Ridge group show that conversion to a spiral ridged machine is impractical, is the complete replacement of our r-f and dee system. We would want probably an external condenser for a higher repetition rate, perhaps 300/sec, with higher dee voltages and a better ion source. Then also we would try to extract the proton beam.

GOTTSHALK, Harvard - How is the $3/2$ resonance used in extraction from an isochronous machine?

BARDON - The presence of a $3/2$ resonance means there is a large radial separation allowing the use of an extraction system such as the CERN coaxial channel.

THE HARVARD "STOCHASTIC" SYSTEM

B. Gottshalk, Harvard

In principle, the stochastic system is the same as at Orsay, Figure 1. A "main oscillator cutoff" circuit shuts off the dee drive just before normal extraction frequency (23.8 mc) is reached, "parking" the protons in an orbit just inside the effective radius of the regenerator. They are brought out by a second r.f. voltage, frequency-modulated at 10 Kc. over a narrow range centered on the extraction frequency and applied to a secondary electrode or cee. This "secondary" program runs continuously.

We will briefly describe some of the design features of our system and what little we know about its performance (it came into operation only a week ago and has been run for about a day so far).

Cutoff system: an ordinary broadcast f.m. receiver is tuned to the fourth harmonic of the main oscillator, brought in from a pickup loop in the oscillator cabinet. (We removed the high-frequency de-emphasis circuit.) The output of the receiver discriminator, mixed with an adjustable DC level, goes to a Schmitt trigger circuit which is adjusted to fire when the cyclotron oscillator passes a given frequency on the way down and recovers when the same frequency is passed on the way up. The Schmitt output is differentiated providing a negative trigger in the first case and a positive one in the second. This system is simple to construct and exceedingly stable because of the effective fourfold improvement of the already quite good receiver stability due to using the fourth harmonic of the main oscillator. The

phasing of the cutoff pulse is changed by varying the receiver tuning.

The "program generator" is simply a monostable flip-flop of adjustable period which triggers on the negative pulse from the Schmitt trigger. The rest of the oscillator cutoff mechanism is complicated mainly by the fact that we are dealing with a grounded-grid oscillator which does not have too much margin of operation to start with, so any additional impedance in the grid circuit would probably put it out of business. Therefore we use the brute-force method, cutting off the cathode current by means of a large triode. Another problem is that the oscillator uses a negative HV supply applied to the cathode; therefore the drive circuit of the gating triode floats at about -7 Kv. A carrier-modulated system (10 mc. carrier) is used to transmit the cutoff signal across this potential difference. This method results in control down to DC (the oscillator can be held off electronically for an indefinite period, which makes some interesting experiments possible). It also eliminates the severe transient problem at turn-on which a DC-blocking condenser would introduce. The rise time at the clamp-tube grid is 1 μ sec. and the decay of r.f. on the dee (some tens of μ sec.) is limited by the Q of the dee system.

We now pass to the subsidiary f.m. system. The signal generator (Figure 2) consists of an 8 mc free-running flip-flop whose bias is varied to adjust the frequency, followed by a frequency tripler, buffer amplifier, and gate. The tripler output is mixed with a 27 mc. crystal oscillator signal to produce a 3 mc beat frequency. This is shaped by a Schmitt trigger and a delay-line clipping system to give a standard pulse every beat. The train of standard pulses is RC integrated and the resulting DC voltage compared to a preset level by a high-gain operational amplifier which feeds a correction

signal to the flip-flop. If, at the same time, a modulation voltage is applied to the flip-flop, the rest of the system has the property of maintaining the average output frequency constant with respect to the crystal. Long-term stability is better than a kilocycle after a brief warmup. Other features are:

1. linear adjustment of the average frequency by a pot,
2. accurate reading of average frequency by a meter across the integrating capacitor,
3. availability of the true modulation envelope from a short-time-constant integrating circuit,
4. Output substantially the same from 22 to 26 mc.

We think that this very stable and flexible signal generator may well be one of the most useful elements of the system.

A buffer amplifier having a bandpass characteristic from 22 to 26 mc boosts the signal from the milliwatt level to about 1 watt, and sends it out to the high-power amplifier. This consists of three conventional tetrode stages, the first using an 807, the second a 4CX300A ceramic tube and the third a 4CX3000A ceramic tube. They are coupled by resonant-line transformers. Because stage 2 draws very little grid current the Q here is artificially spoiled with a shunt resistance. The input capacitances of the second and third stages are shunted by trimming condensers and the final output is coupled to the output line by an adjustable π -matching circuit so that the whole system can be tuned by a panoramic technique. Although it is designed to supply 10 kw of excitation to the cee, it has not been completely debugged and only gives 2 kw at present, which, however, seems to be enough. Figure 3 shows a photograph of the bottom of the final stage chassis.

The cee is about 8" wide and is completely enclosed in a ground plane, facilitating testing outside the cyclotron. It represents quite a departure from the Orsay system. Instead of spoiling the Q of the cee itself, yielding a rather complex structure which must be water-cooled, we built a simple, high-Q structure of welded aluminum, and commercial 3" coax hardware, and spoiled the Q by tapping in a commercial dummy load. This is shown schematically in Figure 1. The resonant frequency can be shifted by altering the position of a home-made shorting plug and the Q can be varied by changing the tapping point. (Since all the characteristic impedances are 50Ω the best match to the input line is when the line and the dummy load are connected at the same point.) The whole system is very compact and easily adjusted. The load is a water-cooled unit made by Corning, whose small size and non-magnetic construction make it well suited to cyclotron use. It is directly cooled by distilled water. It is shown in Figure 4 connected to the cee stub line going away from the viewer. The tuning slug is at the top left. The r.f. voltage measured on the cee is approximately 6kv peak-to-peak.

Performance and observations on the system: Figure 5 shows on the top trace the beam structure with a 10 kc sine wave f.m. modulation frequency. The bottom trace shows the dee r.f. envelope. The photograph was taken with a single sweep using a plastic scintillator and around a two micro-second integrating time constant on the photomultiplier anode. Hence it shows the duty cycle except for possibly r.f. fine structure. Modulation by the main oscillator is a function of cutoff phasing, here set for an integrated beam loss of 20%. (More r.f. volts may make a better compromise possible.) It is seen that the beam comes out in pulses. Each pulse is about 20 μ sec wide giving about a 20% duty cycle. Figure 6 shows the structure of the individual bursts on an enlarged time scale. Each f.m. cee

cycle produces two pulses, once when the sine wave crosses the extraction frequency on the way up, the other when it crosses the extraction frequency on the way down. Any kind of modulation works. Protons always come out at the same frequency; that is, the phasing of protons with respect to the modulating waveform can be varied at will by changing the center frequency. It seems that all that is required is a frequent change of phase of the r.f. with respect to the circulating protons. We have not measured the energy of the stochastically extracted beam yet. The whole system seems to be stable and easy to use.

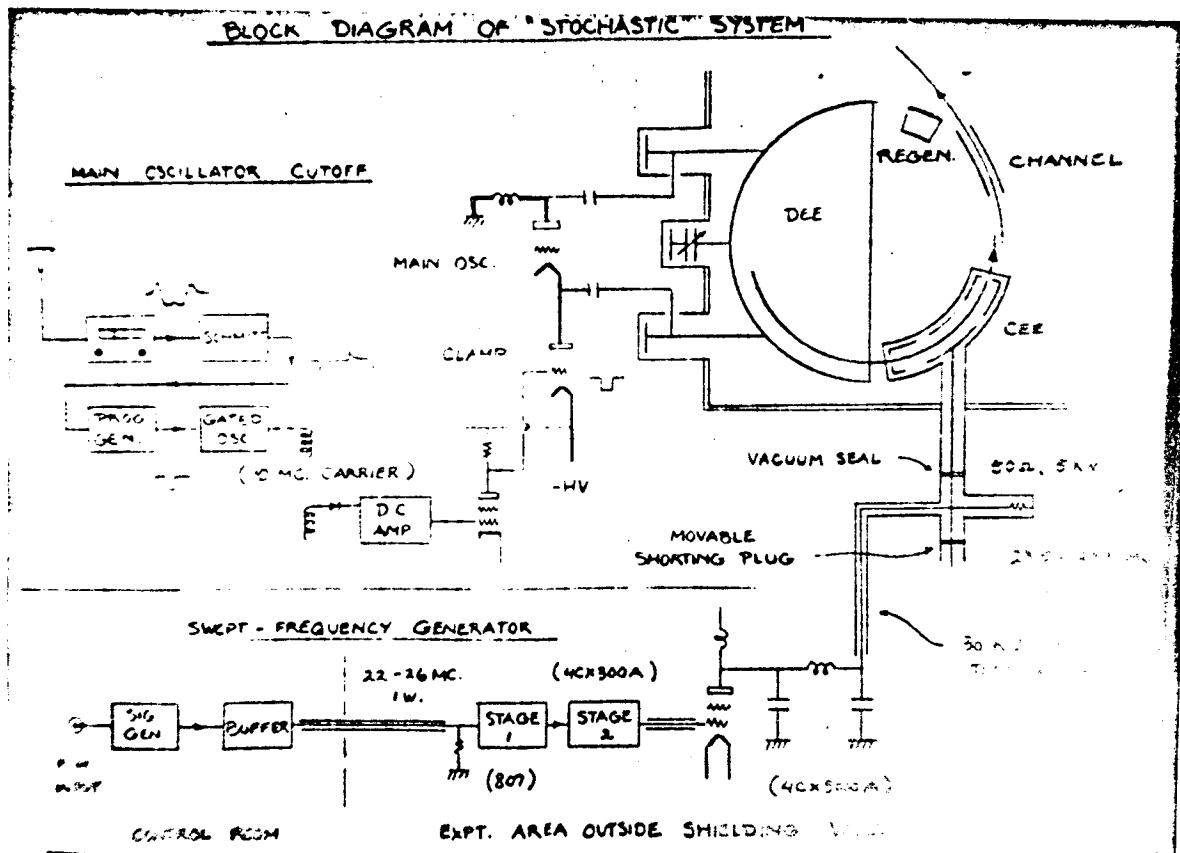


Figure 1 - Block diagram of cee electronics

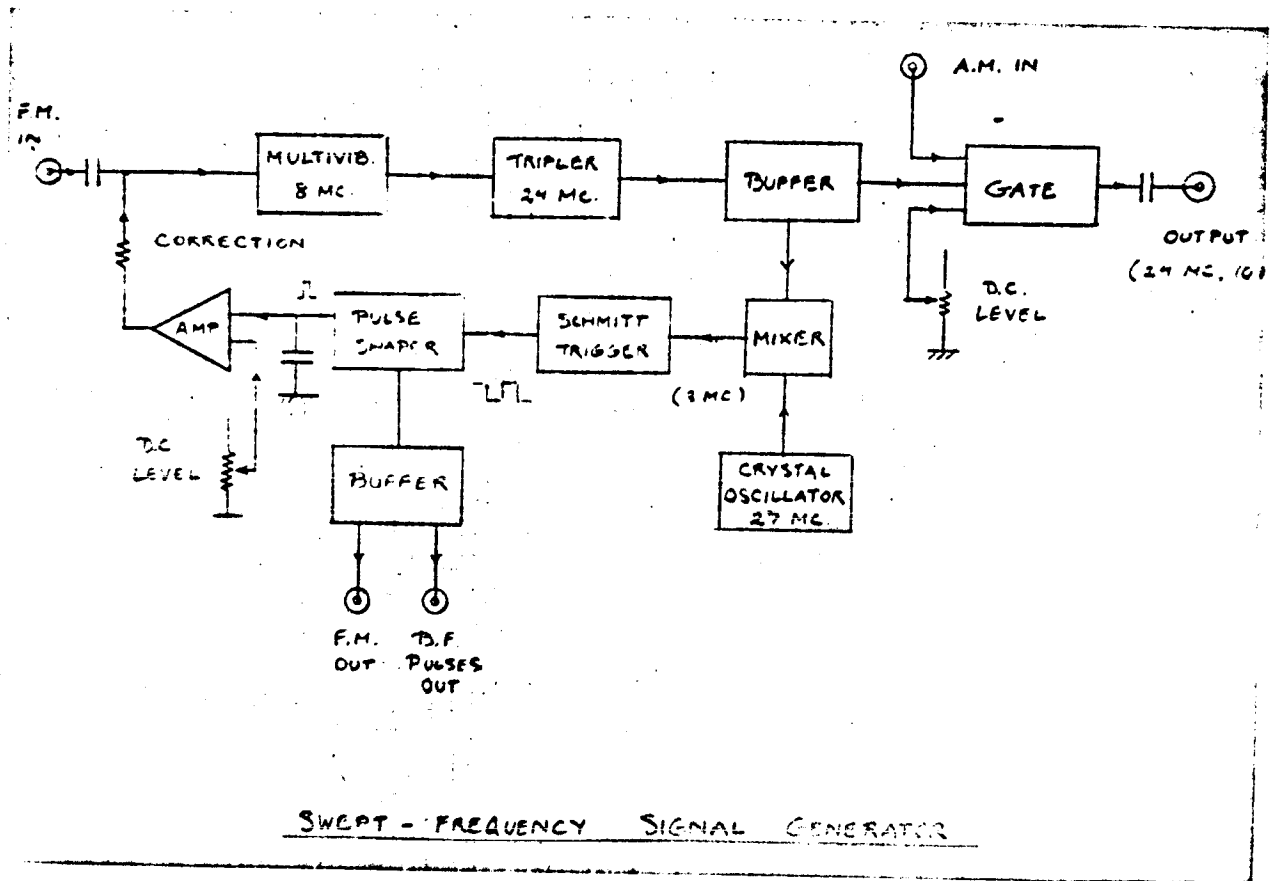


Figure 2 - Block diagram of sweep frequency signal generator

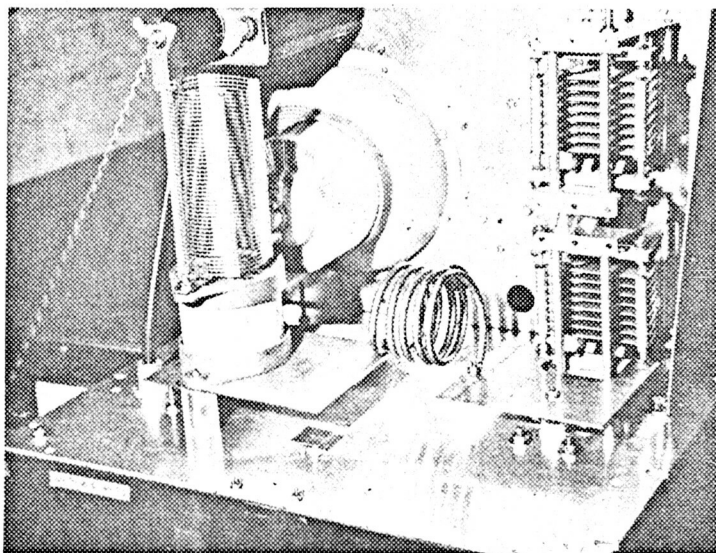


Figure 3 - View of final stage

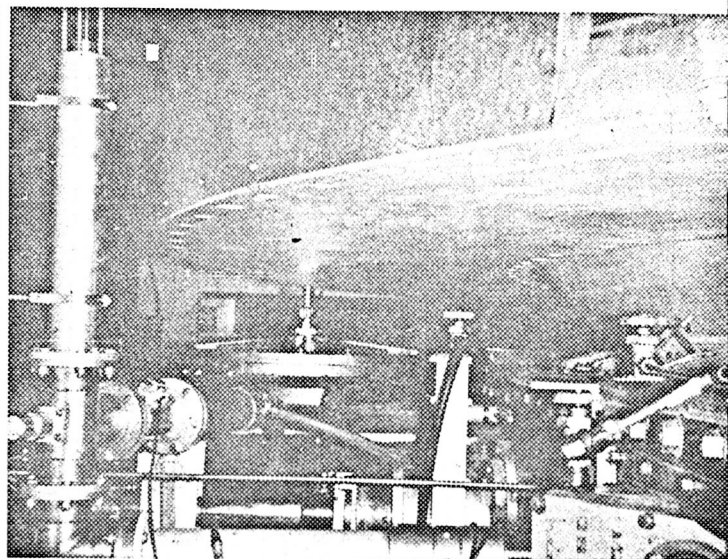


Figure 4 - Cee tuning stub line and water cooled load (pointing away from viewer)

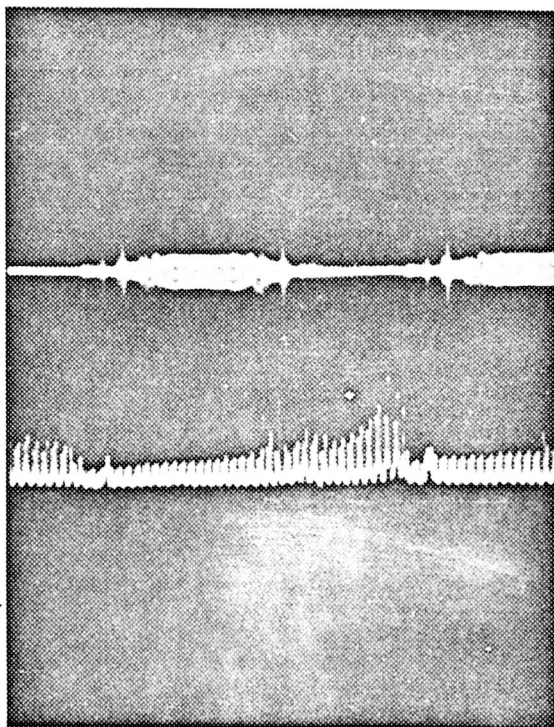


Figure 5 - Cee operation. Top trace is beam time structure taken with a single trace. Bottom trace is dee r.f. envelope.

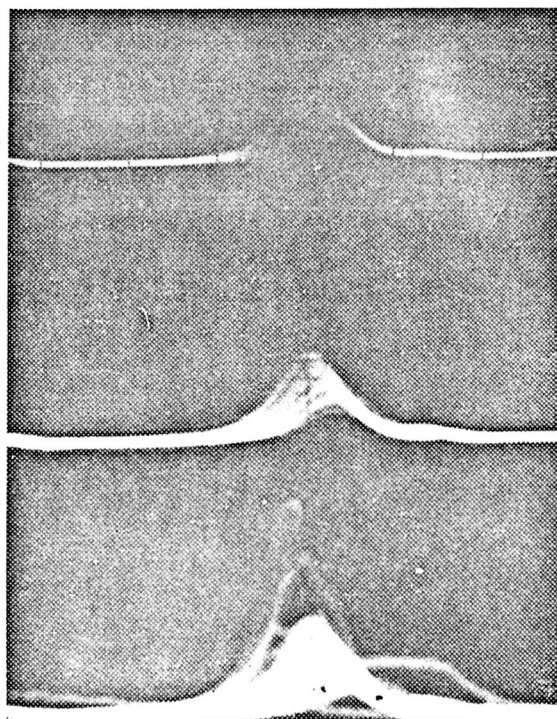


Figure 6 - Single pulse $\sim 20 \mu s$ long produced by 10 kc sine modulation on cee.

CROWE, Berkeley - What was the repetition rate of your sawtooth? Was it 10 kc?

GOTTSHALK - We used 10 kc on everything. However, with sine waves we used frequencies from 20c to 20 kc and got efficient extraction at any frequency. For most experiments, the higher the frequency the better.

GOTTSHALK - to SUZUKI, Carnegie - Could you detail how the pictures of your beam spill were taken? They must have been multiple traces, weren't they?

SUZUKI - Yes, they were multiple traces, but single traces showed the same thing.

GOTTSHALK - What were the integration time constants in the photomultiple tube?

SUZUKI - The pictures showed overshoot pulses from a Hewlett-Packard amplifier, so the time constant was perhaps a microsecond.

GOTTSHALK - If those pictures were taken on the same basis as everybody else's then your system would appear to be about ten times as good as others.

SUZUKI - Yes, we were using noise modulation.

GOTTSHALK - So you do not have the, say, 100 kc. structure which you would get with our type system.

SUZUKI - The 100 kc. component almost vanished with noise modulation. Also our true duty cycle, including r.f. structure, is more than 50%.

(The coincidence curve in Suzuki's paper was shown again.)

GOTTSHALK - Was this curve taken with sufficient resolving time to show the accidental rate between the r.f. peaks going to zero if it actually did?

SUZUKI - Yes, it was.

MONOENERGETIC NEUTRON BEAMS

D. F. Measday, Harvard University

Experiments with neutrons of an energy in the hundreds of MeV have lagged far behind the equivalent proton experiments because of the poor beams and inefficient detectors. For example the proton-proton interaction is quite well understood but our knowledge of the neutron-proton interaction is very hazy. It therefore seems worthwhile to survey the present position and see what improvements could be made.

By what methods have neutron beams above 30 MeV been obtained? Mostly by stripping deuterons or by bombarding a light element with protons. However such beams have a large energy spread. The 100 MeV neutron beam at Berkeley, obtained by stripping 195 MeV deuterons, had an energy spread of 30 MeV. A beam at Harwell from the proton bombardment of beryllium had a spread of 40 MeV with a large tail extending down to zero energy. Of course one can effectively remove this tail in certain simple scattering experiments by placing an energy cutoff in the detector.

However a much neater procedure which is also far more complicated is to utilize the time of flight of the neutrons. At Berkeley in 1952, Ragent and Linlor were able to obtain a resolution of ~ 10 MeV, the maximum beam energy being 180 MeV. At Harwell, Scanlon et al. applied the same principle to the synchrocyclotron there, using

proton bombardment of aluminum as the source. Maximum neutron energy was 135 MeV and the resolution was comparable to Berkeley. However in an experiment to measure the total neutron cross sections of various elements the maximum count rate was 25/sec. The limit was counting loss corrections but there is also the ultimate limit of the repetition frequency of the acceleration cycle. Disadvantages of time of flight techniques are that complex apparatus has to be installed in a cyclotron vacuum tank which is already crowded and also that activation experiments are not possible.

At Harvard we therefore decided to develop an alternative method of obtaining neutrons. The principle is quite simple; deuterium is bombarded by protons and the neutrons knocked on in the forward direction are collimated into a beam. The method was used by Larsen at Berkeley four or five years ago and was quite successful. He obtained a beam of 10^4 neutrons/sec; the beam energy was 710 MeV and estimated energy spread was 6 MeV.

The first figure shows the lay-out at Harvard. The external regenerated proton beam from the cyclotron bombards a deuterium target. The neutrons carried forward at 0° are collimated through an 8 foot concrete wall. There is a 12 inch hole drilled through the concrete. Additional lead and steel shielding is used. The total concrete, steel, and lead wall shielding thickness is 15 feet. The beam is normally 2" x 1" in cross section but can be made larger or smaller. Charged particles are swept aside by a clearing magnet. So far we have stopped the proton beam immediately after the clearing

magnet but a proton transport system has been built to carry the beam as far away as possible. To date, however, this has given a higher background. To vary the neutron energy we change the proton energy by carbon degraders placed in the beam. They are placed before a bending magnet so that none of the primary neutrons produced can go straight down the collimator. An ionization chamber is placed in the proton beam and acts as a neutron monitor. The plates are etched from aluminized mylar and are the same shape as the deuterium target. The total mass in the direct beam is 23 mgms/cm².

The liquid deuterium is held in a 2 mil thick mylar cup, 2 inches in diameter and 5 inches long. The deuterium is cooled by liquid hydrogen and there is also a liquid nitrogen shield in the cryostat. There are 820 mgms/cm² of deuterium in the beam and 24 mgms/cm² of mylar and aluminum heat shield. Therefore, including the ionization chamber, there is altogether a mass which is 6% of the deuterium mass which is in the direct beam. It is important that the deuterium target have a safety line as well as the cooling line. What tends to happen is that no matter how hard you try to keep the deuterium pure some impurities creep into the system. When the deuterium is cooled down by passing through the liquid hydrogen these impurities are deposited in the line and when the deuterium warms up again the line can become blocked. Therefore, a safety line with a valve is essential. As an additional safety precaution it was decided to keep the hydrogen dewar outside the cyclotron vault; the ventilation in the vault isn't

very good so we have a ten foot transfer tube to an outside hydrogen dewar. A new ventilation system was put in with a capacity of 3,000 cubic feet per minute.

The second figure shows a picture of the cryostat inside the vault. The beam comes from the right through the quadrupole pair. The cryostat is seen to the right of the clearing magnet. This magnet bends the protons away from the plane of the figure whereas the neutrons go out toward the left.

Figure 3 shows part of the experimental room and the hydrogen hood. Figure 4 displays the pulse height spectrum of neutrons on a large plastic scintillator. A semi-log plot is used to show the movement of the upper edge spectrum with neutron energy. The channel number on the x-axis is approximately in MeV. Note that for the 160 MeV neutrons the upper edge is diffuse. Figure 5 shows the same information as Figure 4 but on a linear plot with the background indicated. The background is obtained by sliding into the collimator 8 foot long steel rods milled to the rectangular shape of the collimator and then counting in the plastic scintillator. The background does not seem to vary with energy indicating that the shielding between the cryostat and the experimental area is good and the degrader box doesn't give any background. It seems that the background comes directly from the machine.

Figure 6 illustrates a calculated pulse height spectrum from 160 MeV neutrons in the scintillator assuming only hydrogen interactions in the scintillator. At low energies i.e. 20 MeV, a mono-

energetic neutron beam would produce a rectangular pulse height spectrum in the plastic scintillator. At high neutron energies the differential cross section for n-p scattering increases the high and low energy part of the pulse height spectrum; however the scintillator cannot completely stop a 155 MeV proton so the high energy part is severely reduced. These two effects have been included in the rough calculation shown in Figure 6. No contribution was calculated for neutrons on C^{12} which would probably have three times more effect than hydrogen. However the important point is that it indicates that in Figure 5 the incident 160 MeV neutron beam is monoenergetic. The neutron beam energy spread was calculated assuming that the deuteron interaction contributed a 5 MeV width. We obtain a spread of 6.7 MeV at 150 MeV neutron energy ; 8.6 MeV at 100 MeV; 12.6 MeV at 50 MeV.

Estimating the efficiency of the plastic scintillator we calculate that the beam intensity is $2 \cdot 10^4$ neutrons/sec. Original estimates were 10^5 neutrons/sec. The beam is a factor of 10 less at 50 MeV.

For use with present polarized proton targets, a kinematic separation of the scattered proton is necessary. The present method of getting a neutron beam seems the most applicable to this type of target.

In conclusion although one needs an intense extracted proton beam and in spite of a limit to the energy spread of 3 MeV, it nevertheless seems that this method of obtaining a neutron beam can be very useful.

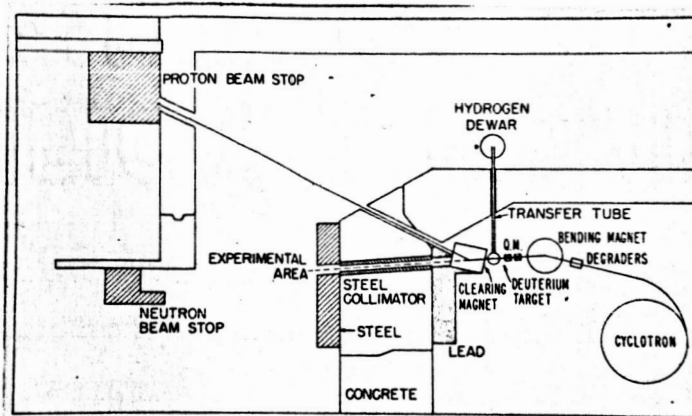


Figure 1 - Plan view of experimental lay out.

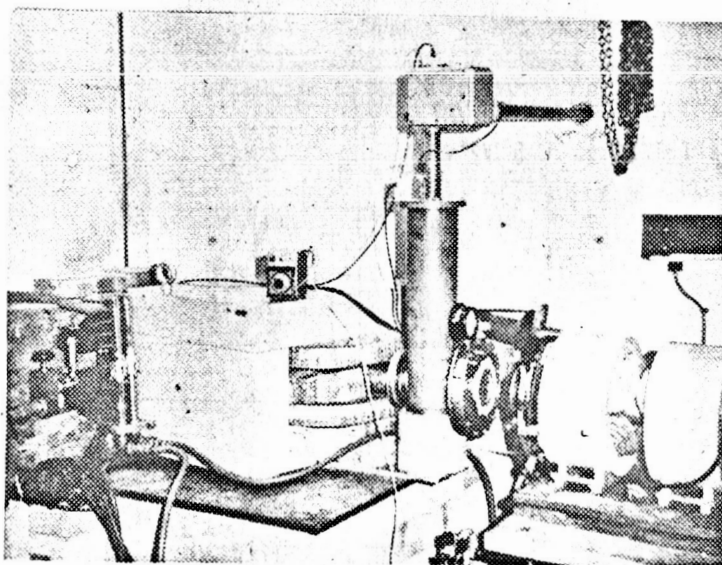


Figure 2 - Deuterium cryostat inside cyclotron vault.

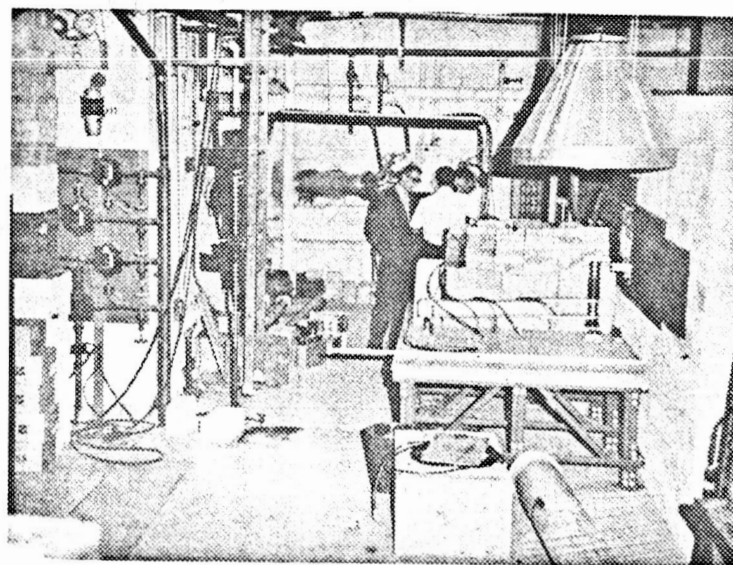


Figure 3 - View of part of experimental room.

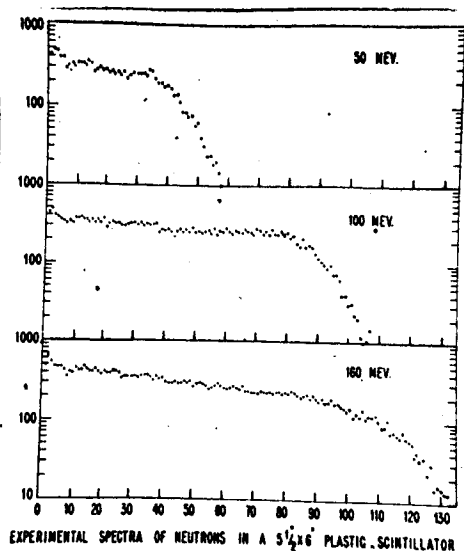


Figure 4 - Pulse height spectrum from neutrons of several energies onto a plastic scintillator.

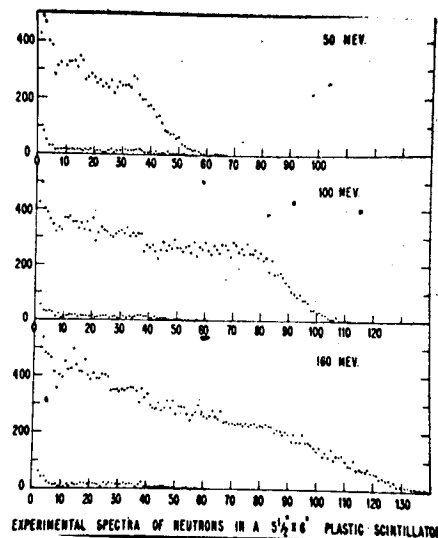


Figure 5 - Pulse height spectrum for neutrons with backgrounds indicated.

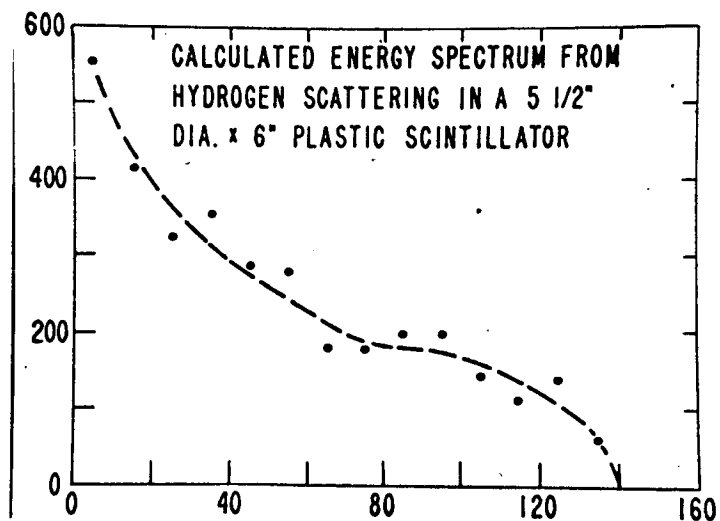


Figure 6 - Calculated pulse height spectrum from n-p scattering in the scintillator for 160 MeV neutrons.

ROSE, Harwell - Over what area did you measure your 2×10^4 neutrons/sec.?

MEASDAY - Our measurement was made for the full 2" x 1" aperture.

MOORE, McGill - What is the intensity of your external proton beam?

MEASDAY - 10^{11} protons/sec. but I don't think all of these are hitting the deuterium target, since the beam at the deuterium target is about 3" to 4" broad while the target is only 2" wide.

ROSE, - I might comment that in our time-of-flight neutron set-up we have about $2 \cdot 10^3$ neutrons/cm.² sec. at 120 MeV neutron energy. Because of this method, we are collecting data over all energies from the maximum on down to a suitable minimum neutron energy.

TELEGDI, Chicago - Why is the energy spread of the neutron beam so small in view of the internal motion of the neutron in the deuteron.

MEASDAY - A calculation done at Harvard, including a final state interaction, came out with a ΔE_n of around 2-3 MeV. Phillips at Harwell has done a separate calculation and came out with the same answer.

ROSE - Since you are looking at neutrons in the forward direction there is less transverse momentum contribution from internal deuteron motion.

FACILITIES FOR BIOLOGICAL AND MEDICAL USES OF THE HARVARD CYCLOTRON

A. M. Koehler, Harvard

In 1959 two neurosurgeons from the Massachusetts General Hospital, Dr. William H. Sweet and Dr. Raymond N. Kjellberg, suggested using a beam of protons from the Harvard Cyclotron for certain types of surgery in the human brain. They referred to similar experiments which were going on at Berkeley and at Upsala. During the next 16 months, the efforts of Sweet and Kjellberg of MGH and Dr. William M. Preston and myself were directed to collimating a suitably small beam, measuring and monitoring the dose delivered, and verifying everything with experiments on animals. In May of 1961 we irradiated our first patient, still using makeshift arrangements in a beam-area shared with physics experiments. A grant was obtained from N.A.S.A. for the construction of an addition to the cyclotron specifically for medical and biological experiments employing proton radiation. The building was completed in July 1963.

The first figure shows the general floor plan. The cyclotron and the extracted beam are shown schematically. The beam is allowed to pass through the physics area into the new operating laboratory. A set of quadrupole magnets refocusses the beam. A thick wall of concrete shields personnel in the control area.

Figure 2 shows the operating laboratory, with the proton beam coming from the evacuated pipe at the left, and passing through the collimator which is suspended from above. Other equipment which is used in treating patients

is also shown: the operating table, an X-ray tube, anaesthesia equipment and a television set for visual monitoring. The collimator consists of a brass cylinder 12 inches I. D. by 30 long and having walls 1.5 inches thick, Figure 3. Inside, there are three aperture plates with removable inserts so that the size of the beam may be changed readily. An ion-chamber is mounted inside the collimator to monitor the beam transmitted to the target. The final aperture of the collimator is mounted on a projecting tube, Figure 4, and the space from here to the surface of the patient's head is filled with water contained in this telescoping absorber.

Figure 5 shows two cross-sectional views of the collimator. The telescoping water absorber can also be used to make phantom measurements of the dose delivered to living tissue. Assuming that water may be substituted for tissue, the probe measures the dose that is actually delivered to the corresponding point in the monkey's head.

A dosimeter consisting of a silicon diode measuring 0.5 mm by 0.5 mm by less than 0.2 mm is imbedded in a plastic block and mounted on a microscope stage, Figure 6. The stage can be driven remotely by small motors, and the vernier scales read by television. This apparatus has been used to map the dose-distribution of various beams. These graphs, Figure 7, show the results for a 3 mm diameter beam. The left graph shows the increase in dose with increasing dE/dx , producing the Bragg peak just before the end of the range. The graphs at the right show the distribution across the beam at several points. Figure 8 shows a similar plot for a beam collimated by a slit of 0.75 mm width.

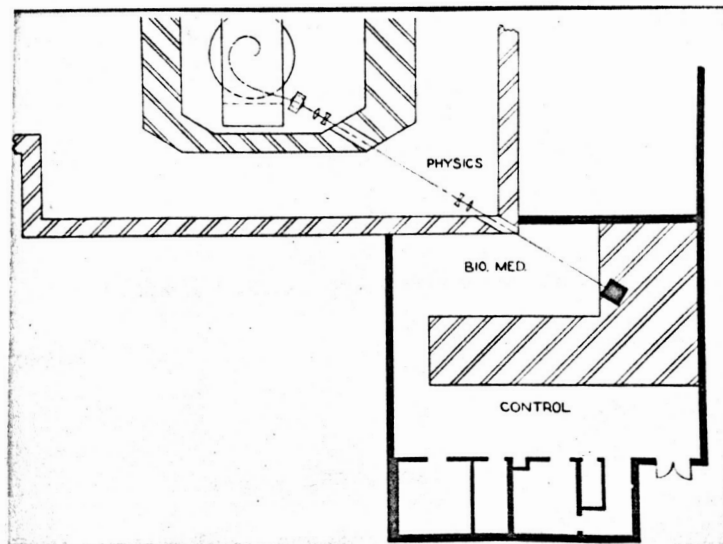


Figure 1 - Floor plan of medical area.

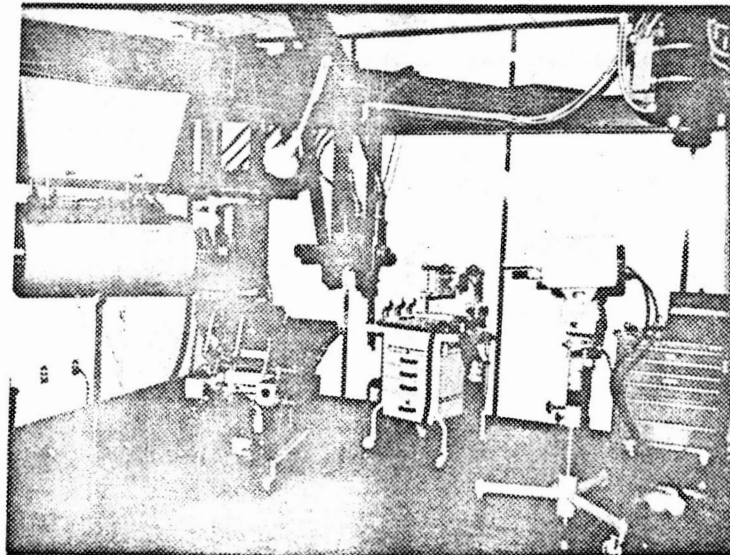


Figure 2 - Operating room. Proton beam comes from evacuated pipe at left.

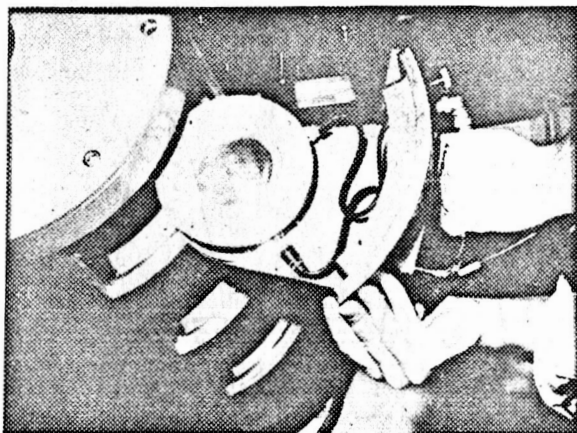


Figure 3 - 12" I. D. collimator

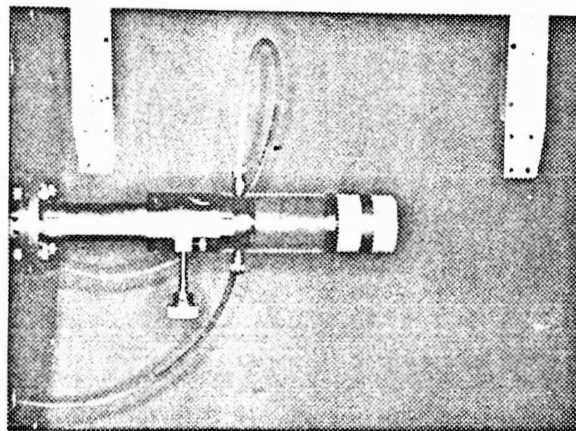


Figure 4 - Final aperture of collimator mounted on projecting tube.

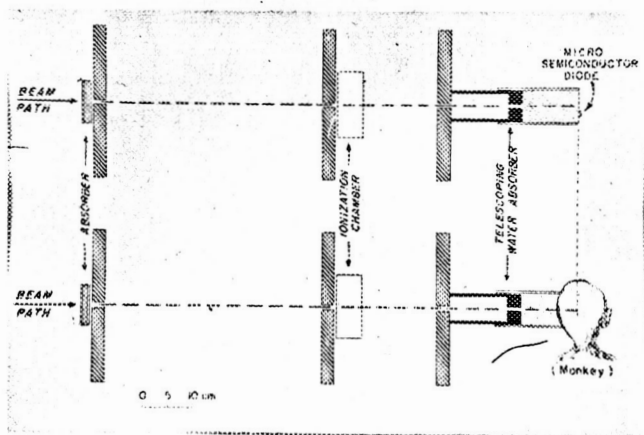


Figure 5 - Cross sectional views of collimator showing telescoping water absorber.

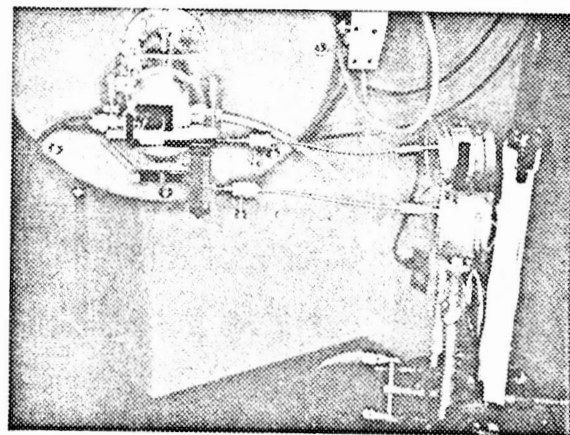


Figure 6 - Microscope stage mount for silicon diode dosimeter.

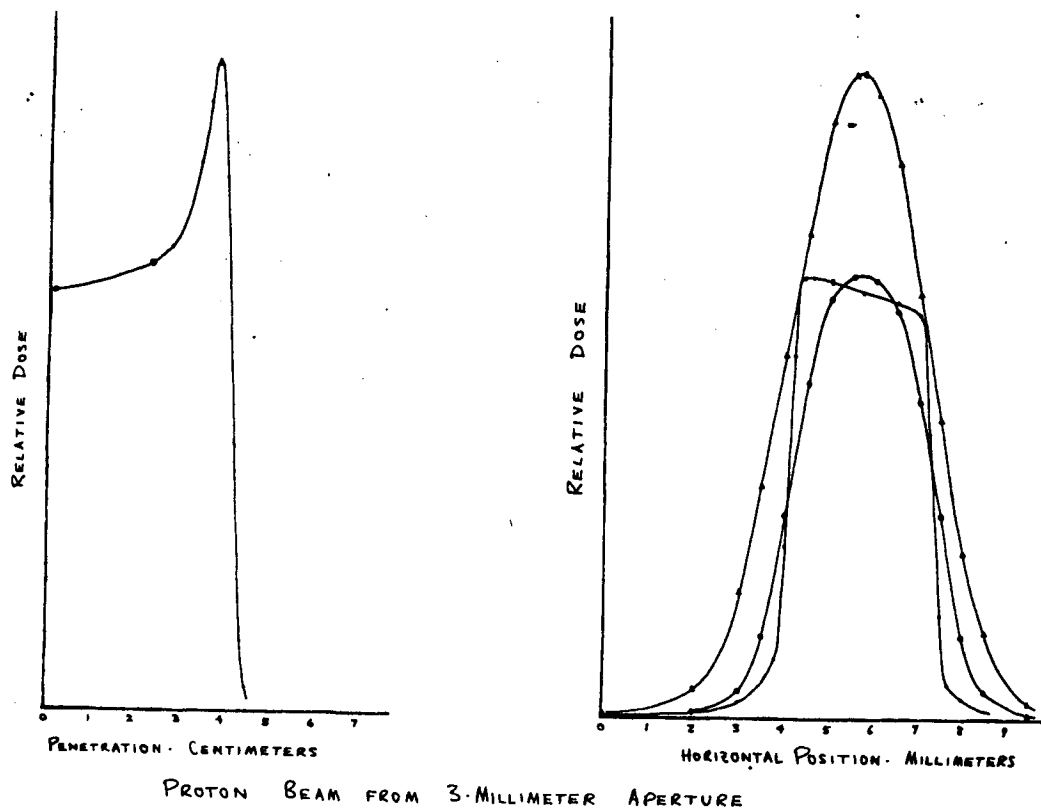


Figure 7 - Dose distribution for 3 m.m. diameter beam.

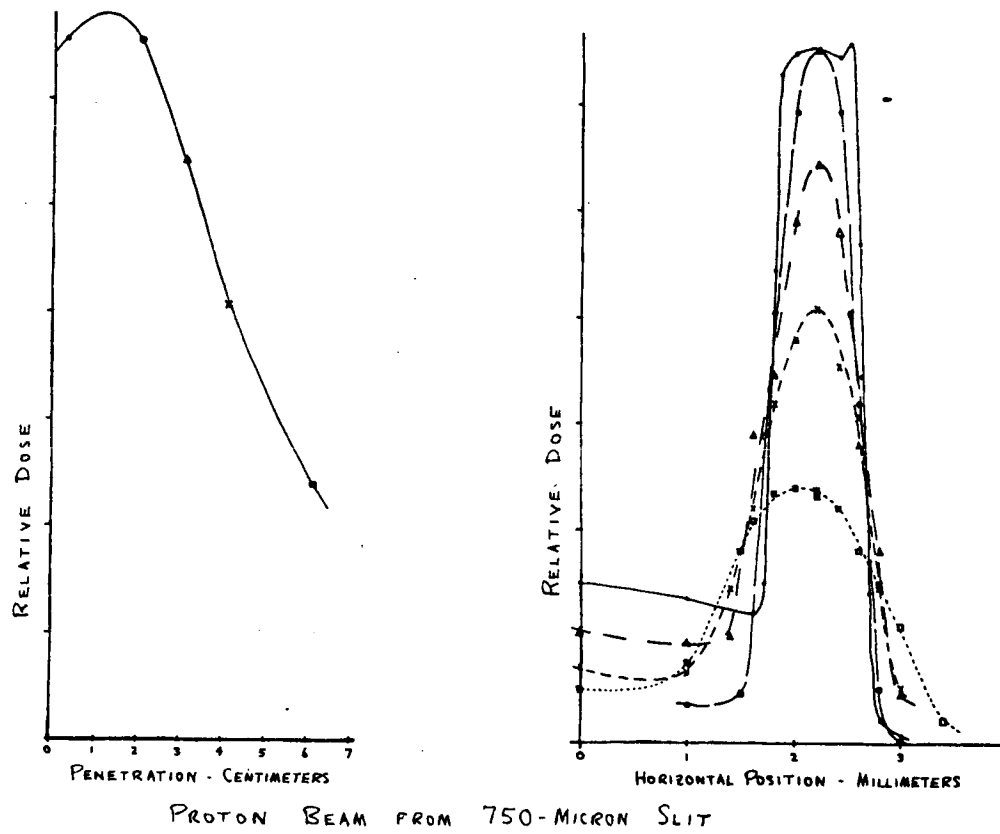


Figure 8 - Dose distribution for .75 m.m. diameter beam.

IMPROVING THE HARWELL SYNCHROCYCLOTRON

George Huxtable, Harwell

The Harwell 110-inch synchrocyclotron is over 15 years old, and there have been no major modifications since it was installed. The machine accelerates protons only, and the internal beam is about 1.5 microamps at 48.5" radius (160 MeV). Figure 1 shows the present layout of the synchrocyclotron pit.

Much of the experimental proton work has required a polarized beam which has been produced by scattering from an internal aluminum target through a magnetic channel. Hence a regenerative extractor has not been installed. The unpolarized proton beam is produced by small angle scattering from a tungsten target. The machine is often used as a pulsed neutron source by electrostatic deflection. Using an 80 kv pulse between two internal plates, the proton sausage is vertically deflected and strikes a target located above the median plane a 2 nanosecond wide neutron burst can be obtained. We propose to alter the machine:

- 1) to accelerate deuterons (and perhaps other particles) as well as protons.
- 2) To increase the internal proton beam to about 20 μ A.
- 3) By installing a regenerative extractor, to increase the external beam by many thousands. Polarized protons could be produced from a scattering outside the machine.

I am not going to talk about beam extraction methods, as we haven't got round to thinking hard about this yet, but it doesn't seem a very difficult

part of the job. We are not proposing to install any spiral ridging on the magnet.

Many of these ideas for improving our machine are attributable to Prof. K. MacKenzie who was with us at Harwell for a few days last summer. I would also like to thank Dr. Anderson of Chicago for supplying a lot of useful information. Our proposals are at the tentative stage, rather than being finalized designs.

MacKenzie has emphasized that the circulating beam is a sensitive function of dee voltage, due to space-charge limitations near the centre. We propose to increase the dee voltage from its present 7.5 kV (peak) to at least 30 KV. This enables a calutron type of ion source to be installed; because of its greater efficiency and the increased dee voltage we expect a factor of 20 increase in beam without too much trouble. This will be at a repetition rate of 1000/sec. compared with 200/sec as at present. At a radius greater than that of the spacecharge saturation region the dee is cut back to become a 90° sector in order to reduce the capacity to earth. (This reduces the effective dee voltage above this radius only by a factor of $\sqrt{2}$. The total effective capacity is less than 400 pfs compared with about 1800 pfs for the present dee system.

To simplify construction and frequency changing, the resonant line is placed in air: a large diameter vacuum insulator (Alumina 24" O.D.) seals the connection and supports the dee completely. The rotating condenser is in a separate vacuum chamber (as in the Orsay machine) with its own pumps (not shown). Again a seal is made with a 24" Alumina insulating disc. Figure 2 shows the proposed r.f. system.

To give a frequency sweep of 24.8 to 20.2 mc/s, the required capacity range is 215 to 500 pfs, and the peak voltage across the condenser varies

between 25 and 35 kV. A padding capacitor (not shown) of 100 pfs has to be added when accelerating deuterons, and the shell over the inner conductor of the line has to be removed, changing the impedance of this section from 12 ohms to 100 ohms.

The blades of the rotating condenser, Figure 3, have a triangular cross section to improve the shape of the frequency sweep as a function of time, and to keep the spacing large when the voltage is high. There are 32 blades, of 30" diameter, so the rotor speed required is only 1900 rpm, and we do not expect serious bearing or rotating vacuum seal troubles at this speed, which is less than that of our present rotor. For pulsed neutron work the speed will be increased to 3000 rpm to get a higher neutron burst rate and a larger synchronous phase angle (i.e. a shorter pulse). The minimum spacing between blades, at the end of the frequency sweep, is .033", and the voltage has to be reduced at this frequency to avoid sparking. This is acceptable as the required energy gain per turn is low. An anode modulator is required for the oscillator, and the voltage can be programmed so that any spill-out of protons which occurs during acceleration due to increase of synchronous phase angle does so at a small radius, so as to reduce activity and heating in the machine.

The estimated power losses in the system are only 10-12 KW; we will use an oscillator triode with about 30 kW dissipation. The oscillator will be of the "fly wheel" type, connected to the resonator at only one point; either directly to a tap on the line as at Orsay, or through a small capacity to the rotor as at Dubna.

The system can be cooled by circulating air or water; air cooling seems simplest. The line is easy to cool, as it is in air. We propose to cool the dee by making the supporting structure a vacuum-tight re-entrant enclosure

into which air is blown through the centre of the insulating disc. The rotor will dissipate about 150 watts, which has to go by radiation.

Power supplies for the cooling fans and the rotor drive are fed in through the bias choke, placed near the voltage node.

The line is bent downwards to keep the median plane as clear as possible to make beam handling easier.

Because of the long thin shape of the resonant system and the limited frequency range we do not expect to suffer from spurious resonances.

At present we use a peripheral cee electrode to improve the duty cycle, and we could use this with the modified machine. An attractive alternative is to trim the frequency sweep at the low-frequency end by a ferrite controllable reactance, which could be capacitively coupled in at the rotating condenser end. If this coupling were made to vary with rotor position, then the ferrite could be 'disconnected' at the high frequency position, where the losses are greatest.

I would like to mention some interesting work which has been done on our behalf by D. Clark and P. S. Rogers at the N.I.R.N.S.:

Tests have been made of small-diameter Calutron-type ion sources with the object of providing a source and puller system small enough to be used in a synchrocyclotron. The small voltage per turn of these machines results in a small initial orbit which would be unable to clear a normalized hooded source.

Sources with chimney outside diameters of 1/8 and 1/16 inch were tried. Figure 4 shows the form and materials. The tests were made on a 4 MeV sector-focussed cyclotron used for central-orbit studies, with a centre field of 13 kilogauss. The dee voltage of this machine is modulated with a 500 μ sec. pulse at 25 p.p.s. to cut down r.f. power and radiation.

The puller was a single post of 0.060" Tungsten wire whose position could be varied. The source position in the gap could also be varied. The dee geometry is shown in Figure 4 in vertical cross-section and plan. Figure 5 shows a plot of proton beam current received on a probe at 1.3 to 1.5 inches radius from machine centre, as a function of peak dee voltage, for the two sizes of ion source. In Figure 6, beam current is plotted against radius at a fixed dee voltage of 7 Kv peak, the source-puller position and orbit trim coils of the machine having been optimized at this voltage for maximum current at 4 inches radius. The effect of D. C. biasing the dee is also shown in Figure 6. Positive bias assists the orbit to clear the structure on the first turn by increasing the energy given in the second acceleration, while negative bias has the reverse effect.

The loss of beam with increasing radius from the machine centre is apparent in Figure 6. This may be partly due to the fact that the magnetic forces at small radii in this machine are defocussing due to a central hole used for injection studies. An improvement will be expected if cones were used at the centre of the magnet.

The currents produced by these small ion sources are less than expected. However, the low voltage threshold indicates that it is feasible to use this type of source in a synchrocyclotron at 7 or 8 kv dee voltage. We plan to try a 1/8" source in the Harwell synchrocyclotron in the near future.

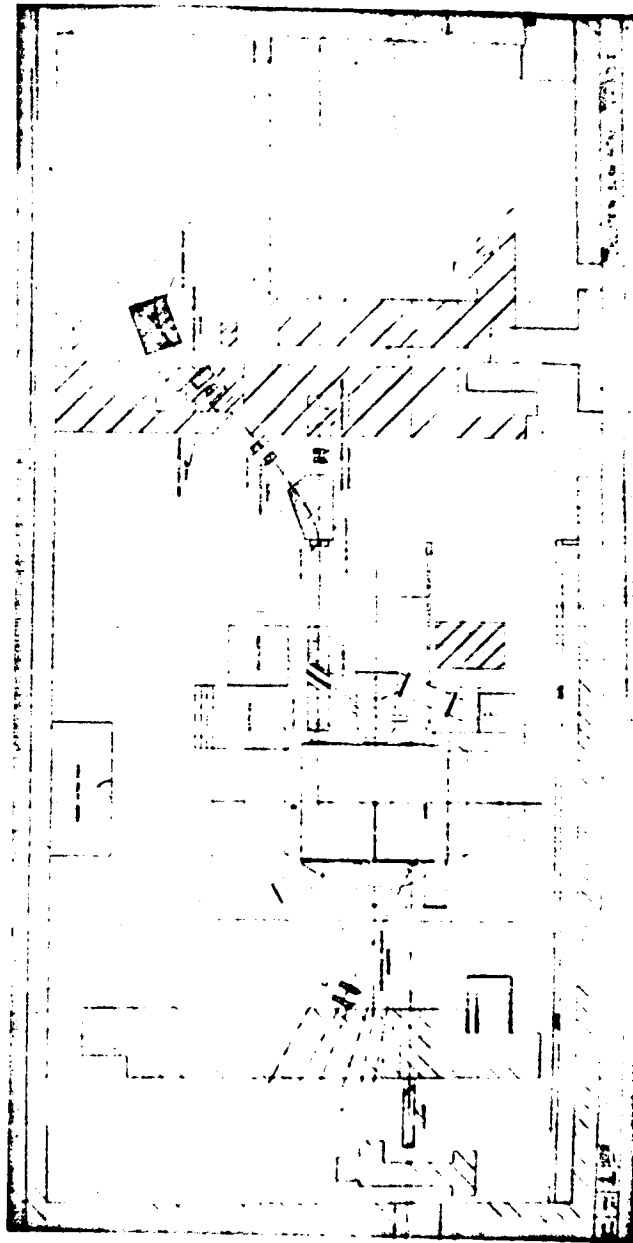


Figure 1 - Present layout of synchrocyclotron pit.

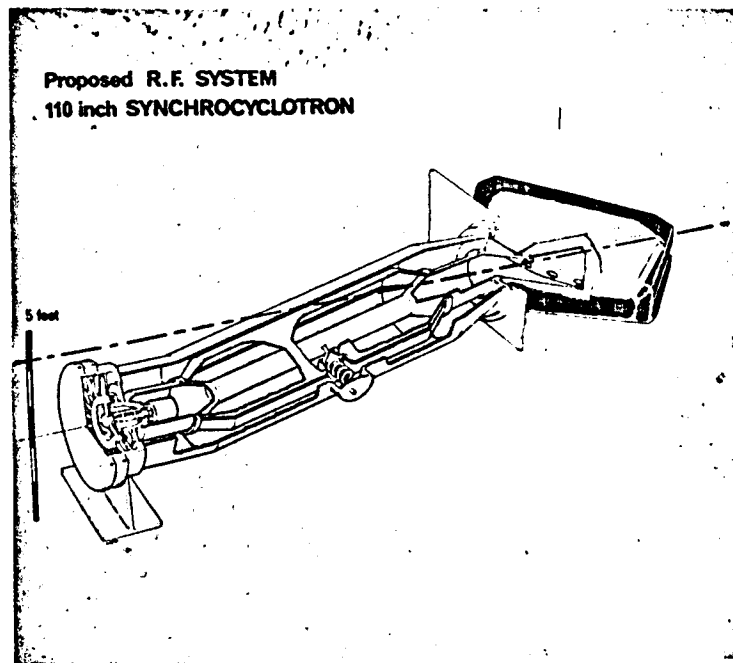


Figure 2 - Proposed r.f. system. The scale at the left is in feet.

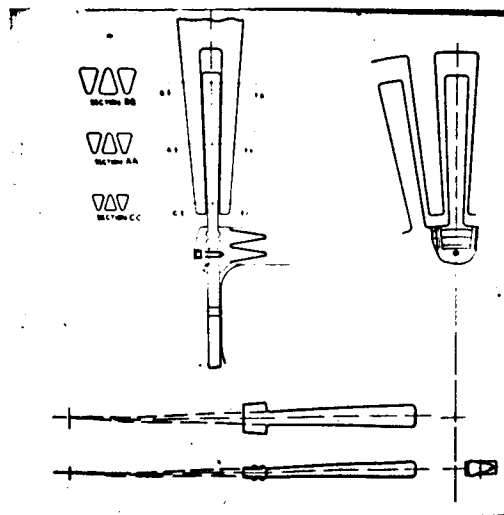


Figure 3 - Proposed rotary condenser. Details of blades.

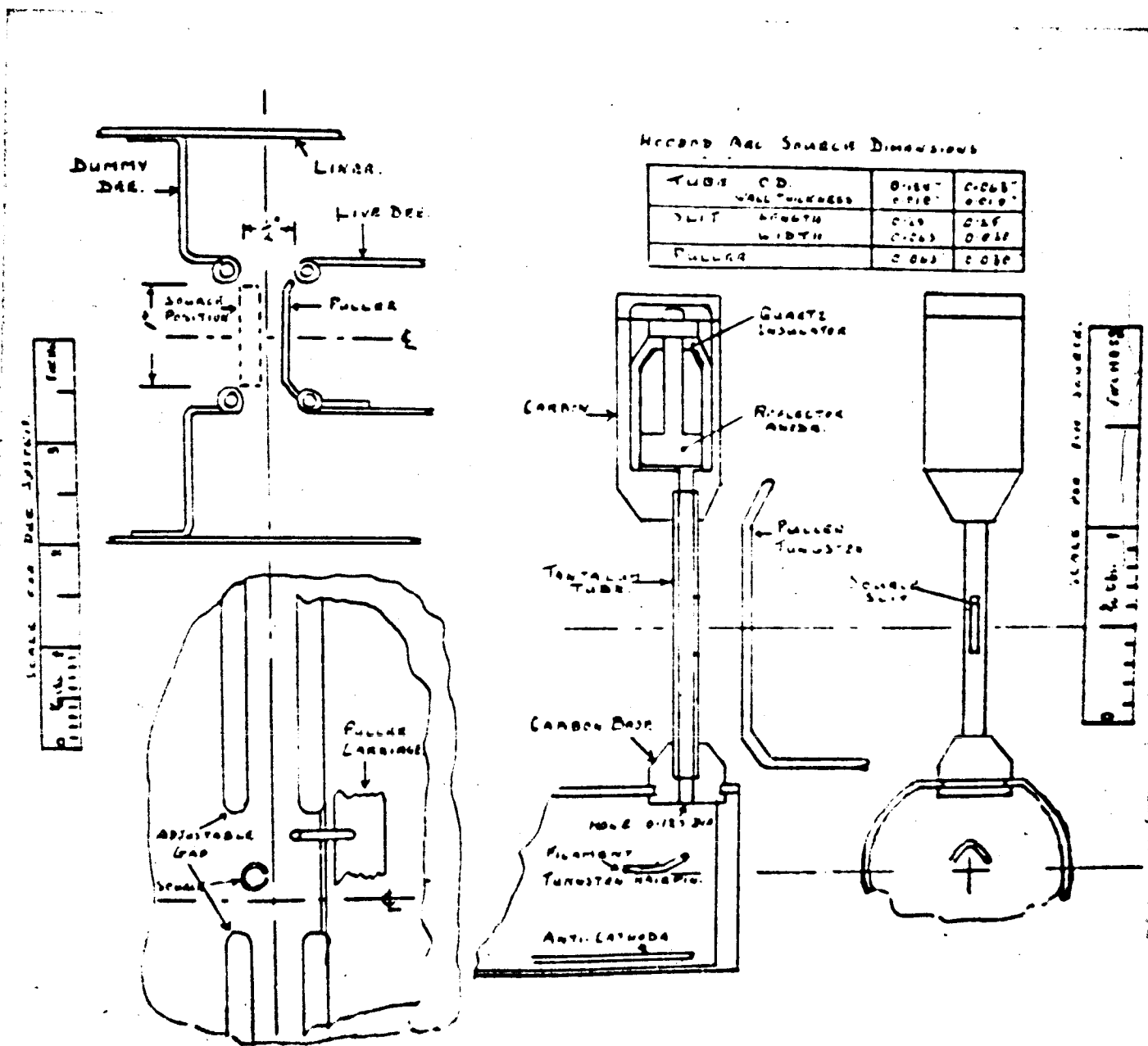


Figure 4 - Calutron ion source detail.

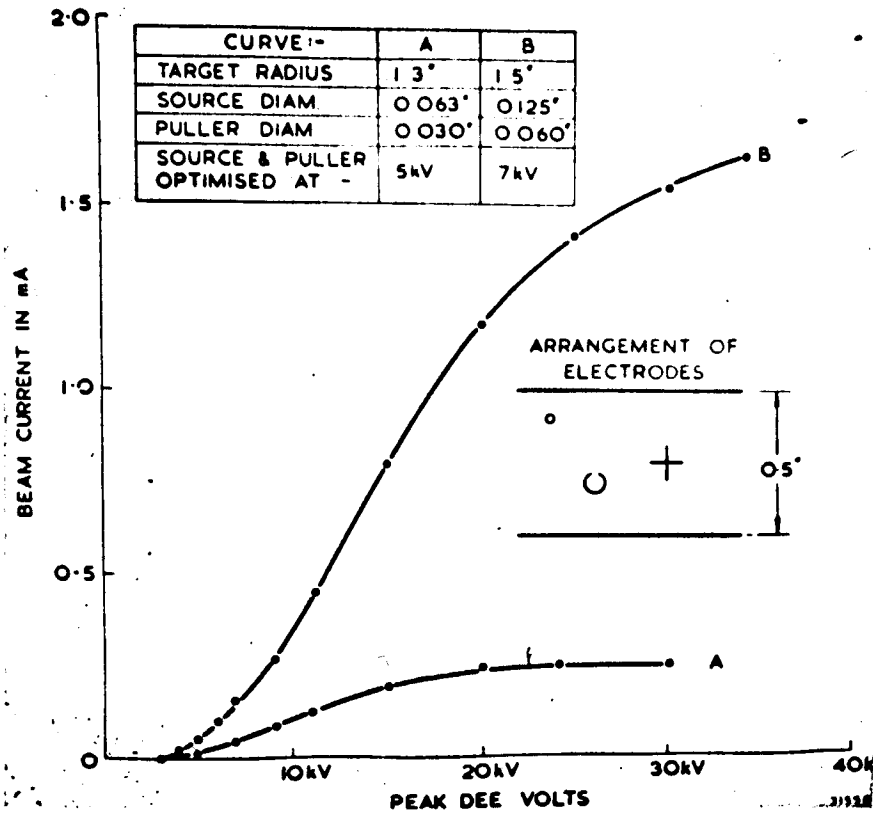


Figure 5 - Calutron ion source variation of beam with dee voltage

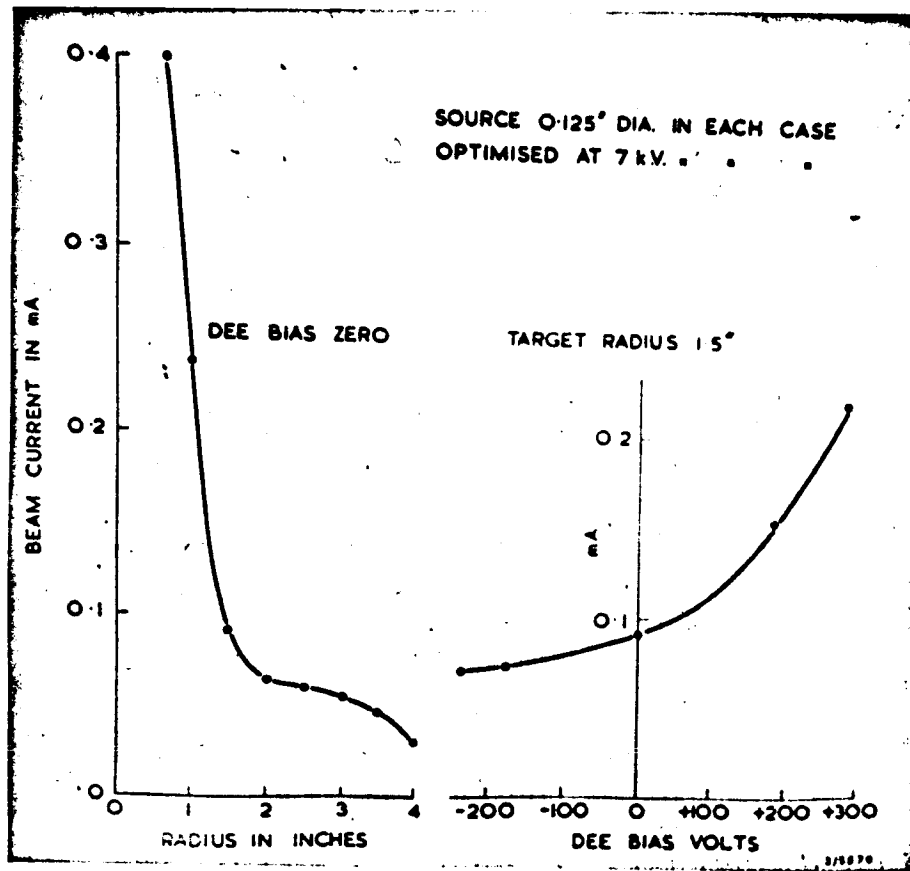


Figure 6 - Calutron ion source variation of beam with radius and with dee bias.

CROWE, Berkeley - What kind of ion source do you have?

HUXTABLE - The same as Berkeley's.

MOLTHEN, Chicago - How do you plan to get your increase in dee voltage; is it more power?

HUXTABLE - Our present dee has a large capacity, nearly 2,000 pfs, whereas the proposed sectorized dee would be around 350 pfs.

KOHLER, Harvard - What are you doing to keep the r.f. currents off your bearings.

HUXTABLE - We use a system similar to that reported at Chicago. We have the blades of the rotor sitting in a ring which is fixed to an insulating disk. A conducting coating is then put on the insulating disk to make a guard ring, so that most of the r.f. is shorted out to ground through the stray capacitance.

SOME REMARKS ON THE ROCHESTER SYNCHROCYCLOTRON

S. W. Barnes
University of Rochester

I will report on a rather elderly machine which has had somewhat of a raffish past. One of its misdemeanors was getting designed without any shielding. As a result of this it has been somewhat of a nuisance to some of the people living nearby.

About three years ago we decided to rejuvenate the machine because it was not fit for the future the way it was. The result was quite an increase in current. I will try to compare the machine before it was torn down with the way it was after.

Let me give some of the usual characteristics of the machine. The energy is 240 MeV; the r.f. system is a quarter wave-length; the dee has grounded stubs and has a flat inner clear aperture of about $2\frac{1}{2}$ inches. It is mechanically grounded and so we have electron sweep grids above and below it to take care of the electron loading. The oscillator is of the grounded grid type operated at about 40 KW. The frequency swing is 18.6 mcs to 26.5 mcs. Figure 1 shows the old rotating condenser. It was 18" in diameter and was made of some 29 zircon ceramic blades covered with silver. This ran very well the first year at 3,000 rpm giving an f.m. repetition rate of 450 cycles per second. It then began to suffer radiation damage as we noticed when the teeth flew off the blades. We had to be satisfied then with various compromises; we went to metal blades but had to drive them at a lower speed. This cut down the beam current.

The machine gave about one microamp when it was running well. This was measured in various ways, e.g. activity from a bombarded target, etc. We started the improvement program with the hope of raising the current from one microampere to 5 microamperes and then to improve the shielding, to improve the duty cycle, and eventually to try to accelerate to $n = 1$. Figure 2 is a view of the machine unshielded, showing the front or research side. The new dee has a clear internal vertical aperture of 6 inches at the center as shown in Figure 3 and narrows down towards the periphery. Figure 4 is a diagram for the new and old condensers. The old condenser was operating in quite a strong magnetic field gradient and meshed with one row of dee stator teeth. We moved the new condenser back 7 inches to get it into a weaker magnetic field and used a pair of rows of dee stator teeth instead of a single row of dee stator teeth as shown in Figure 4. That enabled us to cut down the size so that it is now 13 inches in diameter instead of 18, weighs about 40 pounds, and spins madly. The blades are stainless steel because we wanted to have something that was free of radiation damage. There is no insulator anywhere in the rotor. The blades, because of temperature gradients, are water-cooled by stainless steel pipes which tap into a water-cooled shaft. We were conservative and silver-plated the blades. When we drove them hard the silver began to blister. I think we will just let the silver blister off and run them without the silver on them. We wanted to be able to drive the condenser at a higher rotation rate than before and wanted higher dee voltage and a higher clear aperture. We got higher dee voltage principally by putting a cold trap right beside the rotating condenser.

Figure 5 shows the method of measuring beam current after the above improvements. We used a brass C-probe big enough to stop the protons. First we covered the probe with photographic film and got the $n = .2$ blowup. Then we replaced the photographic film with scintilon, $1/4$ inch thick, inserted the probe again, and ran for a known number of monitor counts mentioned below. Then knowing the amount of carbon in the scintilon and proton-carbon cross section we measured the activity in each of the scintilon pieces, added them up, and came out with a figure for the proton current. This gives the least amount of trouble for self-absorption of the electrons, etc. We did get beautifully straight 20.3 minute decay curves. In general we monitored our beam current by means of an ionization chamber that is buried in one part of the shield. This was calibrated against the C^{11} activity of the scintilon on the probe. The left side of Figure 6 shows the beam current in microamperes, using the C^{11} calibration as a function of rotor rpm for three oscillator power levels, 10, 15 and 20 KW. On the right of Figure 6 we have plotted the behavior of the beam as a function of the power going into the oscillator in kilowatts for various rotor speeds. The data shows currents of more than $5 \mu a$.

Figure 7 shows the shielding that the machine has now, sufficient to make us comfortable for beams of 5 microamps. The cave is covered with a 3-foot roof and that seems to be adequate. Most of the neutron leakage occurs in the median plane. The letters drawn in Figure 7 are positions immediately outside the shield at which we have measured neutron intensities at a current of about $1/6$ of a microampere.

The front of the machine is closed by gondolas carrying 3-foot

brass or lead shields and also carrying a polarized proton port. This generally fits behind the bending magnet whose coils are covered by concrete above and below. Even the 4-foot yokes leaked neutrons at quite a rate and we had to put the concrete outside them.

Figure 8 shows the number of neutrons per square centimeter per second measured with three types of instruments as you walk-around the shield from Z to M using the position notation of Figure 7. The internal beam current is $1/6 \mu a$. Most of the way around we have not more than a few hundred neutrons per square centimeter per second, so the shielding is not so terribly bad. People in the medical school close by have been using whole body counters and before we put in the new shielding, we tripled their background rate which distressed them intensely. So we measured the neutron flux with a BF_3 , a long counter, and a CH_4 counter at various distances (Figure 9) from the machine toward the medical school going as far as 1200 feet. The fast neutrons, the CH_4 counter, fell off as $1/r$, and the slower ones as $1/r^2$.

Figure 10 shows the set-up for a polarized external proton beam. Protons are taken off at a scattering angle of 14 degrees and pass through a quadrupole and bending magnet and to a useable place in the experimental room. The characteristics of the beam are: polarization $91 \pm 1\%$, the mean energy is $213 \text{ MeV} \pm 1 \text{ MeV}$, an energy spread, $\Delta E \sim 6\text{-}10 \text{ MeV}$. Depending upon the setting of slits inside the tank which are not shown in the diagram, we find a beam current through a $3/8$ inch opening of about 2×10^5 protons per second with an angular divergence of $1/4$ degree, full width at half maximum. If the protons are allowed to come through an aperture one inch by two inches with

no collimator following the bending magnet, the beam current is 7×10^7 protons per second.

Figure 11 shows the arrangement for the pion beam at a target in about the same place as the target for the polarized proton beam. The pion beam passes through a steering magnet and enters an iron box shielding counting equipment. This beam has an energy of 32 ± 2 MeV and for 5 microamp internal proton beam consists of about $3 \times 10^4 \pi^+ \text{'S/sec}$ and $1 \times 10^4 \pi^- \text{'S/sec}$ through a crystal that is $1\frac{1}{4}$ inch high by $3/4$ inches.

Figure 12 shows a view of a rotating target which Emery Nordberg built and used. It is completely inside the tank, driven by its own motor, and rides on Atwood machine wheels. This cut down bearing trouble. It is not so bad for use inside $n = .2$. Nordberg found out that when used at the maximum radius it reduces the current so much that it is only occasionally an advantage.

Turning next to tank and target radio-activity, in making measurements of the beam as a function of radius we obtained a measure of the activity on a carbon target $3/8$ inch thick at a very reduced beam level. Then we scaled this reading up to our full beam at 5 microamps. At this current the carbon target would have an activity of 300 r per hour at the end of a 20 minute bombardment. The immediate exterior of the tank has a radiation level varying somewhere between .2 and .8 r per hour the morning after the machine had been shut off at midnight.

After we started the reconversion we heard about the success at the Toyko machine in accelerating protons to $n = 1.0$ and we thought we would try it. To do so we thought we should improve our magnetic field and again Dr. Norberg did this. Figure 13 shows for several radii the

azimuthal variation in the magnetic flux density from 0 to 360 degrees. The dotted curves represent the field before shimming; the solid curves the field after shimming. Norberg managed to reduce the fluctuation by a factor of 10. I should point out that out of 16,700 gauss the variation is no greater than 1 gauss. Its average variation is considerably less than 1 gauss, a fairly uniform field. Figure 14 shows behavior at larger radii using the same notation, $n = 0.2$ at $r = 58"$. We still have variations ≤ 1 gauss. With this good field we hope to have some luck in accelerating to $n = 1$.

Figure 15 shows the internal proton beam current as a function of the radius for two values of main magnet current, indicated by the 103 and 106 millivolt readings. The y-axis is the current normalized to current at $r = 58"$. $n = 1.0$ at 60.5 inches. This data was taken in '49 so it is very old and it is nonsense to have the curve rise at $n \simeq 1$. I have forgotten how we made the measurements in those days. Anyway, the minimum for the 103 mv. reading is probably believable and is about 7%. This minimum for the 108 mv. reading is something like 2%. We turned on the machine for a few minutes the other day and ran carbon probes in at various radii and got 2% of the beam at $n = 1$. Apparently the $n = .2$ and $.25$ resonances are still bothering us. It is interesting that the first time we tried this the other day, we had the vertical aperture restricted by some $1\frac{1}{4}"$ carbon pieces inside the dee at the periphery. We got absolutely nothing beyond $n = .2$. We then took them out and immediately we got 1% of the beam. When we then moved the ion source $\sim \frac{1}{4}$ inch we doubled the beam from 1% to 2%. We think a little more arc adjustment may possibly bring the beam out

in greater intensity to $n = 1$. If it doesn't it may be that distorting the dee somewhat will enable more of the beam to get out through those two resonances. It would be very handy for us to have the beam out there because it should be easier to extract it.

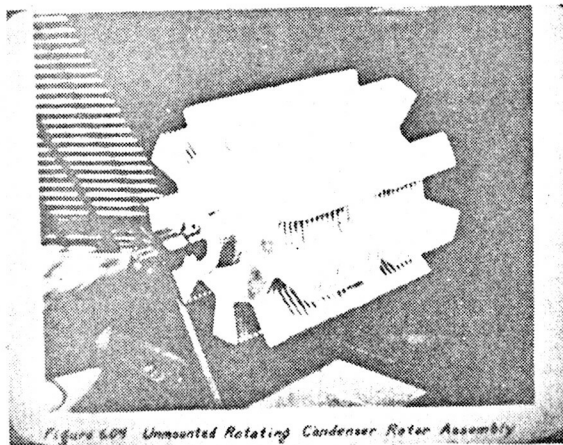


Figure 1 - Old rotating condenser

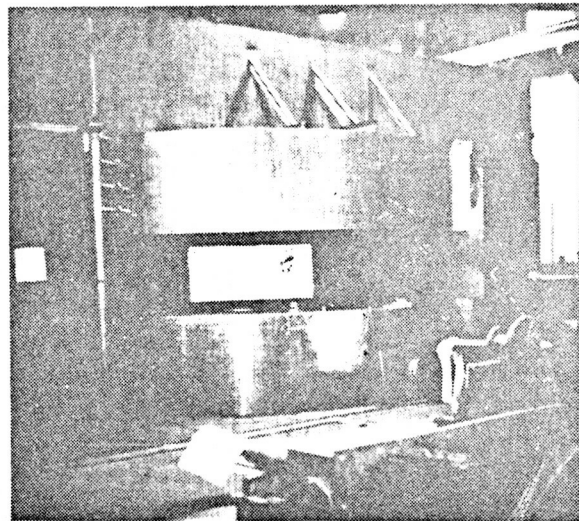
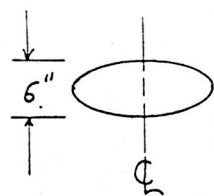
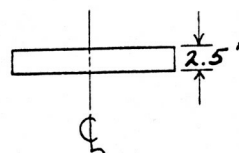


Figure 2 - Research side of cyclotron



a) New dee



b) Old dee

Figure 3 - Elevation, a) new dee, b) old dee

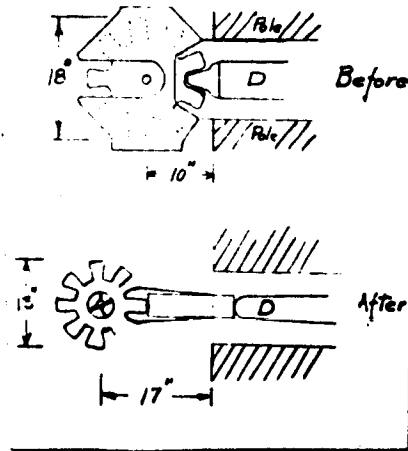


Figure 4 - Elevation sketch of old and new rotating condenser systems.

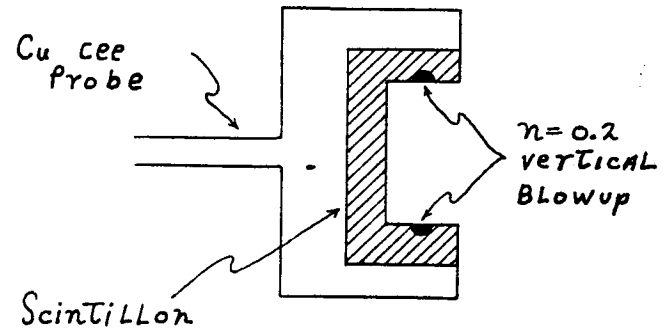


Figure 5 - Probe for activity-type internal current measurement.

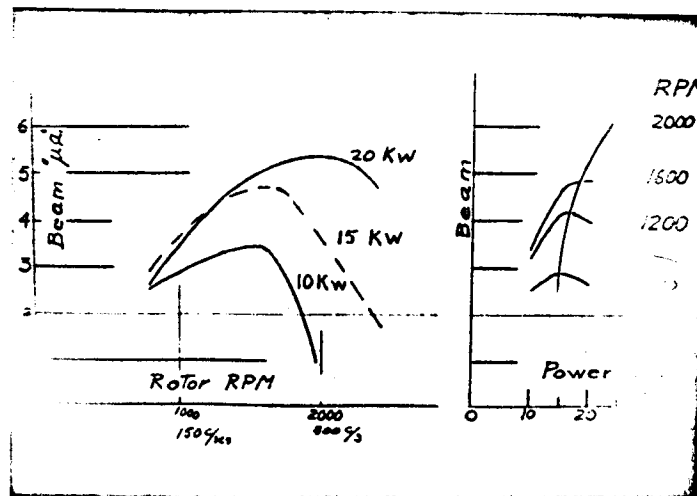
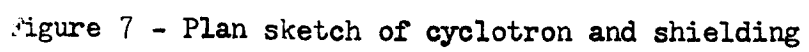


Figure 6 - Beam vs. function of dee oscillator power and repetition rate.



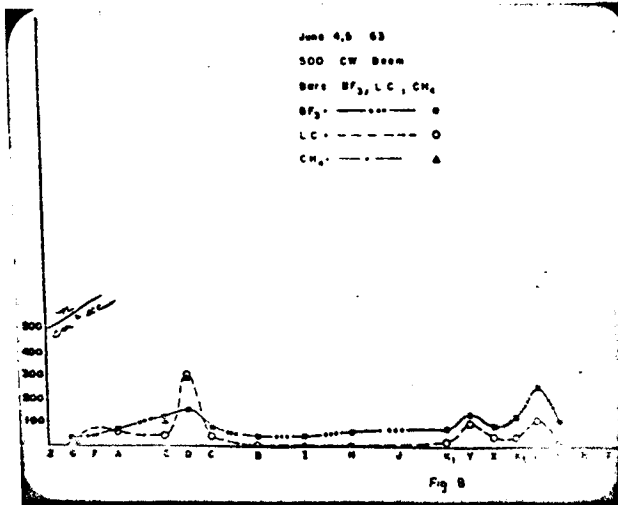


Figure 8 - Neutrons/cm² sec at various locations indicated in Figure 7.

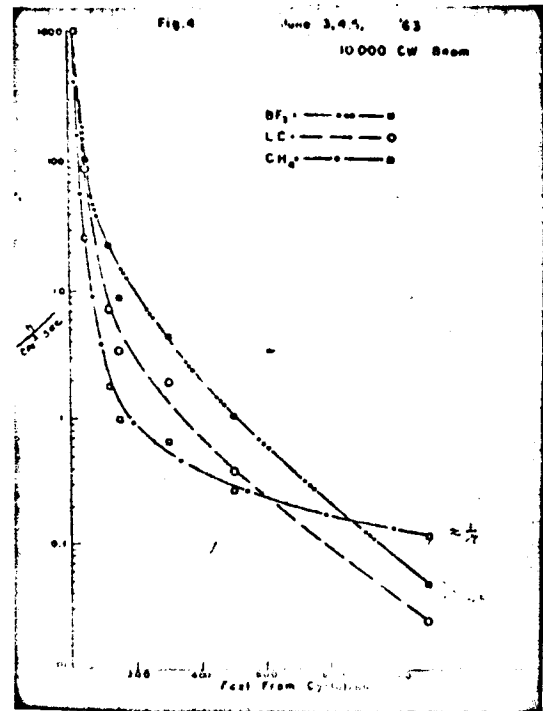


Figure 9 - Neutron flux vs. distance from machine for various types of counters.

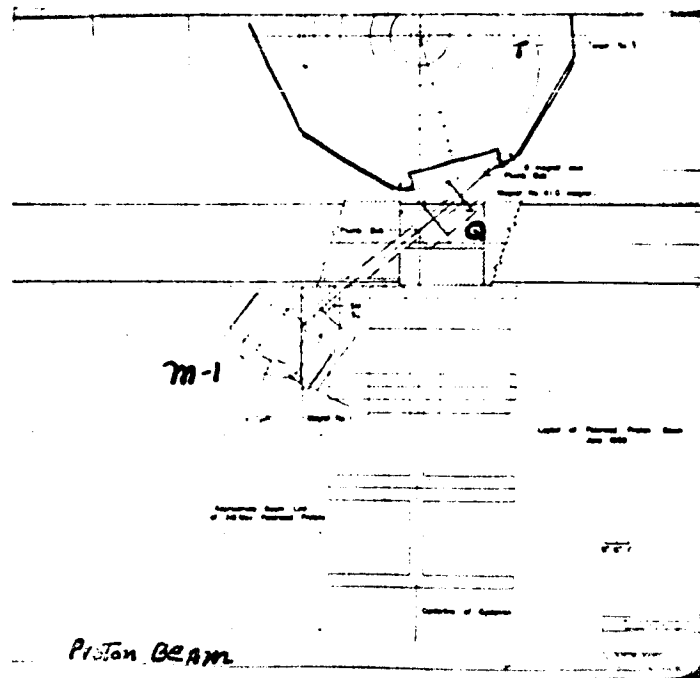


Figure 10 - Plan view for external polarized beam target set-up. 218 MeV polarized proton beam comes from internal target, T, through quadrupole Q, and bending magnet M-1.

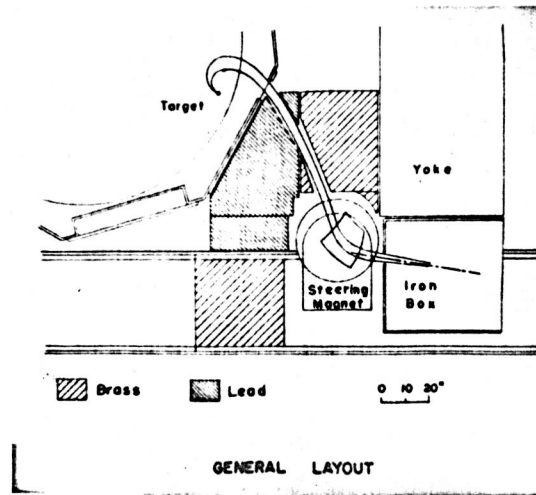


Figure 11 - Plan view of experimental area facility

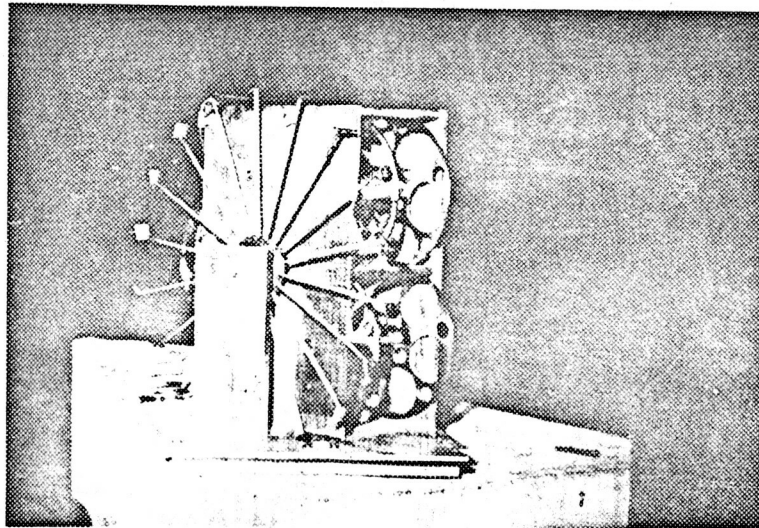


Figure 12 - Internal rotating target assembly

Figure 13



Figure 13 - Asimuthal variation of magnetic field at the radii indicated



Figure 14 - Azimuthal variation of magnetic field at the radii indicated

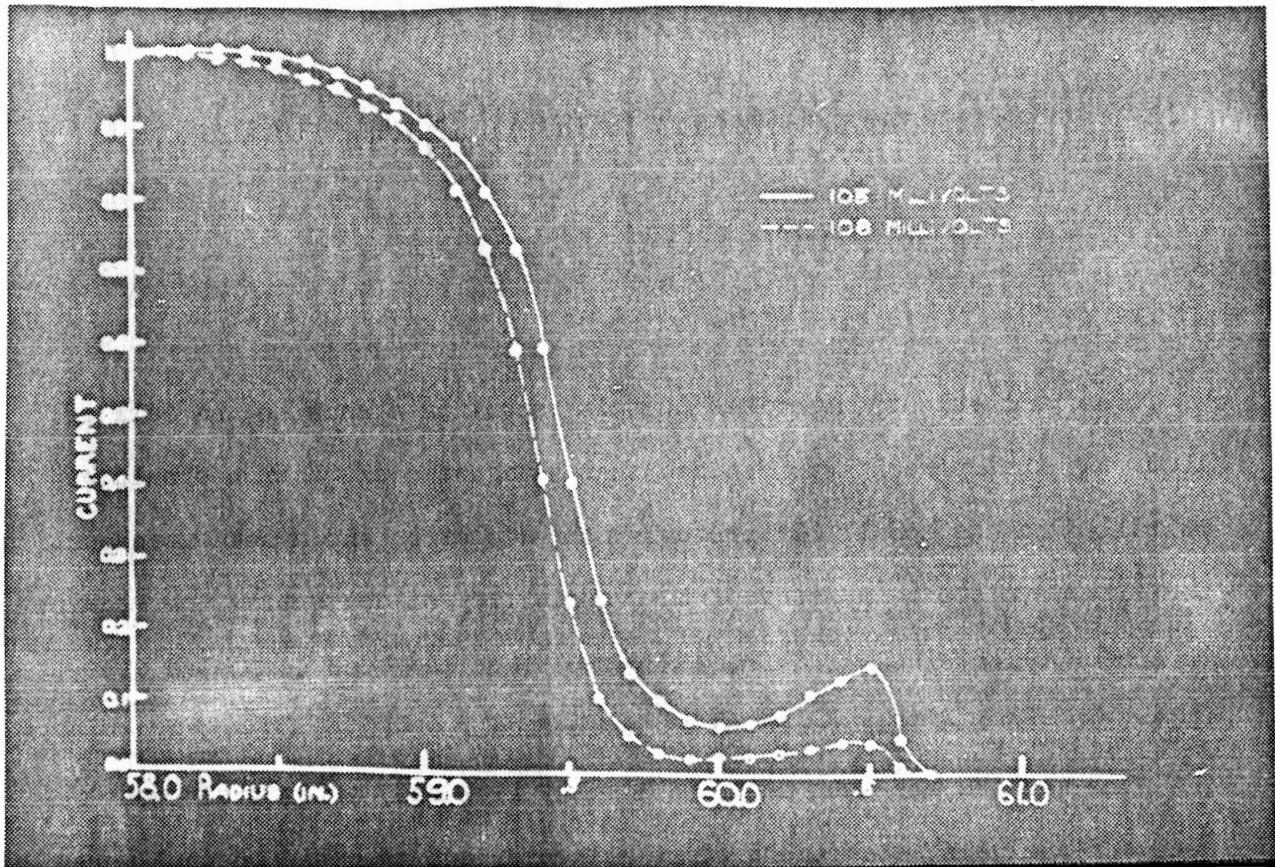


Figure 15 - Internal proton beam current as a function of radius.

WELSH, William and Mary - How did you measure the magnetic field and what accuracy did you obtain?

EMORY, Rochester - We used flux coils and the accuracy was to around 0.1 gauss.

BARNES - comment - I forgot to mention one thing; when we made the current measurements that stopped at 6 μ a, we unfortunately had the ion source about 1/2" out of its optimum position. The positioning motor was burned out. As soon as it was fixed, the current jumped up by a factor of 4/3, so we really had 8 μ a instead of 6 μ a.

SUZUKI, Carnegie - What is your geometry near the ion source?

BARNES - We have a McGill cold cathode ion source.

RECENT IMPROVEMENTS TO THE MCGILL SYNCHROCYCLOTRON

R. B. Moore, McGill

The improvements described in this report date back to the fall of 1960: At that time it was decided that a magnetic extraction should be installed in the McGill 82" proton synchrocyclotron and a beam transport facility developed. A study of the possibility of converting the machine to a sector focusing fixed frequency cyclotron had been completed at that time and the idea rejected as impractical.

The machine was shut down in February 1961 and, after field measurement and analysis, the regenerative extractor and magnetic channel were designed and installed. An external beam was obtained in August 1961.

For the period to December 1962 the machine was used for physics research, using both the internal and the external beams. A relatively crude beam transport system was set up and used by Barton and McPherson to discover and investigate delayed proton radioactivity. A brief description of this system is given in the publication of their work⁽¹⁾. During this period plans were laid for extension of the laboratory and beam transport equipment.

The construction was started in December 1962 and finished in May 1963, and the beam transport system was operational by November 1963.

Beam Extraction

The regenerator follows the design criteria of LeCouteur. Field

⁽¹⁾ Canadian Journal of Physics, 41, 2007 (1963).

measurement and analysis led to a design regenerator strength following the equation

$$\frac{r_o}{B_o} \int \Delta B d\theta = 0.2\rho + 0.40\rho^2$$

for r_o, ρ expressed in inches, θ in radians where r_o, B_o are the values of radius and magnetic field at the last undeflected orbit, ΔB is the field change at $r_o + \rho$ due to the regenerator.

The regenerator was set up to deflect the orbiting protons into a magnetic channel made up of 4" sections with iron walls 2" high and varying from 1/4" thick for the entrance section to 3/4" thick for the exit section. The channel entrance was located to lead the regenerator in azimuth by 64° . In the region of the vertical cross-over of the beam due to the focusing action of the cyclotron fringing field gradient, two channel sections were replaced by pieces of iron forming passive quadrupoles with positive radial field gradient. This enabled a cancellation of the horizontal divergence without an increase in vertical divergence. Minor empirical alterations to the original design of these quadrupoles produced a beam spot 1" high and 2" wide at a distance of 20 feet from the channel entrance.

Mechanisms were provided so that the radial position of the regenerator, and of the entrance and exit of each channel section, could be adjusted without breaking the cyclotron vacuum. The alignment of the regenerator and channel sections was accomplished by using these mechanisms and an insulated copper block as a current measuring device which could be moved along the channel to check the beam transmission.

The original design of regenerator produced an external beam of about 5 nanoamps. Increasing the regenerator strength by 10% resulted in a final

beam intensity of 30 nanoamp. Trimming this beam to avoid collision with bending magnet pole pieces leaves a transported beam of 20 nanoamp, for a final extraction efficiency of about 5%.

The area in phase space of the 30 nanoamp beam is about 1 inch milliradian in the horizontal plane and 2 inch milliradian in the vertical plane (Fig. 1). The 20 nanoamp beam has areas of 1 inch milliradian in both horizontal and vertical planes. The phase space diagrams are obtained by tracing the rays formed by placing in the beam a block of brass with a rectangular array of small holes. Ray tracing was carried out with Polaroid Land Film Packets (Polapan 200, type 52).

The energy of the proton beam is about 98 MeV (uncertain due to uncertainty of range-energy relationship). Its range in pure aluminum is 9710 mg/cm^2 . Its energy spread appears to be less than 1 MeV.

Transport System

A layout of the transport system is shown in Fig. 2. The entrance and exit angles of the 30° and 45° magnets are designed to focus the beam in both horizontal and vertical planes at a distance of one foot from the exit of the 45° magnet. Beryllium degraders are placed at this focus to give a degraded energy beam.

The quadrupole sets are made up of a combination of a 4" quadrupole magnet manufactured by Spectromagnetics Industries and a 6" quadrupole manufactured by Pacific Electric Motor Company. This arrangement is best for our purposes because of the short focal lengths we can obtain with 100 MeV protons in these magnets.

In the center of the switch magnet the gap has been widened to allow a flexible section in the vacuum chamber. This allows the complete transport system after the switch magnet to be moved so as to accommodate the beam

through a bend of $\pm 15^\circ$, this movement being accomplished without breaking the vacuum.

The beam of 20 nanoamp after the second quadrupole set can be reduced to a spot about 0.001 in^2 in area with maximum current in the quadrupole magnets.

The bending magnets were designed at this Laboratory and the iron fabricated by Dominion Engineering Company, Limited. The windings were built in the Laboratory by using Alcan aluminum tape with mylar strip insulation and edge cooling with copper plates. Power supplies and regulation were also designed and built at the Laboratory.

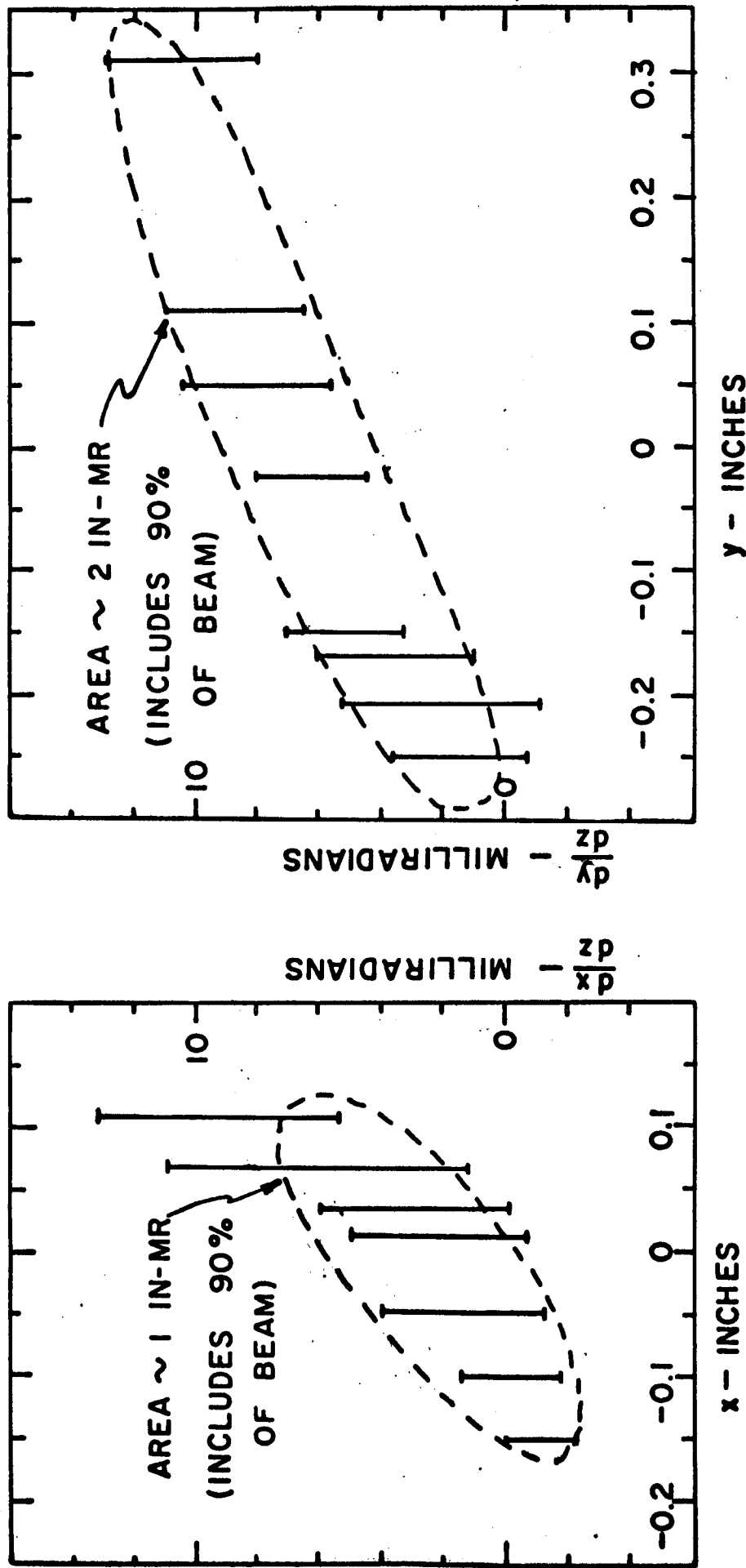


**FIG. 1 - EMITTANCE DIAGRAMS OF EXTERNAL BEAM
55 INCHES FROM CHANNEL EXIT**

(VERTICAL BARS INCLUDE BEAM DENSITIES OF ABOUT 5% OF MAXIMUM AT PARTICULAR COORDINATES. A RIGHT-HAND COORDINATE SYSTEM IS USED.)

EARTH FILL

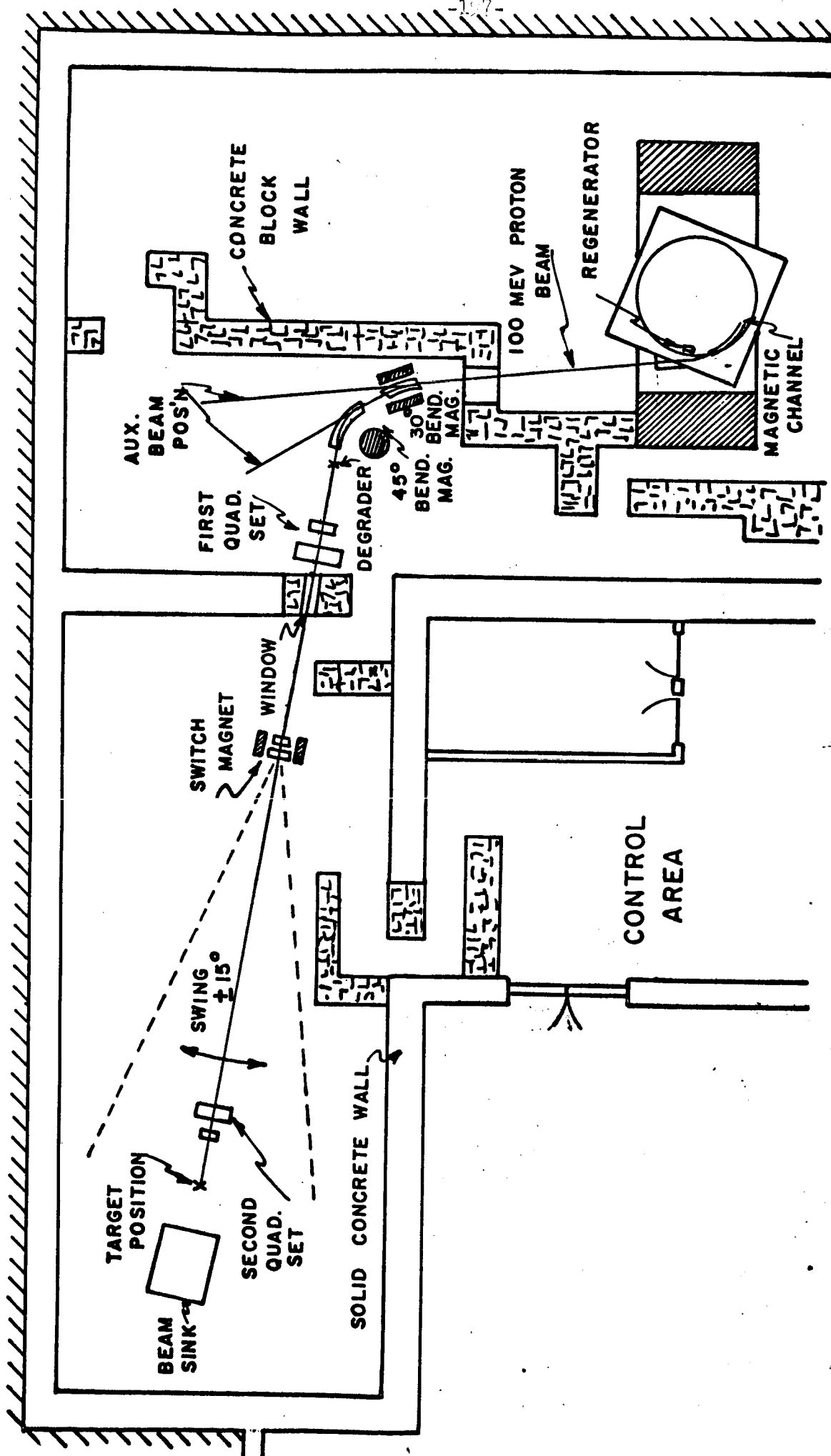


FIG.2 - LAYOUT OF BEAM SYSTEM

IMPROVEMENTS ON THE PRINCETON 18 MeV SYNCHROCYCLOTRON

Ruby Sherr
Princeton University

The Princeton cyclotron is a 17 MeV proton machine. Hearing the talks yesterday, I thought some of our beam characteristics, which are in the same ball park as those of higher energy machines, might be of some interest. About three years ago and for two years before that, we were running with parameters that were something like the following: the internal beam was about .5 microamperes; of this we could get about .07 microamperes deflected. This deflected beam was brought out into the experimental cave through some wedge magnets which, in effect, constituted a quadrupole system (and in fact were in use about three years before quadrupoles were "invented".) With the two sets of wedges we were able to get into a scattering chamber currents of the order of about 1/3 the deflected beam, perhaps 20 nano-amps. It was about this time that we were very worried about trying to do some coincidence experiments and, having heard about the success at the ORSAY synchrocyclotron, we started to initiate a development of that type of apparatus. The first thing we did was to see whether our beam would coast so we put in a plate quench system in the oscillator and found out indeed that the beam did coast when the oscillator was turned off so that one could profitably install a Cee. The interesting thing, however, at this point was that because we were quenching the r.f. off half the time we were able to increase the r.f. voltage the other half f.m. cycle.

Furthermore, it turned out that oscillator breakdown was caused by the average power and not the peak power. Therefore, we were able to go to twice the peak power and the result was that we immediately got up to two microamps internal beam. The conditions now are such that we get about .2 microamps deflected. In the external beam area we now get about .06 to .10 microamperes. We have been striving for a greater energy resolution in the beam and now send the beam through an analyzing magnet and select a section with a 30 kilovolt energy spread. We now get from .004 to .015 microamperes at this energy spread which corresponds to a $\frac{dp}{p} \approx .08\%$. This figure is very interesting because a normal beam spread before the analyzing magnet would vary from 120 to 150 kilovolts. However, it seems that once in a while our beam arrives at the analyzing magnet with an energy spread that seems to be sometimes in the order of 50 kilovolts. We don't understand what it is that makes the beam energy spread change in such a drastic way. Whether this effect has been observed in higher energy machines I don't know.

POSTSCRIPT, April 1964.

Since the Williamsburg Conference we have installed a tungsten wire feeler which points at the open arc as shown in Figure 1. Using an ion source pulser and raising the oscillator plate voltage from 5 to 6.4 kev, we have had an internal beam of $7 \mu a$, a deflected beam of $0.5 \mu a$, and $.03 \mu a$ in our scattering chamber at 30 kev resolution.

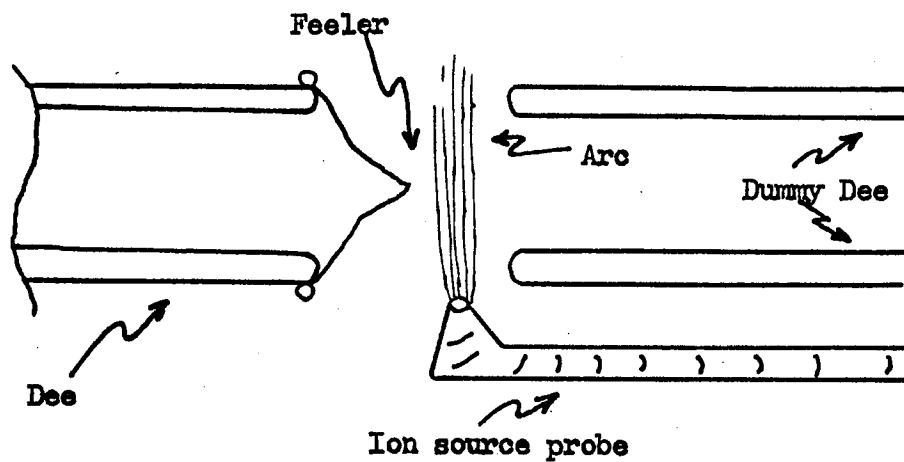


Figure 1 - Arc and feeler assembly in Princeton cyclotron.

CYCLOTRON SPACE CHARGE LIMITS

K. R. MacKenzie, UCLA

INTRODUCTION AND HISTORY

The theory presented in this paper indicates that all cyclotrons, even the fm cyclotron, operate under some sort of space charge limitation. Strangely, it is the fm cyclotron which is most likely to benefit. In such machines the ion source is obviously suspect, but in the main it seems that the dense ion cloud surrounding the source is a more important factor, causing a loss in the vertical direction where focusing forces are weak. Evidence for a limitation of this sort has been accumulating for many years and a good part of the theory in this paper dates back to 1954. A short history including some attempts to raise the space charge limit seems worth recounting.

In the past, space charge has seldom been envisaged as a reason for low intensity. There were far too many obvious troubles such as poor vacuum, sparking, insulator breakage, ion source failures, deflection problems, etc. Most important of course was the relativistic increase in mass. The synchrocyclotron removed this latter limit, but at the expense of a low duty cycle, low intensity, and low deflection efficiency. Recently the low duty factor objection has been largely overcome by beam storage at the final radius followed by extraction in almost continuous fashion by a small auxiliary dee. No cure has been found for the low intensity and low deflection efficiency. Typical numbers are an internal beam of 1 μ a and a deflection efficiency of 1 or 2 percent.

The current in large conventional cyclotrons has for some time been of the order of 1 ma, and with this fact well appreciated, it seems hardly possible to imagine any space charge effects with a beam as small as 1μ a in a synchrocyclotron. It was soon found that no loss of ions occurred beyond a radius of the order of one or two magnet gaps. This established the limitation as being in the central area and it was thought to be due to poor catching efficiency and large oscillations, caused by vertical electric fields and lack of magnet focusing. All sorts of central variations were tried. Dee feelers were of some help, and some improvement was effected by adding small cones to increase the vertical focusing. Subsequent efforts to improve the beam by variations in this region are too numerous to list. Nearly every laboratory tried initial pulsing of the dee voltage. In some cases an extra dee was added near the center. Sometimes the effect of dee bias seemed to be important for proper starting conditions. Several laboratories spent years in developing and testing new forms of ion sources. For a while stochastic acceleration appeared on the scene and was regarded by many as a hopeful solution. While individual improvements were reported, none of these studies produced any variation which is generally recognized as beneficial and is now to be found on all synchrocyclotrons.

After some half dozen high energy fm cyclotrons were in operation a rather unusual fact became quite noticeable. In spite of differences in size, energy and other details of construction, all these machines produced internal beams of approximately 1μ a. For lack of any other explanation, it was gradually accepted that in spite of very small currents, space charge was imposing a limitation of some sort on the output. A dependence somewhere between V and $V^{3/2}$ might be expected. Since all these cyclotrons were running at a dee voltage as high as was consistent with steady operation, there was not much

hope of any large increase in this way. The lack of improvement by initial pulsing of the dee voltage was interpreted to mean that any extra ions that were initially extracted and caught were lost when the voltage was lowered.

About 1954, the Thomas focusing principle was re-discovered and re-activated at Berkeley in the form of two electron models.¹ In scaling to an actual machine the question of any space charge limitation was examined and a simple theory was developed.² It excited very little interest, since with the dee voltages contemplated to overcome field inaccuracies, the limitation was in excess of 100 ma. Some years later it was recognized that the crude theory might be applicable to fm cyclotrons. With several approximations a variation as V^3 seemed probable and indeed it was found that such a dependence had been measured on the 184 in. cyclotron when deuterons were the only particles that could be accelerated.³ A hasty test of the dee voltage dependence, with the 184 in. cyclotron operating on protons, resulted in almost immediate failure of the rotary capacitor brushes and bearings and a long shutdown. With shielding already quite marginal, interest in a resumption of testing met with little enthusiasm. The intensity in the pulse was already too high for many counter experiments, and even if a V^3 dependence was re-measured, there seemed to be no engineering solution which would provide significantly higher dee voltages.

In 1959 a preliminary engineering study was made for the 400 MeV Chicago synchrocyclotron.⁴ The objective was a tenfold increase in output. The recommended design changes were based on the V^3 dependence. The rejected possibilities were vibrating blades, ferrite modulation, and stochastic acceleration. The vibrating blades, with an amplitude dependence as $1/\omega^2$ were incapable of any appreciable increase in repetition rate (which must accompany any increase in dee voltage). This modulation rate was no limitation

with ferrite tuning, but the expense was enormous and there seemed to be no feasible solution to the cooling problem at high voltages. In view of the V^3 dependence, stochastic acceleration appeared hopelessly space charge limited. The remaining choice was a larger rotating capacitor. A tentative design, capable of operating at higher speeds and higher voltages was examined. But the extensive rebuilding job was decidedly unattractive and nothing was done, in the hope that a more promising solution would eventually be found.

As the result of new developments such a solution appears to exist today. The use of magnetic ridges injects a new degree of freedom into the design of the central region by removing the interdependence between focusing and radial fall-off. As a result it appears possible to increase the magnetic focusing near the source, and also shape the rise or fall-off in a way to improve the catching efficiency. Another improvement can be expected by using new ceramic insulating materials in the r.f. system. Even a doubling of the dee voltage results in an order of magnitude increase when the beam varies as V^3 .

THEORY

The ion source itself is well known to be space charge limited, and obeys a $V^{3/2}$ law when the plasma sheath boundary is maintained in a fixed position. In arc type sources with a dense plasma, this limit is usually of little concern. In 1954, Livingston and Jones⁵ showed that one can extract 100 times as many ions from a calutron source as are to be later found in the beam. Furthermore their curves showed that the ion loss occurs in a region very close to the source. Since there is insufficient time for the ions to get out of phase and return to the center, the loss must occur vertically and must be the result of large vertical oscillations or due to space charge.

Effects at Large Radii

At large radii the vertical defocusing space charge force is easy to calculate. We assume no phase slip, so the result applies to either isochronous or frequency modulated machines. The charge per cycle, $Q = 2 \pi \cdot I / \omega$, is contained in an elliptical volume, $1/2 \pi z r \phi \Delta r$, where z is half the beam height and ϕ is the azimuthal extent. Using the relation $eV = m r \omega^2 \Delta r$ where V is the energy gain per turn, we can solve for the charge per unit area normal to the plane of the beam and obtain $\sigma(esu) = (8 m \omega I) / (e \phi V)$. This expression is independent of r as we would expect, since the orbit spacing decreases as $1/r$ and the azimuthal extent varies as r . The vertical focusing force seen by an ion at a height z above the median plane is $e \lambda \pi \sigma$. Equating this force to the magnetic focusing force $m \omega^2 v_z^2 z$, leads to the expression $I(esu) = (\phi V \omega v_z^2 z) / (16 \pi)$. This is identical, except for an unimportant factor of $\pi/4$, with the expression in mks units given by Blosser and Gordon.⁶

$$I(\text{li m}) = A \epsilon_0 \omega^2 v_z^2 (\Delta \phi / 2\pi) (\Delta E / e)$$

As pointed out by these authors, the space charge limited current can vary between wide limits, primarily because of the factor v_z^2 . For example a choice of $V = 60,000$ volts per turn, $\phi = 1$ rad, $z = 1/2$ cm and $v_z = 0.1$ will limit the current to 1 ma. This current will be further reduced when one makes allowance for a reasonable oscillation amplitude and an allowance for field errors. On the other hand if $V = 300,000$ volts per turn, $z = 3$ cm, and

$v_z = 0.3$, the space charge limited current is 300 ma. Although it is probable that some cyclotrons are limited in this way, it seems much more likely that something else is holding the current down to 1 ma.

Effects at Small Radii

If a calutron source is used, the energy gain per turn will essentially be constant, and by making the following assumptions one can argue that the vertical space charge defocusing force is approximately constant everywhere, even at a radius corresponding to the first turn. 1. The ion source is assumed capable of supplying an unlimited amount of current. 2. The ions that finally emerge as useful beam are assumed to start very close to the median plane. 3. Magnetic focusing is assumed to be zero for the first few turns. 4. Electric focusing is neglected. This force decreases with radius and is essentially zero at $r = 0$ when the ions are very close to the median plane. 5. Vertical oscillations are assumed not to exist, since the forces that induce them are assumed to be zero. 6. Magnetic forces, after they enter the picture, are assumed to be some two orders of magnitude larger than space charge forces. These six assumptions remove all the usual defocusing effects and only space charge remains to spread the beam vertically. Eventually the ions will reach a height and radius where magnetic forces will return them toward the median plane. The beam profile will then be of the form shown in Figure 1.

The surface charge density within this profile is seen to be constant at all radii, even near the source, since the height goes to zero faster than the angular width. In practice this is not quite true because the vertical height is not zero at the source and there will be an increased space charge force due to orbit separation. But these are small effects, possibly of the order of a factor of two. All beam outside this limiting profile is lost vertically, and this lost beam exerts no force on the ions inside the beam profile. There is experimental evidence that such a picture can be realistic, as many cyclotrons find that nothing is gained by making the ion

source slit more than $1/4$ to $3/8$ in. high, which means that the useful ions are starting about $1/8$ in. from the median plane. A longer slit just increases dee heating and raises the pressure.

With these assumptions the path of an ion on the limiting profile of the beam is very simple and is governed by $z = 1/2 \text{ at}^2$ until magnetic forces come into play. The exact solution in this transition region is probably different for each cyclotron, and probably must be obtained numerically. Fortunately it is sufficient to assume that this magnetic focusing force enters abruptly at a radius which is designated as r_m . This is argued as follows: In the expression $F_z = m \omega^2 v_z^2 z$, the factor $v_z^2 = (r/B) \partial B / \partial r$ varies initially at least as fast as r^2 , probably nearer to r^3 since $\partial B / \partial r$ is zero at the center. From the relation $z = 1/2 \text{ at}^2$, z varies as t^2 and t in turn varies as r^2 . Thus the ion sees the magnetic force enter as r^6 or r^7 . Such an abrupt dependence means that the vertical motion of the ion is halted in a very short vertical distance and the ion is then turned toward the median plane. Since the usual type of vertical oscillation has been ignored, the subsequent motion will be in the form of a coherent oscillation in which the ion either crosses the median plane or remains on one side.

With the assumption that the magnetic force enters in stepwise fashion as r_m , it remains to simply use the relations $a = F_z/m = (16 \pi \cdot \omega \cdot I) / (\phi V)$ and $t = (\text{no. of turns})/f = 1/2 (m r_m^2 \omega^2 \pi) / \sqrt{e \omega}$ in the equation $z = 1/2 \text{ at}^2$ and obtain

$$I(\text{esu}) = z \frac{\phi}{(2\pi\omega)^3} \left(\frac{e}{m}\right)^2 \frac{V^3}{r_m^4}, \quad I(\text{amps}) = \frac{z}{2} \frac{E_0 \phi}{\pi^2 \omega^3} \left(\frac{e}{m}\right)^2 \frac{V^3}{r_m^4}$$

FM Cyclotrons

The foregoing analysis does not hold in the case of an f.m. cyclotron because open sources are almost always used. The ions gain very little energy in the beginning, so a very dense space charge cloud exists at the center with a functional dependence on radius that seems too complicated to resolve. But again it is possible to make an assumption which makes the whole problem simple. The dense cloud is assumed to exist only near the source. In traversing this region the ions receive an impulse which governs their vertical motion until caught by magnetic forces. The constant vertical space charge force of the previous section is assumed to be small by comparison.

The nature of the beam dependence on this local space charge effect is found at once. The impulse force in this region is $F_z \sim Q \sim I / V$. The impulse $= mv_z = F_z \cdot \Delta t \sim I/V^2$, since $\Delta t \sim 1/V$. $z = v_z t$, and $t \sim 1/V$. Hence we again find a dependence as V^3 , and for convenience we can incorporate this in the previous formula with a constant K to take account of the loss in intensity that results from using an open source. The final formula is then

$$I(\text{amps}) = K \frac{z}{2} \frac{\epsilon_0 \phi}{\pi^2 \omega^3} \left(\frac{e}{m} \right)^2 \frac{V^3}{r_m^4}.$$

When multiplied by the capture efficiency, this formula should predict the output of an f.m. machine. One might think that a variation as V^4 should be predicted since the number of beam bunches varies as the modulation rate, which varies as V. But this is in disagreement with experiment, so it seems likely that the product of catching efficiency and acceptance time is a constant.

EXPERIMENT

In 1954 the center region of a three phase Thomas type cyclotron was studied extensively using a 20 in. diameter model magnet.⁹ The final energy

of 1 MeV was attained in ten to twenty turns so relativistic effects could be ignored. Of the several ion sources used, the calutron type gave the most beam. The aperture was $3/4$ in. by $1/8$ in., which should yield some 60 ma according to the data of Livingston and Jones, (reference 5). To help overcome space charge effects, the extractor electrodes were curved to give some "z focusing", as shown in Figure 2. Under the best conditions the proton beam was 6 ma. The pertinent parameters were as follows: $K = 1$, $V = 100$ Kv per turn, $f = 11$ mc, magnet gap = 13 cm, internal dee height = 5 cm. If these numbers are inserted in the formula, a current of 6 ma is found, provided that r_m is assumed to be 10 cm. This is somewhat less than one magnet gap, but is still a reasonable radius to choose for the onset of magnet focusing. The effect of this parameter is felt as the fourth power, and it is easy to fit almost any cyclotron data by assuming a number of the order of one magnet gap.

The beam vs dee voltage is shown in Figure 3 and at high dee voltages the curve deviates markedly from a V^3 law. From the beam vs radius as shown in Figure 4 at 22 kv, one might deduce that the beam at the source when the voltage is 30 kv would be of the order of 60 ma, which would imply that the ion source is beginning to limit the output.

FM Cyclotrons

Applying the formula to f.m. cyclotrons we might choose gap and beam dimensions about the same as for the 20 in. model we have just discussed. Assuming $V = 10$ kv, $K = 0.1$, and a capture efficiency of 10%, the formula yields a beam current of 0.1μ a. This is about an order of magnitude lower than usually observed, but considering the approximations that have been made, this number might be considered as some sort of agreement. A more sensitive test of the theory is the dependence on dee voltage. Henrich, Sewell, and

Vale (reference 3) made a careful study of the characteristics of synchrocyclotrons and one of the measurements was the dependence on dee voltage, taking care to optimize all other parameters at each reading. They found a V^3 dependence as shown in Figure 5. It happens that the beam observed at 10 KeV per turn in their measurement in 1949 is almost exactly the 0.1μ a calculated above. There are many effects which can be evoked to explain beams 10 times higher than this with lower than 10 KeV per turn. Electric focusing is probably not to be neglected in an f.m. machine since the ions riding at a stable phase angle are subject to strong electric focusing forces.

POSSIBLE FM CYCLOTRON IMPROVEMENTS

Central Ridges

If there is any truth in this analysis, it should be possible to greatly increase the output of a synchrocyclotron. The simplest approach would seem to be the replacement of the central cones with a central ridge structure as shown in Figure 6. The shape of the beam profile would allow the dee skin to be contoured in the same manner and would allow the ridges to come very close to the beam. At the dee voltages in use on f.m. machines the ridges could approach within $1/4$ in. of the dee with little trouble from sparking. The exposed area is small and the r.f. sparking rate is presumably a function of area. The increase in capacity due to the ridges would in first order be offset by the local reduction in dee thickness.

Thin Dee Section

The ridges can come very close to the beam profile if the dee thickness in the depressed region is locally reduced to the order of $1/16$ in. Water cooling is out of the question, so a material such as tantalum would be

appropriate. The heat developed by ion bombardment could then be carried away by radiation. No attention need be paid to local r.f. heating, since it is negligible in this region. Heating by ions could be minimized by reducing the height of the source until only the acceptable ions emerge. Nevertheless it is probable that enough ions will be lost vertically to heat the tantalum to a cheerful red. This surface will remain clean and will probably have less tendency to spark than the rest of the dee.

Calutron Source

A second improvement could be affected by installing a calutron source. Many synchrocyclotrons operate at a dee voltage which will not allow this to be done, but some operate as high as 10 kv, and this is sufficient to permit the beam to clear a small source. A calutron source of small dimensions has not received the attention it deserves. The source of Livingston and Jones with a diameter of $3/8$ in. gave large currents in a field of approximately 3 kilogauss. Experience with calutron sources during the course of the Manhattan Project showed that the possible stable ion density increases with the magnetic field, so it seems reasonable to suppose that an adequate source could be made with a diameter of the order of $1/8$ in. in a field of 15 kilogauss.

The accelerator slit, often referred to as a puller or extractor, is a most important part of the source geometry. In the first turn the combination can remove those ions which will not make the grade, and which would otherwise circulate near the source and add to the space charge. The slit can be curved as in Figure 2. This added z focusing delays the vertical spread and allows use of a longer source.

Higher Dee Voltages

The best way to insure that such a source will work is by using a higher voltage. This means a higher repetition rate of the benefits of a V^3 dependence are to be realized. A rotating capacitor seems to offer the only hope of permitting both higher dee voltage and repetition rate. In a simple half wave system there is a corresponding voltage increase on the capacitor, which means larger tooth spacing. There will be a corresponding increase in tooth size in order to maintain the same capacity, and there may be more teeth to realize the increase in repetition rate. There seems to be no escaping the fact that the capacitor and its vacuum enclosure will increase in size. The design of brushes and bearings present a more formidable problem since the r.f. currents will increase in proportion to the dee voltage.

Most of these difficulties disappear at once if the capacitor is operated in air. While it is true that air will not support the voltage stresses that can be used in a vacuum, it is also true that the vacuum and surface conditions found in most cyclotrons are such that the rotary capacitor does not reliably hold much more voltage than the same capacitor would hold in dry air. Once the decision is made to put the capacitor in air, large size is in several respects no longer a disadvantage. The bigger it is made, the lower the losses, the looser the tolerances and the lower the mechanical stresses. The only problems are the limitation imposed by frequency and the connection through insulators to the dee. The latter problem is greatly eased by using the new ceramics. From the failure standpoint, alumina can be safely used at voltages of 50 kv. Its mechanical strength is exceptionally high and its electrical and thermal properties are equal to or better than quartz.

The frequency limitation is encountered in large machines where the poles are of the order of a half wavelength in diameter. In such cases there is an

advantage in using a dee of some 90 to 100 degrees in angular extent in place of a 180 degree dee. The first harmonic is apparently easily cancelled by a trim coil.⁷ The dee voltage must be raised some 30% to keep the same gain per turn, but the capacity is lowered, and these factors cancel approximately as far as the design problems of the capacitor are concerned. But a net gain is achieved in that the triangular dee lengthens the dee stem distance by approximately $1/3$ the magnet radius.

Reduced Frequency Swing

As a next step simple ridges can be installed everywhere to increase the vertical focusing and reduce the frequency swing somewhat. We note at once that the reduction in frequency swing is achieved at the upper frequency limit which is always a struggle to attain. This means that the capacitor can be located even farther from the center and need cover less range. An increase in repetition rate will result, with an attendant increase in dee voltage.

Improvement in Catching Efficiency

The thin skinned dee allows the central ridges to be very close together. A separation of about an inch is more or less implied in Fig. 6, with $1/4$ in. allowed for r.f. electric fields, $1/8$ in. for the two skins, and the rest for the beam. Strong magnetic focusing should set in at a radius of the order of 1 or 2 inches, making focusing and radial fall-off almost completely independent. A new degree of freedom is now present which should make possible an improvement in catching efficiency. The ions should start in phase if they are to clear a calutron source. Later on they must somehow be shifted to stable a phase angle. A suitable time to do this would be after the onset of magnetic focusing, so that the increase in space charge will cause no losses. It appears that the phase can be shifted at will by simple dips and humps in

the magnetic field profile vs radius. A detailed study of catching conditions with this new degree of freedom should prove most profitable.

DISCUSSION

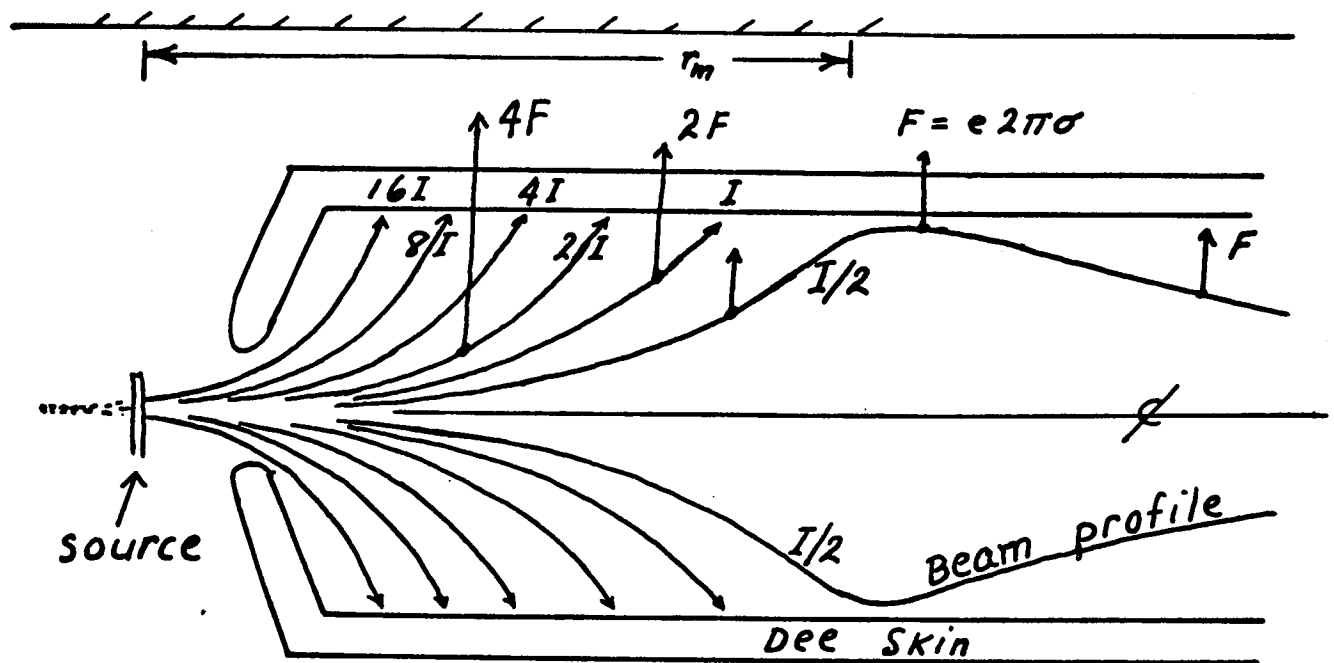
We conclude that there are a number of ways to increase the output of a synchrocyclotron. Let us start with a 1 μa f.m. machine operating at a dee voltage of 5 kv. We will assume an increase to 20 kv, which is not unreasonable in view of the data of Figure 5 in which Henrich et al actually approached such a voltage. Installation of sector cones could reduce r_m by a factor of 2, and a calutron source might introduce a factor of 10. Multiplying these factors together gives a current of 10 ma. The other improvement factors can be held in reserve if this is not sufficient. In an f.m. machine such a current is an average current and the peak value is probably one to two orders of magnitude higher. The calutron sources in their present form would limit this current to a value closer to 1 ma. This is a large beam for a synchrocyclotron and probably very unrealistic, but the assumed factors are reasonable, so there is a good chance that a satisfying fraction can be realized in practice. We note that a step in the direction of higher voltages and repetition rates has been taken in the Philips f.m. machine⁸, where a beam of 20 μa at 160 MeV is obtained with 25 kv and 450 cycles per sec.

ACKNOWLEDGEMENT

The author wishes to gratefully acknowledge the help received through discussions with David L. Judd of the Lawrence Radiation Laboratory, Berkeley, California.

REFERENCES

1. E. L. Kelly et al RSI 27, 493 (1956).
2. K. R. MacKenzie, "Space Charge Effects in Cyclotrons" UCRL Report (1954), (no number).
3. Henrich, Sewell and Vale. RSI 20 12 (Dec. 1949).
4. Preliminary Design Study of the 170 inch Cyclotron by Wm. M. Brobeck and Associates, (May 1960).
5. Robert S. Livingston and Royce J. Jones. RSI 25, 552 (1954).
6. H. Blosser and Gordon, Nucl. Inst. and Method, 13, 101 (1961).
7. D. Clark (Harwell - private communication).
8. G. T. Kruijf and N. F. Verster, Philips Tech. Review, 23, 381 (1961-62).



Ions drift vertically as $z = \frac{1}{2}at^2$

Since $t \sim r^2$, the paths vary as r^4 .

Vertical acceleration \sim charge inside.

\therefore " displacement \sim " "

With dee "feelers", the beam probably diverges slightly at the source. Hence the origin of the $z \sim r^4$ curves is to the left of the source.

Fig. 1.

Beam profile from a calutron type of ion source

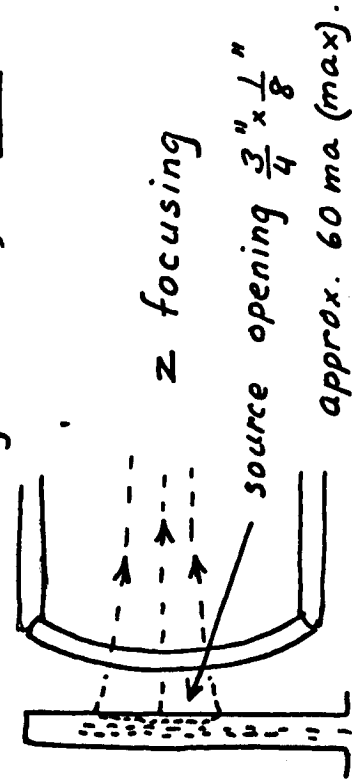
Fig. 2 $I \text{ (amps)} = \frac{h}{4} \frac{\epsilon_0}{\pi^2} \frac{\phi}{\omega^3} \left(\frac{e}{m}\right)^2 \frac{V^3}{r_m^4}$

Example: 20", 3 phase, 1 MeV cyclotron

(Ruby et al, RSI. 27, 490 (1956).

$V = 3$ (dee voltage) = 100 kV max. $f = 11 \text{ mc}$, mag. gap = 13 cm.

$h = 5 \text{ cm}$. Calutron source, with z focusing. $I(\text{max}) = \underline{6 \text{ ma}}$.



Let $\phi = 2$, $r_m = 10 \text{ cm}$

Formula gives 6 ma.

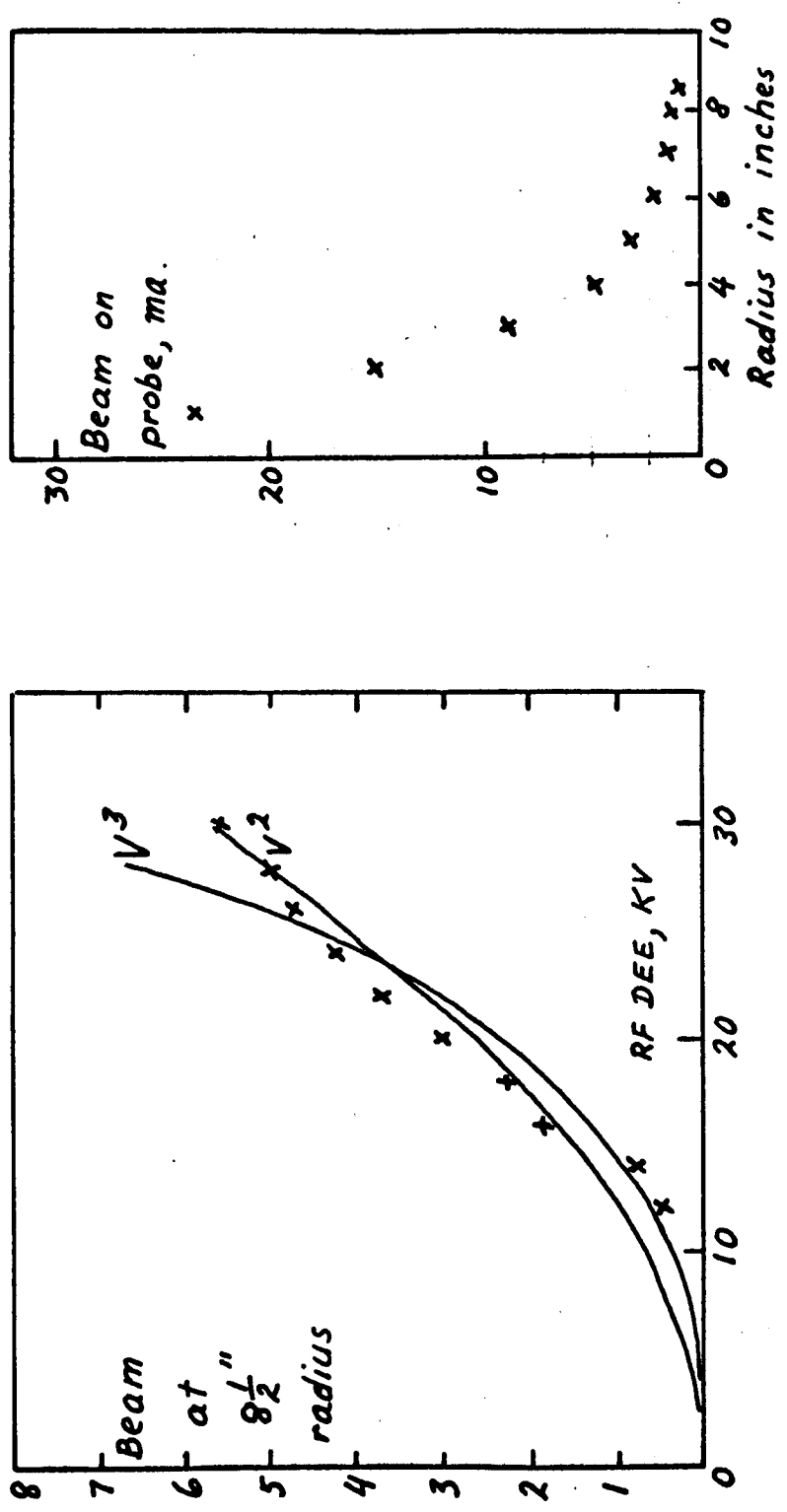


Fig. 3. Beam current vs dee voltage. 'x's indicate data of Ruby et al.
Ruby et al, RSI 27, 490 (1956), (UCRL-1889). Curve shows
tendency to flatten at high dee volts. May be limited at
source. Beam vs radius shows high density near $r=0$

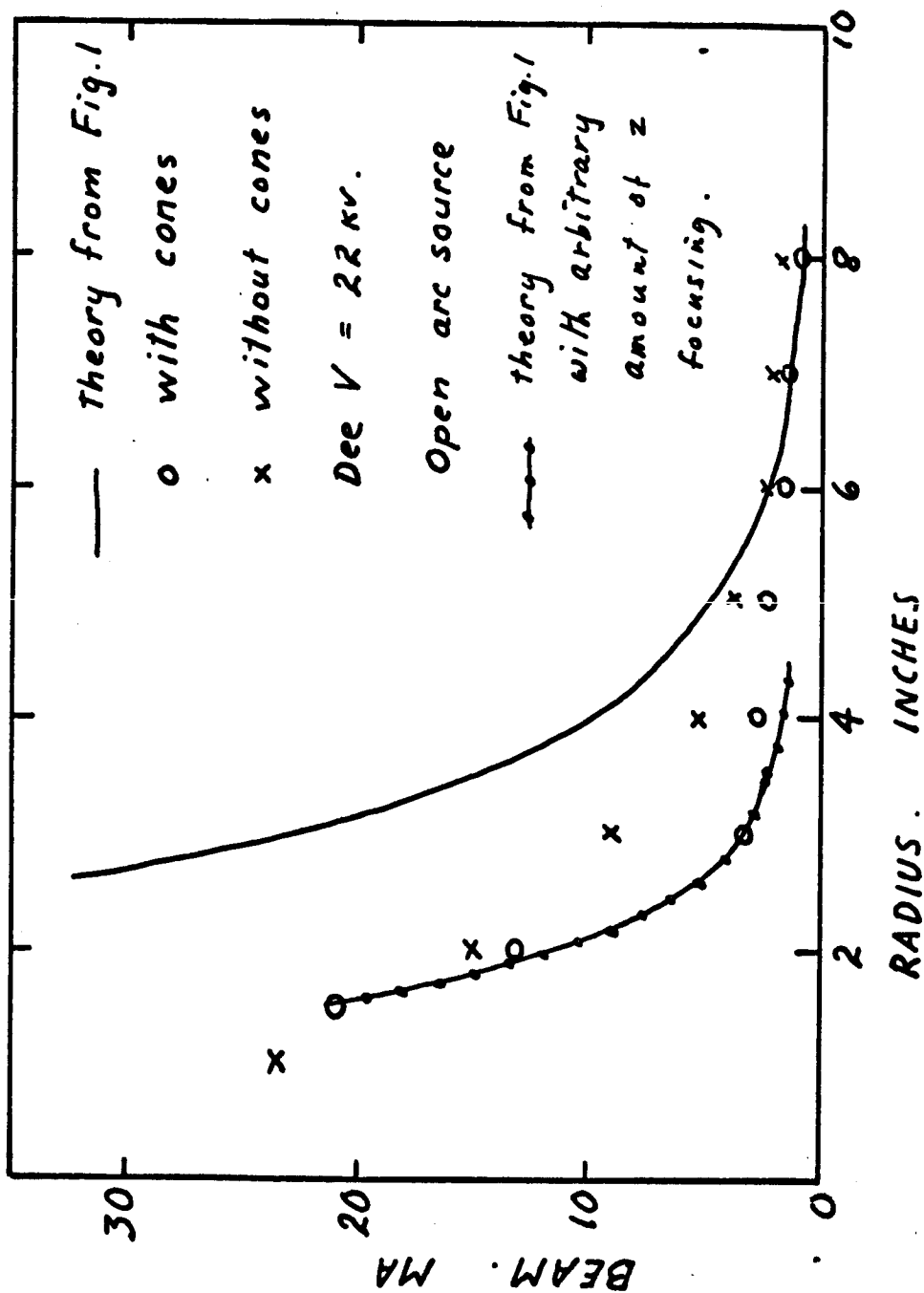
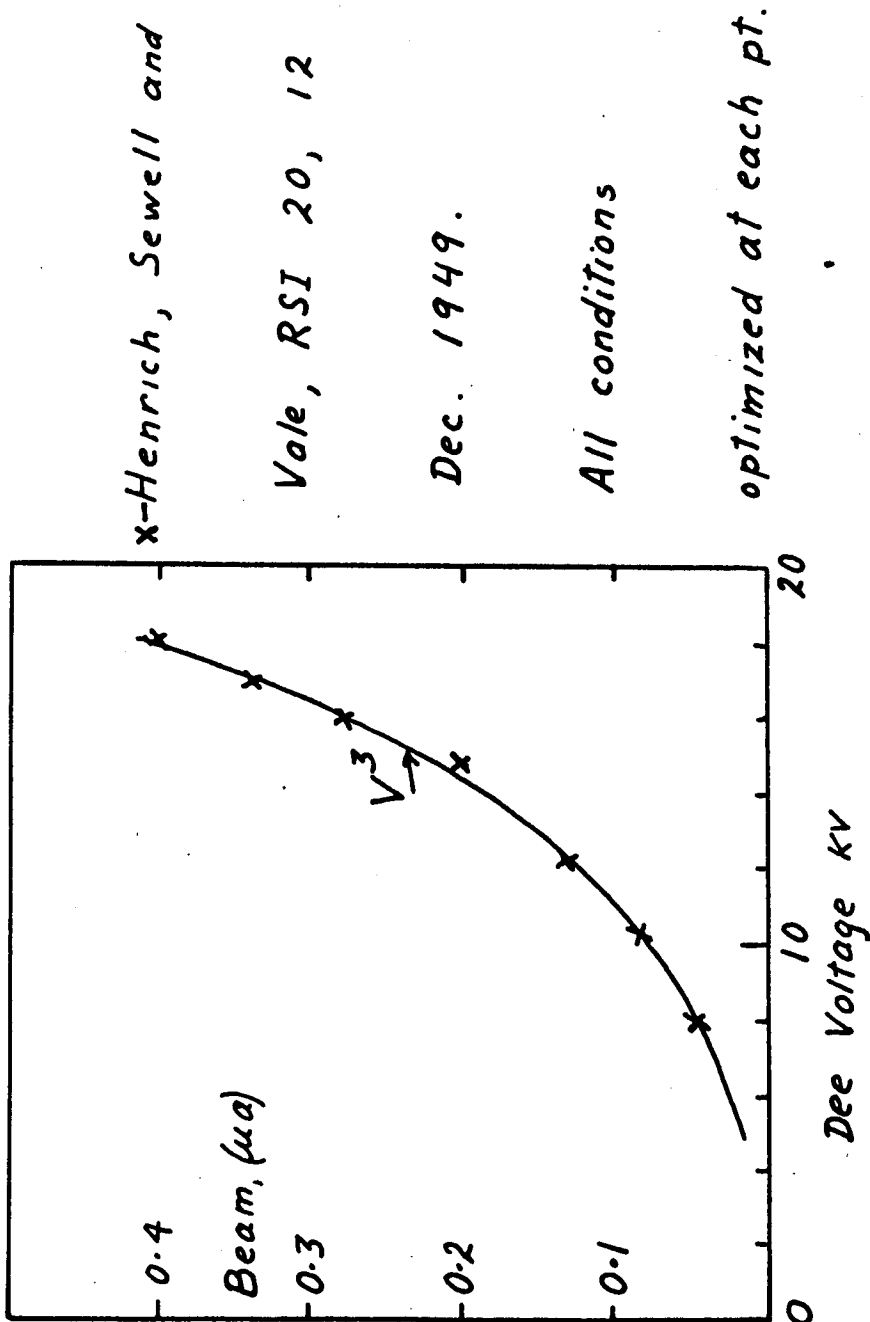


Fig. 4. Beam current vs radius



rep. rate (fm) $\sim V$. \therefore data implies that (acceptance

time) \times (rep. rate) \approx const.

Fig. 5.

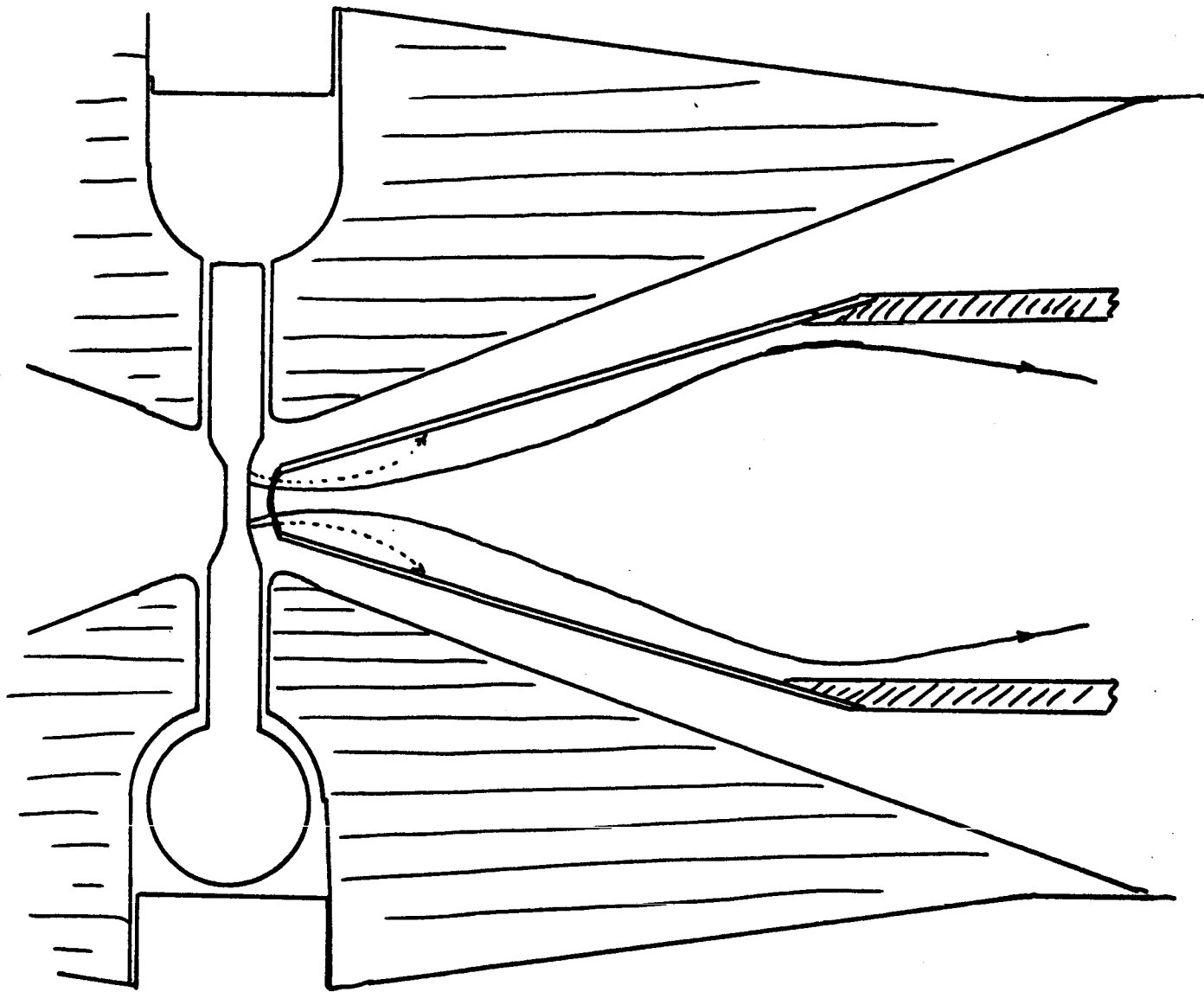


Fig. 6 Cross-section of proposed ion source, replacing the central cover with a central ridge structure.

Deep ridges around source. 3 or 4 fold symmetry. "z" focusing added. Compare with Fig. 1 and note effectiveness of z focusing.

BARNES, Rochester - We balance our rotating condenser at only 2000 r.p.m. in air and it scares you even at that low speed, it howls like a banshee. At higher speeds how are you going to turn a rotating condenser without knocking its blades off from turbulence?

MACKENZIE - There's no problem in air. Rubber tires can be spun at speeds higher than this. Also by filling in the space between teeth with insulating material like polystyrene, there's no vibration. At UCLA about 6 years ago we planned our rotating capacitor so it would make no noise.

BROBECK, Brobeck Associates - You indicate by your theory that only a very small part of the height of the ion source is used. If you put a probe in near the ion source couldn't you experiment to see if there would be a great sensitivity to the position of the probe.

MACKENZIE - I believe you would, although I don't think this has ever been done. For example, the 88" cyclotron at Berkeley has a $1/4$ " height. I consider that to be essentially on the median plane.

GOTTSHALK, Harvard - I notice that the Harwell 90° sector dee was designed under your influence. What would be the optimum angle for such a sector dee?

MACKENZIE - About a 60° - 70° dee in between wedge shaped valleys so the magnet gap would be the same as the dee gap. You would have three-fold symmetry sectors. You just machine them $\pm 1/8$ " as they all are the same, stick them in and put the dee in the 60° valley. It gives a dee with low capacity.

SUZUKI, Carnegie - What about the electric defocussing?

MACKENZIE - I have assumed the electric defocussing is zero because the ions start on the median plane. I'm sure this is not quite right; in fact it may be a rather big factor, but I don't think it's going to make a factor of 10^4 which comes out of the formula.

SUZUKI - We are possibly limited by electric defocussing in the central region rather than by space charge.

MACKENZIE - I don't believe this is true. There's one very easy way to check this. It's possible there's some information on this in a report by Royce Jones and Bob Livingston. They put in d.c. acceleration on the ion source to start the ions horizontally. Since you could give them a small horizontal component with d.c. so they are directed, it takes a lot of electric defocussing to influence them. They are well into the dee before they get much amplitude. I believe that the experiment was unfortunately not very successful for other reasons but this would be a very easy check. But I do not think the electric defocussing is very bad.

SHERR, Princeton - People have used magnetic bumps around the center in the past but they haven't seemed to have achieved much.

MACKENZIE - Oh no, they've been miles away from where the beam is. They are just little cones. You can't put too much in or your frequency range goes up too much.

SHERR - You're suggesting putting in some sort of spider?

MACKENZIE - Yes, which does not change the frequency range appreciably.

QUASI-FREE PROTON-PROTON SCATTERING IN LIGHT NUCLEI

H. Tyren, Uppsala

This is a report on some recent experiments on quasi-free proton-proton scattering in light nuclei which have been performed at the University of Chicago at 450 MeV. There seems to be very little connection between these studies and the main topic of the conference. However, one can perhaps consider this experiment as one illustration of how one could make use of the improvements of the accelerators that we are trying to achieve. We want to make accelerators which produce beams of high intensity, very well defined in energy and with a most favorable duty factor. As I hope to show you these are all machine properties which are extremely desirable in the quasi-free proton-proton scattering experiments which I am going to tell you about.

Protons of high energy have an associated de Broglie wavelength which is short compared to the average distance between the nucleons in a nucleus. The nucleus therefore becomes relatively transparent to such protons and one can describe (p, 2p) reactions in terms of a free proton-proton collision which take place in the nuclear field.

By detecting the two outgoing protons in coincidence in such a way that their energies E_1 and E_2 and their momenta $\hbar\vec{k}_1$ and $\hbar\vec{k}_2$, respectively, are sufficiently well determined, the reaction cross section can be studied as a function of $E_1 + E_2$ (summed energy spectra) or $\hbar\vec{K}$, the momentum transferred to the recoiling residual nucleus (angular correlation

distribution). The conservation laws of energy and momentum imply the relations

$$E_0 = E_1 + E_2 + E_r + E_f$$

$$\vec{k}_0 = \vec{k}_1 + \vec{k}_2 + \vec{K}$$

where E_f is the separation energy for a proton of the A nucleon target when the residual nucleus is left in a final state $|\phi_f\rangle$ and E_r is the kinetic energy of the recoiling residual nucleus. Knowing E_0 and hence the incoming momentum $\hbar\vec{k}_0$ and measuring E_1 , E_2 and the angles θ_1 and θ_2 which \vec{k}_1 and \vec{k}_2 form with the incident beam (here, as in most experiments made so far, \vec{k}_0 , \vec{k}_1 and \vec{k}_2 are chosen to lie in the same plane), one can calculate \vec{K} and E_r , and hence E_f . The summed energy spectra thus give directly the energies of those states $|\phi_f\rangle$ which can be attained in this kind of reaction.

Furthermore, according to the direct interaction model of these reactions a study of the angular correlation distribution for a given E_f should give a considerable amount of information on the motion of the knocked-out proton relative to the residual core in the corresponding state. In order to disentangle this information, however, the distortion of the incoming and outgoing protons due to their interaction with the core must be taken into account. The usual procedure is to assume a definite form from the single-particle wave function describing the motion of the knocked-out proton in the target nucleus with respect to the core, to assume optical potentials describing the distortion of the motions of the incoming and outgoing protons, to compute the resulting angular correlation distribution in the direct interaction model, and to compare this result with experimental ones. If the treatment of the distortion can be trusted, it should be possible to draw conclusions regarding the wave function from this comparison.

One can derive the following relations

$$\frac{d^3\sigma}{d\Omega_1 d\Omega_2 dE} = C \frac{d\sigma^{fr}}{d\Omega} \frac{N_{lj}}{2l+1} \sum_{m=-l}^{+l} |g'_{jl}{}^m(\bar{K})|^2$$

which applies to the symmetric case where $|\bar{k}_1| = |\bar{k}_2| = k$ hence

$E_1 = E_2 = E$, and $\theta_1 = \theta_2 = \theta$. C is a kinematic factor and m is the pro-

jection quantum number corresponding to the orbital angular momentum $\hbar l$

of the single-particle wave function $\psi_{jl}{}^m(\bar{r})$, which enters the dis-

torted momentum amplitude $g'_{jl}{}^m(\bar{K})$ according to

$$g'_{jl}{}^m(\bar{K}) = (2\pi)^{-3/2} \int \exp(i\bar{K} \cdot \bar{r}) \psi_{jl}{}^m(\bar{r}) D_0(\bar{r}) D_1(\bar{r}) D_2(\bar{r}) d^3r$$

where the distortion factors $D_n(\bar{r})$ take into account the distortion of the

incoming ($n = 0$) and the outgoing ($n = 1, 2$) plane waves. $\frac{d\sigma^{fr}}{d\Omega}$ is the

proton-proton differential cross section in the center-of-mass system, taken

at a scattering angle of 90° and at an appropriate energy. Finally, N_{lj}

is the assumed number of protons in the shell characterized by the quantum numbers l and j .

The semiclassical approximation is used for calculating the distortion factors, i.e.

$$D_j(\bar{r}) = \exp\left(-i \frac{E_j' + Mc^2}{\hbar^2 c^2 k_j'^2} \int \psi_j\left(\bar{r} + s \frac{\bar{k}_j'}{k_j'}\right) ds\right)$$

where the integration is taken along the classical paths (here approximated as

straight lines) of the incoming ($j = 0$) and outgoing ($j = 1, 2$) protons.

Here E_j' and $\hbar k_j'$ denote the kinetic energy and relative momentum, respectively, in the rest system of the core.

A computer program, using analytical and numerical wavefunctions is set up by T. Berggren, Nordita, Copenhagen and is now in progress.

Experiments of this type were first done at 185 MeV in Uppsala. Calculations show that the distortions of the incoming and outgoing waves due to absorption and refraction in the nucleus reduce considerably the observable cross sections. These distortions should be smaller at higher energies.

In order to give more information on tightly bound protons in nuclei and in particular to give a closer picture of the true momentum distributions, quasi-free scattering experiments have been carried out at 450 MeV using the synchrocyclotron at the Enrico Fermi Institute for Nuclear Studies, University of Chicago. The results of preliminary experiments using range technique encouraged us to build a much more elaborate instrumentation using two large identical double focusing magnetic spectrometers and a multi-channel electronic detector system for the momentum analysis of the two emerging protons. This equipment has now been used to study quasi-free proton-proton scattering in several light nuclei. A general layout is shown in Figure 1.

The magnets are of the zero gradient fringe focusing type and weigh approximately 30 tons each, Figure 2. The radius of curvature is 135 cm and the deflecting angle 135° . The spectrometers are symmetrically designed and the protons enter and leave the magnets at 51° to the normal of the effective magnetic boundary which is very close to a plane to give correct first order focusing. The solid angle is defined by a slit at the magnet entrance and is 2.4×10^{-3} ster. in the experiment reported. The corresponding plane angle in the horizontal scattering plane is 3.6° . The interior magnetic field is homogenous to about one part in 3000. The spectrometers are pivoted around the scattering center by remotely controlled machinery and the angles are measured with an accuracy of $\pm 0.1^\circ$.

The protons are detected by four momentum channels each consisting of two scintillators in coincidence. The defining crystal has an energy width in the magnetic field range considered, of approximately 1.7 MeV. The other crystal is common for the four momentum channels. The coincidence outputs are combined in an array of 4 x 4 final coincidence and register units. Accidentals are simultaneously measured in identical units. The total energy resolution is approximately 2.5 MeV for the 1.7 MeV channels and the size of the triangular shaped target used. The two scattering angles are equal in the experiment and denoted by $\theta_L = \theta_R$.

Figures 4 - 13 illustrate the results obtained and the table lists the elements which have been investigated and tentative assignments of separated states. Now I want to emphasize the points I mentioned in the beginning, namely what requirements this particular experiment imposes on the beam of the accelerator.

I think it is evident to everybody that it might be possible to obtain rather detailed information on the dynamical properties of nuclei if one could further improve on the precision of this experiment. This requires a proton beam of extremely good quality. I am confident that the spectrometers are good for more precise measurements. One could always decrease the solid angle and the momentum width by decreasing the size of the entrance slit and the width of the detector crystals. This is not feasible with the present duty factor of the beam. It is also somewhat doubtful whether the beam is sufficiently well defined in energy.

To obtain the best possible duty factor we use of course the peripheral auxilliary cee oscillator. From visual observations of the time distribution of the macro-structure of the beam on an oscilloscope the duty factor has been 30% in this experiment. It was found necessary to gate the main program with

the result that some 90% of the beam pulses from the main program are cut off.

In order to investigate whether it would be possible to improve on the duty factor by separating counts in the high frequency structure of the beam we have studied the microstructure in the time distribution with a coincidence circuit of 1/nsec. resolution. The result is shown in Figure 15.

More precise measurements will require higher beam intensity. This can be used to reduce energy spread due to straggling in the target and will also be required to get reasonable counting rates in an improved resolution experiment. The duty factor, including the high frequency part must be improved considerably and the phase space area of the beam should correspond to the desired precision.

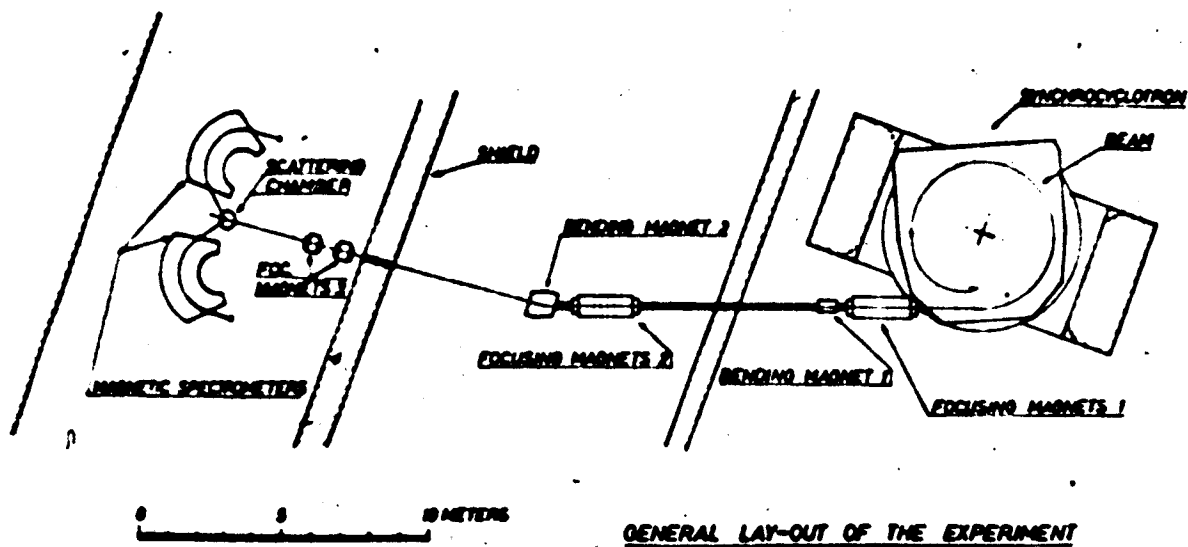


Figure 1 - General layout of experiment

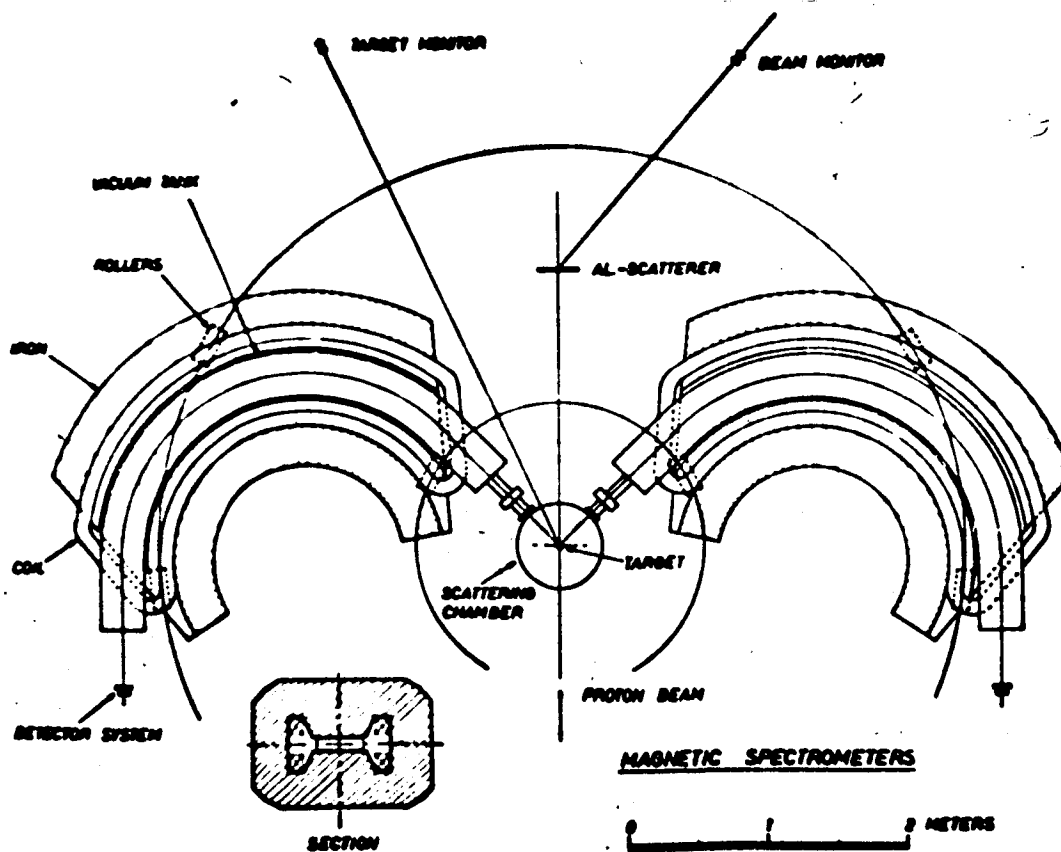


Figure 2 - Magnetic spectrometers, drawing

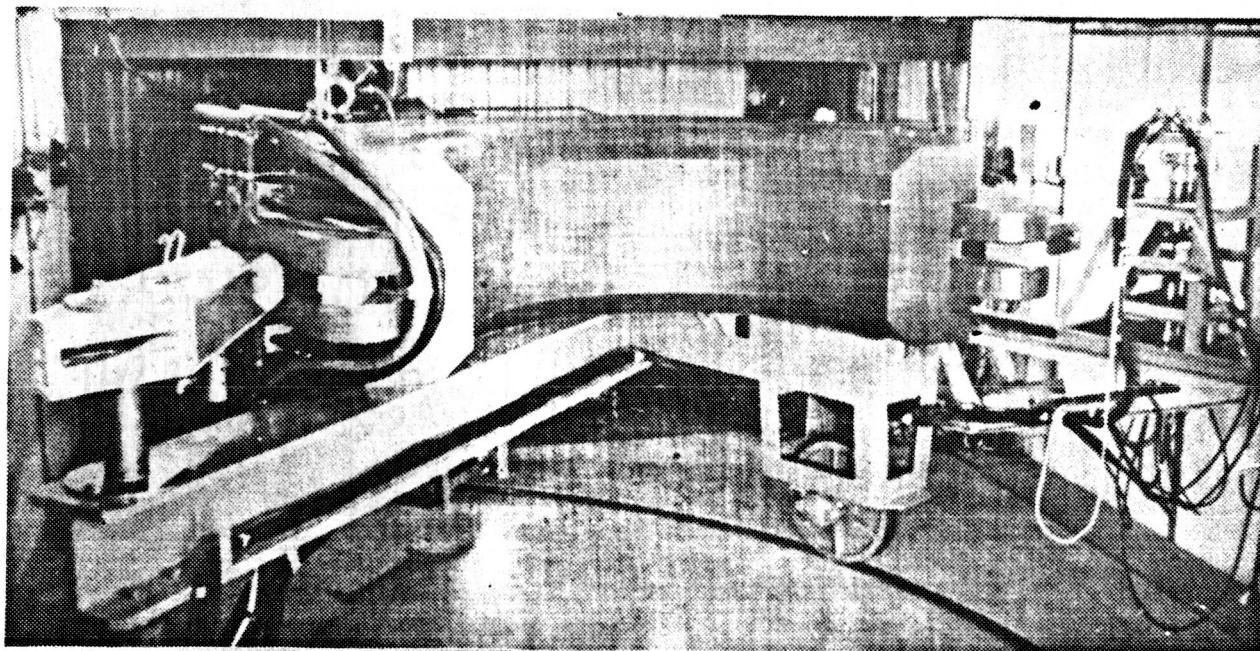


Figure 3 - Magnetic spectrometers

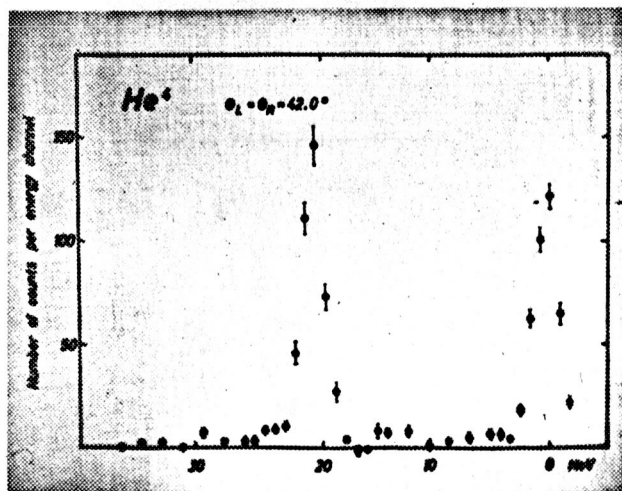


Figure 4 - He^4 energy spectrum 42.0°

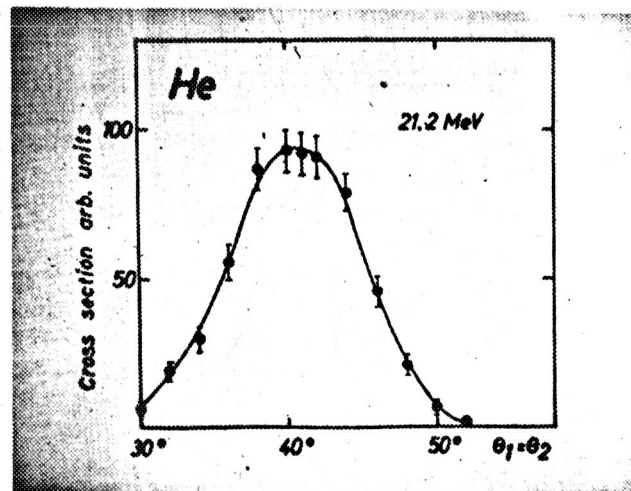


Figure 5 - He^4 angular correlation 21.2 MeV

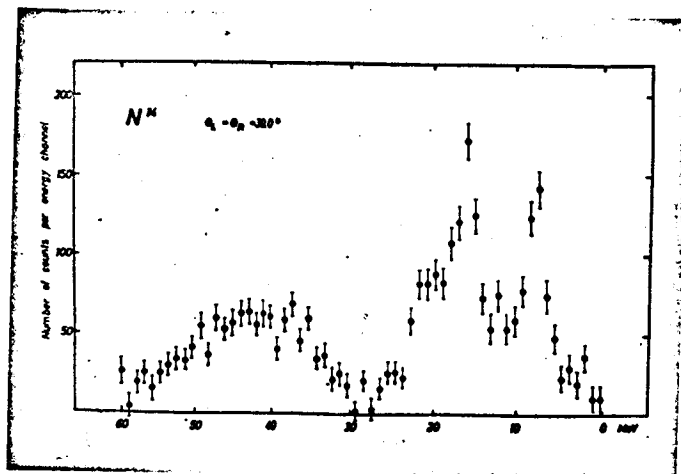


Figure 6 - N^{14} energy spectrum 39.0°

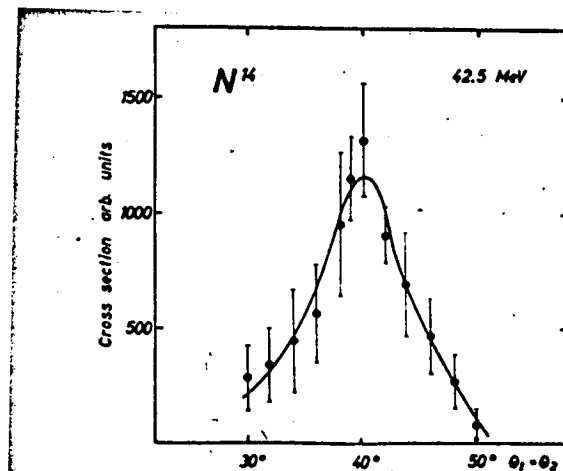


Figure 7 - N^{14} angular correlation 42.5 MeV, $1s_{1/2}$

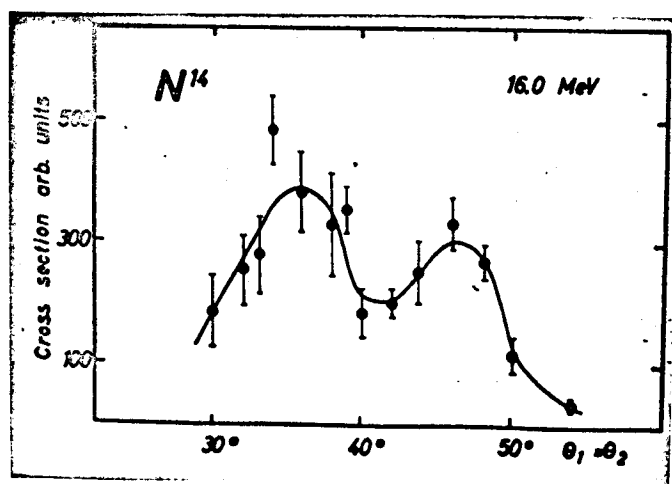


Figure 8 - N^{14} angular correlation 16.0 MeV, $1p_{3/2}$

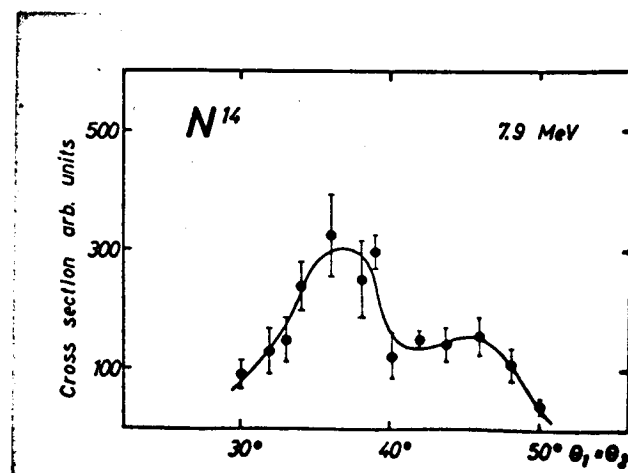


Figure 9 - N^{14} angular correlation 7.9 MeV, $1p_{1/2}$

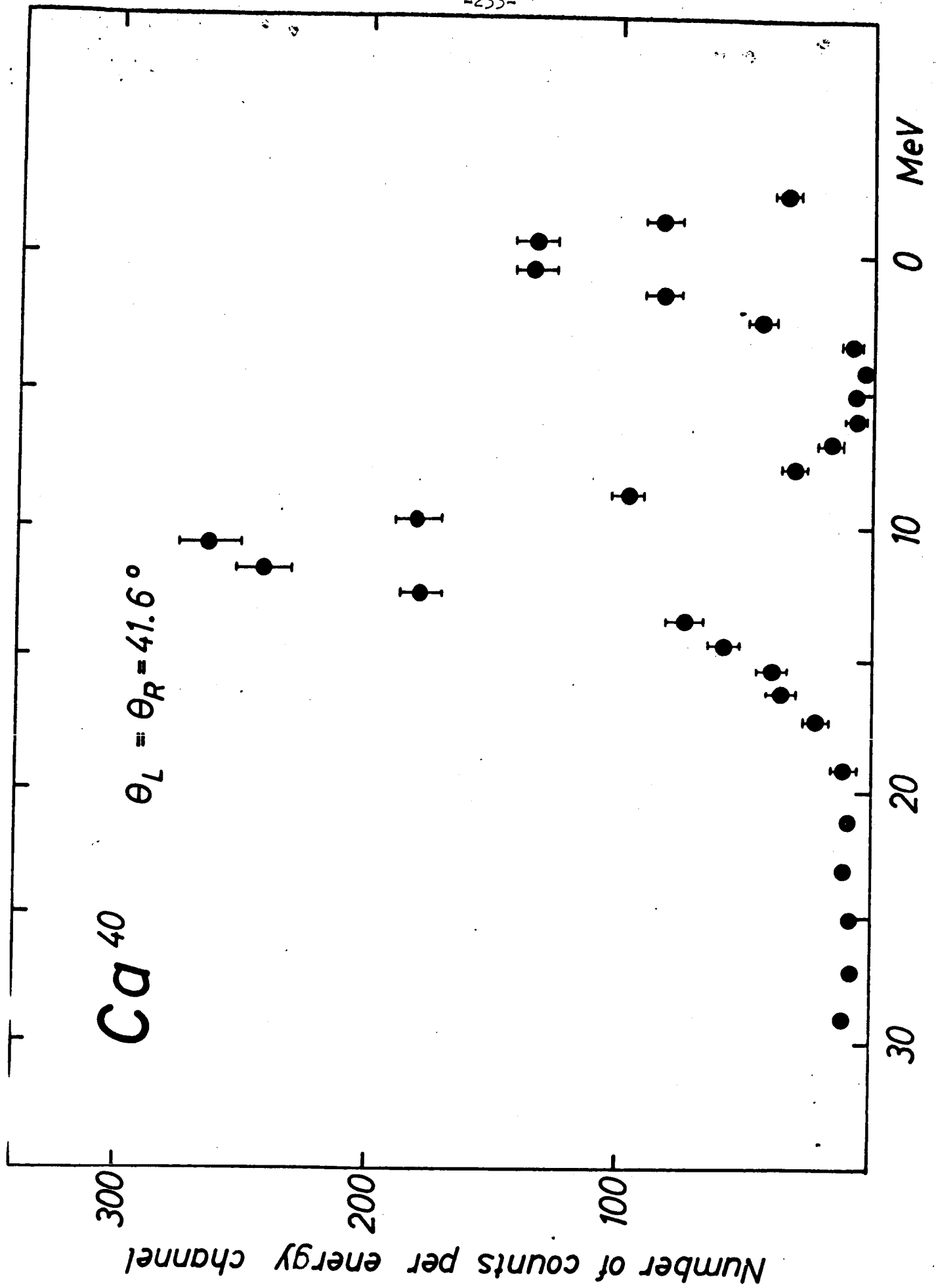


Figure 10 - Ca^{40} energy spectrum 41.6°

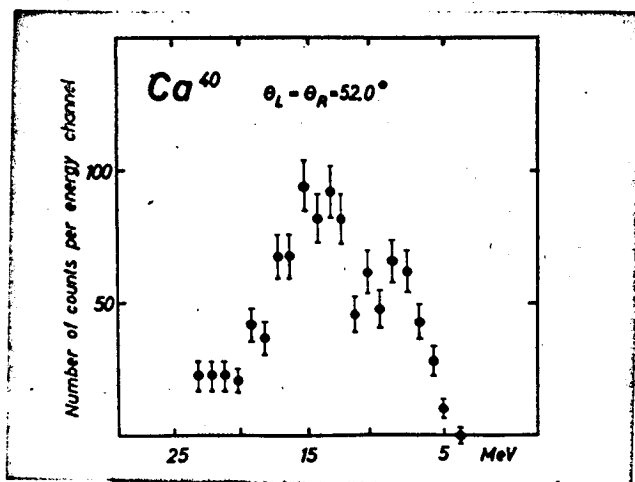


Figure 11 - Ca^{40} energy spectrum 52.0°

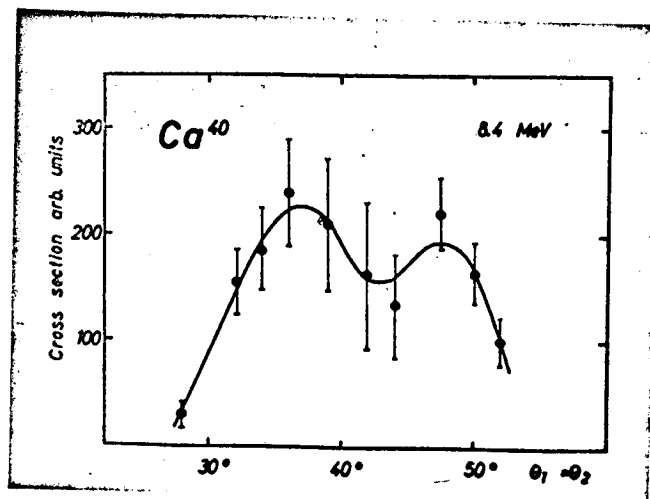


Figure 12 - Ca^{40} angular correlation 8.4 MeV, $1 d^{3/2}$

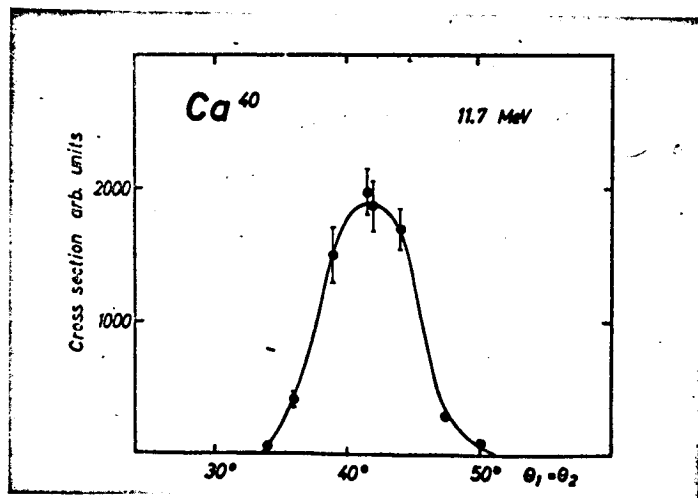


Figure 13 - Ca^{40} angular correlation 11.7 MeV, $2s^{1/2}$

Nuclide	E_B (MeV)			
	(1=0)-type	(1 \neq 0)-type	Assignment uncertain	Existence uncertain
He ⁴	21.2			
Li ⁶	22.3	5.2		
Li ⁷	23.4	10.0		
Be ⁹	26	17.5		
B ¹⁰	32	6.7 16.5		
B ¹¹		11.0 15.1 21.1		
C ¹²	36	16		
N ¹⁴	42	7.9 16.0 20.5		12
O ¹⁶	44	13.1 19.7		
Al ²⁷	16.2	13.7	20.8	
Si ²⁸	13.8	17.7		28 36
P ³¹	7.3		14.1 20.3	29
S ³²	9.6		16.8 27.3 33.7	13
A ⁴⁰	13.7		20.7	17
Ca ⁴⁰	11.7	8.4	15.8	
V ⁵¹	16.4		13.1	21
Co ⁵⁹	14.3			

Figure 14 - Table of results

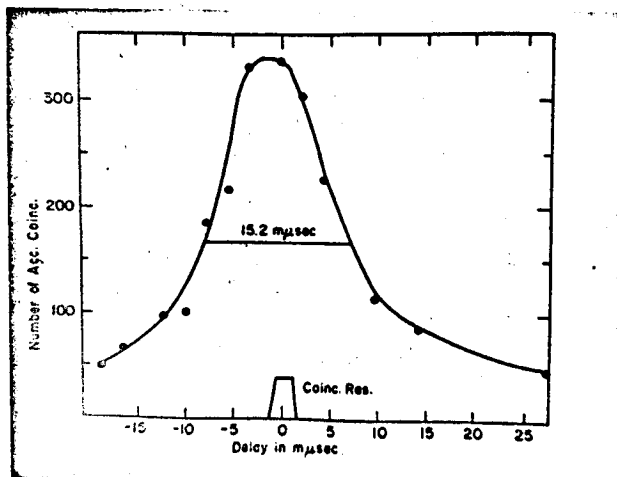


Figure 15 - Coincidence delay measurements

SHERR, Princeton - What energy resolution would you really like to get with these experiments? I was thinking that when you go to the heavier elements like iron and calcium you might like several hundred kilovolts.

TYREN - Yes, 0.5 MeV or so would be most useful, but very difficult to get.

THE MUON CHANNEL FOR THE CHICAGO SYNCHROCYCLOTRON*

I. DESIGN

G. Culligan, H. Hinterberger, H. Øverås**,

V. L. Telegdi and R. Winston***

The Enrico Fermi Institute for Nuclear Studies
The University of Chicago
Chicago, Illinois

Paper Presented by V. L. Telegdi

I would like to point out that the Chicago group is giving two papers on the muon channel; each of these would be pointless without the other. This paper relates to the design aspects, while the companion paper (formally a contributed paper by G. Culligan) covers the performance of the channel. Listed as authors of this paper are the people who were involved in the design: The only persons that should receive particular mention are Mr. H. Hinterberger, who contributed all of the engineering, and Dr. Helge Øverås from CERN, who spent some months in Chicago helping us learn about the subject and who contributed very heavily to the design study. The rest of the people are plain physicists.

As everybody knows, or ought to know, the first muon channel was built at CERN, where it still is in operation. Though I am going to insist that the Chicago channel is totally different from CERN's, it happens to be a copy of the latter in the sense that it too consists

* Work sponsored by contract: Navy Cyclotron No. 2, with the ONR. In addition to this credit line, the authors would like to thank the personnel of ONR for their enthusiastic support.

** Now at CERN, Geneva, Switzerland

*** Now at Department of Physics, University of Pennsylvania, Philadelphia, Pennsylvania

of a long row of quadrupoles and, in fact, does practically everything the same way. But we differed from CERN in that we wanted to build a channel with the following two objectives: (1) to produce low momentum (stopping) muons, and (2) to do this symmetrically for positive and negative muons. The first channel, which gave such a tremendous impetus to muon physics at CERN, was originally designed for one specific experiment, namely high energy muon scattering. Normally one was accustomed to separate pions from muons by range. However, if one wants to preserve the original high momentum of the muons one cannot use this approach. To overcome this difficulty Citron and his collaborators proposed to build a long channel of quadrupoles and catch the μ 's produced therein by π decays in flight.

Figure 1 shows the relationships between the momenta of the pions injected into the channel, and those of the resulting muons. Figure 1a illustrates the situation for high (relativistic) pion momentum, $p \approx 400$ MeV/c. The resulting decay muons cover a momentum band, extending roughly from the injected pion momentum, p_π , down to about $p_\pi/2$. In the muon scattering experiment one selects, by means of a bending magnet, a certain band of decay muons as far from p_π as indicated by the cross-hatched region in Fig. 1a. For low (non-relativistic) pion momenta the situation looks somewhat different, viz. as sketched in Figure 1b. For $p_\pi \approx 150$ MeV/c, the band of muon momenta extends from a little above p_π to around $p_\pi/3$. This situation corresponds to that of the Chicago channel. We designed it essentially trying to get the maximum number of stopping muons, and to achieve this for muons of either sign. We also hoped from the beginning that the muons from our channel would

be polarized. From the state of the theory it wasn't very clear whether we would succeed in this or not. In actual practice we do have very highly polarized muon beams, and you will hear Dr. Culligan on that topic.

Now, how did we go about designing this channel? One could give a tremendous discussion of this, but I shall be brief. The design essentially consists of three steps: (a) choose an injected pion momentum, p_{π} , (b) decide on the center of the decay muon band momentum to be extracted; (c) select quadrupoles according to (a) and (b). With regard to (c), Citron and Øverås have given a detailed discussion of properties of quadrupole channels. The basic approach which one may follow is, however, available in many text books on synchrotron theory. A channel is a succession of focusing and de-focusing lenses as indicated in Figure 2. At least in the limit of infinitely many lenses, it has obviously a phase space acceptance and general transport properties which have been discussed ad nauseam by the synchrotron people who arrange lenses in a ring. It turns out that the phase space acceptance of such periodic systems is represented by an ellipse, Figure 3. Its area A can be written as

$$A = r^2 k f (ks) \quad (1)$$

Where

f = known function of ks

r = radius of each quadrupole (bore)

k^2 = Quadrupole magnetic gradient/momentum = G/p

s = magnetic length of each quadrupole

There are certain natural limitations on the gradient G . For $r \approx 10$ centimeters, we can achieve $G \approx 10^3$ Gauss/cm, which is a sort of constant of nature. In order to choose momentum p_π one really needs mysterious quantities like

$$\frac{d^2 \sigma}{d\Omega dp} (p_\pi, \theta)$$

where θ is the angle of π production. I say mysterious because you will find that our knowledge of π production cross-sections is in a very sad shape indeed. One does not find the relevant data anywhere -- only very scattered data at a few energies, and generally not for useful targets like Be. We were primarily interested in negative pions; for these the only thing one has to know is that $d\sigma / d\Omega$ is largest $\theta = 0$, i.e. in the forward direction which for π^- is an accessible one. The further choice, that of the momentum p_π , determines the orientation of the channel uniquely in virtue of the Störmer, or impact parameter, theorem

$$\Delta L_z = L_z(r_2) - L_z(r_1) = e \Phi(r_1, r_2) = p(b_2 - b_1) \quad (2)$$

i.e. change in angular momentum = e , the particle's charge, times the flux in annulus (r_1, r_2) with

$$L_z(r_i) = r_i \sin \psi(r_i) p \equiv p b_i,$$

where ψ is an angle of obvious meaning, and b_i is the impact parameter at r_i . Clearly, for forward emission, $b_1 = r_1 = r_t$, the target radius, b_2 , the channel impact parameter, can then be obtained from (2).

In our case, with an old machine, the choice of p was largely

determined by b_2 , i.e. by compatibility with existing installations. For a new machine, such as the one planned at Langley Field, the converse would be true. We knew that π^- production by 450 MeV protons is rather flat for $150 \text{ MeV/c} \leq p_{\pi} \leq 180 \text{ MeV}$, and within this range our choice ($p \simeq 155 \text{ MeV/c}$) was dictated by the available space.

Eq. (2) is a first integral of the (horizontal) equation of motion, and says nothing about the orbits $\varphi(r)$, i.e. about the relative azimuth $\varphi = \varphi(r_2) - \varphi(r_1)$ of channel and target. Inasmuch as the channel inclination $\psi(r_2)$ as well as the channel entrance plane radius $r_2 = r_C$ are fixed once the channel is installed, it is convenient to know φ vs. ψ at r_C for all possible orbits (for the definition of φ and ψ , see Figure 4). Such a plot is known as the Michaelis plot.

Figure 5 obtained by an explicit computer calculation, represents the π^- orbits in an X, X' plane, the horizontal phase plane at the channel entrance radius r_C . The coordinates X, X' are defined in terms of φ and ψ by

$$\begin{aligned} X &= r_C \varphi_C \cos \psi_C \\ X' &= \varphi_C + \psi_C \end{aligned} \tag{3}$$

where we imply $\varphi(r_1) = 0$, and the subscript C indicates the value of the indexed variable taken at the intersection between the circle $r_2 = r_C$ and the channel axis. We call a plot such as Figure 5 a modified Michaelis plot. To see what a given channel will accept in the horizontal plane, one has to take the ellipse that corresponds to that channel and lay its center on top of the corresponding point, (eqn. (3)), on the

Michaelis plot. Before we had a channel we were extracting 160 MeV/c π 's from the cyclotron with a pipe. The effective phase space area of that beam transport device, as an ordinary pipe can also be called, is indicated by the parallelogram in the lower left hand side of Figure 5. (Upon reversing the cyclotron field, one has essentially the same geometrical orbits for pions of the conjugated sign. Hence we can intercept both backward π^+ 's and forward π^- 's of the same p_π .) The ellipses characteristic of some particular channel, entered into the Michaelis plot (labelled D and F" in Figure 5), enable one to see the pion spectrum captured by that channel. Thus for example, ellipse D extends from 200 to 160 MeV/c.

Figure 6, given here for comparison, shows the modified Michaelis plot for the CERN cyclotron. The CERN channel has, in view of the muon scattering experiment, an orientation (impact parameter) favoring forward π^- at 400 MeV/c. For a fixed (absolute) impact parameter, reversing the magnetic field but not switching the sign of the particles corresponds going from a positive impact parameter (upper dotted line,

$\psi_C = + 0.125$) to negative impact parameter (lower dotted line, $\psi_C = - 0.125$). The straight lines are the loci of acceptable orbits, and the second line leads to low energy beams. One has, of course, to adjust the target azimuth to the momentum chosen. So CERN keeps the channel fixed, displaces their target and manages to get high and low energy μ^- beams by this technique. They do not at the present time seem to get good positive beams; theirs is a "negative" channel.

At Chicago, pion beams were selected formerly by rotating a meson pipe wheel. When we decided to install the muon channel we didn't have much freedom to choose our impact parameter. As $p_\pi = 155$ MeV/c

sounded reasonable and the corresponding channel wouldn't conk into anything in particular we put it finally in at the position shown in Figure 7, having to make a hole through the shielding wall. I'll later make much ado about one feature in which we differ from CERN - namely that we have a gigantic vertical matching lens, in fact, a lens that has exactly twice the magnetic aperture of the quadrupoles of the channel. In Figure 7 you can see the 29 lenses constituting the channel, and at the left, our experimental area with the final bending magnet and a somewhat modest lead collimator (actually a big wall). Behind the collimator is the experimental apparatus, for instance the one to which Dr. Culligan will refer in the companion paper.

Having decided, mostly on the basis of a practical channel location, on $p\pi \approx 155 \text{ MeV/c}$, we pursued from the beginning the philosophy (which turned out to be a good one !) that even for a muon beam there is nothing better that one could do than to trap as many pions as one could. This is not obvious, because one might, for instance, want to optimize the channel by exciting it so as to make its phase space acceptance optimal for the decay muons, rather than for the injected particles. Our philosophy has been to select the muon band indicated by the cross-hatched area in Figure 8a, e.g. a band that embraces the injected $p\pi$. Note that the injected spectrum has a low momentum cut-off, but no high momentum cut-off, as indicated in Figure 8b.

Figure 9 represents essentially the area of the (horizontal) acceptance ellipse of the channel, Eq. (1). It is a classic curve from any synchrotron book. It is seen that to obtain the maximum area one should have no gap t at all. The maximum of $f(k_s)$ occurs at a

canonical number well known from synchrotron theory, viz. for fixed k the area A is maximum at $ks = 1.25$. Also, $f(ks) = 0$ at $ks = 1.86$; thus if s is fixed and k is increased (p decreased), one will not accept backward decaying muons if one is not very careful. From a graph like Figure 9 we selected $s \approx 28$ cm and, in pursuance of the philosophy that gaps are not good for you, adopted the following principle for the actual lens design: Let the lens have physical length L , such that the effective magnetic length will be $L + r$, (thus for $s = 28$ cm, $r = 10$ cm, make $L = 16$ cm) and squeeze the copper needed for the specified excitation into the space between L and s , as shown in Figure 10. This is not the traditional approach: Formerly people put in as much copper as they could in order to cut their power bill, and put up with some gaps t . We decided not to care about the power bill, but rather to make the lenses touch each other physically as well as magnetically. Thus at CERN, I believe, $s \approx 40$ cm and $t \approx 15$ cm, whereas we have $s = 28$ cm, and $t = 3$ cm.

Having decided how to maximize the π -acceptance, we come to the much more tough question as to how to maximize the muons. At the time Citron, Øverås and their collaborators proposed the CERN channel, computers were not readily available to them. Thus they made analytically some approximate estimates for the exceedingly complicated problem of the trapping of muons from pions decaying in flight within the channel. Since we built the channel, another physicist at CERN, Fronteau, has written a complete program that solves this problem exactly.

Figure 11 shows the fraction of decay muons transmitted according to Fronteau's program. This holds for decay muons formed in the channel.

One basic flaw in comparing the actual channel to such a treatment is that of direct injection of muons into the channel which is very hard to allow for theoretically. So I shall always talk as if the cyclotron did not spontaneously inject muons, although it does so in great numbers. From the full Frontoau theory one sees that one can trap many more muons per decay for a finite channel than for an infinite channel. The explanation of this is very simple: The notion of an acceptance ellipse is valid only for an infinitely long channel, i.e. infinite in terms of the "wavelength" λ of the (quasi) periodic motion of particles in the channel. Pions whose representative phase points lie outside the ellipse in the entrance phase plane are ultimately bound to hit the walls of an infinite channel. Now the actual length of the channel is of the order of the mean decay length of the pions, viz. 28 ft = 28 lenses in our case, while λ turns out to be of the order of 6 lens pairs \approx 12 ft. Thus the pions injected outside the ellipse have a good chance to decay into muons when travelling on orbits that would ultimately hit the channel walls, and these muons can in turn be trapped. Similarly, decay muons formed towards the end of a finite channel have a better chance of being trapped than in an infinite channel. So the approach of overlaying the channel ellipse on the modified Michaelis plot may be very elegant, indeed, but it doesn't allow for injected muons and for the non-saturation of wall hitting. That's done by the Frontoau program which follows the fate of pions and muons in gory detail. Figure 11 shows that there is a big difference between the two treatments. The cross in Figure 11, the one that we have to bear, represents the operating point of our channel, and of course, indicates that it is well

designed.

Figure 12 shows the product of the fraction of decay muons transmitted times the pion acceptance. Again with our choice of parameters we are operating at the conditions indicated by crosses, i.e. slightly below the theoretical maximum.

Now let us turn to the mechanical design of the quadrupoles. I would like to emphasize that our design is due to Mr. H. Hinterberger; its great elegance is perhaps due to the fact that he had never designed any quadrupoles before, and they may look rather unconventional. Traditionally, quadrupoles have all sorts of octagonal return yokes or otherwise complicated shapes. But when one does orbit theory one always thinks of the channel as of an object of cylindrical symmetry. (one uses, of course, Cartesian coordinates, and distinguishes between vertical and horizontal phase planes). So the thought strikes one: Why not make a really cylindrically shaped quadrupole lens?

Figure 13 shows a channel lens, with $r = 10$ cm. A cast ring forms the return yoke. Such rings, with a dimensional tolerance of 1-2 mills, can be centrifugally cast and are quite cheap. The pole pieces, attached to them with screws, have a profile intermediate between hyperbolic and circular, which we copied from M. Morpurgo's design at CERN. They were obtained by machining a long bar to the required shape, and then cutting it into pieces. The copper was wound onto these pieces and epoxy impregnated in place (Pacific Electric did this job). Each quadrupole weighs about 0.75 tons, and costs around \$2,000 to make.

Figure 14 gives perhaps a better idea of how small the Chicago quadrupoles really are; the man who holds them up is very strong and is

admittedly not the smallest man we could find. Figure 15 shows the CERN quadrupole lenses. It is worth recalling that the CERN and the Chicago channel lenses have the same bore, $r = 10$ cm. The Chicago lenses, owing to the smaller volume of copper, have a somewhat larger power consumption. We are very satisfied with them, and use a (twice) blown up version of them for vertical matching.* Fifteen channel quadrupoles are placed in a tunnel in the shielding wall (figure 16), the remainder being placed on two tables, in sets of six (Figure 17) and of eight. One of these is normally against the shielding wall, and either or both tables can easily be removed. As can be seen from Figure 16, the lenses in the shielding wall are placed on a rail to facilitate set-up.

We have so far seen how the orbits hit the channel in a horizontal plane. Now we have to worry about the vertical plane. This too can be discussed very elegantly in terms of phase space. It can, however, be discussed with less elegance but perhaps with more clarity in terms of ray optics.

Figure 18 shows ray paths for three possible channel set-ups. The bottom set-up constitutes an obvious, but not necessarily optimal possibility. Here one pushes the channel (with its first lens vertically focusing) right up against the cyclotron window, (W, -W). As has been pointed out by F. J. M. Farley and others, the cyclotron field can be treated, as far as its vertical action is concerned, as a lens, e.g. this field produces a virtual image T' of the internal target, T. One

* People interested in such lenses should contact H. Hinterberger directly.

would like to accept into the channel all the rays that fill up the window which in our case is 16 in. high. The bottom set-up does not accomplish this. Next consider the rays that come from T' up to the window, $(W, -W)$, and insert a lens into the window which will make these rays converge. Then pull the channel (with its first lens defocusing) back to the distance indicated by the top set-up in Figure 18. Here the vertical channel acceptance fills the window, and the matching lens causes the full aperture, $\pm W$, illuminated by the virtual target, to fill the cone of rays from the channel. Thus one collects as much as one can. From the image and object distances, using Newton's formula for lenses, one readily derives the one relevant thing, namely the focal length of matching lens (quadrupole). Retaining such a lens, another possibility, shown as the middle set-up in Figure 18, is to start the channel with a vertically focusing section. Since the two rays A and B cross one has to pull the channel yet farther back in this case. There is no point to this, as it spoils the horizontal collection. Thus the top set-up is optimal; in our case it turns out to give a gain in intensity of a factor three.

Vertical phase plane representations of the above situations are given in Figure 19-21. In Figure 19, the target is shown as the strip (HG) which intercepts the vertical acceptance ellipse, F, by the hatched amount (LK). By inserting a magnetic lens into the aperture $(W, -W)$, making the channel initially vertically defocusing, and moving its entrance plane back to $\ell = 99$ cm, one switches strip (HG) in Figure 19 to strip (QP) in Figure 20, and drifts ellipse D (Figure 19) into ellipse D' (Figure 20). (The ellipses of initially vertically focusing

and defocusing channels differ by a reflection about the X' axis at their entrance plane.) Figure 21 indicates the effect of moving the channel further back, (viz. to $\ell = 181$ cm), and making its first lens vertically focusing. It is seen that this yields vertical, but not horizontal matching.

In practice, to make a matching lens one has to make a quadrupole of the required focal length (80 cm) and aperture (40 cm). This was very easily done by simply blowing up all the dimensions of our standard quadrupoles (Figure 13) by a factor of 2. Mr. Hinterberger ingeniously provided us with a very large cyclotron window to exploit fully this lens.

Figure 22 shows an elevation schematic of the channel, cyclotron window, and matching lens. The matching lens itself is mounted telescopically to allow for adjustment. G. Culligan and I have made some rough calculations that indicate that one can build matching lenses for much higher momenta than ours (~ 160 MeV/c) without any effort. Thus one can, even in practice, use vertical matching at such momenta with considerable profit.

The Chicago channel has by now worked satisfactorily over a period of a year. It is not only used as muon channel, but also as a pion channel (the lenses beyond the shielding wall are in that case removed). In fact it is hard to imagine how we could live without it; it has given us 15 fold increase in muon intensity. Aside from anything else, it takes one farther away from the cyclotron which is an advantage. The total cost of the project, including the excavation of an addition to the experimental area and a 900-KeV power supply (solid state) was \$300,000.

A full report on the channel design, as well as another on its performance, are being prepared for publication.

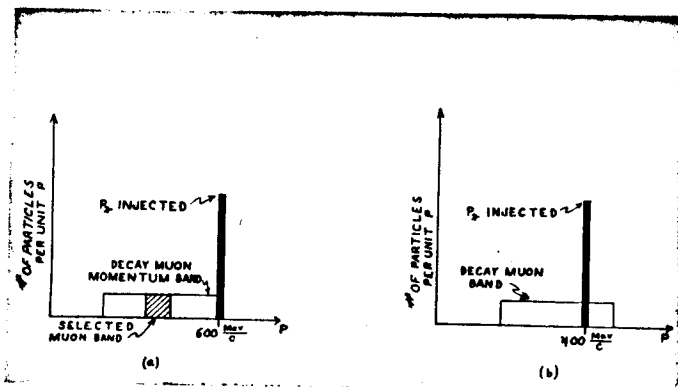


Figure 1 - Relationships between the momenta of the pions and the resulting muons. 1 (a) high pion momentum, relativistic; 1(b) low pion momentum, non-relativistic.

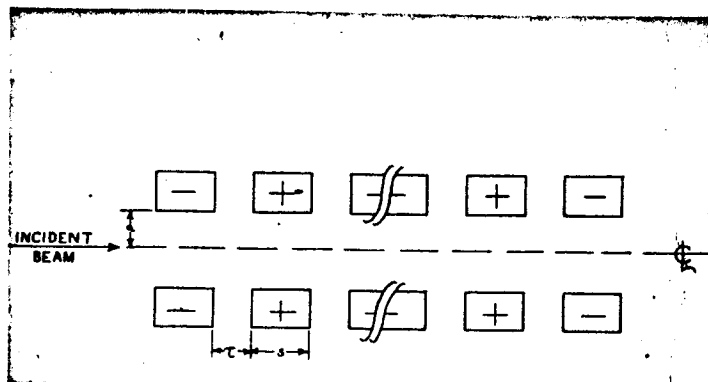


Figure 2 - Quadrupole channel schematic:

F = horizontally focussing quadrupole
D = horizontally defocussing quadrupole
t = quadrupole separation
s = effective magnetic length per section

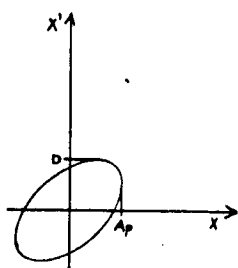


Figure 3 - Horizontal or vertical phase space acceptance ellipse of an infinite quadrupole channel. D = maximum divergence and A_p = maximum aperture of the acceptance ellipse.

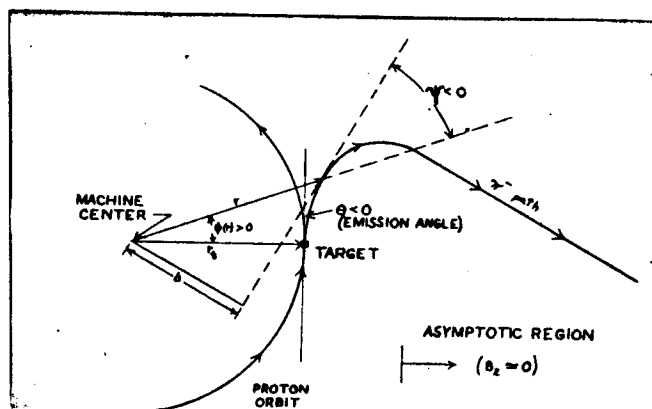


Figure 4 - Pion path in horizontal plane

b = impact parameter =

$$\frac{1}{|p|} \vec{r} \times \vec{p} = r \sin \psi$$

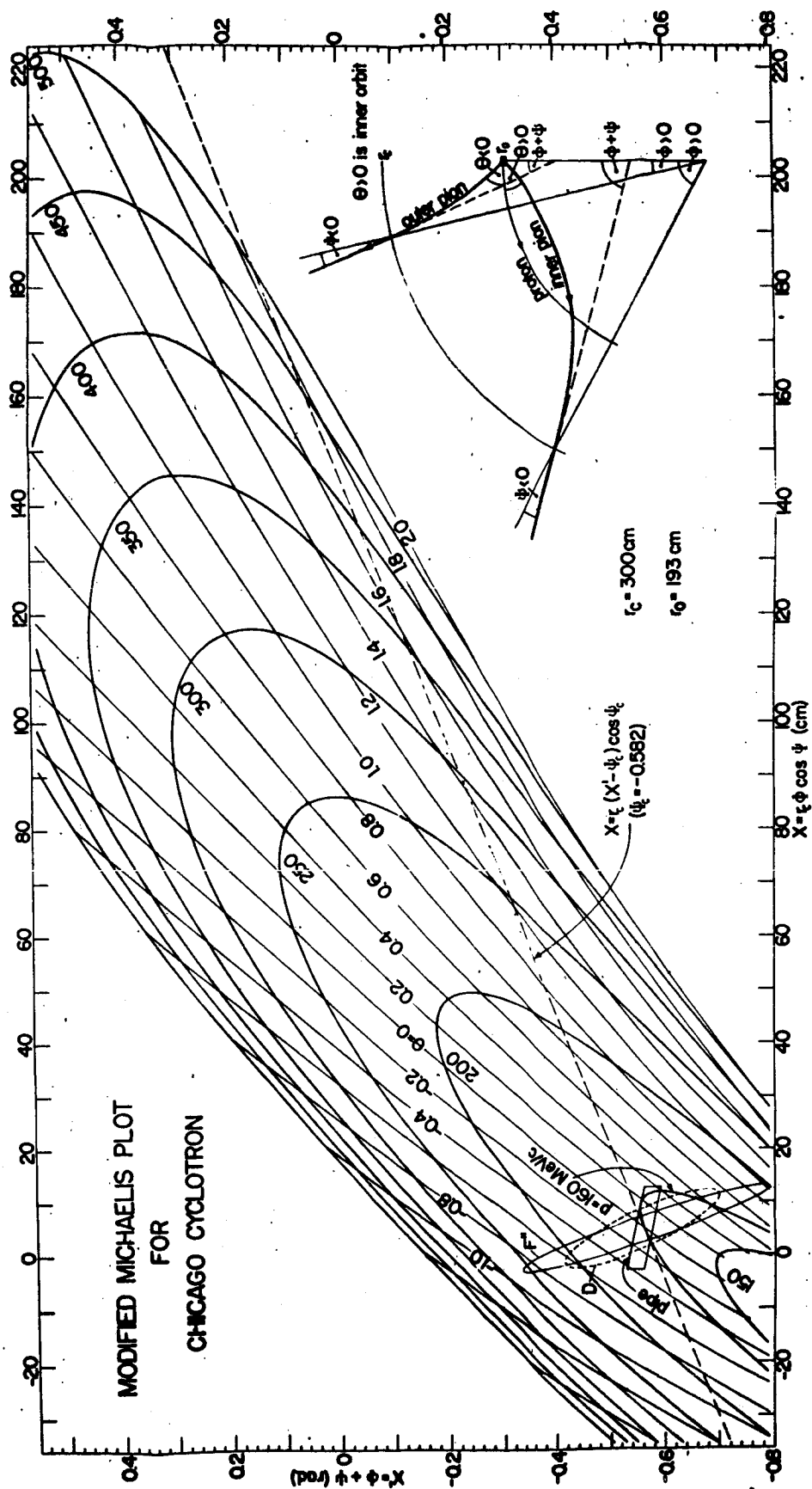


Figure 5 - Modified Michaelis Diagram. Plotted are the quantities $X = r_c \phi \cos \psi$ and $X' = \xi \phi \cos \psi$ for negative pion orbits originating in a target ($\phi_t = 0$) at several emission angles, ϕ , in radians and momenta p_π in MeV/c. r_c is taken at 300 cm. $\theta = 0$ corresponds to forward emission. The diagonal broken line represents the locus for a fixed impact parameter, given by $X = r_c (X' - \psi_c) \cos \psi_0$.

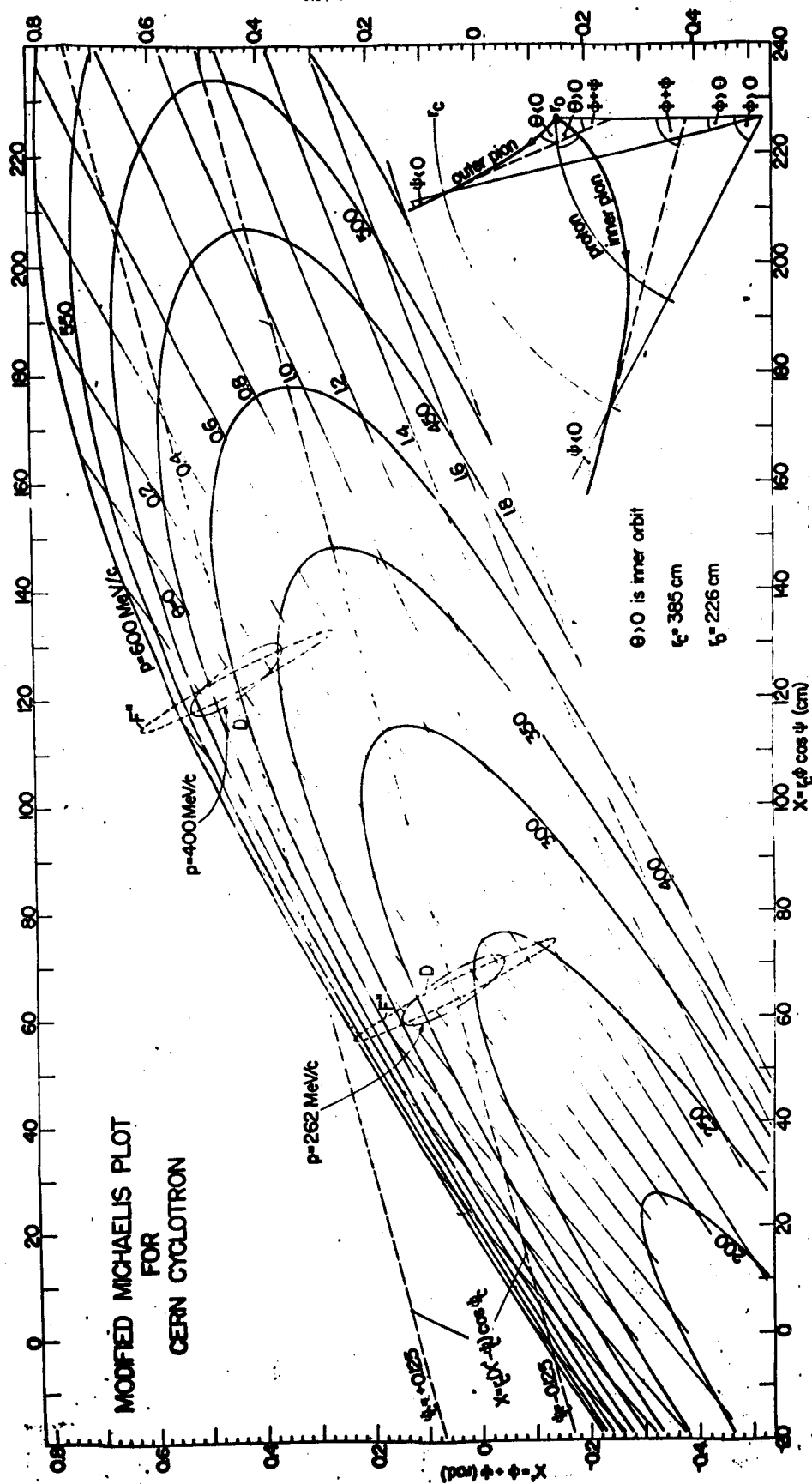


Figure 6 - Modified Michaelis plot for the CERN synchrocyclotron. Ellipses are acceptance plots for the CERN channel. Diagonal broken lines are loci for given impact parameters.

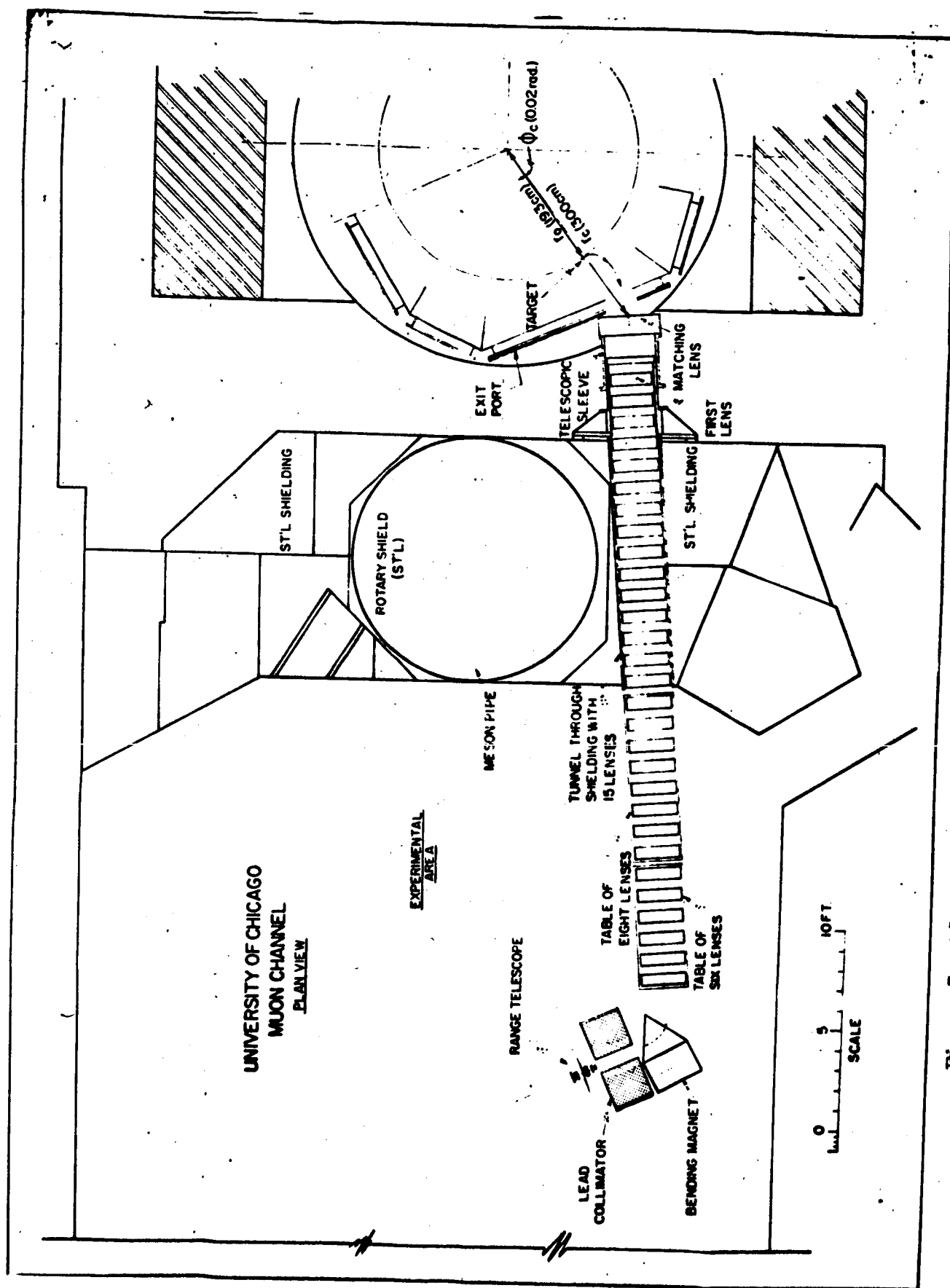


Figure 7 - Plan view of Chicago muon channel and experimental area.

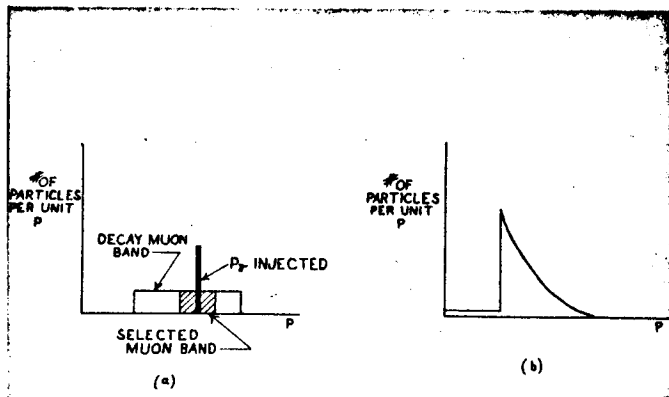


Figure 8 - a) Relationships between the momenta of the pions and resulting muons. The cross-hatched area represents the muon momentum band selected by the Chicago channel. b) Pion momentum spectrum for the Chicago channel; apparent is the low-momentum cut-off.

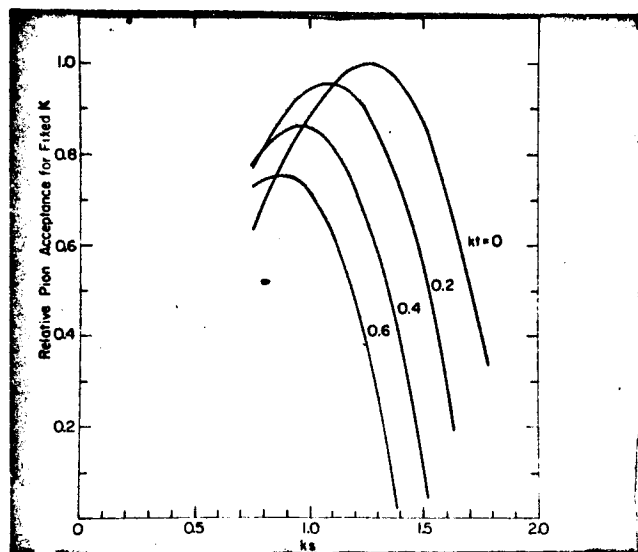


Figure 9 - Pion acceptance area vs. ks for infinite channel (for fixed k):
 s = magnetic length of each quadrupole
 t = gap length between quadrupole sections
 k^2 = quadrupole strength parameter
 $= (\text{magnetic gradient})/p$.

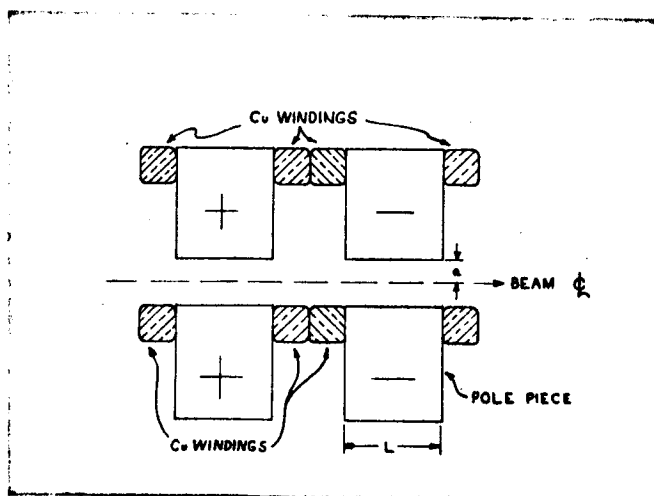


Figure 10 - Winding schematic for a quadrupole pair to minimize drift space t between lenses.

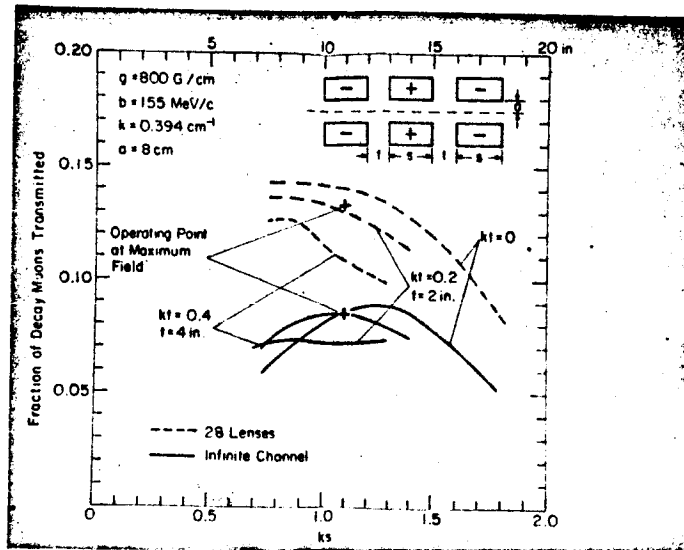


Figure 11 - Fraction of decay muons transmitted/pion decay. Notation is the same as in Figure 9..

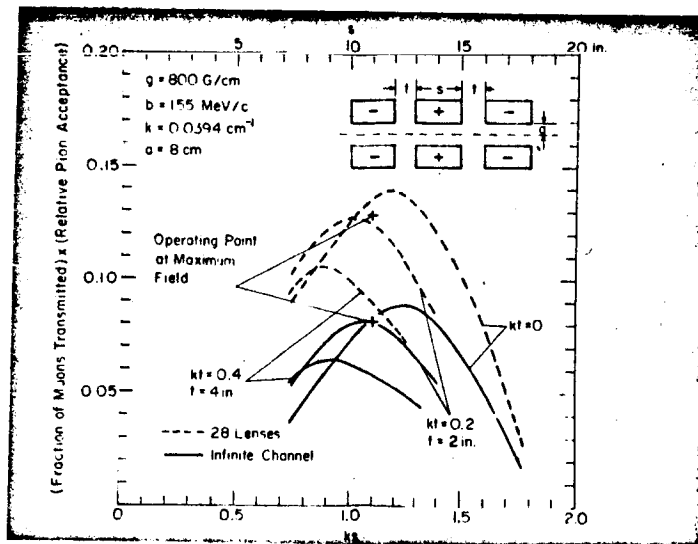


Figure 12 - (Pion acceptance) x fraction of transmitted decay muons, as a function of ks and t for channels.

TYPICAL LENS (MUON CHANNEL)

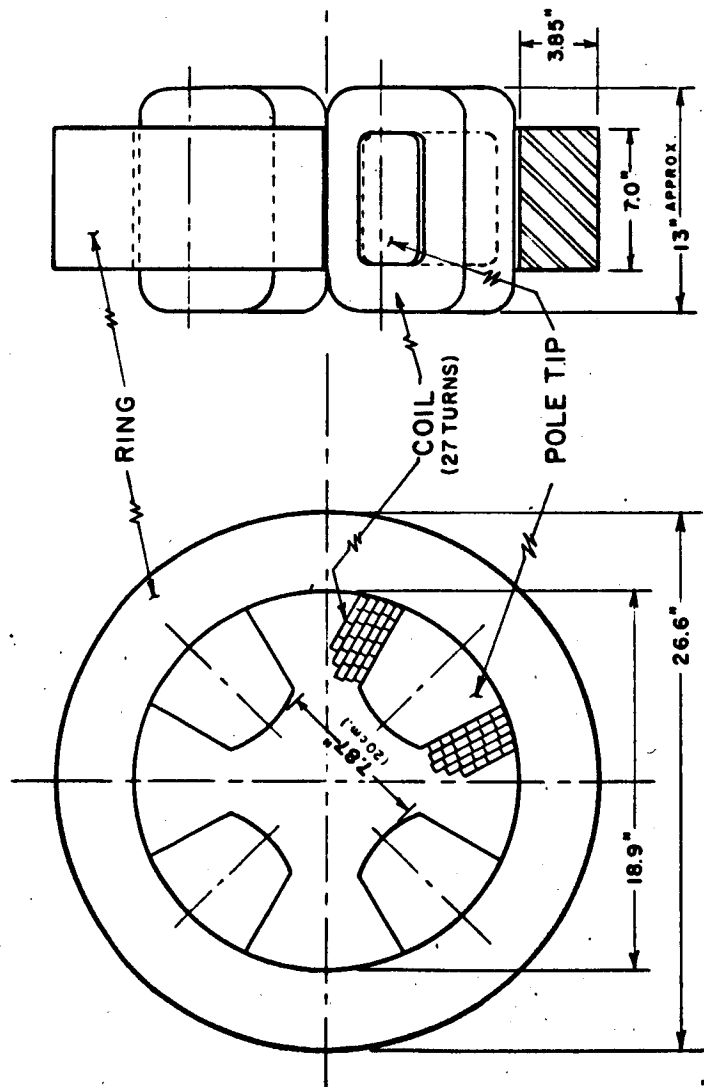
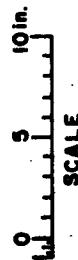


Figure 13 - Mechanical design characteristics of a typical channel lens.



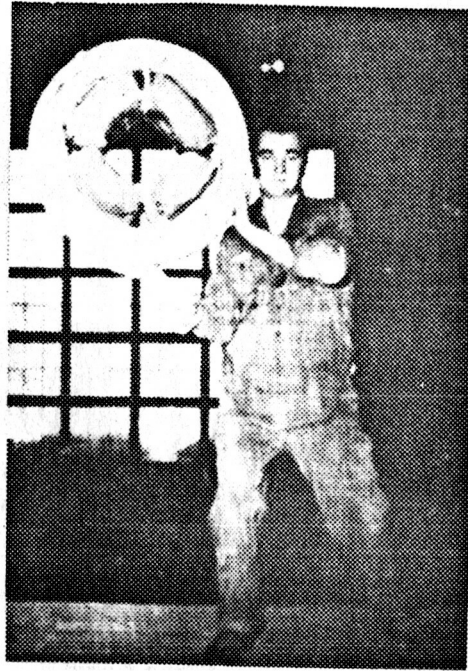


Figure 14 - View of typical Chicago lens (quadrupole).

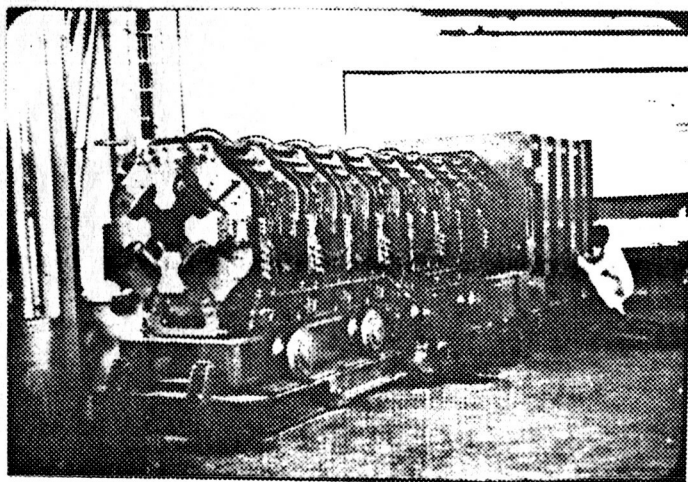


Figure 15 - View of CERN quadrupole channel.

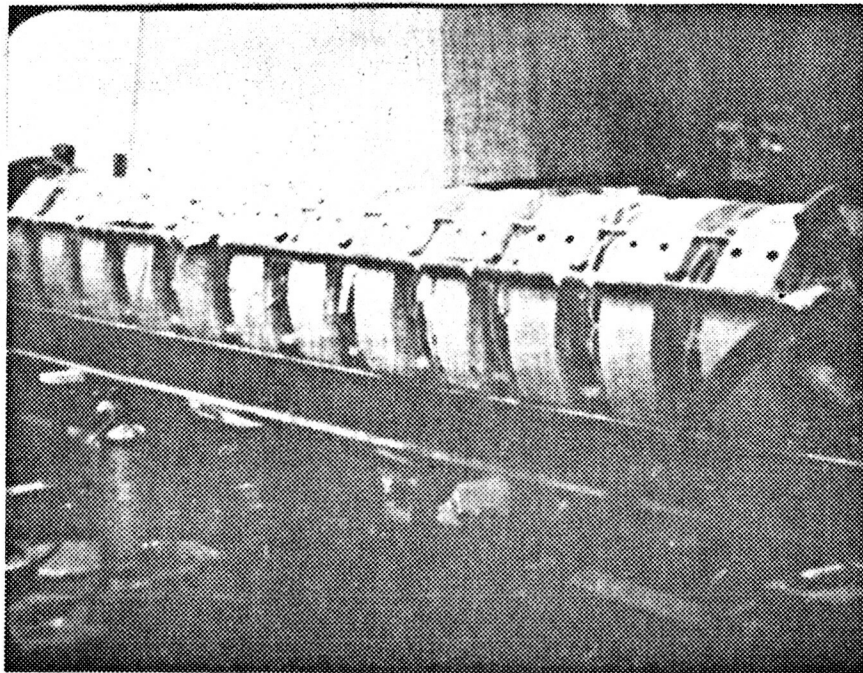


Figure 16 - Train of 12 lenses normally lodged in the steel shielding wall.

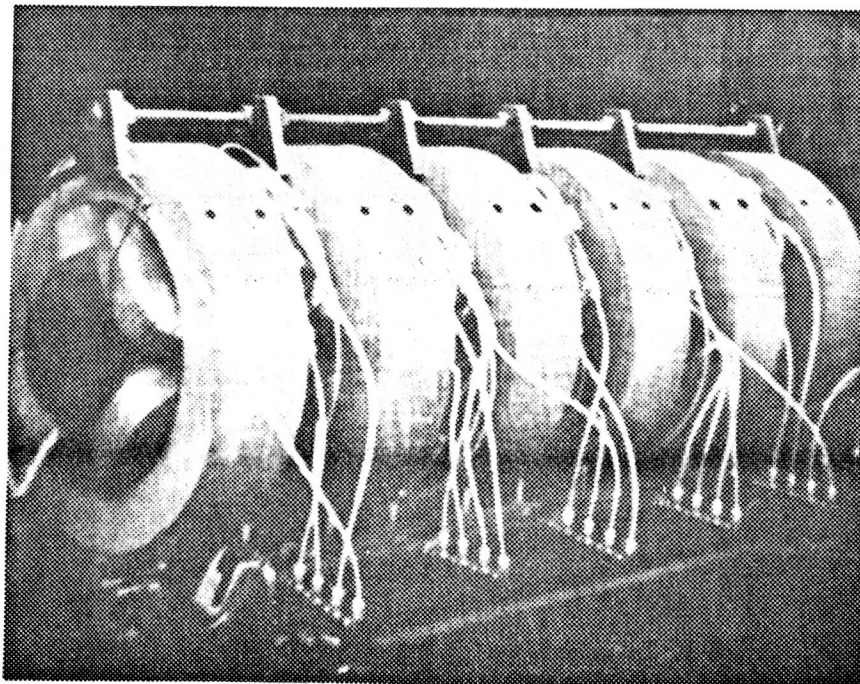


Figure 17 - Table with six lenses.

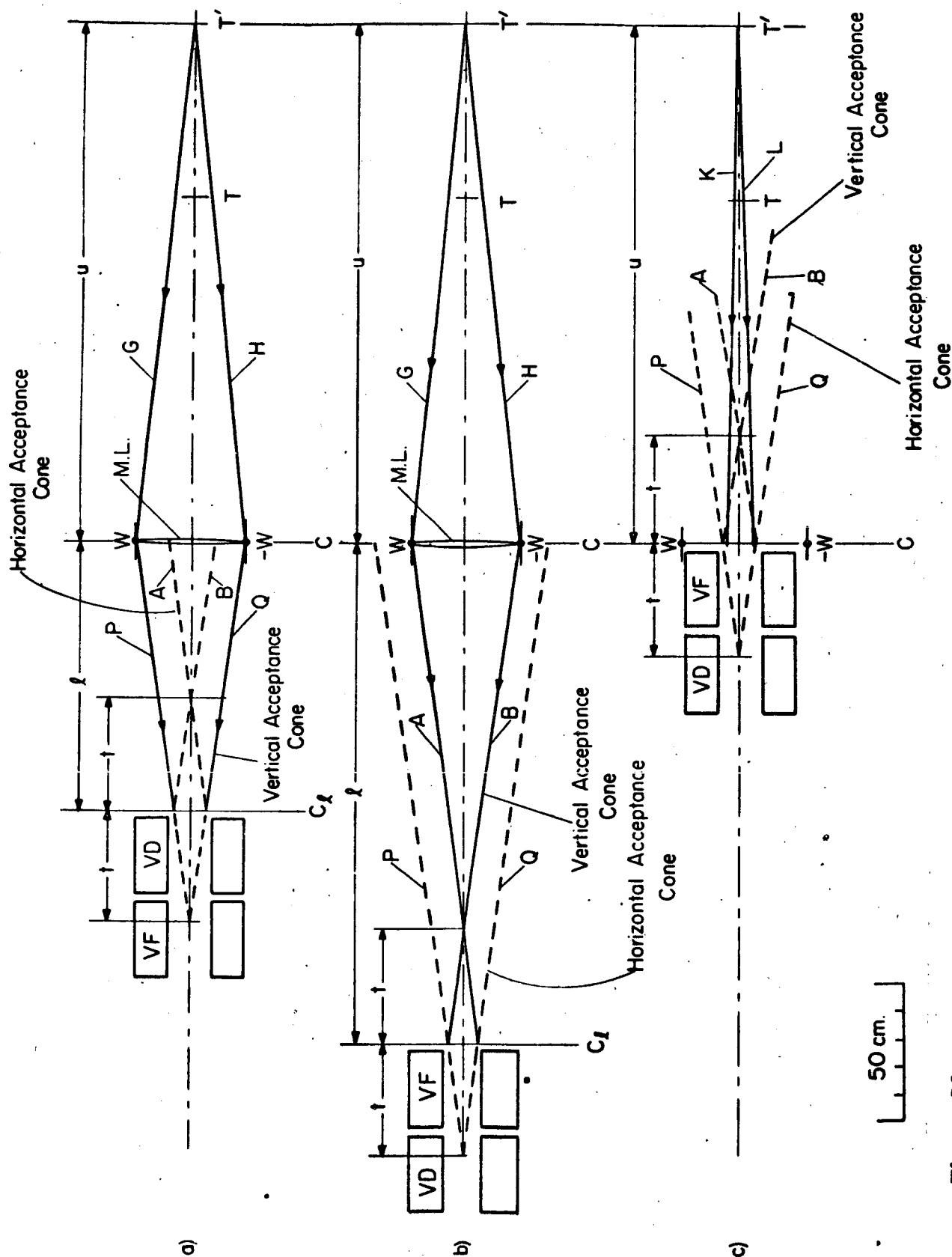


Figure 18 - Ray tracings for various situations of vertical matching of channel to cyclotron: (a) matching lens, channel vertically defocussing, (b) matching lens, channel vertically focussing, (c) no matching lens, channel vertically focussing.

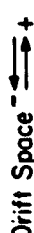


Figure 19 - Vertical phase space plot at channel entrance plane. Target strip S and ellipse F represent the same situation as Fig. 18(c), i.e. first channel lens vertically focussing and no matching lens. Ellipse D and strip S_m represent a set-up with a matching lens and the channel vertically defocussing, but with the channel entrance plane at C. This set-up is not shown in Fig. 18.

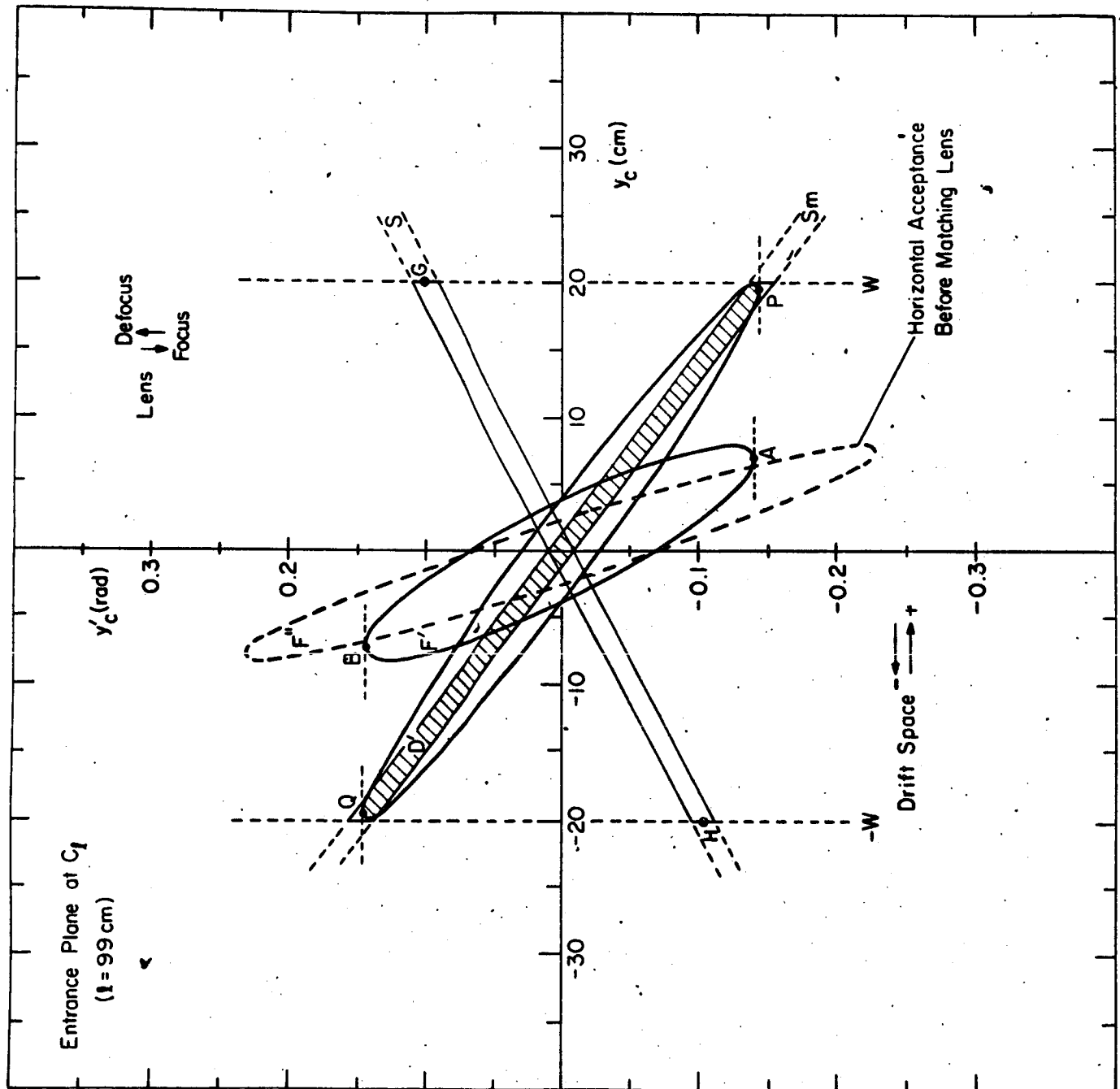


Figure 20 - Vertical phase space plot, with drift space $l = 99$ cm. between channel and cyclotron window. Strip S_m and ellipse D' correspond to Fig. 18(a).

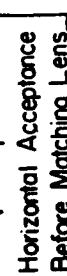


Figure 21 - Vertical phase space plot. Ellipse F' and target strip S_m correspond to Fig. 18(b) where channel, first lens vertically focussing, is moved back by $l = 181$ cm.

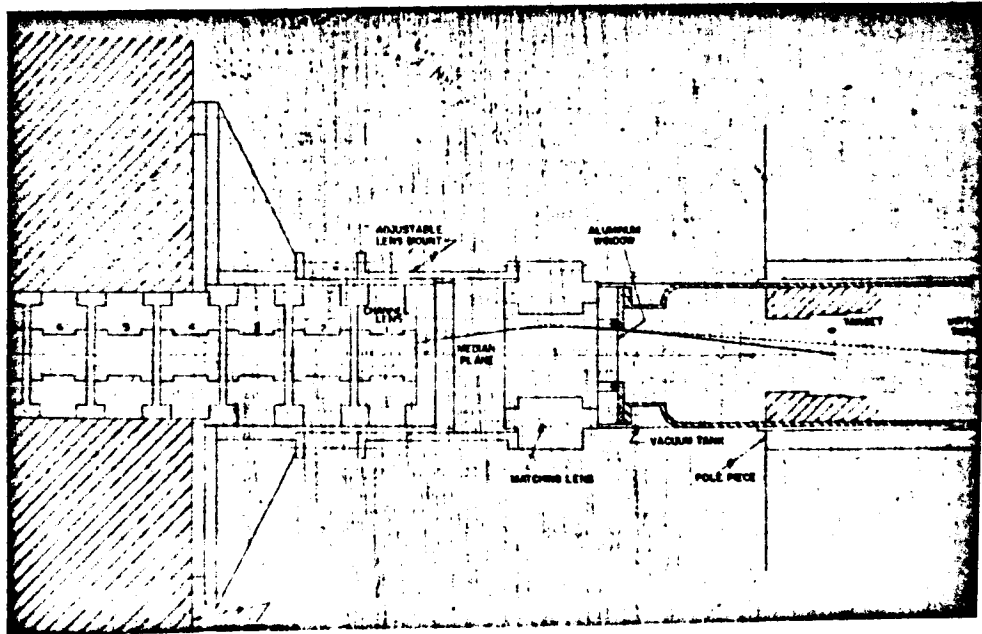


Figure 22 - Elevation schematic of cyclotron vacuum tank, matching lens (M.L.), and first part of channel. Cross-section plane, through M.L. and channel only is rotated by 45° with respect to true vertical plane in order to show pole piece structure of lenses.

KOEHLER, Harvard - What is the power consumption of the quadrupoles?

TELEGDI - The quadrupoles are built to obtain their maximum gradient when operated at two thousand amperes. It turns out, however, that there's very little benefit in operating like that. The consumption is 32 k.w. at 2 thousand amperes and roughly a factor of $3\frac{1}{2}$ less where we work. The quadrupoles are not ideal from the point of view of power consumption because of the little copper that we have in the windings.

THE MUON CHANNEL FOR THE CHICAGO SYNCHROCYCLOTRON*

II. PERFORMANCE

G. Culligan, R. A. Lundy, V. L. Telegdi,

R. Winston** and D. D. Yovanovitch

The Enrico Fermi Institute for Nuclear Studies -
The University of Chicago
Chicago, Illinois

Paper Presented by G. Culligan

I am going to discuss the measurements of the beams we get from the muon channel and the methods by which they are measured. Figure 1 shows the range telescope we use to determine the intensities of the μ , π , and electron components of the beam. It is essentially a copy of the telescope which was used for the same purpose in CERN. We have a Cerenkov counter, 3, which is 90% effective for electrons, behind a piece of carbon (C) to reduce the efficiency for muons below threshold. The Cerenkov counter is removed after the electron contamination has been measured. We next have a variable aluminum absorber followed by two counters (4 and 5), a stopping counter (6 star) and an anti-coincidence counter, (7). The pion content is measured with the so-called star counter (6), which is a device which was developed at Dubna and exploited at CERN. It is operated so that negative pions which stop in it produce large pulses which we subsequently select with a discrimi-

* Work sponsored by contract: Navy Cyclotron No. 2, with the ONR. In addition to this credit line, the authors would like to thank the personnel of ONR for their enthusiastic support.

** Now at Department of Physics, University of Pennsylvania, Philadelphia, Pennsylvania

nator. It is insensitive to muons. The muon content is measured by counting the decay electrons out of 6 into 7 and 8 in anti-coincidence with 5, the solid angle being calibrated with π^+ mesons. We make these measurements directly in front of the muon channel. Most measurements were made using negative beams. The intensities of the negative and positive beams are, however, roughly equal.

Figure 2 shows the electronics, and Figure 3 shows the pulse height spectrum of the star counter. The π^- 's produce the upper spectrum with the tail; μ^- 's produce the lower spectrum which cuts off very sharply. When the star counter is 1% efficient for μ^- 's, it is 30% efficient for π^- 's. It is an extremely useful device. I certainly was very surprised that it was capable of discriminating against μ^- 's with this efficiency. Figure 4 is the discriminator curve of the star counter placed in our channel beam after a bending magnet. We operate at a bending magnet current which is such that we have the maximum number of particles entering the counter telescope. At the optimal muon range, we have a π/μ stopping ratio which is less than 6 parts in 10^4 , as may be seen from the star counter discriminator curve (Figure 4).

Figure 5 is the channel negative pion excitation curve with the matching lens operated at a fixed current of 1200 A. The pion intensity is, of course, a function both of the channel and matching lens current. The absolute maximum of the function occurs when both the lens and the channel are operated at 1200 A. The gain is measured relative to the intensity we observed with both the channel and matching lens de-excited, i.e. using the channel as a regular beam pipe. The predicted excitation curve was obtained using Fronteau's program, integrating over the acceptance ellipses of the channel, and taking into

account the differences in momenta of particles accepted. I point out that we made some reasonable assumptions in calculating this curve; we could, however, make somewhat different assumptions which would not be too unreasonable and change the predicted curve up or down by the order of 30%. The net pion gain into all space (incidentally we performed a beam scan which is why we don't have many points on the excitation curve) is about 25 relative to a pipe. The excitation curve was taken at the end of the muon channel, but before the bending magnet.

Figure 6 shows the pion range curve taken at the end of the channel. The broken line is the predicted range curve obtained using Fronteau's program. There is quite reasonable agreement between the results and theory for the π^- 's both for the range curves and the excitation curves. The situation in the μ^- case is not so clear.

Figure 7 is the μ/π ratio in our counter telescope. We didn't have sufficient time to measure the μ/π ratio for a number of different positions of the counter telescope. It is taken with the counter telescope on the beam axis. You can see that we have perhaps 30% more μ 's per pion than we expect.

Figure 8 shows the range curve for muons. There are two peaks apparent; one at approximately 30 gm/cm^2 $A\ell$ due to forward decay from the pions and in the center of mass one at approximately 5 gm/cm^2 $A\ell$ due to backward decay from the pions in the center of mass. Only the backward and forward muons are trapped by the channel. Muons with large angles of emission strike the walls of the channel and are not transmitted. Again you see that there is not particularly good agreement between the theory and the experiment. There are obviously components in this curve which we don't take into account with the naive theory.

Now I wish to discuss the situation after the bending magnet. Figure 9 shows the polarization of μ^+ 's which have been momentum selected with the bending magnet. The polarization is relative to that which one normally obtains under regular pipe operation. We calibrated our "polarization measurer" in the regular μ^+ beam. One sees that the beam is highly polarized in one direction at 150 MeV/c momentum, and about equally polarized in the opposite direction at 75 MeV/c momentum. We thereby confirm that the second peak in the μ^- range curve indeed corresponds to the backward decay muons in the center of mass system.

Figure 10 shows range curves which have been obtained (in tight geometry) by a number of experimenters who have used the beams since we finished construction. Each of the range curves show two peaks. The left peak corresponds to pions, the right to muons. The upper left range curve was taken with a strong focussing magnet similar to that used at CERN. This was later replaced by a conventional wedge magnet which increased our intensity by a factor of 2. These various range curves are compatible. There are some fluctuations in beam intensity, but our average intensity is about 200 K per second into a 5 x 5 inch square counter, 60 cm from the edge of the bending magnet. The bottom right range curve corresponds to an experiment in which the only convincing measurement of the beam composition after the bending magnet was made. We found 23% e^- , 35% π^- and 42% μ^- . These fractions do, however, depend on the counter geometry used because the momentum spread of the μ^- 's before the bending magnet is much larger than that of the π^- 's. The π/μ ratio was obtained by decomposing the range curve into the somewhat arbitrary components shown. The Cerénkov counter is slightly efficient for muons, and hence, for range curves

taken with this counter, the true muon rates are about 15% higher than those indicated. We have calculated from the range curves that we can stop 20 K per second μ^- 's in a 10 cm diameter, 6 cm (9 gram Cu equivalent) long cylinder of polyethylene, (CH_2), one meter from the magnet edge.

It is interesting to try to see if our intensities are consistent with the internal proton beam which we have in the cyclotron. At the design momentum (160 MeV/c) we accept 1.7 rad-cm phase space area in the horizontal plane, and with vertical matching, all particles which are 20 cm above or below the median plane. These figures may be used to calculate the solid angle subtended at the target. We find $\Delta\Omega\Delta p = 1.7$ MeV/c - sterad at 160 MeV/c. We accept a range of momentum 155 - 200 MeV/c however, and the horizontal acceptance decreases with increasing momentum. In addition, the vertical matching is complete at only one momentum since the focal length of the matching lens is momentum dependent. We have not calculated in detail the reduction in solid angle produced by these effects, but we consider it reasonable to assume that in truth we subtend a solid angle, say, of 0.9 ± 0.3 MeV/c - sterad at the target. The forward production cross-section for negative pions by protons on Be at 450 MeV proton energy is about 5 microbarns per steradian for 160 MeV/c pion momentum. Using this cross-section, we calculate from the assumed solid angle that the observed intensity of 1.6×10^6 /sec particles accepted (with stochastic extraction) corresponds to 1 μA of protons interacting in 1 gm of Be. The internal target is about 9 gm/cm² of Be. We do not know, however, the fraction of the beam which intercepts target or the average number of traversals; but, nonetheless, it would seem that the internal current is about one or two tenths of a microamp,

i.e. within a reasonable range for the stochastic acceleration system.

An example of the experiments which can be done with the muon channel, is indicated in Figure 11 which shows the pulse height spectra in a NaI crystal produced by mu-mesic X-rays from some low Z materials (Boron, Carbon, Nitrogen and Oxygen). The spectra are exceptionally free from background, even at energies as low as 10 keV. The reason for this is apparent from Figure 12 which shows the geometry used. We observed the X-rays at 135 degrees with respect to the incident muon beam, with no-anti-coincidence counter before the NaI crystal. The background in this geometry was so low that one could see the 75 keV carbon K line without requiring a coincidence with the incoming muon. The targets were in general about $1/2 \text{ gm/cm}^2$ thick and stopped about 500 μ^- 's per second. This experiment removed a disagreement between the observed and predicted ratios of K-to-L X-rays in some light elements, and is a convincing demonstration of the type of experiment which is now possible using the muon channel.

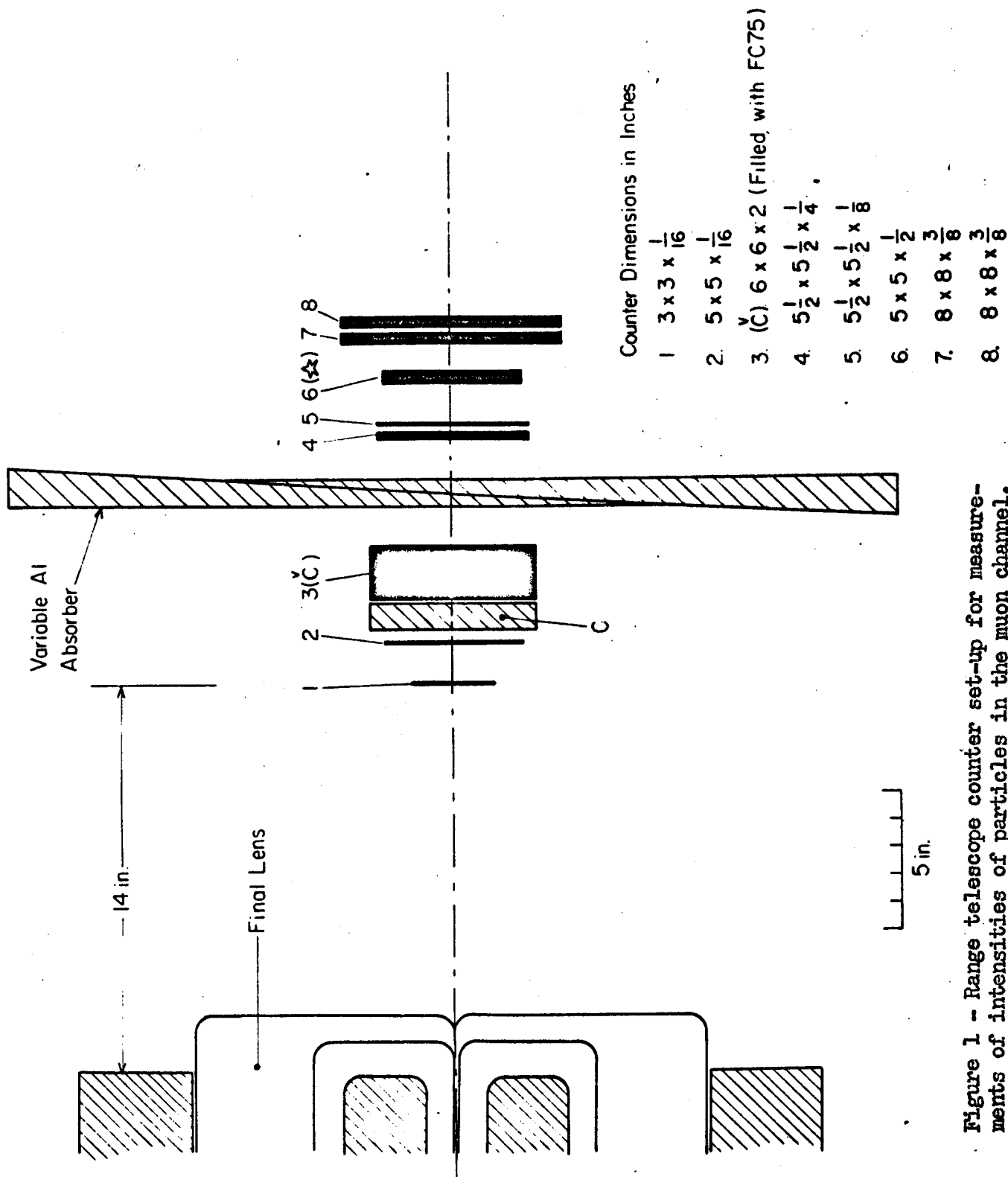


Figure 1 -- Range telescope counter set-up for measurements of intensities of particles in the muon channel. Counter 3 is a Cherenkov counter and counter 6 is a star counter.

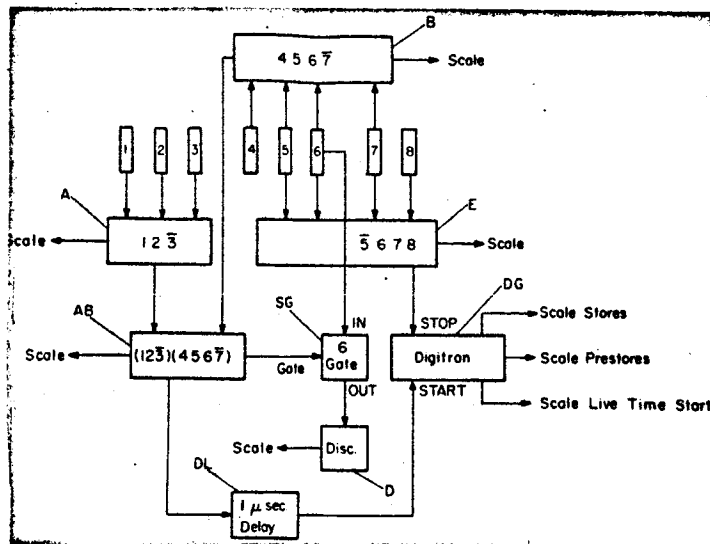


Figure 2 - Block diagram of electronic logic system for the range telescope.

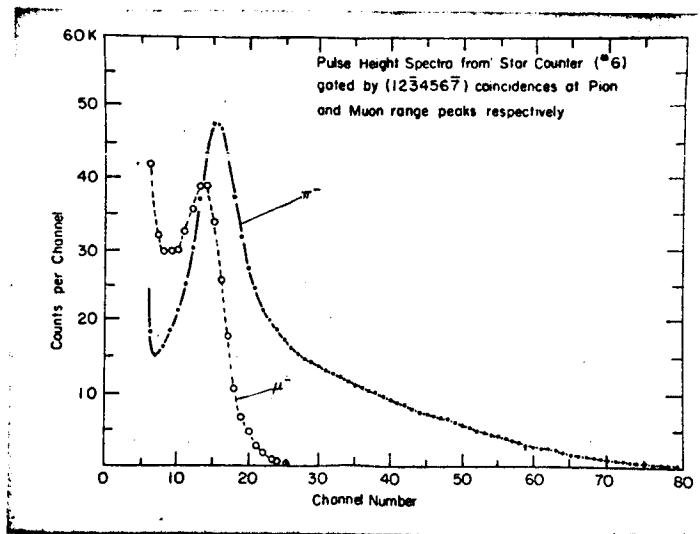


Figure 3 - Star Counter Pulse Height Spectra.

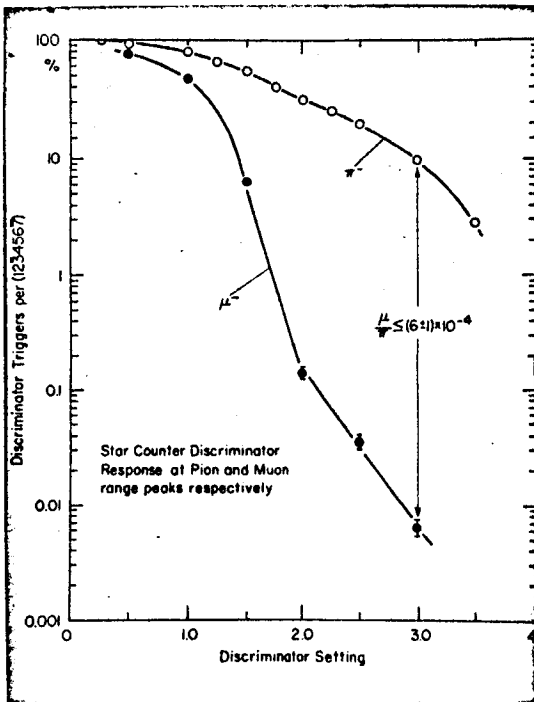


Figure 4 - Discriminator curve for the star counter. Counter set-up.

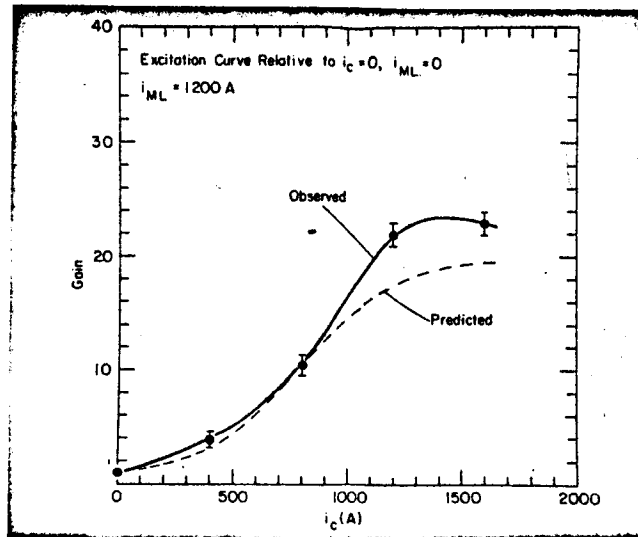


Figure 5 - Channel gain for negative pions as a function of excitation current. M.L. = vertical matching lens discussed previously operated here at 1.2 KA.

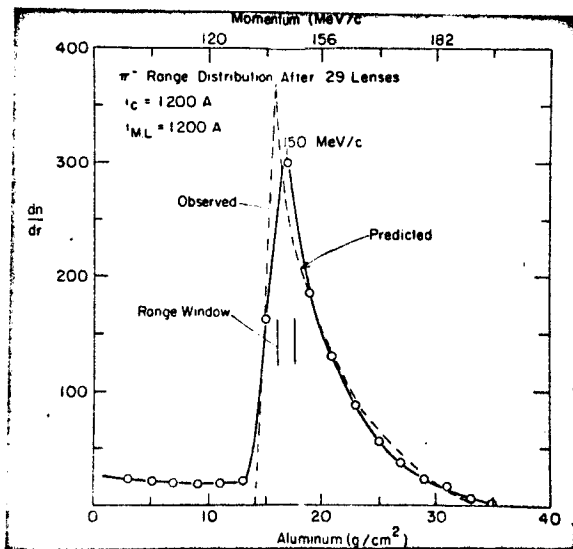


Figure 6 - Range curve for pions.

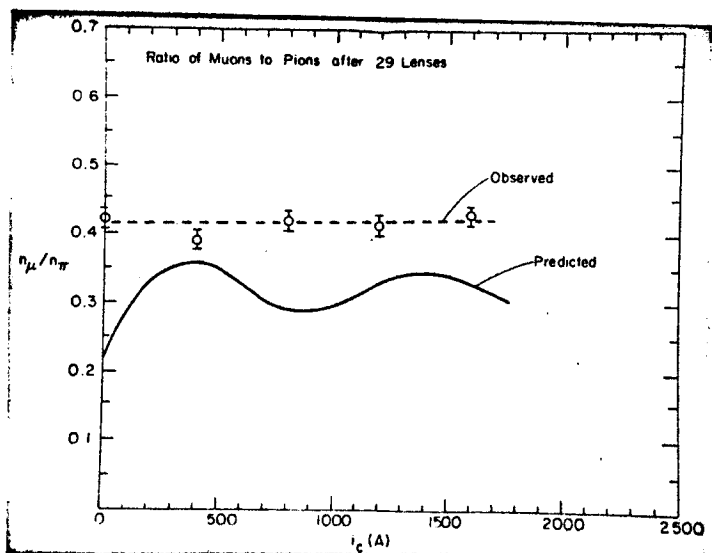


Figure 7 - μ/π ratio for channel vs. excitation current.

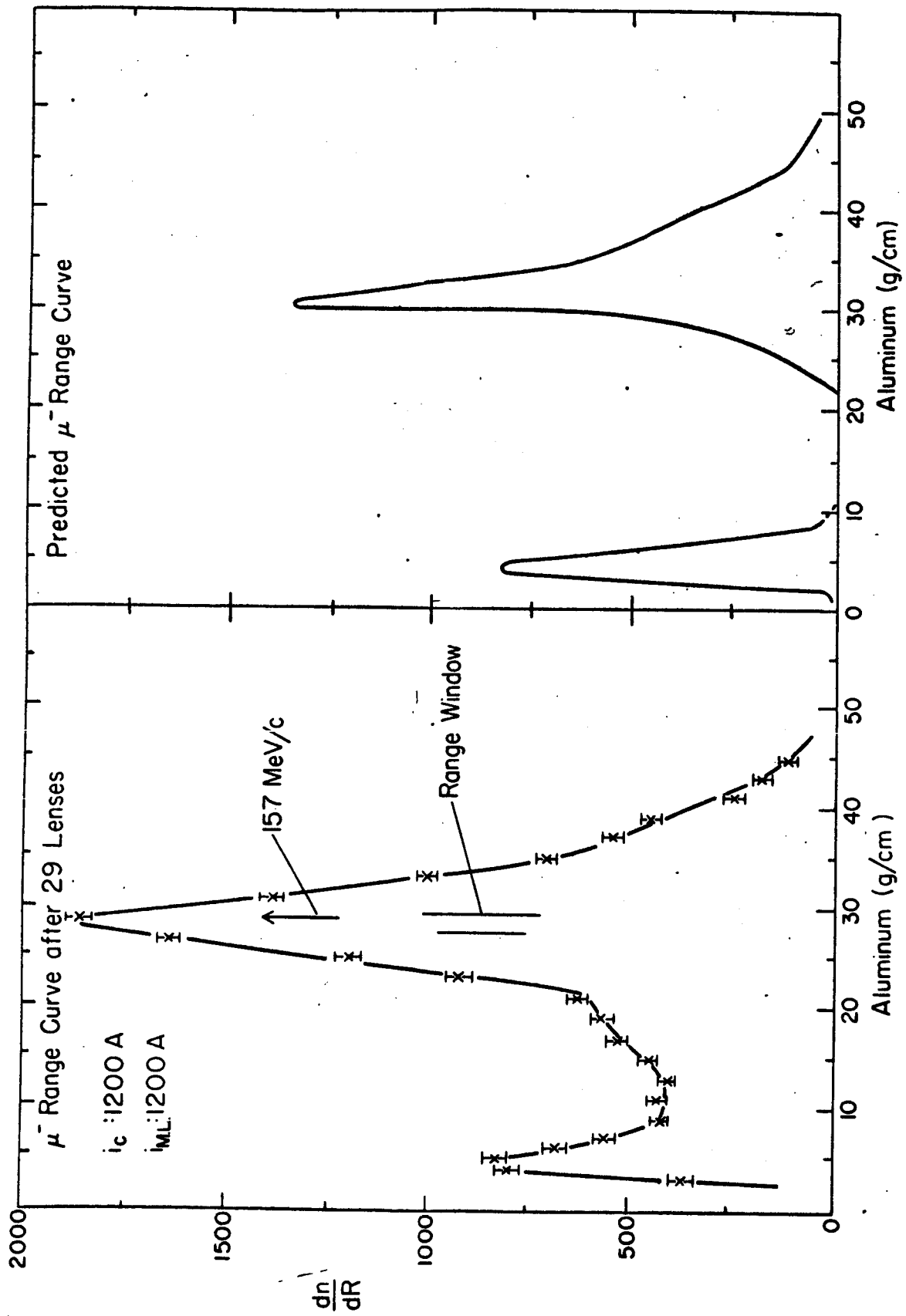


Figure 8 - Range curve for muons.

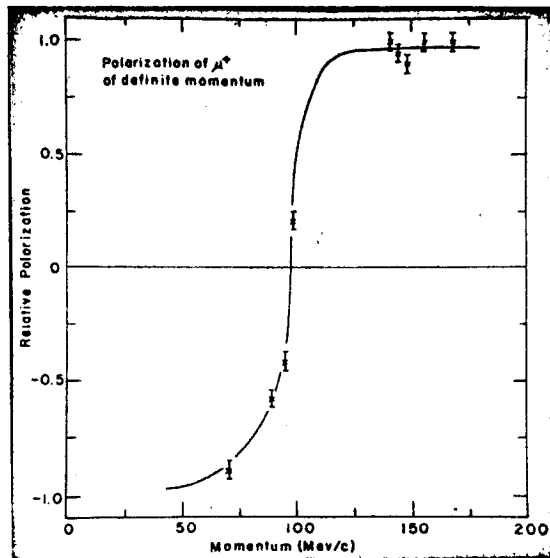


Figure 9 - μ^+ polarization vs. momentum.

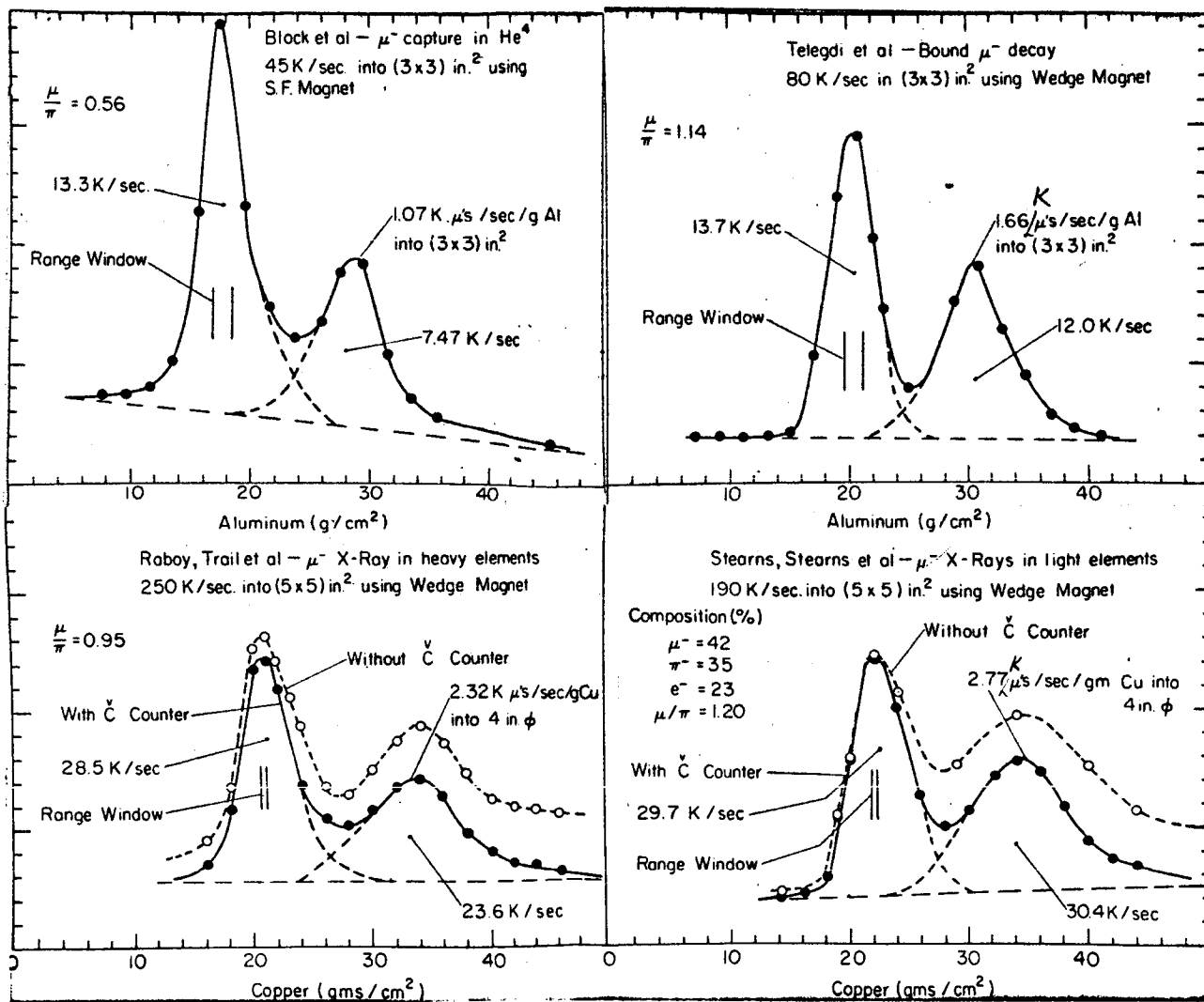


Figure 10 - Range curves obtained by several experimentors. The left peak in each of the range curves correspond to pions, the right correspond to muons.

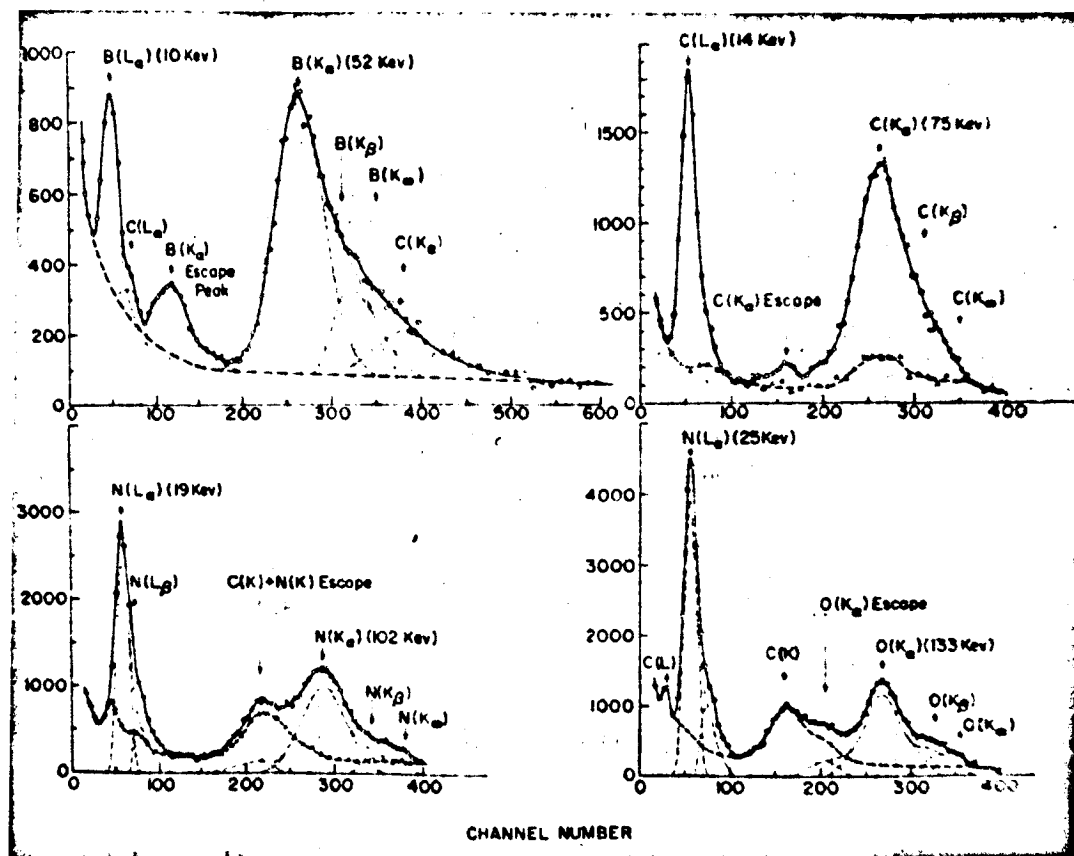


Figure 11 - Pulse height spectra of mesic X-rays in low Z materials.

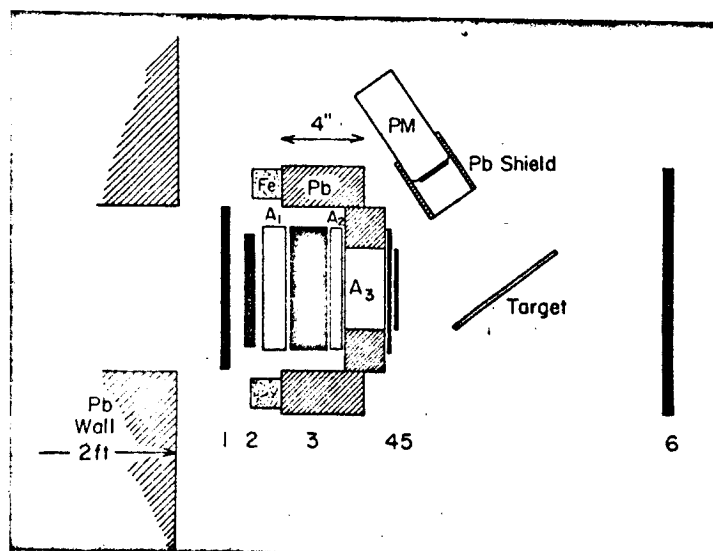


Figure 12 - Counter set-up for mesic X-ray experiment.

ECKHAUSE, William and Mary - Could you tell me what are the advantages of your channel over the one at CERN.

CULLIGAN - I think our intensities are comparable with those at CERN.

MICHAELIS, CERN - If I read your results correctly, you stop something of the order of 30-50 muons per gram, and I believe we use to stop around 80 muons per gram of carbon. So I think we now get around three times what you have at Chicago.

CULLIGAN - and this is operating under a pion peak?

MICHAELIS - Yes.

CITRON, CERN - one would expect your channel to perform 3 or 5 times better than ours....but the thing you have against you is that you are operating at a lower proton energy ... so your pion spectrum is not as favorable.

CULLIGAN - Your impact parameter is reasonably well chosen. 260 MeV/c corresponds roughly to the peak in pion production at (your) energy. We have chosen an impact parameter which was variable. There is the uncertainty in the factor of increase in muon intensity which one can expect upon raising the proton energy from 400 to 600 MeV. I don't know what that would be.... As I pointed out, I made a calculation in terms of the solid angle which our channel subtends at the target and we obtain a beam of 1 μ a.- gm of Be. Now what would be a comparable figure from the CERN cyclotron.

CITRON - 1 μ a.

CULLIGAN - This is 1 μ a -gm; our target is in truth 5 grams thick.

TELEGDI - The performance of the channel can best be judged by switching it off. You can simply compare the flux when you have first an empty pipe at a given distance with the flux when the channel is working, as Dr. Culligan has shown. The performance can be judged simply by the excitation curve. Anything else depends on what you put in front. There are ample reasons to assume that we are putting in something different from what you are putting in. We have a 450 MeV machine. From what little we know here about these things we think we have somewhat less current--and less production cross section. The channel excites as theory predicts it should and for us it is an improvement by a factor of 15. Now if we put in more at the front of the channel we would get more out. Now in the absolute sense this channel has the one advantage of (being) symmetrical in charge. That is what we have done by our particular choice of impact parameter. By the way, the intensities given by Dr. Culligan could be generously multiplied by a factor of 2 or 3 to allow for the fact that they all are taken with a stochastic beam. In addition to the channel excitation curves, you can also perform excitation curves for the vertical matching lens by itself, which also performs according to theory.

ROTATING CONDENSERS

M. Foss, Carnegie Tech.

Because there is current interest in this type of equipment I would like to tell you about the Carnegie Institute of Technology rotating condenser. Our condenser has had over ten years of satisfactory operation.

One interesting feature is the main bearings. These are 120° nylon sleeve bearings operating in cooled Myvane oil. The 240° annulus not occupied by the bearing is used as an oil duct. The original nylon sleeves are still in service and show no perceptible wear.

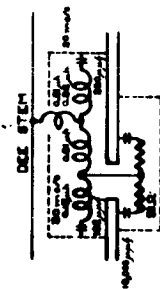
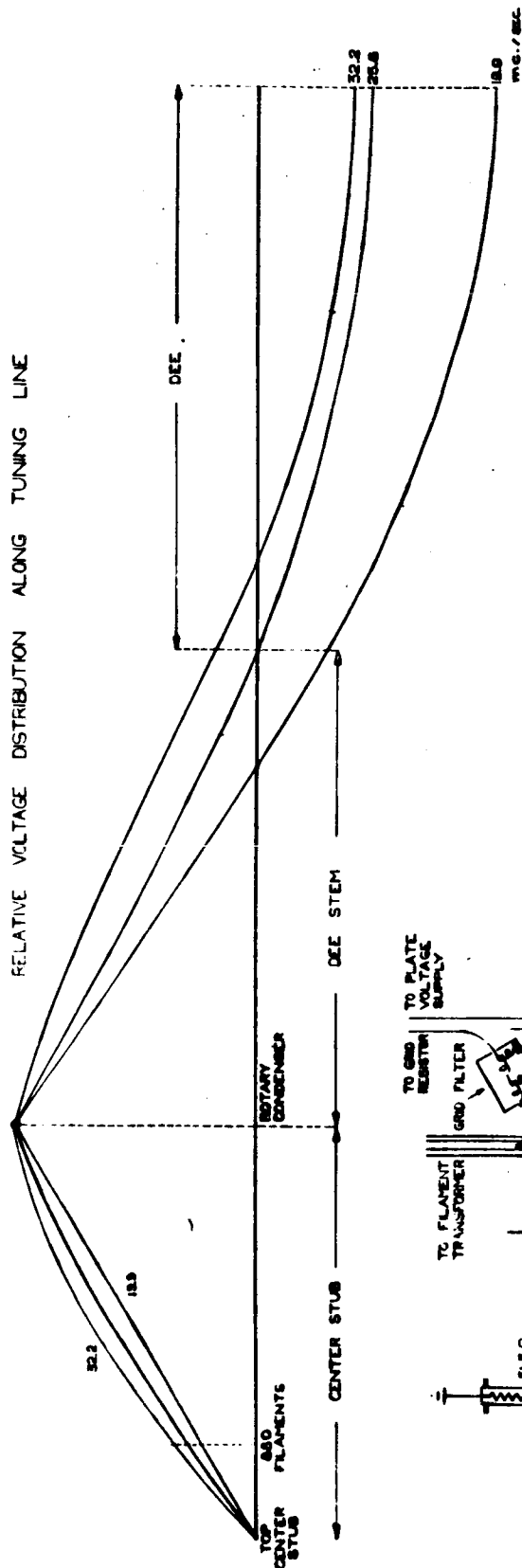
The main bearing oil is kept out of the vacuum by modified 3-1/2 inch Crane seals. The rotating seal is made between a ceramic alumina ring and a non-porous graphite ring. The original seal between the shaft and the rotating ring has been replaced by an "O" ring. The spring which holds the rings together has its turns shorted together with braid to prevent r.f. resonances.

If the shaft has an axial resonance in the operating band of frequencies the oscillator may not operate at the resonant frequency of the line. To keep the axial velocity high (in a line which is necessarily capacity loaded) the inductance was kept at a minimum. The axial velocity in the one meter long toothed region is $c/3$. By using an appropriate impedance between the toothed region and the bearings a resonant frequency of 33 megacycles per second was achieved.

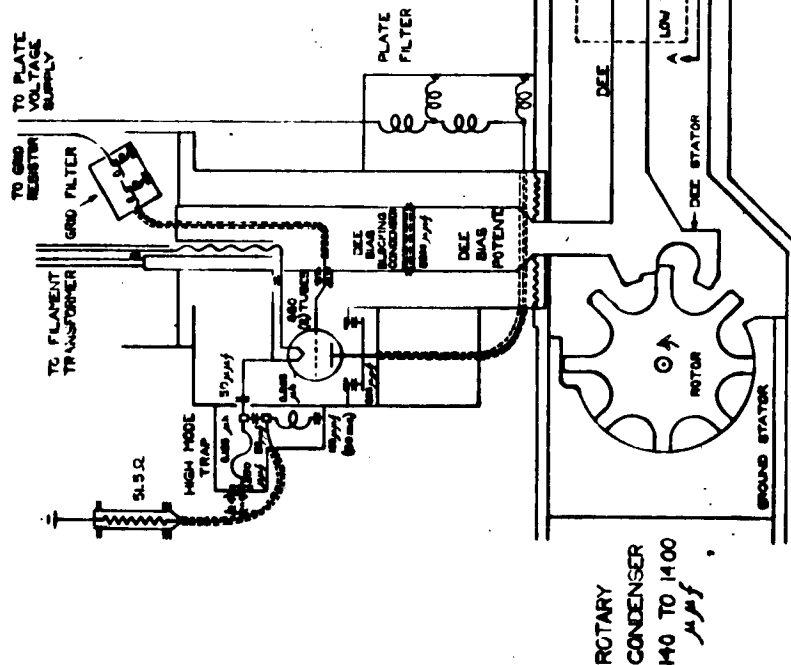
One end of the shaft sticks out of the vacuum tank. It is used for a drive sheave, thrust bearing, and shaft water cooling connections. This end was subject to excessively high r.f. voltages which broke the bearing bracket insulators. To overcome this problem the bearing bracket was grounded and the shaft connected to the bearing bracket by brushes. There are now two resonances one at 5 and one at 40 megacycles per second.

Our condenser was designed to deliver 400 pulses per second (3000 RPM) and use 50% of the time accelerating beam. However, we operate at 200 pulses per second.

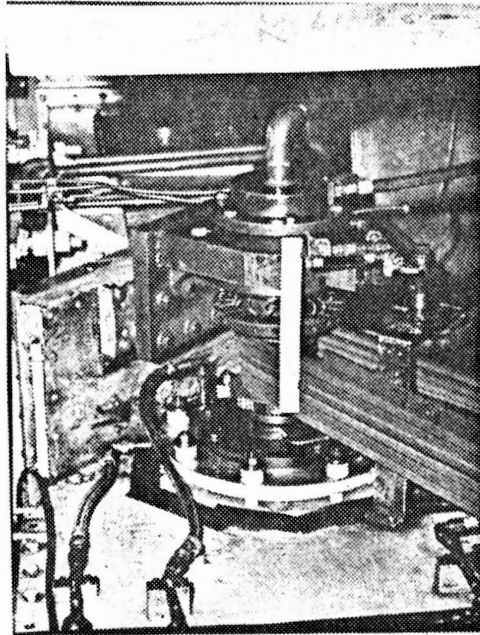
The brushes and water seal limit the speed. Both of these will be improved to allow operation at 300 pulses per second. It is not clear that we will be able to reach 400.



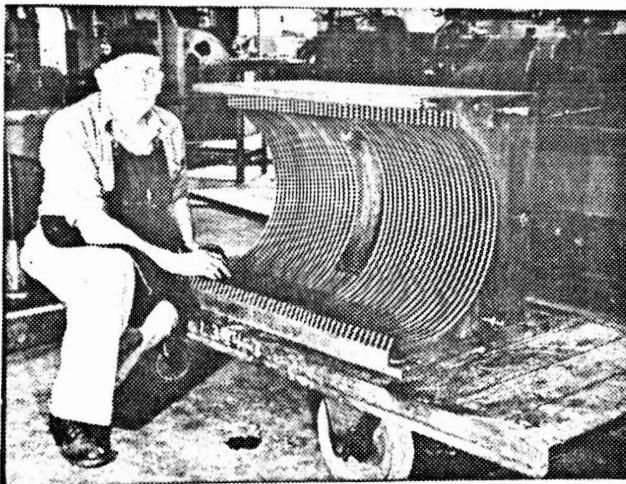
SECTION A-A



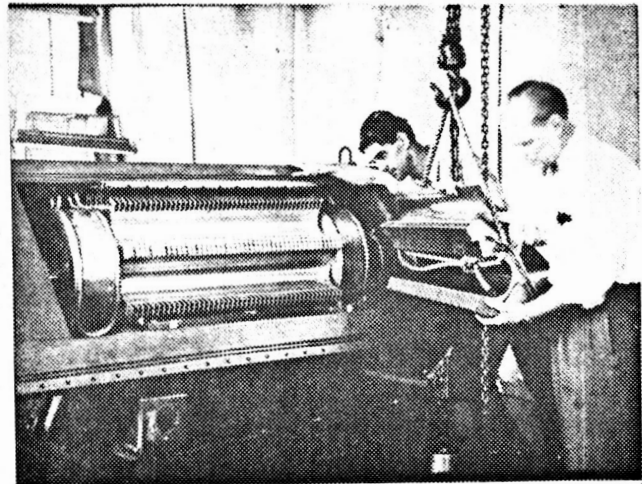
The CIT grounded plate, grounded grid, grounded cathode oscillator. The plate bypass condenser is $8000 \mu\mu f$ (note error), grid bypass $1200 \mu\mu f$ each, and filament bypass $70,000 \mu\mu f$. The outstanding drawback to this system is the low impedance which the tubes drive.



Bearing insulation and oil pipes, the optical comutator, belts, brushes, bearing bracket, and water seals. This region acted as a step up transformer when the bracket was insulated from ground. To avoid this the bracket was grounded and brushes were installed to ground the shaft.



Ground Stator - The hole was put in for pumping. 5 rows of rotor teeth are in the stator at maximum capacity.



Condenser Assembly - Note that the teeth are cut only deep enough to give the required clearance, 2 mm. in the ground stator and 3 1/3 mm. in the "D" stator. This minimizes the axial inductance.

BEAM STRETCHING BY EXCITATION OF RADIAL OSCILLATIONS

J. R. Wormald, University of Liverpool

I should say at the start that I will only talk about a particular mode of beam stretching, i.e. that applied to an internally produced pion beam. It was actually Arthur James who first realized what was going on and did most of this work. B. Collinge designed the r.f. oscillator and the auxiliary electronic equipment. We stumbled upon this method accidentally a few months ago and so the work is not yet complete. I can only give you a sort of current progress report. It all started off with a quite conventional cee system primarily for the proton users since they had to put up with a normal duty cycle of .8%.

The arrangement inside the tank is shown in Figure 1. I have left out the peeler-regenerator and extraction channel because I'm only talking about internally produced pions which come out from a target at a radius of $69\frac{1}{2}$ inches through an angle of about 90 degrees and off to the screening wall to the right. The cee is four inches high, the same height as the dee, and four inches deep. Figure 2 shows the frequency program which we originally used. The main r.f. comes down to 19.2 megacycles, the dee oscillator is switched off and the cee oscillator is switched on. It has the same repetition rate as the dee oscillator and is run by another oscillator tuned by

its own rotating condenser on the same axis as the main condenser to give a frequency swing of 250 kilocycles. We obtained a beam with a duty cycle of the order of 16%. This duty cycle is measured by comparing the rates on two scalers; one with 1 microsecond dead-time and the other with a .1 microsecond dead-time. Hence any duty cycles I mention ignore r.f. structure. The efficiency in this mode was about 50%. We originally tried it with a proton beam, then we tried using it on the internal pion target and obtained about the same performance--50% of the pion beam and a duty cycle about 16%.

We weren't very happy with this 50% because we are rather short of pions in Liverpool, so we were trying to vary all the parameters to see if we could improve things when Arthur James noticed that pions were coming out when they hadn't any business to. We then changed to the frequency program which is shown in Figure 3. I thought we were unique in having the frequency gap of 19.40-18.71 mcs, but from yesterday I gather that Chicago also has it. The main r.f. comes down to 19.4 megacycles. (The scale is nonlinear.) Then it is turned off. We decreased the cee frequency swing to \sim 50kcs and kept the cee running all the time. At the bottom of Figure 3 is a histogram of the actual output of pions. There is a short spike lasting about 80 microseconds and contains about 10% of the beam. The rest is spilled out in two parts. The first occurs when the frequency of the cee is going down and the lesser part occurs as it is going up. With this system we have managed to get the performance

of 100% of yield of pi minuses with a duty cycle of about 38% and, although we haven't checked it yet, we believe that if we did cut out the 10% in the spike the duty cycle would be 50%. We haven't managed to get quite as good a performance with the positive pions; so far we haven't managed to get more than 75% yield and a duty cycle of 27%, but, as I said, we are still developing this system and we are still not quite certain why there is this difference between π^+ and π^- ; they come out from a target in the same position, down the same channel.

A picture of the beam is shown in Figure 4. Displayed are the spike containing 10% of the beam, the group coming out while the cee frequency is decreasing, and the group coming out as the frequency goes up again. An explanation of this is that the cee is not in fact being used as an accelerating electrode, but as a deflector and that we are in fact inducing radial oscillations, the frequency being given by $(1-n)^{1/2} \omega_c$. We assume that the cyclotron frequency, ω_c is the frequency at which we stacked the beam, that is, the frequency at which we turned off the dee, 19.4 megacycles. We are swinging the cee through quite a small frequency range, less than 50 kilocycles around about the 18.7 Mc/s region.

This corresponds to a value of $n \simeq 0.07$. We have never actually measured our magnetic field accurately enough to say that is the value of n , but it seems not impossible.

Furthermore we can try to explain the difference between the performance obtained with π^- where we have achieved 100% yield,

and the $\pi^+ S$ with a 75% yield. It is possible that this is due to the effect of the peeler and the regenerator; they are supposed to start acting on the beam when it gets out to a radius of 69 inches. Since our target is at $69\frac{1}{2}$ ", it is possible that if we stacked the beam just outside the target the peeler and regenerator would be just beginning to have some slight action. Hence when we are getting out $\pi^+ S$, by sending the beam around in the way which we normally do when we try to get out protons, the peeler and regenerator may be perhaps producing too much radial oscillation amplitude and not leaving it all to the cee. On the other hand if we are sending the beam around in the opposite direction, as we do when we are making $\pi^- S$, it is possible that the peeler and regenerator may be having the effect of reducing radial oscillations, making our sausage narrower. Thus there is a smaller range of radii, a smaller variation in n , and so possibly a smaller range of radial oscillation frequencies. We've got no evidence for that, it just happens that way and it will be interesting, although we haven't finished these investigations, to see what other people think about them or if they care to try it on their machines to see if they can get similar results.

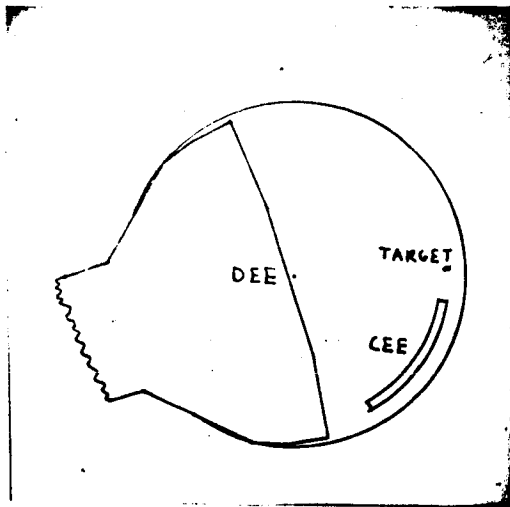


Figure 1 - Plan view target and cee inside cyclotron tank.

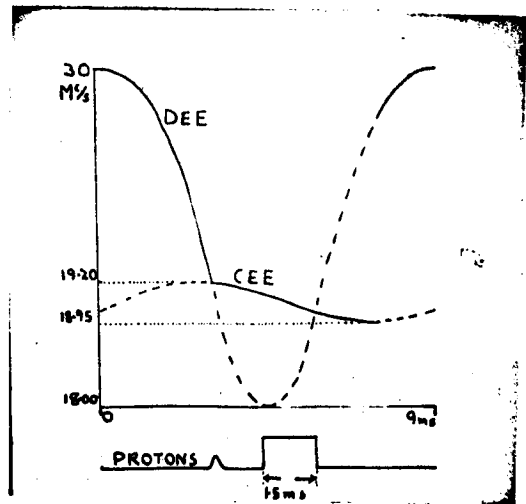


Figure 2 - Frequency program used initially. Bottom line shows beam time structure.

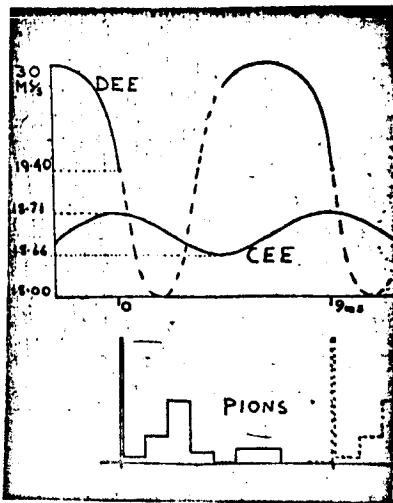


Figure 3 - Frequency program used finally. Bottom line shows beam time structure.

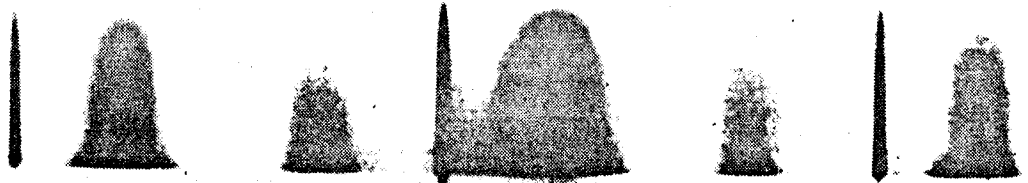


Figure 4 - Photograph of beam time structure.

CROWE, Berkeley - Do you ever observe that the pion yield from a target at such a large radius depends upon the position of the regenerator? Is your regenerator movable?

WORMALD - No, it is fixed and as it is rather radioactive now, we don't want to go near it.

CROWE - As you move the target in - inside the regenerator radius - do you lose pions rapidly?

WORMALD - Yes, we do lose beam rather rapidly as we go to smaller radii.

CROWE - Is it possible that you have the beam being regenerated and striking the target with reasonably large radial oscillations-- e.g. do you have a great deal of turn separation due to the regenerator action?

WORMALD - Well, I shouldn't think so at this radius. The regenerator goes on working for several inches and it only has a half inch before it hits the target.

CROWE - One of the problems of operating with internal targets is that the turn-to-turn separation is so small that you don't get a very long effective target length in the beam direction. I believe Harvard claimed they could get much more from an internal target by a regenerator which gave a few tenths of an inch radial oscillation at the target. Possibly your target is in such a position that it would be struck by positively regenerated protons. In your machine there's a proton path crossover (node) after the regenerator, going in; does this occur before the target or after it in the beam direction?

WORMALD - It's close but I can't remember just which side of the target it is.

HUXTABLE, Harwell - What happens when you leave the frequency on the cee constant?

WORMALD - It's awful-- we get at best 5% duty cycle and still only 50% yield. We must have some frequency wobble. We haven't tried varying the range of the wobble.

FUNSTEN, William and Mary - If you excite by radial oscillations, it seems you would need coherence for many cyclotron revolutions. I don't see how you can get that with the precession of your orbits.

TELEGDI, Chicago - If you excite radial oscillations, you work as an extractor rather than an accelerating electrode. Wouldn't you also expect that you would need singularly little power to do this. We find that we have to pump in a lot of power which makes one think of the accelerating mode. But if you are hitting a resonance, you could do this with relatively little power.

WORMALD - I don't know the power figure, but I think the cee is operating at about 3 k.v.

RESIDUAL RADIATION STUDIES

by

C. B. Fulmer, K. S. Toth and M. Barbier

(Presented by C. B. Fulmer)

ABSTRACT

The reliability of estimates based on calculation of residual radiation to be encountered in meson producing accelerators was tested by comparing calculated residual radiation levels with experimental data. A computer calculation was used for determining the γ -ray dose rates near slabs of material after irradiation by a beam of fast protons incident normal to the slab surface. The calculated and experimental decay curves agree within a factor of two of three. Examples of practical application of the calculation are discussed.

An important part of the development program for any accelerator capable of producing beams of particles that induce spallation reactions is a realistic appraisal of residual radiation levels that will result from operation of the machine. Such an appraisal will help to ascertain the shielding and remote handling facilities needed for the safe operation and maintenance of the machine and associated experimental facilities. Costs for unnecessary facilities can thus be kept to a minimum without incurring unanticipated delays in maintenance operation due to residual radiation levels.

This paper is part of such a study⁽¹⁾ that was made for the proposed ORNL Mc² Cyclotron, which is designed to accelerate 100 μ A of protons to an energy of 810 MeV. The approach used was to calculate the residual radiation levels by using published spallation cross section data. The results were compared with experimental activation data. The calculations were done at Oak Ridge and the experimental data were obtained at the CERN Synchro-Cyclotron.

A formula was derived for calculating γ -ray dose rates outside slabs of materials irradiated by fast particles. It is assumed that a collimated beam of particles impinges normal on the slab. The incident beam intensity I_0 is attenuated in the material by the macroscopic geometric cross-section Σ_t . In a straightforward manner an expression for the total dose rate D_j at a point a distance d from the slab due to all activity from spallation product j in the slab is obtained.

$$D_j = \text{const } I_0 \Sigma_j E_j (1 - e^{-\lambda_j t_B}) e^{-\lambda_j t_c} \int_0^{X_{\text{MAX}}} \frac{e^{-(\Sigma_a + \mu_j)x}}{(x + d)^2} dx$$

Σ_j is the macroscopic production cross section for activity j , E_j is the gamma energy, λ_j is the radioactive decay constant, t_B is the irradiation time, t_c is the cooling time, μ_j is the absorption coefficient of the slab material for the gamma radiation, X is the depth in the slab, and X_{max} is either the slab thickness or the range of the incident particles in the slab material, whichever is smaller.

The analytical evaluation of the integral yields a slowly converging infinite series; therefore numerical integration is used to evaluate D_j . For the total dose rate at a given point the D_j 's for all the spallation products must be evaluated. Since the amount of computation is enormous, the work was programmed for the IBM 7090 computer. ⁽²⁾

Cross sections for the production of spallation products in the slab material were taken from published studies. ⁽³⁻⁷⁾ The computation determines the dose rate, for specific bombardment and cooling times, at the slab surface, at 10 cm from the surface, and at 1 meter from the surface.

Samples of several materials were exposed to protons inside the CERN Synchro-Cyclotron vacuum tank for a period of three months. The samples were then removed and decay curves were measured for the γ -radiation emitted. Some of these curves are shown in Slide 1. To provide a test of the computer calculation discussed above, dose rate decay curves were computed from a 3-month bombardment with a 1- μ A 600 MeV proton beam on samples of C, Al, Fe, and Cu 1 mm thick. These samples were selected because they are the most common materials to be used in the construction of an accelerator and associated equipment and because spallation reactions in these materials have been extensively studied. The experimental and computed decay curves are compared in Slide 2. These have been normalized where the aluminum decay curves flatten out, i. e. where Na^{22} is the dominant activity in aluminum. The shapes of the two sets of curves are very similar. The ratios of the experimental to the calculated curves are in most cases unity within a factor of two.

Residual radiation induced by spallation neutrons must also be considered. The usual assumption is that fast neutrons produce the same types of spallation reactions as fast protons. Samples of several materials were exposed to fast neutron fluxes at the CERN Synchro-Cyclotron for a period of six weeks. Decay curves were measured for the gamma radiation induced in

these samples. Some of these are shown in Slide 3. A comparison of these curves with those shown in Slide 1 shows similar shapes of the curves for each material. If the two aluminum decay curves are normalized on the flat part of the curves, the ratio of the curves for other materials are unity within less than a factor of two.

As a check on the absolute normalization of the computed decay curves thin samples of various materials were exposed to a monitored proton flux (1.06×10^9 p/(cm² sec) for a period of three hours at the CERN Synchro-Cyclotron and the decay curves measured. The previously measured counting efficiency of the NaI crystal was used to convert the γ -ray counting rates to absolute dose rates. Theoretical dose rate decay curves were computed for C, Al, Fe, and Cu for the same beam intensity and bombardment time. The experimental and computed curves ^{are} compared in Slide 4. These curves have not been arbitrarily normalized. The shapes of the two sets of curves agree quite well. The discrepancies in absolute magnitude are not too surprising when the experimental errors involved in a bombardment of short duration by a beam of low intensity are considered.

As an example of an application of the computer calculation, dose rates were calculated for a 100 μ A beam of 810 MeV protons striking a 4 cm thick copper and a 5 cm thick aluminum target for a period of 100 hours. The residual radiation dose rates at a distance of 1 meter from the targets are plotted as a function of cooling time in Slide 5. For a 1 μ A beam the dose rates would be two orders of magnitude lower than those shown on the slide.

The comparison of Slides 1 and 3 shows that the computer calculation described above can be used to determine residual radiation levels due to fast neutron induced activation. The principal modification needed is one that considers distributed fluxes rather than collimated beams of incident particles. It can be shown that if one considers plane slabs of infinite lateral extent, the residual radiation level outside the slab will be about the same after irradiation

with a uniform flux of 10^8 particles/(cm² sec) as that obtained for a collimated beam of 1 μ A at a distance of 1 meter from the slab if the bombardment and cooling times are the same. The latter is readily determined with the computer program. Thus the computer program can be used to determine upper limits to the residual radiation levels from distributed fluxes.

The computer calculation was used to estimate the residual radiation level inside CERN Synchro-Cyclotron. For this calculation the incident beam was attenuated by a factor of -0.5/cm in agreement with the experimentally measured specific activation as a function of depth in the pole face.⁽⁸⁾ The computed value was increased by a factor⁽⁹⁾ of 4 for fast-particle build-up in the stopping material and by an estimated factor of 10 to account for oblique incidence. The activity was assumed to be uniformly distributed over the pole face area. The decay curve of the residual radiation after 1000 hrs of cyclotron operation is shown in Slide 6. The experimental points shown in the slide were measured at 30 widely distributed locations throughout the cyclotron 15 days after a shutdown. For the detector used, 10^6 counts/sec of 0.5 MeV gammas corresponds to about 1 R/hr. The fast particle flux is not uniformly distributed on the pole faces; thus the distribution of the experimental points is not surprising.

The same type of calculation was applied to the Mc² cyclotron. 10 μ A of incident protons were assumed. The estimated ranges of residual radiation dose rate after 1000 hrs of operation are shown in Slide 7. The upper curves are for pole faces of iron and copper (sector coils). The lower curves show the calculated residual radiation levels if the pole faces are covered with 4 cm of carbon. The results indicate that residual radiation can be reduced by more than an order of magnitude by covering the pole faces with a few cm of carbon.

REFERENCES

1. A more complete discussion of this study is presented in a paper by Fulmer, Toth, and Barbier that is to be submitted for publication in Nuclear Instruments and Methods.
2. J. B. Ball and C. B. Fulmer, ORNL Report 3554.
3. M. Honda and D. Lal, Phys. Rev. 118, 1618 (1960).
4. P. Benioff, Phys. Rev. 119, 316 (1960).
5. G. Rudstam, E. Bruninx, and A. C. Pappas, Phys. Rev. 126, 1852 (1962).
6. J. Hudis, I. Dostrovsky, G. Friedlander, J. R. Grover, N. T. Porile, L. P. Remsberg, R. W. Stoenner, and S. Tanaka, Phys. Rev. 129, 434 (1963).
7. E. Brunnix, High-Energy Nuclear Reaction Cross Sections I, CERN Rpt. 61-1, January (1961), and II, CERN Rpt. 62-9, February (1962).
8. J. P. Blaser, Ch. Perret, M. Barbier, and J. Dutrannois, p 157-164 in CERN Rpt. 63-19 (1963).
9. B. J. Moyer, Data Related to Nuclear Star Production by High-Energy Protons, Lawrence Radiation Laboratory (June 20, 1961) (unpublished).

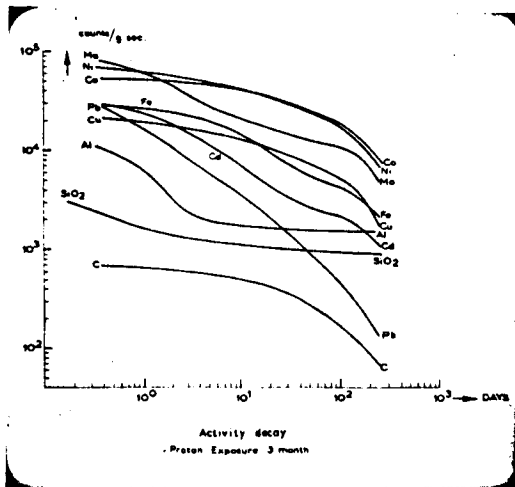


Figure 1 - Specific activity as a function of cooling time for various materials irradiated with 600-MeV protons for a period of 3 months.

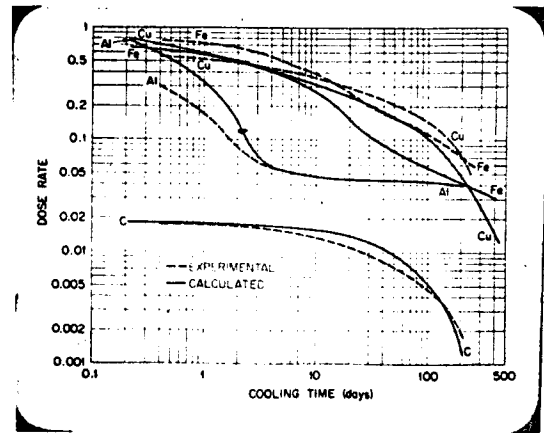


Figure 2 - Calculated and experimental residual radiation decay curves for carbon, aluminum, iron, and copper activated by proton-induced spallation reactions.

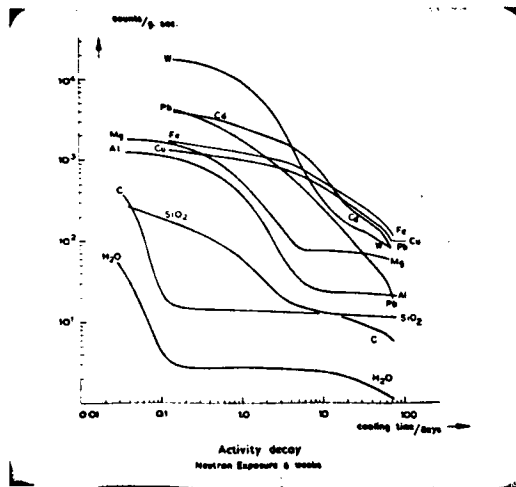
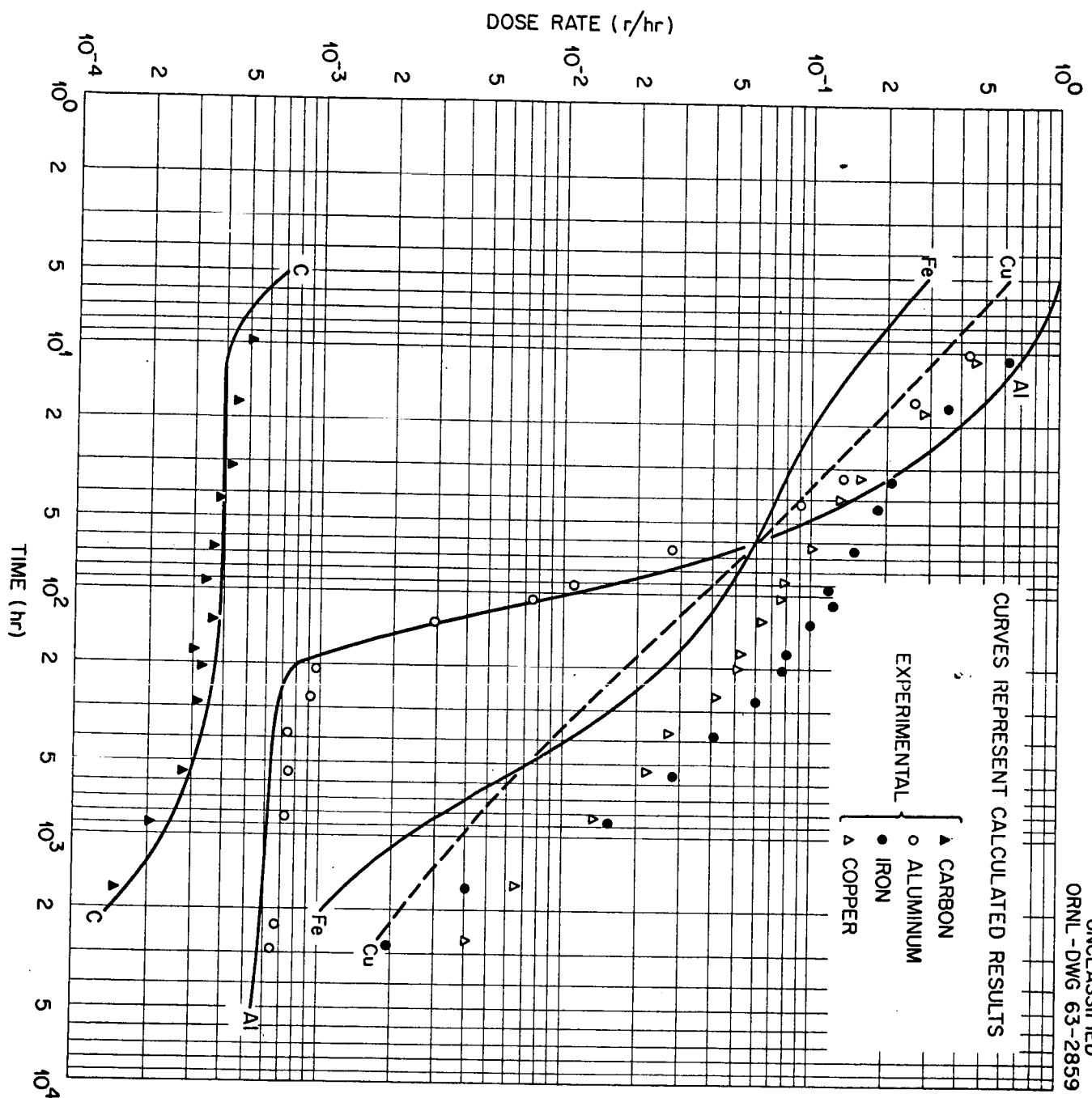


Figure 3 - Specific activity as a function of cooling time for various materials irradiated by spallation neutrons for a period of 6 weeks.



UNCLASSIFIED
ORNL - DWG 63-2859

Figure 4 - Comparison of calculated and experimental measurements of residual radiation levels after 3 hrs. irradiation. The proton beam was monitored for the experimental data.

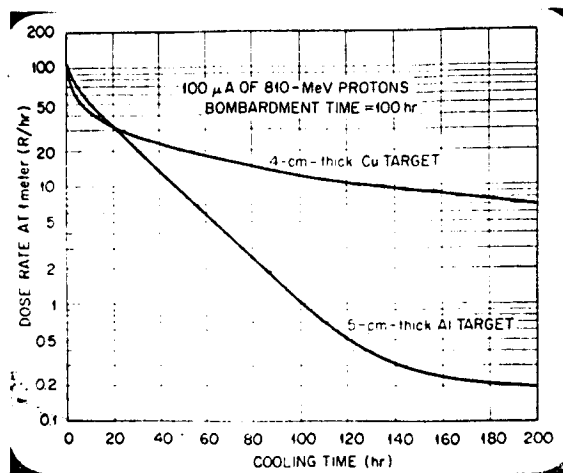


Figure 5 - Calculated residual radiation dose rates at one meter from copper and aluminum targets after 100-hr bombardment with 100- μ A of 810 MeV protons.

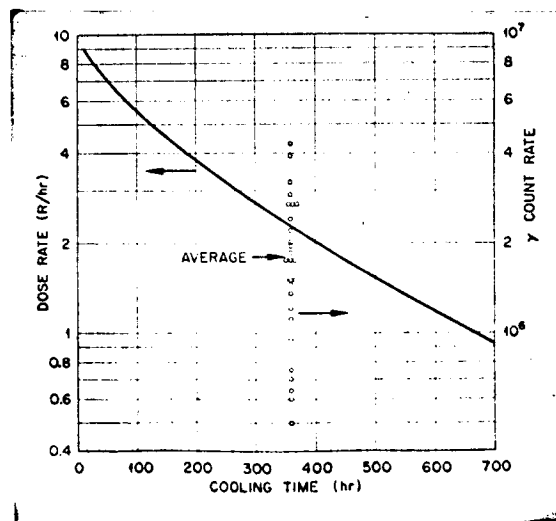
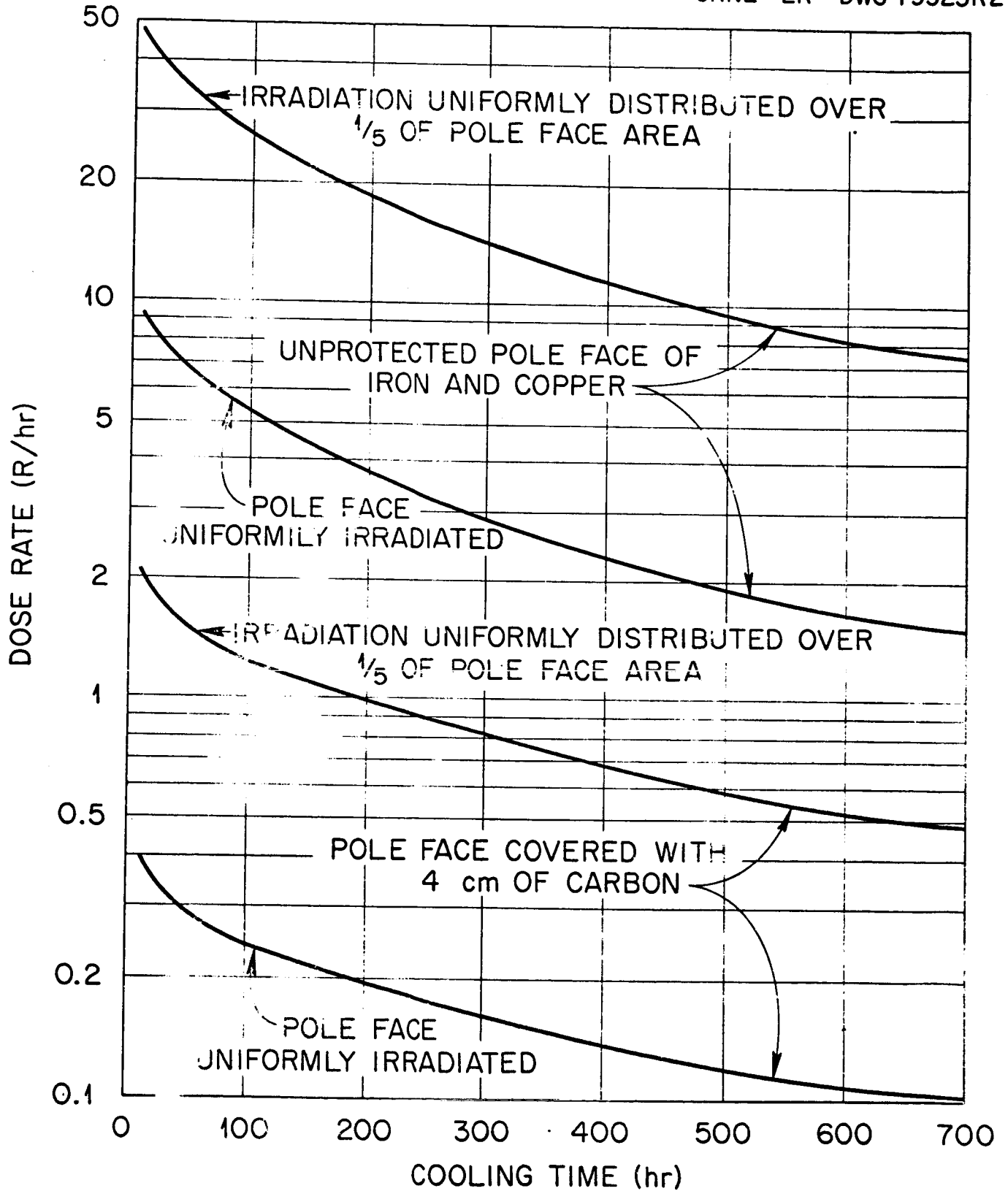


Figure 6 - Residual radiation levels in CERN Synchro-Cyclotron gap. Solid curve is calculated. The experimental points were measured 15 days after cyclotron shutdown. For the detector used, 10^6 counts/sec of 0.5 MeV gammas corresponds to ~ 1 R/hr.

Figure 7 - Calculated residual radiation levels in the Mc² Cyclotron after 1000 hr operation with 10 μ A of protons being scattered into the pole faces by the beam extraction apparatus.

UNCLASSIFIED

ORNL-LR-DWG 79525R2



N64-28164

ENGINEERING DESIGN
OF THE SPACE RADIATION EFFECTS LABORATORY*

W. M. Brobeck
Brobeck Associates

Requirements

The requirements which determined the general design of the SREL are the following:

1. The availability of proton beams from 20 MeV to 600 MeV.
2. The availability of electron beams from $\frac{1}{2}$ MeV to 10 MeV.
3. The ability to bombard targets up to one foot square in area with these beams, either simultaneously or separately.
4. Primary beam currents within the capability of existing FM cyclotrons and electron accelerators.
5. Reduced energy proton beams of 10^{10} particles per second above 70 MeV and 10^9 particles per second below 70 MeV.
6. The ability to change space irradiation targets with a minimum of down time.
7. Provision for the future use of the accelerators in scientific research.

Selection of the Accelerators

As the high-energy proton beam is the most expensive to produce, a most important problem was the selection of a cyclotron design. As the current

*Under Contract NAS1-1947 for the National Aeronautics and Space Administration

output of existing machines was adequate and as time was limited, there appeared to be good reason to copy the design of an existing machine. Three such machines meet the energy requirements--those at Berkeley (730 MeV), Dubna (680 MeV), and CERN (600 MeV). The CERN design was selected for a number of reasons. It was the smallest machine that met the energy requirement; it was built largely by commercial fabricators, in particular the radio-frequency system was available commercially; and it performed well. The CERN laboratory offered its complete cooperation in our copying their design.

The electron acceleration requirements were met by the provision of two commercially available machines. For the range from $\frac{1}{2}$ MeV to 3 MeV, a "Dynamitron" manufactured by Radiation Dynamics, Inc. is provided. This is a DC machine using a voltage-multiplying circuit driven through capacity coupling from an RF supply at ground potential. For the range of 3 MeV to 10 MeV, a microwave linear accelerator manufactured by the ARCO division of High Voltage Engineering Corporation is used.

Production of Variable Energy Proton Beams

The production of the reduced energy proton beam was a problem less easily solved than the selection of the cyclotron. It was determined that a combination of degrading and extraction from an intermediate energy would cover the range from 600 MeV to 50 MeV with acceptable intensity and energy spread. Below 50 MeV, no solution other than the provision of a separate small cyclotron has been found. For the present, this second cyclotron is not included in the project. Other papers to be presented during this meeting will describe the extraction, degrading, and beam transport systems.

The Building

The arrangement of the building was intended to provide maximum flexibility in the experimental areas and to shield the neutron radiation by means of walls

located close to the targets rather than by the use of distance. The first increment of the building is shown in Figure 1. The location of the cyclotron and the two electron accelerators can be seen. Two separately shielded space-irradiation target rooms are provided, one of which is used for both electron and proton irradiation. The building has a total of 55,000 square feet of floor area. It includes a high bay area approximately 140 feet by 240 feet, and a two-story support building having about 28,000 square feet of floor space. The high bay area is served by a crane having two 25-ton hooks.

As permanent shielding is less expensive than movable blocks, the cyclotron cave itself is surrounded on three sides by permanent walls, and a single long wall is extended to the north. The thicknesses of these walls vary from 16 feet to 24 feet. The electron accelerator rooms and the irradiation target rooms are shielded by concrete blocks. Ordinary concrete is used except for the west shielding wall which is high density concrete. Horizontally moving doors which may be relocated are used for the rooms shielded by blocks, and vertically moving doors which descend into a pit below the floor level are used for the cyclotron cave. The roof shield over the cyclotron and proton areas consists of 8 feet of ordinary concrete. The total volume of shielding is about 11,000 cubic yards of which 7000 are in movable blocks. Dr. Burton Moyer assisted in the design of the shielding.

The beam centerline is $4\frac{1}{2}$ feet above the floor. The ceiling height in the experimental and electron accelerator rooms is 10 feet, and in the cyclotron room it is 16 feet.

The support building includes a utility section and a combined accelerator control and data room, with the remaining area used for offices, small laboratories, and shops. All power supplies, except the power supply for the cyclotron magnet, are housed in the utility section. A total of 2300 kilowatts

of DC power is supplied to the magnets. The total electrical load capacity of the building is 6000 kilovolt-amperes.

Beam Transport Systems

Proton beams must be transported a total of approximately 230 feet and electron beams approximately 90 feet. The proton transport system conducts protons to either of the two proton target areas. The system has an aperture of 8 inches diameter and includes a variable degrader as a permanent feature.

The electron transport system permits conducting the beam from either electron accelerator to a target in the accelerator room and to the combined target area where the electron and proton beams can be brought into the same line.

Provision for Scientific Use

The CERN cyclotron design provides for the emission of proton and neutron beams from opposite sides of the magnet. Taking advantage of this feature, the building is divided into three areas--the space-irradiation area to the northwest, the neutron-meson area to the south, and the experimental proton area to the east. The space-irradiation area is included in the present construction contract, and the neutron-meson area is presently being planned. These areas are shown in Figure 2. The neutron-meson area is similar to that at CERN. The shield wall between this area and the cyclotron will be of iron for the first ten feet above the floor. The wall is formed of blocks designed to be handled by the overhead crane. Provision will be made for neutron and pi meson beams to pass through the wall, as well as for the mu meson channel similar to that at CERN.

To reduce the scattered neutrons in the room, a minimum of shielding material will be used inside the building. Primary neutron beams will be stopped in an earth bank outside the building. An external earth backstop

is practical in this case due to the good collimation of the primary neutron beam. No roof shielding is required over this area.

The data room for the neutron-meson area is located against the west wall as shown in the slide. It is shielded from scattered neutrons by a wall of ordinary concrete blocks. Control and instrument wiring is distributed in ducts around the walls of the experimental area and to overhead terminal boxes in the data room. Built-in controls and instruments are held to a minimum. Additional wiring can be added in the wireways without disturbing the wires already installed. Fifteen circuits providing a total of 2900 kilowatts of DC magnet power and corresponding water-cooling service are distributed through the neutron-meson room.

The proton experimental area shown in Figure 3 has not been authorized yet and exists as a preliminary design only. The plan is to provide a well-shielded area for the primary proton beam adjacent to a less heavily shielded area in which reaction products can be observed. The location of the proton area beyond the east shield would permit its construction while the rest of the facility is in use. This figure also shows a possible location for a 50 MeV cyclotron.

Three sides of the building face unobstructed outdoor areas into which beams can be brought if long flight paths are required. The building can be extended to the north, east, or south if this should be necessary. In general, it is felt that this facility provides an unusual degree of flexibility and freedom from physical restraints on future experimental work.

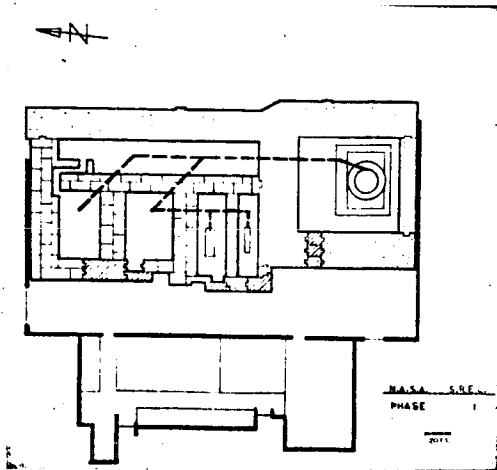


Figure 1 - Plan layout of SREL facility showing Phase I area.

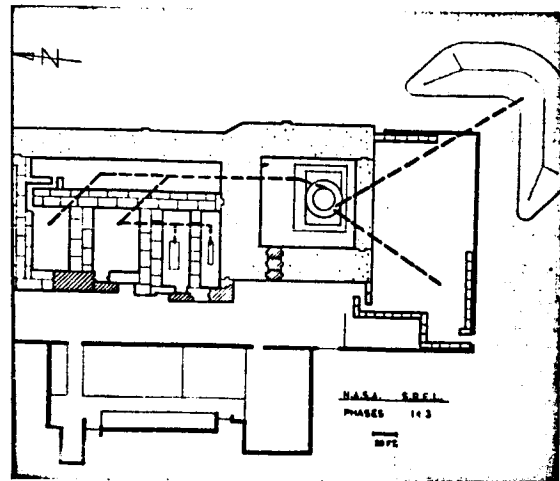


Figure 2 - Plan layout of SREL facility showing neutron-meson experimental area.

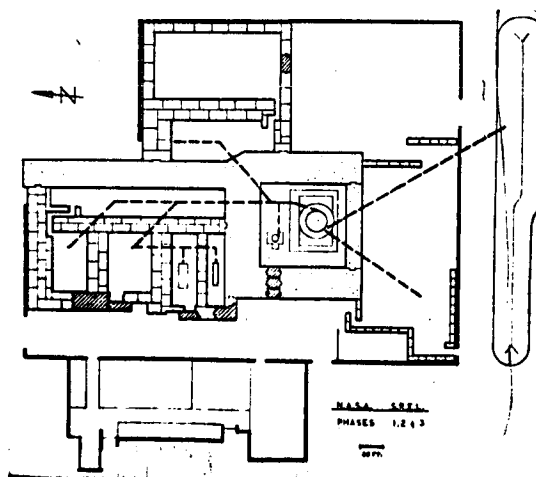


Figure 3 - Plan layout of SREL facility showing additional proton experimental area.

N64-28165

THE USE OF MULTIPLE DEES IN THE FM CYCLOTRON

W. M. Brobeck
Brobeck Associates

The possible advantages that encourage investigation of the use of multiple dees are:

1. The possibility of an increase in the beam current proportional to the number of dees.
2. The possibility of eliminating the moving parts inherent in mechanical frequency modulation.

The first advantage arises from the fact that a number of bunches of ions equal to half the number of dees are simultaneously accelerated. These bunches are separated widely enough so that each would be independent of the other and no space charge limitation on the number of bunches would apply. As the central dee could have the same voltage applied to it that would be used on a single dee of the conventional machine, it is reasonable to expect that each starting bunch would have the same charge as in the conventional machine. The losses during acceleration are not quite as easy to compare. However, there is good reason to expect no greater loss in acceleration through a series of dees than with a single dee if the starting dee voltage were maintained. If this were found to be true, the output would be proportional to the number of bunches accelerated per second and, hence, to the number of dees.

The possibility of eliminating moving parts arises from the fact that the frequency range and the capacity to ground of each dee can be considerably

reduced below that of a single dee. The corresponding reduction in volt-amperes per dee may make possible "broad band" dee systems driven off-resonance to vary the frequency.

The disadvantage of multiple dees is primarily the complication of the many separately excited dee systems. Furthermore, if mechanical tuning is not used, there is a problem in holding down the radio-frequency power or volt-amperes to keep the cost of the radio-frequency system within reason. As Dr. Crowe has pointed out, the disadvantage of the radioactivity produced by increased beam current may be avoided by limiting the beam near the source to control the amplitude of radial oscillation and by taking the improvement in increased extraction efficiency.

The configuration of a ten-dee system and the accelerating conditions are illustrated by the following figures.

Figure 1 shows the relative proportions of a set of ten dees based on the same ratio of maximum-to-minimum frequency for each. In practice, the outer dees would be designed to subtend less than 180 degrees to reduce their capacity. Another variation would be to place alternate dees on opposite sides of the pole face. Although this might involve a problem of interference with the extraction system, it would considerably reduce the capacity of each dee to its neighbors and hence reduce the power required.

Figure 2 illustrates the passage of the bunches successively through the dees. When the ions cross a gap, the dees on each side of the gap are driven in phase while the voltage is gradually reduced on one and increased on the other. There is reason to expect that the motion of the ions would be unaffected by their passing from one dee to the next. The effect of changes in accelerating force during the radial oscillations, which have an amplitude comparable to the radial dee gap, should be unimportant as their frequency

is so much greater than that of the phase oscillation. From the standpoint of the phase motion, only the average position of the ion is important. Electrostatic focusing forces at the dee edges are negligible compared to the magnetic focusing existing.

This figure also shows why there are half as many bunches as dees. Because ions are being accelerated only half of the time in the conventional FM cyclotron, the output of the multidee system, relative to that of the single dee machine, is proportional to the number of dees.

Figure 3 shows the frequency program of the dees. Each dee is successively switched from one to another of a series of oscillators. As shown, there are ten oscillators for ten dees. Five of the oscillators are in use at one time. Switching of the oscillators permits driving two dees from one oscillator during the time that the ions cross from one dee to the other, and so holding the voltage the same on adjacent dees as the ions cross the radial gap.

Calculations have been made for the radio-frequency power required with the use of ten dees in a cyclotron of the CERN design. The Q was taken as $2.0 (f / \Delta f)$, where Δf is the frequency range of the dee. This was based on the relation $Q = 2.5 (f / \Delta f)$, derived by Ferger and Susini in CERN Report 60-41, with an allowance for frequency overlap of the dees. The RF power is calculated as ω / Q times the energy stored in the dee capacities. The peak dee voltage was taken as 20 kilovolts peak-to-ground. With the dees all on one side of the pole as shown in the slide, the maximum RF power came out to be 3300 kilowatts. With alternate dees on opposite sides of the pole, the calculated peak power is 1100 kilowatts. The average power would be about half of the peak power. A reduction of dee voltage would, of course, reduce the power, but at the expense of loss in output.

In general, it appears that a multidee system is a feasible method of increasing the output of a synchrocyclotron. Further study based on an actual design for the radio-frequency system seems justified.

Acknowledgments

I wish to thank Mr. Robert Thomas and Mr. Thomas Mongan for their assistance in preparing this paper.

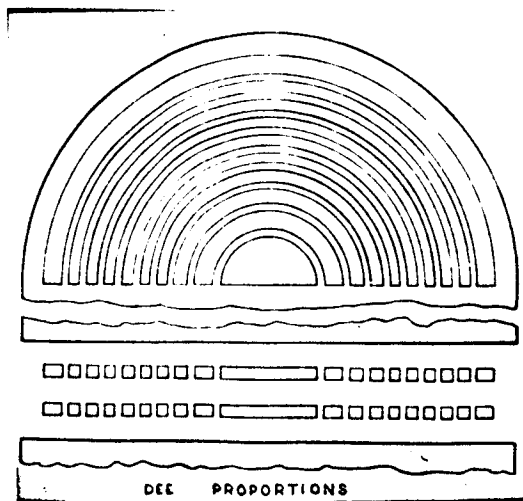


Figure 1 - Positions of the set of 10 dees based on the same ratio of max.-min. frequency for each.

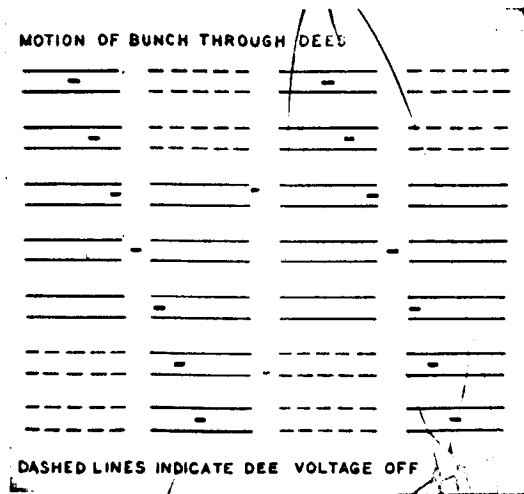


Figure 2 - Passes of bunches successively through the dees.

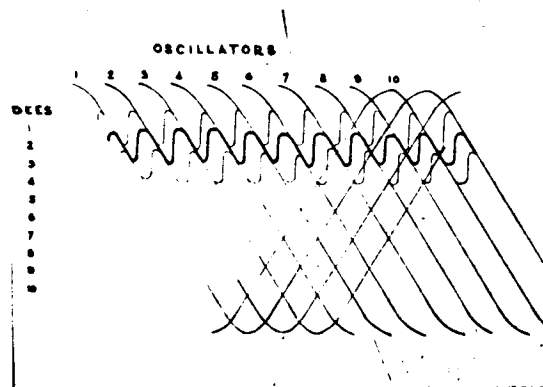


Figure 3 - Dee frequency programs.

N64-28166

BEAM TRANSPORT SYSTEM FOR THE NASA 600 MEV SYNCHROCYCLOTRON*

R. F. Nissen
Brobeck Associates

The proton beam transport system will be handling primary proton beams with energies of 600 and 300 MeV and degraded beams with energies as low as 20 MeV. Although the synchrocyclotron is essentially a copy of a 600 MeV synchrocyclotron at CERN, the beam transport system was designed specifically for the NASA installation.

Figure 1 displays the layout of the magnets and the associated hardware. The beam transport system has two branches. Both branches are identical, and only one is shown.

The magnet, M1, just outside the machine is a steering magnet which serves to direct the beam down the beam tube. It is necessary because extraction may take place at either 600 MeV or 300 MeV, and the beam does not leave the machine at the same angle in each case. Actually, the magnetic channels in the machine are designed so that the extraction orbits at the different energies intersect at the center of magnet M1.

After the degrader, the beam is bent 45 degrees in order to eliminate particles and gamma rays originating in the degrader.

The beam is monitored for cross-sectional shape and intensity at three points between the synchrocyclotron and the target. The first point is just after leaving the machine, the second point is right before the degrader, and the last point is slightly ahead of the target.

*Under Contract NAS1-1947 for the National Aeronautics and Space Administration

Finally, there are vertical and horizontal collimating slits a little way upstream from the targets. The beam optics are such that the horizontal and vertical dimensions of the beam at the collimator correspond to the dimensions of the beam at the target. Since the collimator setting can be read and adjusted from the control room, the size of the beam spot on the target can be determined without monitoring the beam at the target.

In Figure 2 the ray diagrams show the degraded beam from the synchro-cyclotron to the target. The phase-space diagrams show the radial and angular acceptance of the beam transport system.

Only the ray diagram for the nominal energy is shown on this slide. The off-energy ray diagrams and phase-space diagrams look fairly similar even though the beam spot accepted by the beam transport system moves off axis in the horizontal plane. The spot size on the target remains essentially the same.

The degrader effectively splits the beam transport system into two sections. The first section focuses the beam emerging from the synchro-cyclotron onto the degrader; the second section transports the degraded beam from the degrader to the target. As the beam goes through the degrader, it is magnified considerably, both in the horizontal and vertical planes.

For the first section, an effort was made to image the emerging synchro-cyclotron beam spot onto the degrader. Actually, the beam spot on the degrader ended up a little smaller than the emergent spot.

The second part of the system was designed primarily to transport the degraded beam with minimum loss rather than to focus the beam. The exit face of the degrader was regarded as the source, rather than the crossover, due to the large angular deflection of the beam as it is being degraded.

For the same reason, the degrader was moved as close to the first quad as possible, the limiting factor being this quad's ability to focus the beam.

As a result of these design considerations, we get the maximum intensity at the target, but a rather large image.

Each bending of the beam is accomplished with two bending magnets and one quadrupole pair. The reason for using a quadrupole pair between the bending magnets instead of the horizontally focusing singlet normally used is that the source is a large diffuse spot, and the single quad would give such a large vertical magnification that most of the beam would be lost.

The first single quad is placed where the horizontal beam is very small and would, therefore, be practically unaffected, while the vertical beam is large. It is then possible to adjust the vertical beam independently of the horizontal beam to get the maximum use out of the last three quadrupoles. These three quads work as a rather assymetrical triplet.

Looking now at the horizontal and vertical phase-space diagrams at the degrader, we see that the shaded area is the phase-space accepted from the degrader and carried to the target.

These areas were obtained by a computer program entitled OPTIK, written by Thomas J. Devlin of the University of California Lawrence Radiation Laboratory, and described in UCRL-9727.

The lines shown represent the limiting magnet apertures in phase-space projected back along the beam onto the source.

The degrader is used to reduce the primary beam energy from 600 or 300 MeV to the energy desired for a particular experiment. The reduction is accomplished by multiple scattering of the beam particles in the coulomb field of the atomic nuclei in the copper block. For the calculations of beam intensity, all beam particles making elastic or inelastic nuclear collisions

were considered to be lost. Figure 3 shows the value of the beam intensity in protons per second at the target for beams degraded from 600 MeV to 300 MeV and from 300 MeV to 20 MeV.

Figure 4 shows curves exhibiting the change in angular divergence of the beam emerging from the degrader as it changes its energy from 600 MeV to 300 MeV, or from 300 MeV to 20 MeV.

Figure 5 shows the radial growth of the beam emerging from the degrader when the energy is changed from 600 MeV to 300 MeV, or from 300 MeV to 20 MeV.

These curves were calculated using methods suggested by Dr. Burton Moyer, Lawrence Radiation Laboratory, Berkeley, and by using a computer program, INTENS, developed by Mr. C. Hoard, William M. Brobeck and Associates. INTENS computes the intensity of the beam at the target by weighting and measuring the areas of the phase-space diagrams.

When the degrader is not being used, the situation looks a little brighter. The violent magnification caused by the degrader is absent, and it is possible, by adjusting the triplet at the end of the beam transport system, to focus the beam and obtain a small beam spot on the target as shown in Figure 6.

The phase-space of the beam emitted by the CERN machine, of which this machine is a copy, is included in the phase-space diagrams for comparison. This ray diagram shows the nominal energy only.

Figure 7 shows ray paths for the off-energy beam. The beam is focused to the approximate size of the correct energy beam and is fairly well centered on the axis at the target. The beam shown is one per cent off the nominal energy. This is the approximate maximum energy divergence of the CERN cyclotron beam and, hopefully, the NASA cyclotron will not exceed that.

In conclusion, I feel that the system has achieved the design objectives of maximum beam intensity on the target at all energies.

I gratefully acknowledge the assistance of Dr. Burton Moyer, Dr. Kenneth Crowe, Norman E. Jorgensen, and Edward L. Prichard on this project.

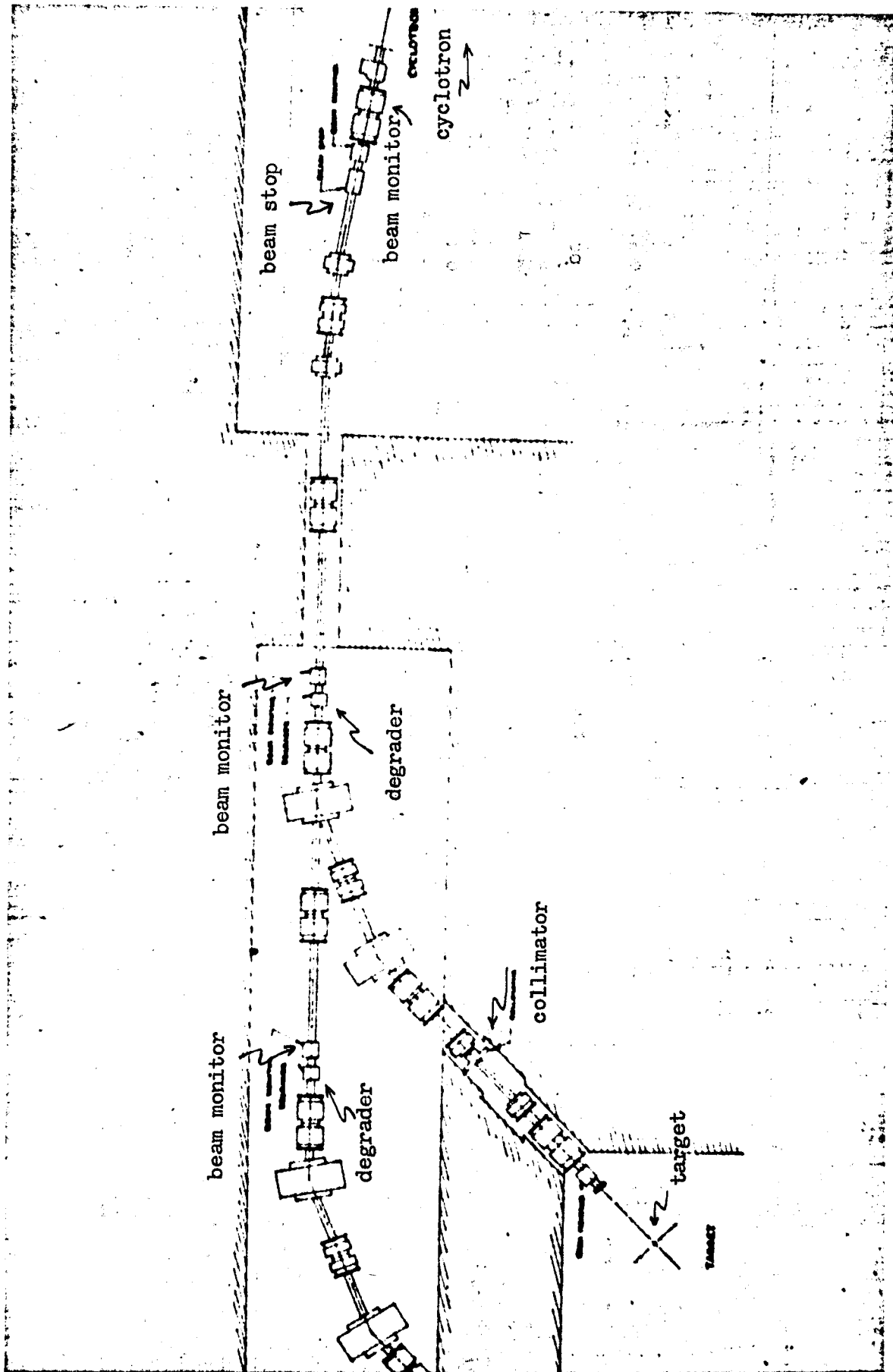


Figure 1 - Magnet layout for SREL beam transport system.

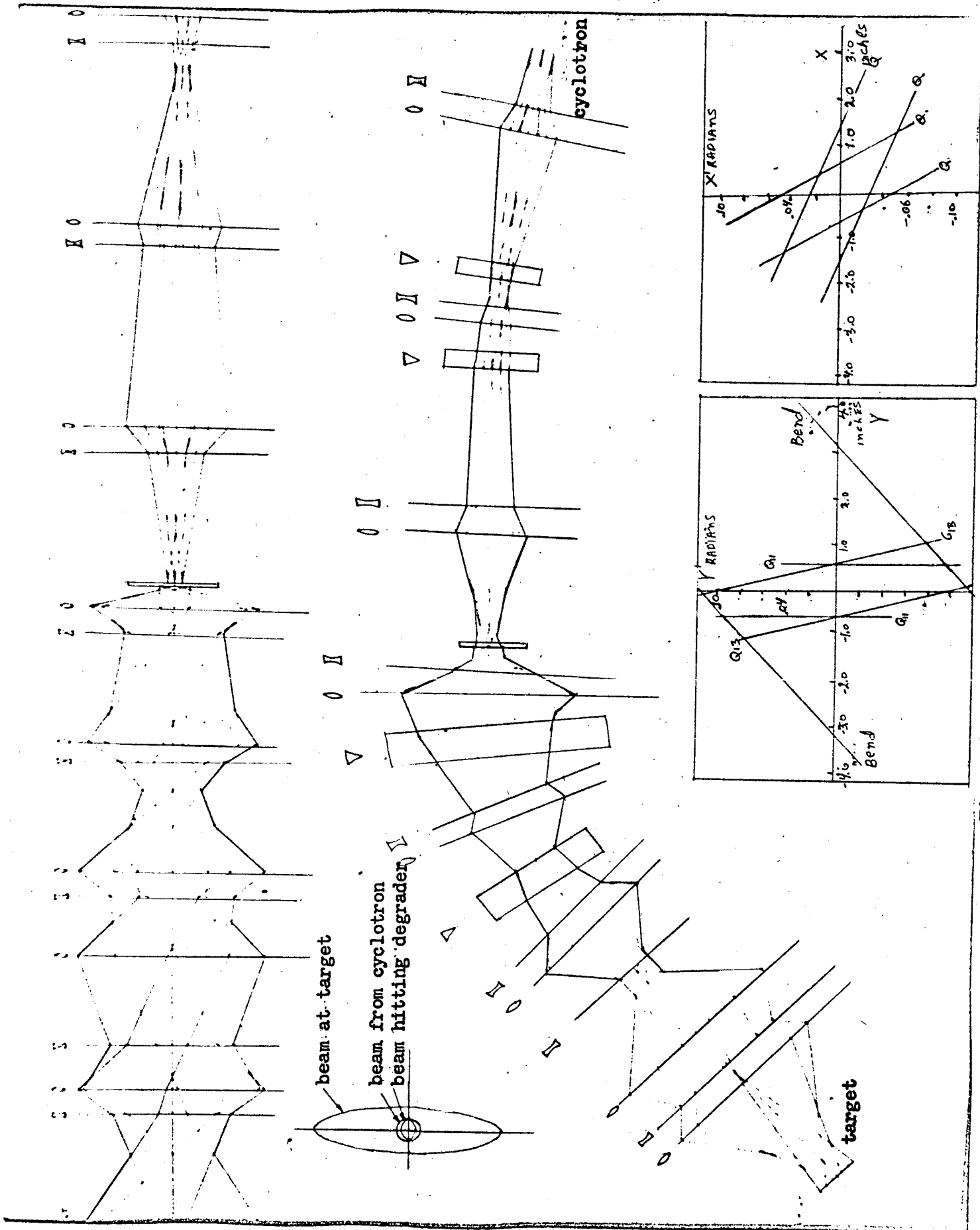
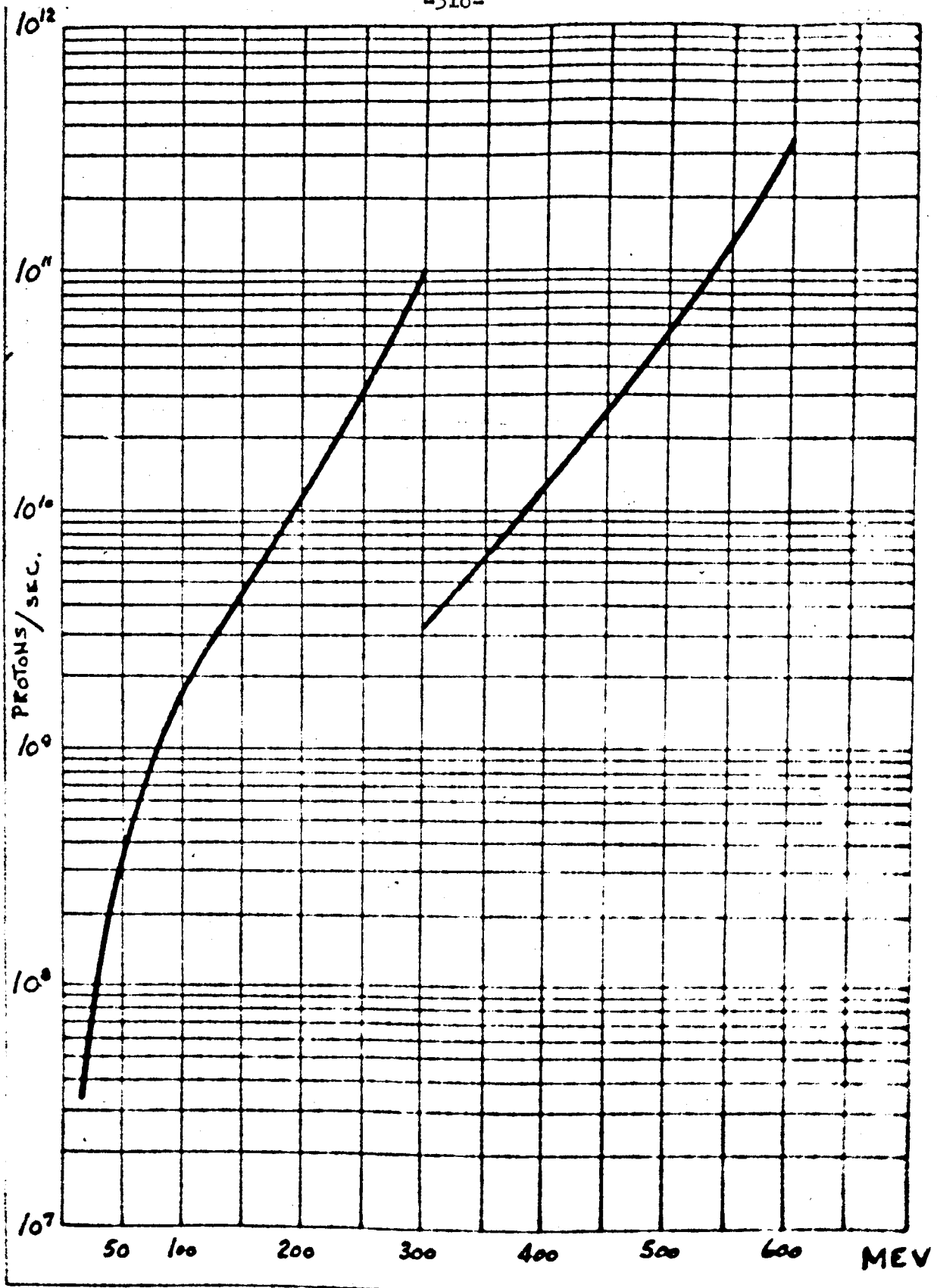


Figure 2 - Degraded beam ray envelope diagrams.



BEAM INTENSITY AT TARGET

Figure 3 - Beam intensity in protons/sec. at target or beam energy.

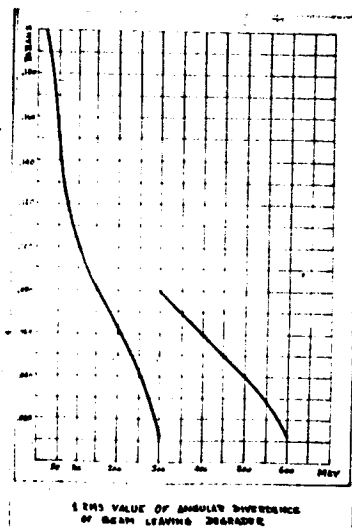


Figure 4 - Angular divergence in radians of beam emerging from degrader as a function of energy.

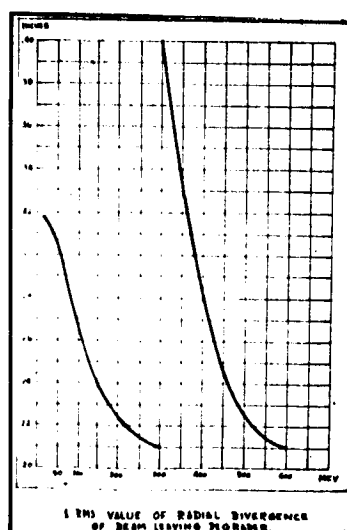


Figure 5 - Radial divergence in inches of beam leaving degrader as a function of energy.

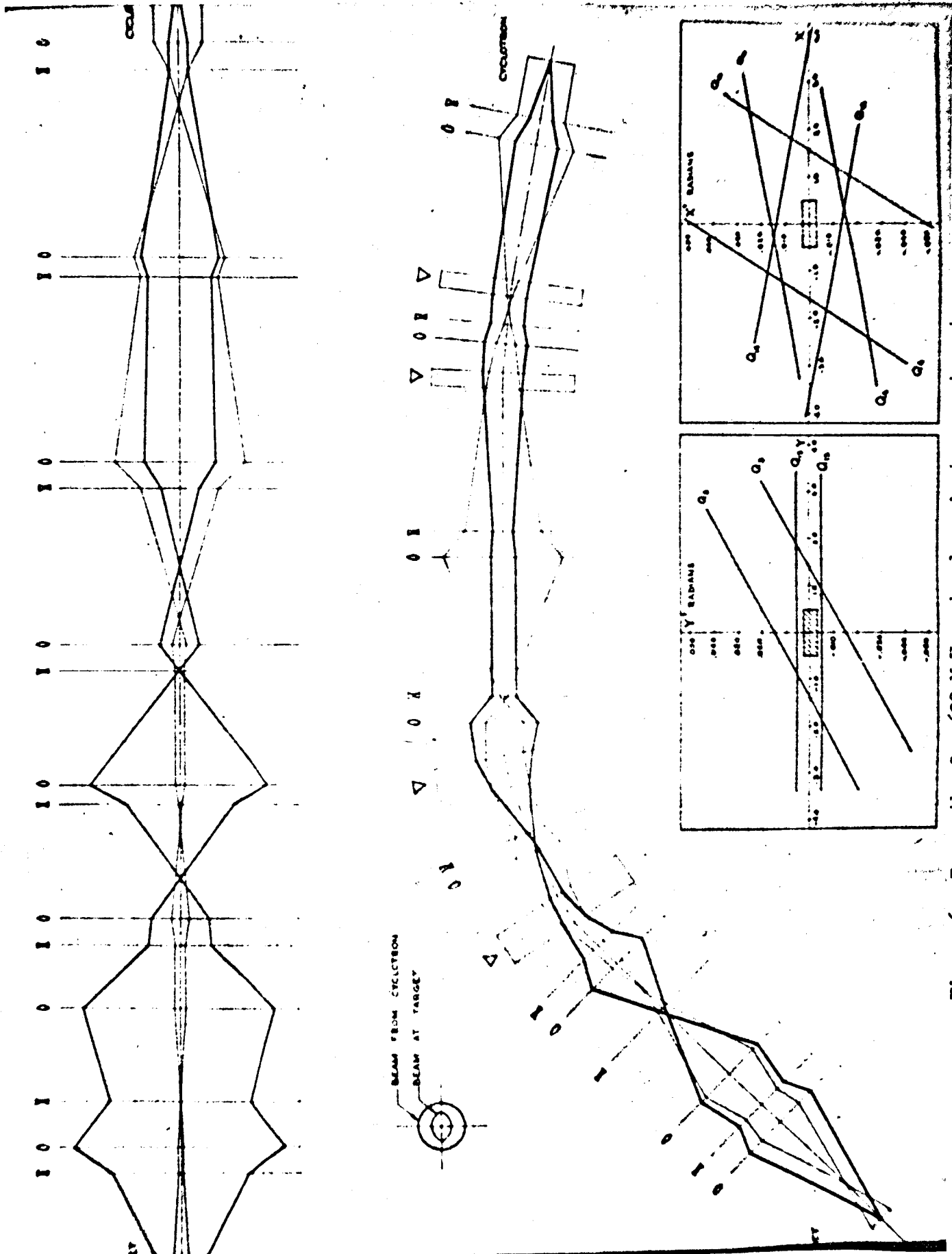


Figure 6 - Ray paths for 600 MeV proton beam in transport system (no degrader).

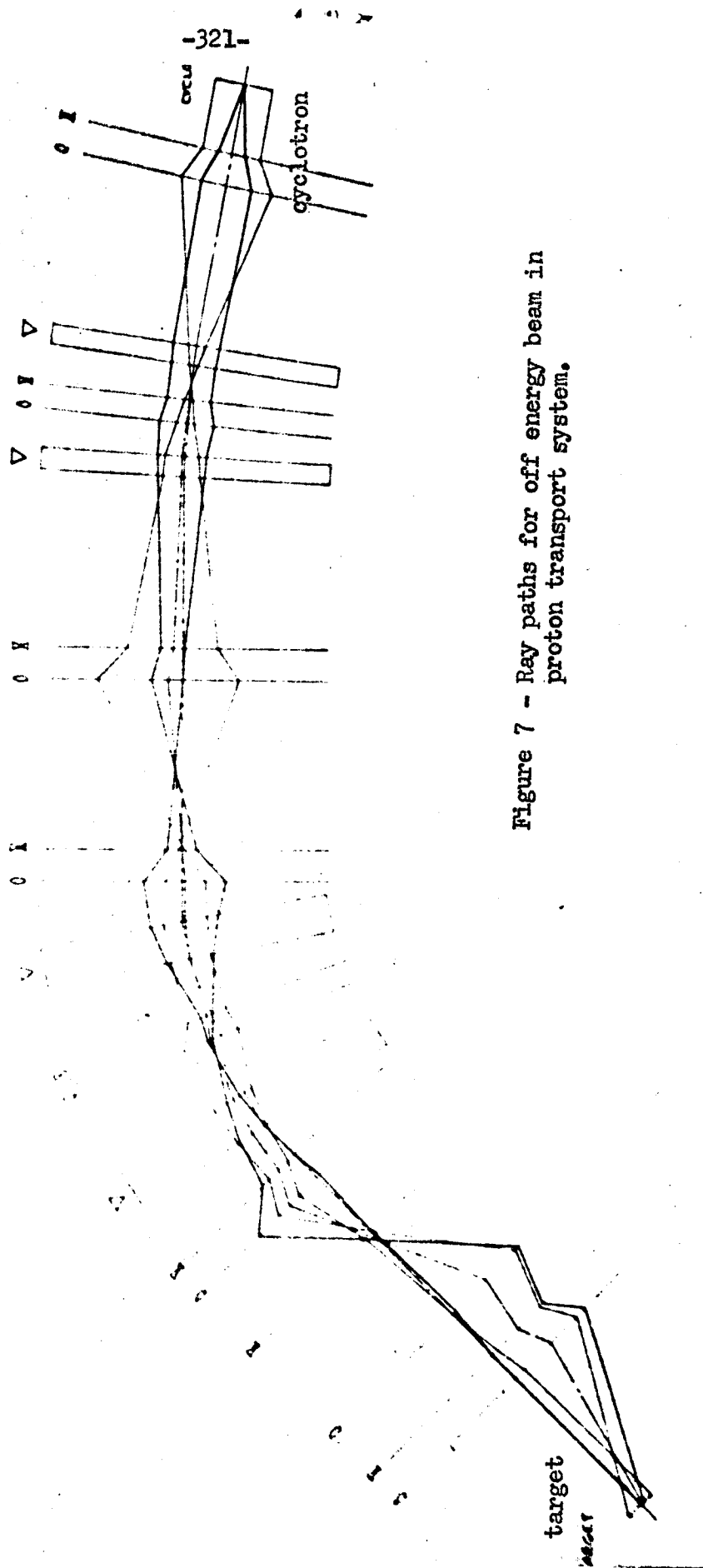
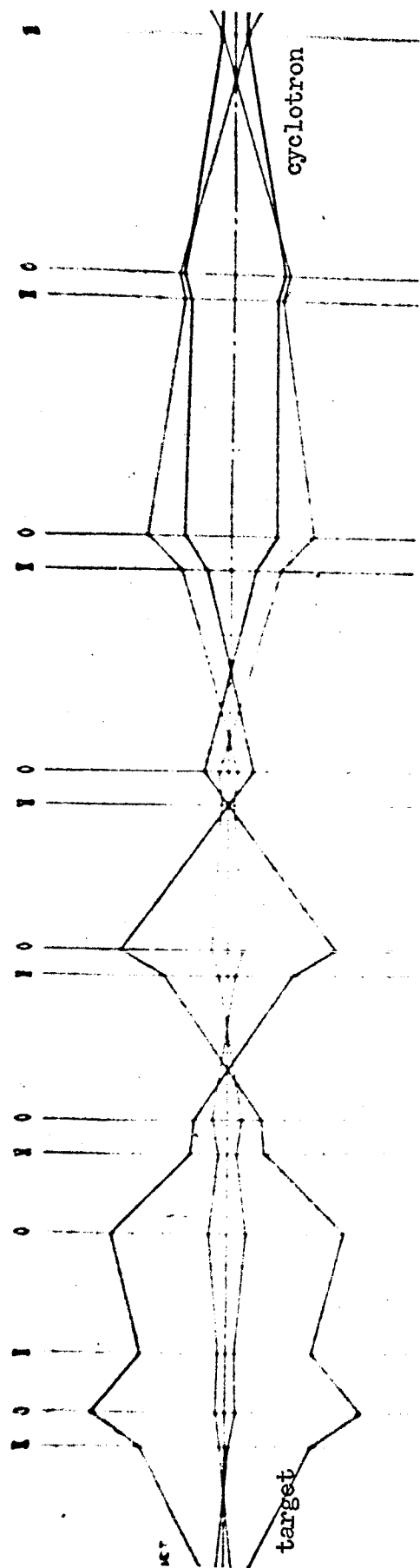


Figure 7 - Ray paths for off energy beam in proton transport system.

MOORE, McGill - How much of your beam is lost through the transport system?

NISSEN - We feel that 100% of the undegraded beam reaches the target.

THE DESIGN OF A 300 MEV EXTRACTION SYSTEM

for the

NASA, SREL SYNCHROCYCLOTRON*

N64-28167

J. R. Mulady
Brobeck Associates

The SREL synchrocyclotron is to be an exact copy of the CERN synchrocyclotron, except for the provision of external beams of less than full energy. Proton energies in the range of 50 MeV to 600 MeV and their effects on experimental equipment in space are of particular interest to the group at Langley Field. In order that these effects might be studied in detail, it is felt that external proton beams with intensities of the order of 10^{10} protons per second and energy spreads of less than plus or minus five per cent should be provided by the SREL accelerator over this range of energies.

Several methods of obtaining reduced-energy beams were considered. These included: reduced conventional field, reduced azimuthally varying field, decreased radius of deflection, and degrading beam energy. Analyses of each method were compared with regard to energy range, attenuation, degree of modification to the existing CERN design, effect on schedule, cost, and operating experience. On the basis of these analyses, it appeared that the most feasible method of obtaining variable energy beams would be by a combination of the extraction of two primary beams, one of full energy, and one of reduced energy from a reduced radius, and the degrading of these beams to the required intermediate energies.

*Under Contract NAS1-1947 for the National Aeronautics and Space Administration.

Extraction from much reduced radius has never previously been attempted to our knowledge. However, the theoretical analysis of extraction well inside the pole edge has been made and extraction from the linear portion of the field has been accomplished with several synchrocyclotrons. Thus, there is no question of any fundamental problems arising.

The choice of 300 MeV for the second of the primary beams was dictated mainly by limitations on the reduction in ambient field that can be obtained in the magnetic channel which conducts the extracted beam to the pole edge. This channel must be compensated so as not to seriously affect the circulating beam before it can be deflected into the channel entrance. If the walls of the channel are made thick so as to provide more shielding, the rate of increase in the field reduction obtained between them decreases rapidly because the additional iron is added at a greater distance from the region of interest. However, the amount of compensation required rises rapidly, as the added iron is closer to the circulating beam. This situation is particularly acute for the entrance sections which are at the smallest radius, and thus are closest to the circulating beam. The problem is further complicated by the need for gradient focusing which reduces the amount of shielding that can be realized. Calculations indicated that three to four kilogauss reduction in ambient field is the maximum that can be reasonably obtained in the first few sections of the channel, and no more than six kilogauss can be obtained over the remainder of the channel. These values, when applied to the lowest average value of field obtainable in the synchrocyclotron without loss of linearity over the region of interest, indicate that extraction from any radius smaller than about 60 inches is too uncertain to base a theoretical design on. This radius corresponds to an energy of about 300 MeV.

Calculations were then made of the intensities that can be expected if this energy were chosen. (See Figure 1)

The intensity of the circulating beam at any reduced radius is at least as great as at full radius as all full energy beam must pass through the lower radius during acceleration. Thus, there is no fundamental reason for the intensity of the beam extracted at lower energies being less than that of the beam extracted at full energy. However, the state of development of full energy extractors is certainly more advanced than that of any reduced-energy-extractor which might be used. Accordingly, a factor of three reduction has been used in estimating the intensity of the 300 MeV extracted beam in the results shown in this figure. As can be seen, intensities fall slightly below the desired values in some regions. Extraction at 300 MeV thus appears to be a good compromise.

Peeler-Regenerator System

The peeler-regenerator scheme of beam deflection was first proposed in 1950 by J. L. Tuck and L. C. Teng (Ref. 1) and first applied by them on the University of Chicago Synchrocyclotron. In 1951, K. J. LeCouteur (Ref. 2) at the University of Liverpool developed the solution for linear fields and described the conditions required for vertical stability. K. J. LeCouteur and S. Lipton (Ref. 3) later extended the solutions to the case of nonlinear fields where the peeler is replaced by the natural fall-off of field with radius. The CERN 600 MeV extraction system is an example of this latter type of system.

The linear field deflection system consists of two elements (see Figure 2): the peeler, a region of field which decreases with increasing radius; and a regenerator, a region in which the field increases in strength with increasing radius. These two regions of modified field together

increase the amplitude of the natural radial oscillation and stop the precession of the center of rotation of the particles about the center of the accelerator, causing the maximum amplitude of the radial oscillation to occur repeatedly at one azimuth. If this radial gain per turn is made large enough, and if vertical "blow-up" does not occur, the particles can be made to step over the inner wall of the channel. Once in the channel, they are partially shielded from the magnetic field of the cyclotron and are conducted out of the cyclotron and into a beam transport system.

The choice of deflector lengths and position was first made on the basis of calculations which followed in detail the first order linear approximations given by LeCouteur. The strength of the regenerator required was calculated to be about 734 gauss per inch for an effective angular distance of 15 degrees, and the peeler, of similar angular length, to be minus 468 gauss per inch. The angle between them turns out to be about 60 degrees. (Variations in these parameters were made later for reasons to be described.)

Although it was felt that the solutions obtained using the formulas of LeCouteur were correct, a series of drawings were made to provide additional confidence, as well as a better feeling for the action of the peeler-regenerator deflector. The first graphical analyses were done assuming the field index to be zero. In the CERN synchrocyclotron, the actual index of field, n , is about 0.03 in the region of this deflector. This is certainly close enough to zero to contribute only a very small error to the analysis.

A particle of correct energy and radius was then traced step-by-step through its last four or so turns in the deflector. After several false starts, a very satisfactory picture of the action of the deflector on the

particle was obtained. The phase angles and the radial growth of the induced oscillation were studied in detail by this method and were found to agree very closely with the results calculated by the methods of LeCouteur.

The graphical analysis of the 300 MeV system was later repeated, assuming a gradient field of the proper value and taking into consideration the precession of the center of rotation of the particles before deflection. Again, the results agreed within the errors due to pencil line widths. All of these graphical analyses were made at one-quarter scale.

As an additional check on our methods, a graphical analysis was made of the Liverpool deflector system as it is described by A. V. Crewe and J. W. G. Gregory (Ref. 4). The results were better than could be reasonably expected, and the positions of the minimum and maximum radial oscillation amplitude and the position of the virtual image were found to agree with those reported in detail.

The deflection system was further checked by use of the "Optic" program which has been described in the paper by Nissen on the beam transport system.

Iron Calculations

The field between two uniformly and axially magnetized iron bars can be calculated if it is assumed that the field is due only to effective poles at their ends. We can write the field due to the surface charges of element dA (assuming the bars to be infinitely long):

$$dH = \frac{k \cdot \sigma \cdot dA}{z^2} \cos \theta$$

We can then integrate over the rectangular poles and obtain the gap field as:

$$H = 8k\sigma \tan^{-1} \left[\frac{\tan^2 \theta_y \cdot \tan^2 \theta_x}{1 + \tan^2 \theta_y + \tan^2 \theta_x} \right]^{1/2}$$

For saturated iron, $8k\sigma \simeq 13,600$ gauss.

In order that the effect of one or more blocks, which are situated symmetrically about the median plane of the magnet of the cyclotron, might be easily calculated, a computer program we call CP-20 was written for the IBM 7094.

The physical system calculated in this program is shown in Figure 3. The computer program represents each block by sets of dipoles, at positions corresponding to the upper and lower surfaces of the block. Each block within the magnet gap gives rise to an infinite sequence of images in the iron of the pole tip. The effective strength of these images is a function of the incremental permeability of the pole tip iron. If the poles become completely saturated ($\mu = 1$), the effective strength of these images is zero. Only the first two pairs of these images are considered in the program. In the interest of conservative design, the incremental permeability of the pole tip iron has been taken to be 100.

For these calculations, it was assumed that the bars are of infinite length, which is certainly fair for all except the very end sections of the channel. For the calculation of the end effects, at the channel entrance, the peeler region, and the regenerator region, computations were made by hand.

Blocks positioned as shown in the slide act to increase the magnetic flux density between them. Blocks such as this form the basis for the regenerator. The same program is used to calculate the effect of single blocks, such as are used to form the peeler and the channel walls by making the gap between a pair of blocks equal to zero.

The required shapes of the regenerator, peeler, channel, and compensation iron were determined by a sort of jigsaw puzzle method. A large number of sizes of blocks were analyzed by the computer which produced their effects at 0.1-inch increments along the median plane. These blocks were then stacked together on paper until the desired field shape was obtained. This was a tedious and time-consuming process, especially in the light of the great number of iron sections required for this system. However, it seemed to provide the only really feasible method of accomplishing the design.

Channel Optics

The beam optics for the magnetic channel were calculated by use of the "Optic" computer program mentioned earlier. The requirements on the channel were that its entrance occur about four and one half inches beyond the equilibrium radius (radius at which deflection begins) and that it conduct the beam out of the vacuum tank through the existing proton beam window. The angular extent of the channel cannot exceed 180 degrees as there is not room between the dees for a channel. These requirements were fulfilled by a channel in which the radius of curvature of the beam has only two values. The first 60 inches of the channel provide a shielding of about 3.5 kilogauss, and thus a radius of curvature of about 73 inches. The last 180 inches of channel length provide an average shielding of about 5.8 kilogauss, and thus the beam radius is about 86.5 inches in these sections.

The channel was broken up into 30 sections, each about eight inches long. These were then treated by the program as bending magnets. Many computer runs were required to develop a design which provides the required beam focusing without unobtainable field gradients. The present channel is relatively weak-focusing, in that it provides only one cross-over point in each plane. The gradients in the channel alternate and vary between 200 gauss per inch and 700 gauss per inch. A radial gradient exists in only about one half of the 30 sections.

The aperture of the channel was made as large as was consistent with the required field reduction and compensation. The entrance aperture is nominally one inch in the horizontal plane and three inches in the vertical direction. The passage through the channel widens out to about 1.2 inches beyond the peeler region, to 1.4 inches near the regenerator, and to 1.6 inches at the exit, in the horizontal direction. The vertical aperture increases to four inches over the last half of the channel length. Because of the difficulties mentioned previously with compensation of the channel near its entrance, and also so that the maximum amount of channel length could be realized, the peeler has been made part of the channel. That is, the inner wall of the first 10 degrees of the magnetic channel has been compensated so as to provide the required peeler field. The resulting change in peeler length (from the original design value of 15 degrees) required adjustment of the angular position of the regenerator, the angle between the respective centers of the peeler and regenerator being reduced to about 58 degrees. Orbit calculations with the computer indicate that this change restores the deflector performance originally calculated.

Mechanical Design

As shown in Figure 4 the mechanical design of the extraction system provides the maximum amount of flexibility for change. The channel consists of 30 separate and individually adjustable sections, most of which are about eight inches in length. The first two sections also perform as the peeler. The regenerator is made up of two sections. Each section of the channel and regenerator is supported on its own adjustable base. These provide a radial adjustment of one and one-half inches, an azimuthal adjustment of one-half inch, and an angular adjustment of eight degrees. The C-blocks, which support the channel walls, and the threaded rods on which the compensation bars are mounted, provide an additional radial adjustment of one-half inch. The channel walls are made up of several thicknesses of iron plate so that the shielding can be easily adjusted by the removal or addition of iron in increments of 0.1 inch.

The extraction system and the necessary flip targets, beam chopper, and beam clippers will be mounted on aluminum plates called "platters." The size of the platters (96 in. x 180 in.) is such that it is impractical to change them through a vacuum lock. Consequently, the accelerator tank must be opened to atmosphere and the platters changed through an opening opposite the dee region. The 600 MeV extraction system will be mounted on a similar plate. We expect that the two systems can be interchanged within 24 hours, including pumpdown time, after the crew becomes familiar with the process. Handling equipment has been designed to reduce the time required, and thus the radiation exposure that will be incurred during these changes.

The design of a working extraction system requires a combination of theoretical analysis and experimental work in the accelerator. Although this system has been designed as far as possible from the experience with similar

systems at synchrocyclotron installations around the world, it is still only the first step towards the realization of an extracted 300 MeV beam. A great deal of work will have to be done after the system is installed in the NASA synchrocyclotron. Accurate mapping of the actual fields in the peeler and regenerator regions and in the channel will be required. The compensation will have to be adjusted to minimize the harmonic distortion due to the large amounts of iron which make up the system. The final adjustments will then have to be made with the accelerator in operation on the basis of data from beam photographs and from probes.

Although the design presented here is only a beginning, we feel confident that this system can be made to provide the beam intensity and quality that is necessary for the experimental work planned by the Langley Field group.

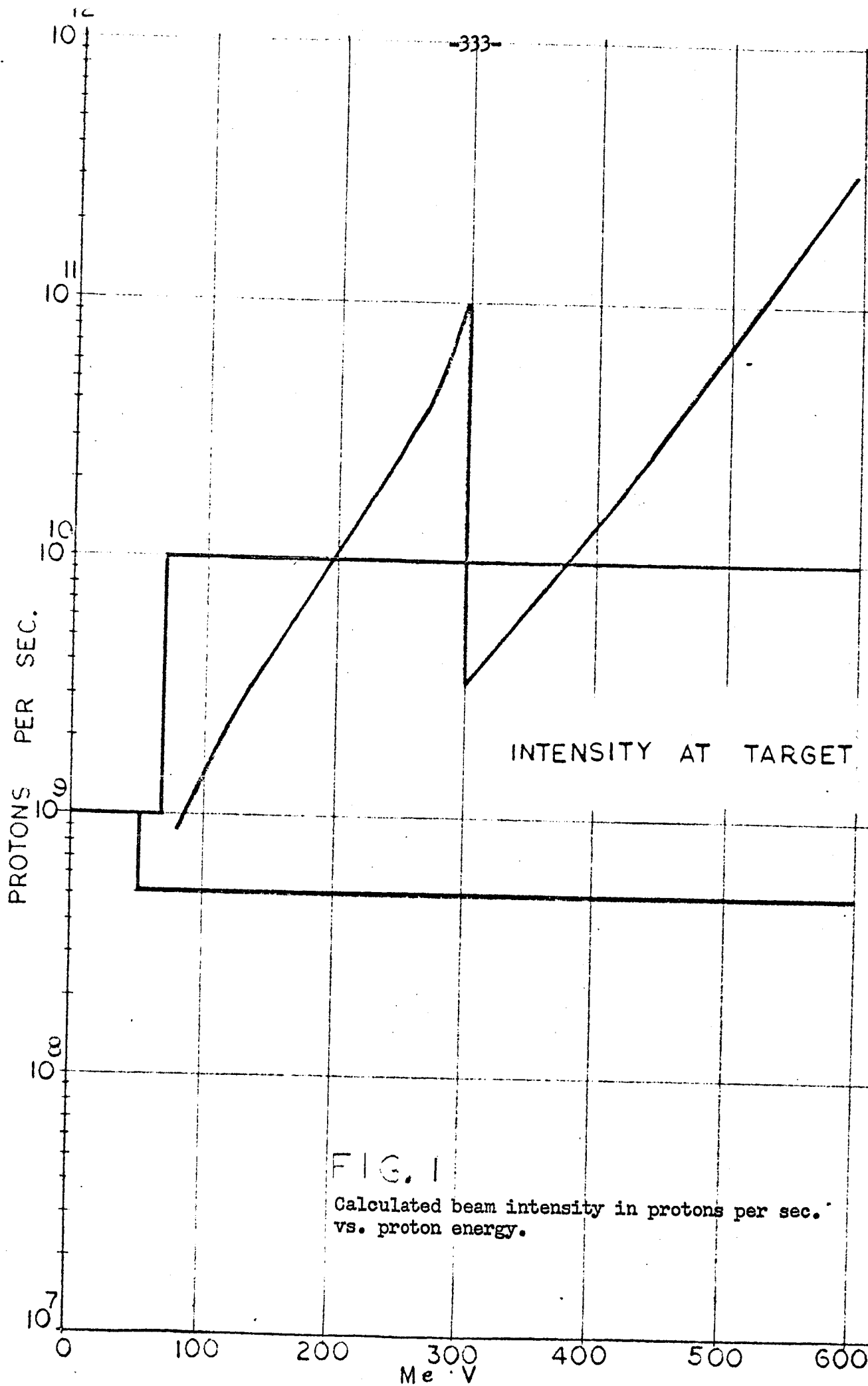
Acknowledgments

The calculations and design work discussed in this paper were a group effort. I wish to particularly acknowledge the help of Dr. Ken Crowe of the Lawrence Radiation Laboratory who served as our consultant on this problem and without whose help this design would never have become a reality.

Major contributions were made by William M. Brobeck, John S. Alcorn, Edward L. Prichard, Norman E. Jorgensen, and Guenther E. Schmidt.

References

1. J. L. Tuck and L. C. Teng, Synchrocyclotron Progress Report III, University of Chicago, Chap. VIII (1951).
2. K. J. LeCouteur, "The Regenerative Deflector for Synchrocyclotrons", Proc. Roy. Phys. Soc. 64, 1073 (1951).
3. K. J. LeCouteur, and S. Lipton, "Non-Linear Regenerative Extraction of Synchrocyclotron Beams", Phil. Mag. 46, 1265 (1955).
4. A. V. Crewe and J. W. G. Gregory, "The Extraction of the Beam from the Liverpool Synchrocyclotron", Proc. Roy. Phys. Soc. 232, 242 (1955).



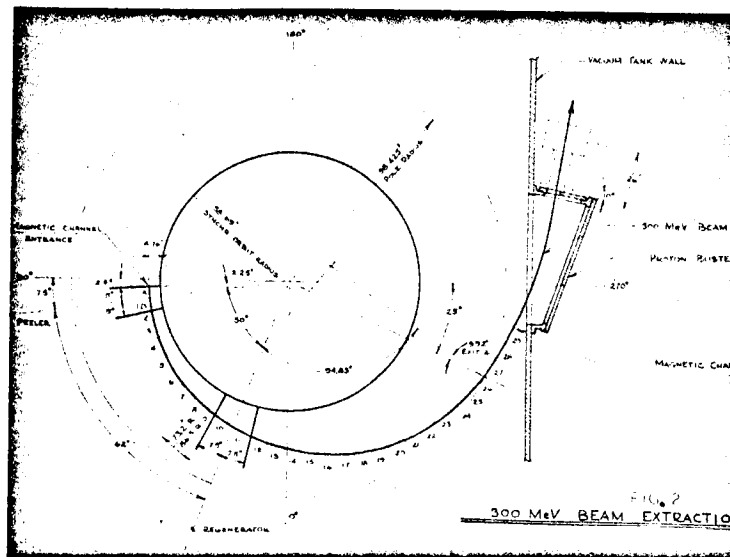


Figure 2 - Plan layout of 300 MeV extraction system.

PHYSICAL SYSTEM OF TWO BLOCKS
ARRANGED SYMETRICALLY IN UNIFORM
MAGNETIC FIELD .

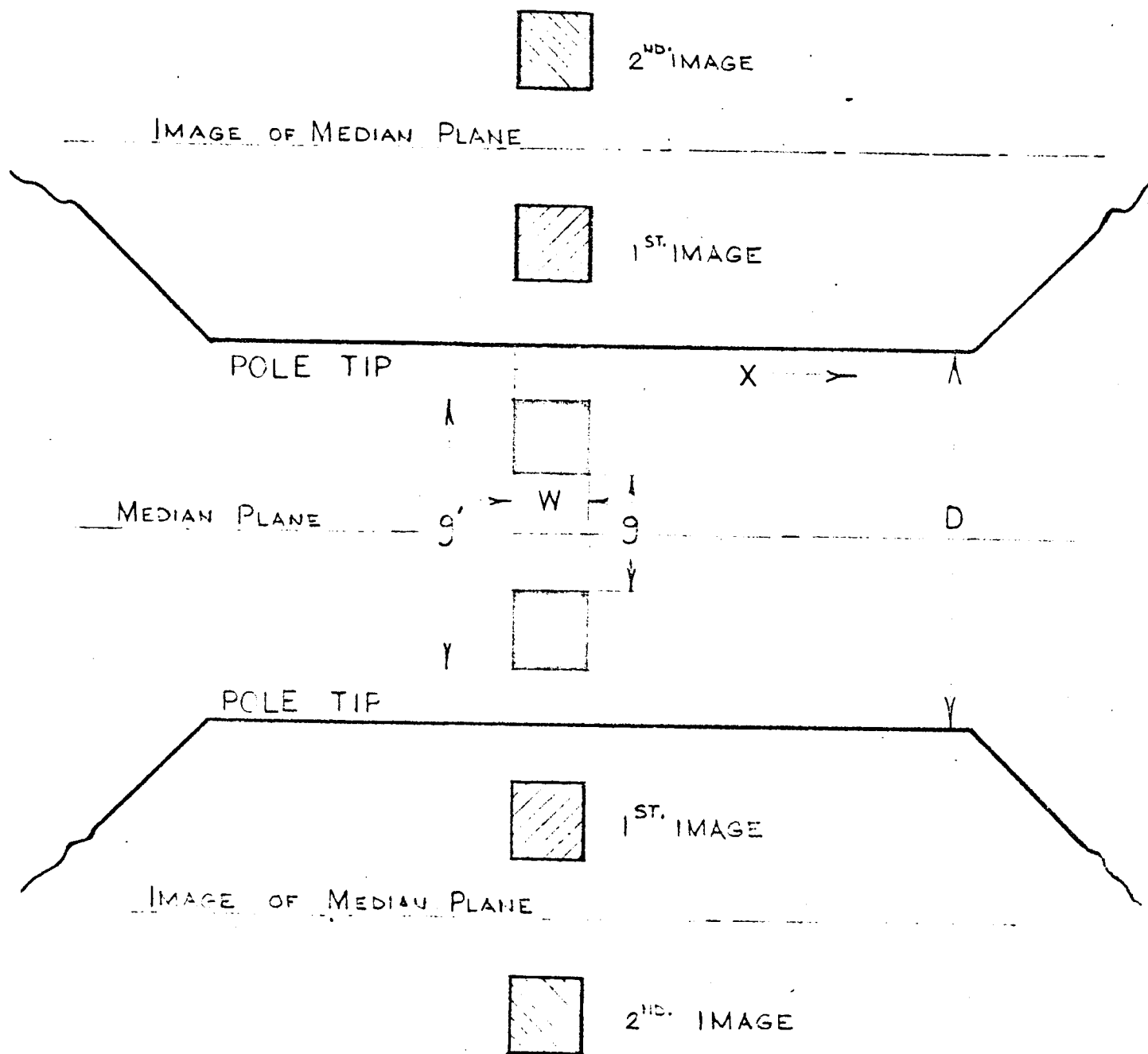


FIG. 3

Images of two magnetic blocks in a uniform magnetic field.

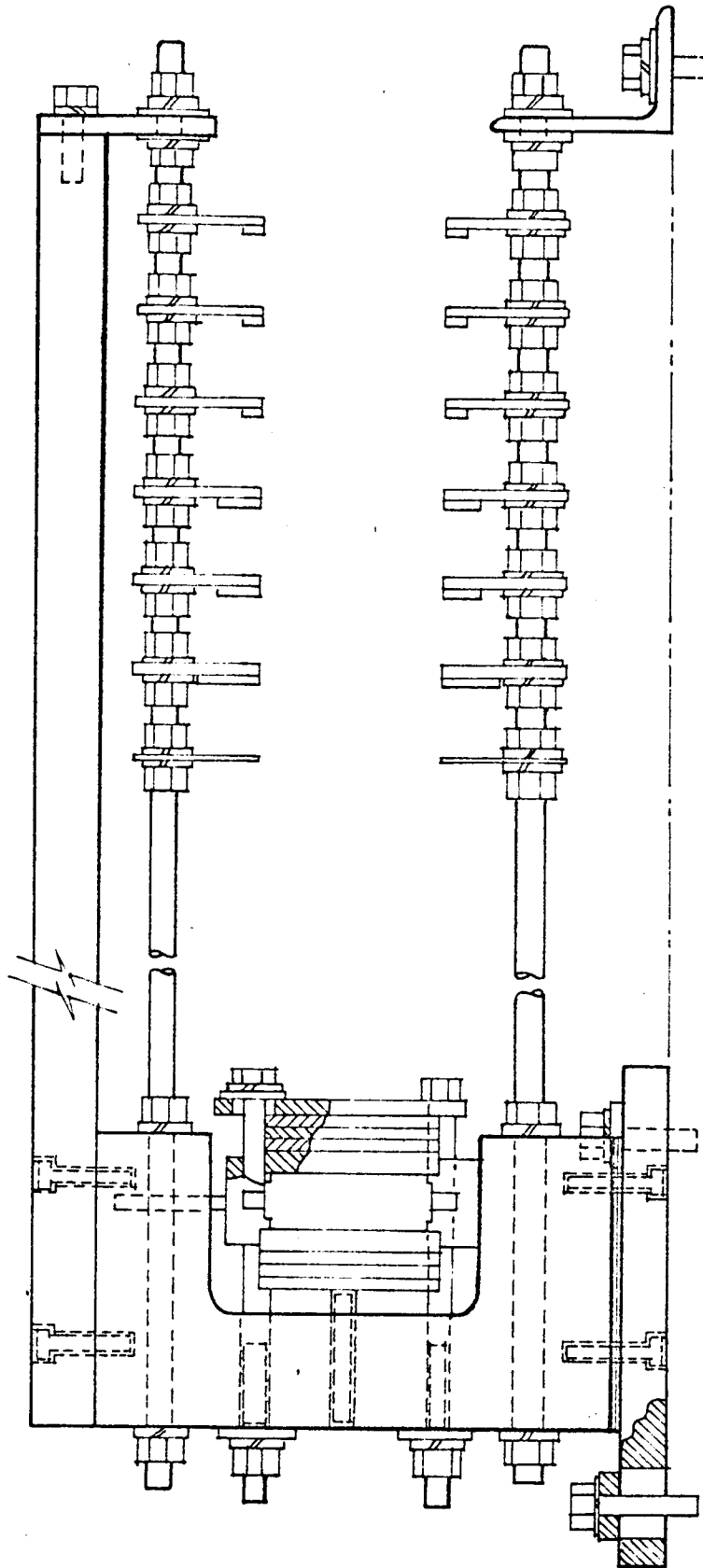


FIG. 4
MAGNETIC CHANNEL ASSEMBLY

SUMMARY

Kenneth M. Crowe
Lawrence Radiation Lab

A new pion producing machine is being constructed close to the Williamsburg campus and we have learned its requirements for space environmental studies have apparently been satisfied by copying an existing CERN machine. It is clear to everyone here that the fundamental physics of this type of machine will continue to evolve only if the machines themselves continue to grow. From the talks we cannot help noticing that one by one the machines have eliminated the differences which gave one machine a temporary edge over the others. As far as currents, duty cycles, reliability, the new machine will be welcomed to join the club.

However, we can be confident that S.R.E.L. will produce some surprises if only in spurring the old machines into facing up to the challenge for more beam. Many of us have speculated on what we would do with more than 1 μ A of beam and when the excitement of MacKenzie's speculations are turned into hardware something is bound to give.

Let me first summarize the results reported here in connection with standardization of beam intensities and duty cycle.

Operating conditions change and the best performance does not correspond to the usual. No one really cares what the current is. The questions are:

What do you do that is different?

Where do you get all the pions, muons, and external protons?

What new phenomena have appeared which may explain irregularities in our operations?

What can we do to improve our own machines?

Questionnaires which are being prepared by each of us are, we hope, up to date. I will venture to predict that the current per accelerating cycle is remarkably constant; i.e., those beams in excess of $1 \mu A$ occur in proportionally higher rep-rate machines.

The new duty cycles, we agree, are not altogether equivalent, although it is suggested that differences may diminish if one measures by a uniform technique; for example, the accidental rate of beam particles with good time resolution (< 5 ns) at the full operating intensity. The high efficiency (65%) and excellent duty cycle (50%) Suzuki reported at Carnegie Tech is at least twice that of the average reported in similar systems elsewhere.

The experience at Liverpool and Chicago on the success of the extraction cees which seem to indicate that particles are knocked out rather than pulled out may lead to unscrambling some unexplained idiosyncrasies of the systems. However, it seems to be agreed that everyone is satisfied that in actual performance further major improvements are necessary.

The efficient extraction of protons is, however, far from a satisfactory situation. I will risk concluding that every suggestion for increasing the beams above $10 \mu A$ must include an overhaul of the extraction system. Although computer codes exist and new suggestions are being tried on paper, most of the operating machines are reluctant to rebuild their extraction devices except as part of a major reconstruction program because of the intense radioactivity in these areas. As we have heard, S.R.E.L. and Carnegie are exceptions and hopefully forthcoming computer results may shed a new light on to this program.

It is my firm opinion that if the internal beam were 100 times the present beam, simple restrictions in the vertical height of the beam at $\sim 1/4$ maximum radius would help and if the excessive radial oscillations could be controlled, existing regenerations would probably be satisfactory.

Results from the Tokyo cyclotron in 1961 (Sanada, Suwa, and Suzuki) in which 60% of the beam enters the extraction deflector beyond $n = 1$ have not been reproduced elsewhere. Reports from attempts at Rochester and Carnegie to pass through $n = .2$ and $.25$ were not encouraging, although my previous remarks (page 108) on quality of the internal beam would apply equally to these results.

As far as machine activity is concerned calculations from Fulmer, Oak Ridge, and Barbier, CERN, were presented which indicated a significant reduction in ambient activity can be obtained with graphite lining of components. More detailed studies with the computations on specific problems, i.e., scattered beams from meson targets, regenerated beam which does not leave the machine would certainly provide impetus to fill the remaining open space with graphite and lead.

The pion and muon beams were discussed in several papers. The results of performance of the muon channel which Telegdi and Culligan reported were encouraging.

As Telegdi mentioned, pion cross sections in such things as beryllium are only available in scattered form. Results from Berkeley and CERN will be available soon on such mundane problems.

In terms of an argument for intense external beams, the experience gained in the past three years at Berkeley is that the intense π^+ and neutron beams are obtained exclusively in external proton beams. Whether the muon channel designed for μ^+ in an internally produced beam would compete with the natural 5% μ^+ contamination is doubtful presently. However, for μ^- the situation still favors the internal target: for example $\sim 10^6 \pi^+/\text{sec.}$ in the proton cave and $10^6 \pi^-/\text{sec}$ inside meson cave are obtained at 300 MeV pion, where 10% of the beam is extracted. With 50% extraction, however, we may

well scrap internal targets. It is encouraging to attempt an optimization for designs of muon channels based on beautiful success of Telegdi's channel.

Improvements of FM Cyclotrons

Several papers which open the possibilities for realizable gains in intensity for the obsolete synchrotron were presented.

W. Brobeck presented a paper based on the use of multiple dee systems. In one system he considered 10 dees operation on five bunches simultaneously. The required r.f. power of ~ 3.5 megawatts seems to be the expensive drawback.

He then considered the application of Mura beam stacking systems where the center of the machine extracts many times, depositing beam at an intermediate radius, and then the main dee extracts it to full radius. Calculations by Swenson at MURA and CERN¹ and others show that reasonable gains are expected if one can obtain the voltages and corresponding bucket sizes to make a reasonable match to the bucket brigade.

Calculations are in progress at Berkeley on an analogue to the machine using ~ 20 up-going buckets to explore if the process is indeed reasonably efficient.

The Chicago Group explained a plan to utilize efficiently the r.f. off-time for a pair of acceleration dees. A factor ~ 4 is reasonably expected. Further increase due to increased dee voltage may cause even more gain.

R. Sherr asked me to mention that no one has reported on studies of axial injection or neutral ion injections with a stripper foil, although both may have real possibilities.

¹
CERN Internal Report, AR/Int. SR/61-19.

K. MacKenzie, with his two reports on the feasibility of an f.m. cyclotron meson factory and cyclotron space charge limits, has in my opinion blown the lid off the $1 \mu A$ ceiling. It is a clear departure from the previous attacks along a fundamental path. He considers the vertical motion near the ion source and concludes that the defocussing space charge force is offset by the magnetic focussing in an abrupt region, the onset occurring at the radius r_m . Applying this to solve for the current he obtains

$$I = \frac{Z \phi V^3}{\omega^3 r_m^4}$$

where Z is the vertical height of the dee, V is the dee voltage, ω the frequency, and ϕ the azimuthal extent. The experiments seem to confirm the V^3 dependence and the factor of proportionality can be adjusted to fix up all the assumptions (electrostatic defocussing, etc.) and approximations.

In summary, I believe that studies of the type suggested by MacKenzie's paper should be made with particular attention to scale. The improvement program at CERN with a nearly full scale model of the center of the machine would be ideally suited to verify the suggestions in every detail. The considered opinions of most is that there must be a wealth of possibilities when the starting conditions can be explored. It seems likely that unless someone thinks of something terribly wrong in the results of this paper, we can expect a major improvement in synchrocyclotron beam in the foreseeable future.

FOSS, Carnegie - We're trying two steel bars that run between the dees at about $1\frac{1}{3}$ " off the mid-plane to get the focussing started in a hurry. The field decreases radially which should, I think, make two fold symmetry work.

CROWE - Are you going to do these tests on the machine itself?

FOSS - Yes.

CROWE - Do you feel that you disagree with my comment about actually doing experiments on the inside of a hot cyclotron?

FOSS - No.

TELEGDI, Chicago - About putting a channel at the end of an external beam: You can compare the solid angle subtended at an internal target by such a channel with the solid angle subtended at an external target. We all believe that we extract about 3% (of the protons) and the comparison becomes obvious. But, however, the positive pions are produced more copiously than the negative pions. But the question still is of solid angle.

CROWE - There's one other factor--that is the multiple traversals and the effective thickness of the internal target.

TELEGDI - Multiple traversals help us.

CROWE - This is just about compensated by the fact that one uses about $10''$ of polyethylene target in our external beam. But these factors are very close to the same.

MACKENZIE, UCLA - I was reminded that I had forgotten to add a little experimental evidence which is in the write-up. Phillips has built a

machine for Saclay. In their report in the last issue of Phillips Technical Review, they report 20-25 μ a. internal beam and 0.7 μ a. deflected with a regenerative deflector. They do it by putting 25 k.v. on their dee with a repetition rate of 450 cy./sec.

CROWE - If the frequency is 450 cy./sec... that's a factor of 8 (in frequency above ours). Therefore if they have 25 μ a. maybe ... that's... 3 (μ a.), which is in the experimental error of agreeing with my statement; namely, it looks like 1-2 μ a. scaled back to 60 cy./sec.

MACKENZIE - Yes, they do not use a calutron source. That factor in front (of my equation) takes care of all disagreement....(laughter)

SIEGEL, William and Mary - What is the energy of that machine?

MACKENZIE - 160 MeV.

CROWE - The efficiency of their extractor sounds rather poor.

BEGER, CERN - I would like to start a discussion of beam intensity measurement. It seems difficult to compare the methods that each group uses in making beam current measurements. I propose adopting a standard method for all machines, so at least we can make relative comparisons between machines. As soon as we know the number of multiple traversals, the height of the dee, and the vertical focussing of the machine we can measure the beam intensity by using the thermal power developed in the target.

CROWE - I agree with the motion except I want to caution everybody that if the beam circulates and runs into a long target and there is any tendency for the beam to be regenerated, then the uncertainty in whether

the effective length of penetration is of the order of a few inches or something of the order of 6-8 inches makes this comparison risky, but it is worth it. The other thing is that misalignments with respect to the inside of the machine can cause errors. In the past we have used a device for such measurements consisting of a flag of graphite with a polystyrene foil inside. The whole thing is mounted on a probe. Then one measures the activity of the front half, the back half and the piece in the middle, for several different thicknesses of targets and then one knows all the necessary parameters. Now this method certainly can be used in all other laboratories provided you know what the limiting aperture is, since near the final target radius the trajectories of the particles vertically may not be known. In our machine it is not known what the performance is within the last 3"-4" of extraction. So I would like to suggest that you move a good 10" inside any questionable variation of the magnetic field. Be sure the measurement is made far enough in so that details of field fall-off do not make this comparison invalid. Then I don't care whether you use thermocouples, activities, or pion or neutron yields; we know the cross-sections, we can make those comparisons.

TELEGDI - I am very much in favor of the Beger proposal. I would like to make a suggestion along the same line which may be more practical for the physicists as opposed to the machine people. We all seem to use the same kinds of targets. Most people use beryllium targets, some use copper targets for positive pions. The sizes of these targets, in the machines I know of, is also about the same. Now if we could go a step further, and agree that we all own identical targets with identical heat sinks, then we could, in the course of our regular experiments, just communicate how many watts we are measuring.

CROWE - I would like to remind you of a previous remark: People who build

machines don't like to quote the average performance of their machine.

GOTTSHALK, Harvard - A recent report from Rochester by Thorndyke shows they improved their energy resolution from an internal polarizing target by a factor of 2 by putting a lip on the target. The principal is that the protons pass through the lip, lose a small amount of energy, perform a radial oscillation and hit the target solidly on the next time around. This principal could be used in either a calorimetric or Farady type of device.

SIEGEL - There seems that part of the difficulty in standardization is whose standard shall we use. Now Beger has a thermocouple design and I think there is a real virtue in Prof. Telegdi's point of view that if we all measure heat, everybody knows what it means.

CROWE - Would Beger be willing to send us all a drawing of his thermocouple design?

GOTTSHALK - If we are looking for a standard I'm not quite sure why it should be heat rather than charge. The secondaries have been shown to be a relatively small problem in a Faraday device, so there remains only the problem of grazing incidence which is the same for a calorimetric or a charge type of device. So you just have a block and measure the current from it.

CROWE - My comment about the block is that it reads the wrong sign (of current).

BEGER - For those not running with internal targets, possibly installing a standard target on a flip target holder would do for making these measurements.

TELEGDI - In connection with a flip target, we at Chicago use a main fixed target with our muon channel. We have placed a vibrating target at a

different azimuth but at the same radius, $\pm 1/8"$, as the main target, and brought it into the beam. The vibrating target was visible through our meson pipe. By some adjustment of the vibrating target, we have been able to cut the beam exactly in two and parasite with ourselves, e.g. we use two simultaneous internal targets.

FOSS, Carnegie - The subject hasn't been discussed very much here, but some places are doing a lot of work in getting more data out of a given amount of beam...collecting data in cores, using numerous detectors and doing two experiments at the same time. This is an important area for future development.

OPERATING CHARACTERISTICS
OF
EXISTING FM SYNCHROCYCLOTRONS

SYNCHRO-CYCLOTRON PARAMETERS

(January, 1964)

Name of Laboratory Carnegie Institute of Technology NRC

A. Beam Properties

Vertical Spread In Internal Beam	(2 x) 0.75"
Radial Spread of Internal Beam	(2 x) 2 "
Energy of Internal Beam	425 MeV
Radius of Internal Target	67"
Current in Internal Beam	1 μ a
How Measured	

Energy of Extracted Proton Beam	437 MeV
Energy Spread of Extracted Proton Beam	1 MeV
Geometrical Size of Extracted Beam in Experimental Area	2" x 4"
Proton Flux in Extracted Proton Beam	$10^7/\text{cm}^2/\text{sec}$
Beam Stretching Method Used With Internal Beam	noise + r.f. on cee
Percentage of Normal (Unstretched) Internal Beam Which is Stretched by Above Method	65%
Duty Cycle (% on Time)	90% (50% n sec)

B. Ion Source Description

Hot cathode 1/8 in. diameter port in graphite 5" below center	
Pulsed?	Yes
Estimated Current Emitted by Source	1 ma

C. R. F. System

Frequency Swing	32 - 20 mc/sec
Repetition Rate	200 pps

R. F. Voltage

10 kv

Oscillator D. C. Input

7 kv

Duty Cycle

50%

Internal Height of Dee

6" to 4"

Description of Capacitor

400 - 1400 *per sec.*

D. Magnet

Diameter

141.67"

Gap

15.615"

Center Field-Strength

20,520 Gauss

Power Consumption

360 kw

Radius where $n = 0.2$

68.4

Radius where $n = 1.0$

69.4

Accuracy of Magnet Shimming at

$n \approx 0.2 \pm 2$ Gauss

Amplitude of First Field Harmonic

Relative to Mean Field

.05%

Amplitude of Second Harmonic Relative

to Mean Field

.05%

CERN 600 MeV SYNCHRO-CYCLOTRON PARAMETERS (JANUARY 1964)

MAGNET :

Diameter	5,00 m
Magnet gap	45 cm max., 36 cm min.
Centre-field strength	19,53 kG
Power consumption	0,95 MW
Radius, where $n = 0,2$	226,8 cm

RF SYSTEM :

3/4 λ -system with series C (Tuning fork)	
Grounded grid self-excited oscillator	
Repetition rate	54 cps
Frequency swing	30,0 Mc - 16,4 Mc
RF voltage	5 kV - 30 kV
Oscillator DC input	~ 15 kW
Duty cycle	50%
Free height of the D	12 cm

VACUUM :

Working pressure	$3 - 5 \times 10^{-6}$
Pumping speed of oil	
diffusion pumps	$2 \times 12,000 \text{ l/sec}$

BEAM FEATURES :

Ion source	Cold cathode, pulsed
Internal target position	223 cm
Beam intensity at 210 cm	~ 1,6 μ A
Regenerator and magnetic	
(iron) channel for external	
proton beam	

SYNCHRO-CYCLOTRON PARAMETERS

(January, 1964)

Name of Laboratory University of Chicago

A. Beam Properties

Vertical Spread In Internal Beam	2" at 76" RAD.
Radial Spread of Internal Beam	
Energy of Internal Beam	450 MeV
Radius of Internal Target	76"
Current in Internal Beam	1 μ a
How Measured	thermocouple

Energy of Extracted Proton Beam	450 MeV
Energy Spread of Extracted Proton Beam	< 1 MeV
Geometrical Size of Extracted Beam in	
Experimental Area	1 cm ²
Proton Flux in Extracted Proton Beam	
Beam Stretching Method Used With	
Internal Beam	stochastic cee
Percentage of Normal (Unstretched) Internal	
Beam Which is Stretched by Above Method	50%
Duty Cycle (% on Time)	50% macroscopic

B. Ion Source Description

Pulsed?	yes
Estimated Current Emitted by Source	

C. R. F. System

Frequency Swing	28.4mc \rightarrow 18.2mc
Repetition Rate	78 cps (95 max.)

R. F. Voltage

14 kv

Oscillator D. C. Input

25 kw

Duty Cycle

1/4

Internal Height of Dee

4 1/2"

Description of Capacitor

rotating condenser

D. Magnet

Diameter

170"

Gap

14" → 18"

Center Field-Strength

18.6 kg

Power Consumption

650 kw

Radius where $n = 0.2$

76.5"

Radius where $n = 1.0$

79"

Accuracy of Magnet Shimming at

$n \approx 0.2 \pm$ _____ Gauss

Amplitude of First Field Harmonic

Relative to Mean Field

Amplitude of Second Harmonic Relative

to Mean Field

SYNCHRO-CYCLOTRON PARAMETERS

(January, 1964)

Name of Laboratory Harvard Cyclotron Laboratory

A. Beam Properties

Vertical Spread In Internal Beam	<u>0.5" just before regenerator</u>
Radial Spread of Internal Beam	<u>approx. 3" peak to peak</u>
Energy of Internal Beam	<u>~ 160 MeV</u>
Radius of Internal Target	<u>41.5"</u>
Current in Internal Beam	<u>approx. 0.5 μa</u>
How Measured	<u>current from brass block</u>

Energy of Extracted Proton Beam	<u>160 MeV</u>		
Energy Spread of Extracted Proton Beam	<u>1.5 MeV open; 0.4 MeV with slits</u>		
Geometrical Size of Extracted Beam in Experimental Area	<u>7mm H x 12mm W, full beam</u>		
Proton Flux in Extracted Proton Beam	<u>3 x 10¹⁰ prot./sec. open</u>		
Beam Stretching Method Used With Internal Beam	<table><tr><td>shaped (1) condenser- teeth</td><td>cee</td></tr></table>	shaped (1) condenser- teeth	cee
shaped (1) condenser- teeth	cee		
Percentage of Normal (Unstretched) Internal Beam Which is Stretched by Above Method	<table><tr><td>~ 100%</td><td>~ 80%</td></tr></table>	~ 100%	~ 80%
~ 100%	~ 80%		
Duty Cycle (% on Time)	<table><tr><td>5%</td><td>~ 15%</td></tr></table>	5%	~ 15%
5%	~ 15%		

B. Ion Source Description

Pulsed?	<u>~ 3A peak ~ 100 ms</u>
Estimated Current Emitted by Source	<u>~ 0.6A peak total; ~ 75ma. peak ions</u>

C. R. F. System

Frequency Swing	<u>29.6 mc \rightarrow 23.6 mc</u>
Repetition Rate	<u>variable up to 300 pps</u>

R. F. Voltage

~ 9 kv

Oscillator D. C. Input

15 kw

Duty Cycle

Internal Height of Dee

varies from 4 to 1 $\frac{1}{2}$ in.

Description of Capacitor

coaxial cylinder geometry
16 teeth, shaped to increase
extraction time

D. Magnet

Diameter

95" pole tip

Gap

approx. 12"

Center Field-Strength

19.7 kg.

Power Consumption

160 kw

Radius where $n = 0.2$

42 in.

Radius where $n = 1.0$

Accuracy of Magnet Shimming at

$n \approx 0.2 \pm$ _____ Gauss

Amplitude of First Field Harmonic

Relative to Mean Field

Integrated field defect less
than 0.2 Kg - inch ⁽²⁾

Amplitude of Second Harmonic Relative

to Mean Field

(1) LEFRANCOIS; Rev. Sci. Instr. 32, 986 (1961)

(2) CALAME, et al ; Nuclear Instruments 1, 169 (1957)

SYNCHRO-CYCLOTRON PARAMETERS

(January, 1964)

Name of Laboratory Harwell

A. Beam Properties

Vertical Spread In Internal Beam

Radial Spread of Internal Beam

Energy of Internal Beam

Radius of Internal Target

Current in Internal Beam

How Measured

$\pm 3''$

160 MeV

48.5"

1.5 μ a

current in thick stopping target

Energy of Extracted Proton Beam

Energy Spread of Extracted Proton Beam

Geometrical Size of Extracted Beam in

Experimental Area

Proton Flux in Extracted Proton Beam

Beam Stretching Method Used With

Internal Beam

Percentage of Normal (Unstretched) Internal

Beam Which is Stretched by Above Method

Duty Cycle (% on Time)

no extraction system, beam scattered
out through channel

± 1.5 MeV

6 mm. square

10^7 polarized 10^8 unpolarized

synchronous acceleration by cee

80% but only 45% for external
beams

70%, but less for ext. beams
(not counting r.f. structure)
cold cathode, penning-type

B. Ion Source Description

Pulsed?

Estimated Current Emitted by Source

yes

C. R. F. System

Frequency Swing

Repetition Rate

26 - 18.8 mc (only use 248 - 202mc)

200/sec

R. F. Voltage

8 \pm 1 kv

Oscillator D. C. Input

10 kw

Duty Cycle

45%

Internal Height of Dee

3.75"

Description of Capacitor

One ring of 4 rotor blades

D. Magnet

Diameter

110"

Gap

12" max.

Center Field-Strength

16.2 kg

Power Consumption

360 kw

Radius where $n = 0.2$

50.2"

Radius where $n = 1.0$

Accuracy of Magnet Shimming at

$n \simeq 0.2 \pm$ _____ Gauss

Amplitude of First Field Harmonic

Relative to Mean Field

Amplitude of Second Harmonic Relative

to Mean Field

SYNCHRO-CYCLOTRON PARAMETERS

(January, 1964)

Name of Laboratory Columbia University Nevis Laboratories

A. Beam Properties

Vertical Spread In Internal Beam	<u>1"</u>
Radial Spread of Internal Beam	<u></u>
Energy of Internal Beam	<u>385 MeV</u>
Radius of Internal Target	<u>72"</u>
Current in Internal Beam	<u>.5 - 1.0 μa</u>
How Measured	<u>Thermocouple and activation</u>

Energy of Extracted Proton Beam	<u>none</u>
Energy Spread of Extracted Proton Beam	<u></u>
Geometrical Size of Extracted Beam in Experimental Area	<u></u>
Proton Flux in Extracted Proton Beam	<u></u>
Beam Stretching Method Used With Internal Beam	<u>vibrating target</u>
Percentage of Normal (Unstretched) Internal Beam Which is Stretched by Above Method	<u>80%</u>
Duty Cycle (% on Time)	<u>30%</u>

B. Ion Source Description

Pulsed?	<u>yes</u>
Estimated Current Emitted by Source	<u></u>

C. R. F. System

Frequency Swing	<u>28 - 17 megacycles</u>
Repetition Rate	<u>60 C.P.S.</u>

R. F. Voltage

~ 6 kv - 10 kv

Oscillator D. C. Input

6 kv

Duty Cycle

Internal Height of Dee

5"

Description of Capacitor

Internal rotating condensers,
(along open end of dee, on diameter)

Magnet

Diameter

16 1/4"

Gap

18" at center, 1 1/4" at edge

Center Field-Strength

17.8 kgauss

Power Consumption

600 kw

Radius where $n = 0.2$

7 1/4"

Radius where $n = 1.0$

Accuracy of Magnet Shimming at

$n \approx 0.2 \pm$ 20 Gauss

Amplitude of First Field Harmonic

Relative to Mean Field

Amplitude of Second Harmonic Relative

to Mean Field

SYNCHRO-CYCLOTRON PARAMETERS

(January, 1964)

Name of Laboratory Lawrence Radiation Laboratory, Berkeley, California

A. Beam Properties

Vertical Spread In Internal Beam	2"
Radial Spread of Internal Beam	6" to 10"
Energy of Internal Beam	740 MeV.
Radius of Internal Target	81"
Current in Internal Beam	1 - 2 μ A
How Measured	Activity
Energy of Extracted Proton Beam	740 MeV.
Energy Spread of Extracted Proton Beam	+ 6 MeV.
Geometrical Size of Extracted Beam in Experimental Area	3" Dia. to 1/2" Dia.
Proton Flux in Extracted Proton Beam	.1 μ A to .02 μ A and less
Beam Stretching Method Used With Internal Beam	Synchronized Auxiliary Electrode
Percentage of Normal (Unstretched) Internal Beam Which is Stretched by Above Method	50%
Duty Cycle (% on Time)	50%

B. Ion Source Description

Hooded arc heated with r.f.

Pulsed?	Yes.
Estimated Current Emitted by Source	$\sim 50 \mu A \propto + < 10"$

C. R. F. System

Frequency Swing	38 to 19 MC
Repetition Rate	64 cyo/sec.

R. F. Voltage

10 KV.

Oscillator D. C. Input

Duty Cycle

50%

Internal Height of Dee

4"

Description of Capacitor

Vibrating Reed

D. Magnet

Diameter

~ 188.75" Pole Tip

Gap

~ 12" (14" at Center)

Center Field-Strength

23.1 K. G.

Power Consumption

2.5 M.W.

Radius where $n = 0.2$

82.2"

Radius where $n = 1.0$

85.0"

Accuracy of Magnet Shimming at

$n \approx 0.2 \pm$ _____ Gauss

Amplitude of First Field Harmonic

Relative to Mean Field

10 gauss

Amplitude of Second Harmonic Relative

to Mean Field

~ 100 gauss

n at Extraction

~ .02

SYNCHRO-CYCLOTRON PARAMETERS

(January, 1964)

Name of Laboratory University of Liverpool, England

A. Beam Properties

Vertical Spread In Internal Beam	(about 2 in.)
Radial Spread of Internal Beam	(about 4 in.)
Energy of Internal Beam	383 MeV
Radius of Internal Target	$69\frac{1}{2}$ in.
Current in Internal Beam	about 1 μ a
How Measured	carbon irradiation

Energy of Extracted Proton Beam	383 MeV
Energy Spread of Extracted Proton Beam	< 2 MeV
Geometrical Size of Extracted Beam in Experimental Area	$\sim 1/2$ in ²
Proton Flux in Extracted Proton Beam	2×10^{11} sec ⁻¹
Beam Stretching Method Used With Internal Beam	peripheral cee
Percentage of Normal (Unstretched) Internal Beam Which is Stretched by Above Method	π^- 100%, π^+ 75%
Duty Cycle (% on Time)	π^- 38%, π^+ 27%

B. Ion Source Description

Pulsed?	yes
Estimated Current Emitted by Source	

C. R. F. System

Frequency Swing	29.8 to 18.0 Mc/s
Repetition Rate	115 sec ⁻¹

R. F. Voltage

about 5 kv

Oscillator D. C. Input

8 kv, 4 A

Duty Cycle

Internal Height of Dee

4 in.

Description of Capacitor

rotating - 6 sets of blades,
1150 r.p.m.

D. Magnet

Diameter

156"

Gap

~ 14"

Center Field-Strength

19 kgauss

Power Consumption

910 kw

Radius where $n = 0.2$

Radius where $n = 1.0$

Accuracy of Magnet Shimming at

$n \simeq 0.2 \pm$ _____ Gauss

Amplitude of First Field Harmonic

Relative to Mean Field

Amplitude of Second Harmonic Relative

to Mean Field

SYNCHRO-CYCLOTRON PARAMETERS

(January, 1964)

Name of Laboratory Radiation Laboratory, McGill University

A. Beam Properties

Vertical Spread In Internal Beam	<u>~ 1/2 in.</u>
Radial Spread of Internal Beam	<u>~ 2 in.</u>
Energy of Internal Beam	<u>100 MeV</u>
Radius of Internal Target	<u>36 in.</u>
Current in Internal Beam	<u>1 μa</u>
How Measured	<u>Cu Block</u>

Energy of Extracted Proton Beam	<u>100 MeV</u>
Energy Spread of Extracted Proton Beam	<u>1 MeV</u>
Geometrical Size of Extracted Beam in	
Experimental Area	<u>1 in² - 10⁻³ in² (Focused)</u>
Proton Flux in Extracted Proton Beam	<u>1 - 1.5 x 10¹¹</u>
Beam Stretching Method Used With	
Internal Beam	<u>none</u>
Percentage of Normal (Unstretched) Internal	
Beam Which is Stretched by Above Method	
Duty Cycle (% on Time)	

B. Ion Source Description

Pulsed?	<u>Yes</u>
Estimated Current Emitted by Source	

C. R. F. System

Frequency Swing	
Repetition Rate	<u>400 cps</u>

R. F. Voltage

~ 12 kvp

Oscillator D. C. Input

8 KV

Duty Cycle

0.25

Internal Height of Dee

2 in. to 1 in.

Description of Capacitor

Rotating

D. Magnet

Diameter

82 in.

Gap

7 1/2 in.

Center Field-Strength

16,800 gauss

Power Consumption

180 KW

Radius where $n = 0.2$

36.8 in.

Radius where $n = 1.0$

38.0 in.

Accuracy of Magnet Shimming at

$n \approx 0.2 \pm \underline{30}$ Gauss

Amplitude of First Field Harmonic

Relative to Mean Field

~ 0.1%

Amplitude of Second Harmonic Relative

to Mean Field

0.1% (r = 15 in) - 0.03% (r = 36 in)

SYNCHRO-CYCLOTRON PARAMETERS

(January, 1964)

Name of Laboratory Laboratoire de Physique - Orsay, France - Nucleaire, (Taken from
Phillips Tech. Rev. 12, p. 381
61/62 and Journal de
Physique et le Radium Vol. 21
May, 1960.

A. Beam Properties

Vertical Spread In Internal Beam

Radial Spread of Internal Beam

Energy of Internal Beam

Radius of Internal Target

Current in Internal Beam

How Measured

160 MeV Protons

80 MeV Deuterons

123 cm. maximum radius

20 μ a

Energy of Extracted Proton Beam

Energy Spread of Extracted Proton Beam

Geometrical Size of Extracted Beam in

Experimental Area

Proton Flux in Extracted Proton Beam

Beam Stretching Method Used With

Internal Beam

Percentage of Normal (Unstretched) Internal

Beam Which is Stretched by Above Method

Duty Cycle (% on Time)

157 MeV protons

$\Delta E \simeq 3$ MeV

4 x 8 cm., 3 m behind exit of
extraction system without quadrupoles

.7 μ a

Cee system used with external
beam.

20-25% for external beam.

B. Ion Source Description

Pulsed?

Estimated Current Emitted by Source

cold cathode

Yes, pulse length = 1 ms.

C. R. F. System

Frequency Swing

Repetition Rate

25.0 - 20.2 Mc/s for protons

450 c/s

25 kv

 $\leq 30 \text{ kw}$

Duty Cycle

20 cm $r = 0$, 10.4 cm $r = 132$ cm.
8.5 cm $r = 137$ cm.

rotary capacitor

D. Magnet

2.80 meters

30 - 40 c.m.

16.30 kg

Power Consumption

Radius where $n = 0.2$

Radius where $n = 1.0$

Accuracy of Magnet Shimming

* 15 Gauss

Amplitude of First Field Harmonic

Relative to Mean Field

Amplitude of Second Harmonic Relative
to Mean Field

650 tons

SYNCHRO-CYCLOTRON PARAMETERS

(January, 1964)

Name of Laboratory University of Rochester 130"

A. Beam Properties

Vertical Spread In Internal Beam	at target $\pm 3/4"$
Radial Spread of Internal Beam	1.5"
Energy of Internal Beam	240 MeV
Radius of Internal Target	n = .2 Target at 58 1/2"
Current in Internal Beam	5" to 6" measured 7" to 8"
How Measured	under proper conditions Cll activity of scintillon on C probe at n = .2
Energy of Extracted Proton Beam	213 \pm 1 MeV
Energy Spread of Extracted Proton Beam	\pm 6 to 10 MeV
Geometrical Size of Extracted Beam in Experimental Area	\bigcirc -3/8" to \bigcirc 3/4"
Proton Flux in Extracted Proton Beam	
Beam Stretching Method Used With Internal Beam	In past a rotating target, soon a cee
Percentage of Normal (Unstretched) Internal Beam Which is Stretched by Above Method	Rotating target 1/3" to 1/4"
Duty Cycle (% on Time)	\approx 30%

B. Ion Source Description

Pulsed?	yes
Estimated Current Emitted by Source	xx

C. R. F. System

Frequency Swing	18.5 - 29.6 mcs.
Repetition Rate	200 to 330 cy/sec.

R. F. Voltage

≈ 15 kv

Oscillator D. C. Input

10 to 25 kw

Duty Cycle

$\approx 1\%$

Internal Height of Dee

5" to 3"

Description of Capacitor

metal rotating condenser

D. Magnet

Diameter

130"

Gap

11 3/8 to 12"

Center Field-Strength

16,750 gauss

Power Consumption

Radius where $n = 0.2$

$58\frac{1}{2}"$ $n = .25$ at $r = 58"$

Radius where $n = 1.0$

$60\frac{1}{4}"$

Accuracy of Magnet Shimming at

$n \approx 0.2 \pm 1$ Gauss

Amplitude of First Field Harmonic

Relative to Mean Field

± 1 gauss

Amplitude of Second Harmonic Relative

to Mean Field

FREQUENCY-MODULATED CYCLOTRON DATA SHEET

Name of machine INSJ 160 cm Synchro- and Variable Energy Ordinary Cyclotron
 Institution Institute for Nuclear Study
 Address Tanashi-Machi, Tokyo, Japan
 Person in charge Junpei Sanada
 Person supply data Junpei Sanada Date January 1964

<u>Present Fields of Research</u>	<u>% of Time</u>	<u>History and Status</u>
<u>Isotope production</u>	<u>30</u>	Construction started <u>April 1954</u>
<u>Nuclear Reaction and Structure</u>	<u>30</u>	Completion date <u>(exter. beam)</u> <u>Dec. '58</u>
<u>"on beam" hrs/wk</u>	<u>100</u>	Scheduled operation <u>120 hrs/wk</u>
		Magnet cost <u>\$220,000</u>
		Total cost <u>\$650,000</u>

Design Specifications

<u>Magnet</u>	<u>Design energy and particle</u>
Core dia. <u>212 cm</u>	<u>57 Mev</u> <u>protons</u>
Pole tip dia. <u>160 cm</u>	<u> </u> Mev <u> </u>
Beam radius, max where n=1 <u>76.6 cm</u>	Oscillator type <u>self-ex, gnd-g</u>
Field gap, center <u>25 cm</u>	Pre-exciter <u>no</u>
Field, center <u>15.5 k-gauss</u>	Oscillator tube <u>8T-50</u>
Field, where n=0.2 <u>15.0 k-gauss</u>	Osc. d-c input, max <u>60 kw</u>
Radius, where n=0.2 <u>71 cm</u>	Osc. r-f output, max <u>25 kw</u>
Power <u>135 kw</u>	Frequency range <u>20.3 to 24.3 Mc/s</u>
Weight, Fe <u>243</u> Cu <u>21.8 tons</u>	Modulation method <u>rotating condenser</u>
Winding solid strip <u>2x32, 2.2x28mm</u>	Repetition rate <u>max. 2250 pulses/sec</u>
Cooling <u>oil bath</u>	Acceptance time <u>30μs</u> r-f deg
Dee aperture <u>7.8 cm</u>	Dee-to-ground <u>max. 20 kv, peak</u>
Dee bias, d-c max <u>-2000 (-100 used) V</u>	Shielding <u>concrete, 150cm sides</u> <u>and 96 cm top</u>
Beam extraction, type <u>E. S. Int. def. at n=1</u>	
Ion source, type <u>hot cathode, open D. C.</u>	

ACTUAL PERFORMANCE DATA

Internal Beam

	Protons	Deutrons	Alphas	
Energy, Mev	51~57			
Frequency range, Mc/sec	20.3~24.3			
Mag. field, k-gauss	15.5			
Dee-to-ground, peak, kv	10			
Duty cycle, %	1.5~30*			
Internal Beam, stable Time averaged, μ a	2.4			
Energy spread, %	0.7			

* By stochastic extraction

External Beam

Particle	Flux (part./cm ² -sec)	Beam Area (cm ²)	Energy (Mev)	Energy Spread
p	50% of internal beam at exit port of vacuum tank			

Ext. beam "piped" 30 ft to target. Beam analyzing magnet used?
under preparation

Unusual Features of Installation

By exchanging r-f systems and lowering the magnetic field, the machine is used as a variable energy ordinary cyclotron. High efficient extraction of the beam with an electrostatic internal deflector at $n=1$ was succeeded. Debunching of the beam pulse was also accomplished by the stochastic extraction.

Published Articles Describing Machine

1. S. Kikuchi et al., "A 160 cm Synchro- and Variable Energy Ordinary Cyclotron", J. Phys. Soc. Japan 15, 41, 1960
2. S. Suwa et al., "Efficient Beam Extraction from a Synchrocyclotron at $n=1$ ", Nuclear Instrument & Methods 5, 189, 1959
3. J. Sanada, S. Suwa and A. Suzuki, "Efficient Beam Extraction at $n=1$ and Debunching of the Beam for Synchrocyclotron", Proceedings of 1961 Brookhaven International Conference on High Energy Accelerator, page 311-313, Sept. 6-12, Upton, New York.
4. A. Suzuki, "Debunching of the Beam Pulse for the Synchro-Cyclotron", Japanese Journal of Applied Physics, Vol. 2, No.2, pp. 106-113, February, 1963

SYNCHRO-CYCLOTRON PARAMETERS

(January, 1964)

Name of Laboratory The Gustaf Werner Institute, University of Uppsala,
Uppsala. Sweden

A. Beam Properties

Vertical Spread In Internal Beam	<u>2 cm at 100 cm radius</u>
Radial Spread of Internal Beam	<u>(around 7 cm)</u>
Energy of Internal Beam	<u>185 MeV (max. 192 MeV)</u>
Radius of Internal Target	<u>100 cm</u>
Current in Internal Beam	<u>0.2-0.5 μa (max. meas. 1 μa)</u>
How Measured	<u>Activation Na₂₄, Cl₁₁, in- sulated Cu to μa-meter</u>
Energy of Extracted Proton Beam	<u>185 MeV</u>
Energy Spread of Extracted Proton Beam	<u>\leq 0.2 MeV</u>
Geometrical Size of Extracted Beam in Experimental Area	<u>Normally 4×4 mm², can be varied</u>
Proton Flux in Extracted Proton Beam	<u>4×10^{10} protons/sec.</u>
Beam Stretching Method Used With Internal Beam	<u></u>
Percentage of Normal (Unstretched) Internal Beam Which is Stretched by Above Method	<u></u>
Duty Cycle (% on Time)	<u></u>

B. Ion Source Description

Cold cathodes of Uranium
Penning type

Pulsed? Pulsed (5-30 usec pulses)
Estimated Current Emitted by Source

C. R. F. System

Frequency Swing 33.2 - 25.8 MHz
Repetition Rate 250/sec

R. F. Voltage

5-10 kV

Oscillator D. C. Input

5 kW

Duty Cycle

8 cm

Internal Height of Dee

Condenser rotating in air

Description of Capacitor

D. Magnet

Diameter

230 cm

Gap

25 cm mean

Center Field-Strength

21.5 kgauss

Power Consumption

445 kW

Radius where $n = 0.2$

102 cm

Radius where $n = 1.0$

Accuracy of Magnet Shimming at

$n \simeq 0.2 \pm$ _____ Gauss

Amplitude of First Field Harmonic

Relative to Mean Field

Amplitude of Second Harmonic Relative

to Mean Field